Interactions of Neurotrophins and their Receptors

by

Allan Bates

A dissertation submitted in partial satisfaction of the requirements for the degree of

Doctor of Philosophy

in the

Institute of Molecular Biosciences

at

MASSEY UNIVERSITY, NEW ZEALAND

2003

ABSTRACT

Supervisors

Prof. Pat Sullivan, Ph.D. Massey University, Palmerston North, New Zealand.
Prof. Uri Saragovi, Ph.D. McGill University, Montreal, Canada.
Prof. E. N. Baker, Ph.D, Auckland University, Auckland, New Zealand.
Prof. William Mobley, MD., Ph.D., Stanford University, Palo Alto, California, U.S.A.

In order to investigate the interactions of neurotrophins with their receptors, a number of different domains of the extra-cellular regions of the TrkA, TrkB and TrkC receptors were expressed and the interactions of neurotrophins with these domains were investigated by biosensor. The entire extracellular domains of all three receptors were expressed in the yeast *Pichia pastoris,* while the leucine-rich regions and the immunoglobulin-like domains were expressed as MBP-fusion proteins in *E. coli.* Peptides representing the second leucine-rich regions and purported neurotrophin-binding domain of TrkA, TrkB and TrkC were synthesized. Proteins expressed in *Pichia pastoris* were purified by anion, cation and metal chelating columns; proteins expressed in *E. coli.*, were purified on amylose columns. All recombinant Trk proteins were covalently attached, using EDC/NHS chemistry, to the methyldextran surface of a biosensor cuvette. Extensive kinetics measurements of the interactions of the neurotrophins with immobilized recombinant proteins established a difference in the binding interactions of NGF with TrkA compared with the interactions of BDNF with TrkB and NT-3 with TrkC. All NGF interactions with TrkA proteins showed biphasic kinetics. Interactions of BDNF and NT-3 with TrkB and TrkC showed monophasic kinetics. No interaction of NGF with the immunoglobulin-like domain of TrkA was observed for those proteins expressed in *E. coli*, however the interaction of BDNF was observed with the immunoglobulin-like domain of TrkB when expressed in *E. coli.* Interaction of NGF and BDNF was observed with the leucine-rich domain of TrkA and TrkB respectively. These results differ from previously reported studies, both *in vivo* and *in vitro,* of the interactions of the extra-cellular domains of the Trk receptors with neurotrophins. Previous studies have claimed to establish exclusive interaction of the neurotrophins with either the leucine-rich or immunoglobulin-like domains of the Trk receptors. The interaction studies reported here show a clear interaction of neurotrophins with both leucine-rich and immunoglobulin-like domains of the Trk receptors.

These interactions have similar affinity. This result suggests that the interactions of neurotrophin and receptor may be more complex than previously suggested. It is conceivable that neurotrophins bind initially to the leucine-rich domain of the receptor, followed by movement to the Immunoglobulin-like domain and the initiation of phosphorylation of the intra-cellular domains or internalization of receptor and bound neurotrophin. Kinetics studies of the synthetic peptides failed to show that these represent the exclusive neurotrophin-receptor interaction domain as previously reported. These results suggest that the development of small molecule mimetics of the neurotrophins as a therapy for Alzheimer's and other neurological diseases may be more complicated than previously envisioned.

ACKNOWLEDGEMENTS

Rita Levi-Montalcini, the co-discoverer of the neurotrophin NGF and eventual Nobel Prize winner, began her studies of the protein shortly before the outbreak of the second-world war. She continued her studies in the confines of her home throughout the allied bombing campaign of Italy. After the war, the studies were continued in Europe, the United States and South America. It would be difficult to find a more inspiring story than the trials and difficulties of one scientist in the pursuit of knowledge, than that of Levi-Montalcini. My own project presented in this thesis, has taken me from the United States to Japan, New Zealand and Canada and often seemed so close to failure that it seemed prudent to abandon the entire study. I owe a great deal to those that encouraged me to continue.

An ancient Chinese myth relates the story of an emperor who commissions a noted sculptor to fashion the emperor's likeness out of a piece of jade from a nearby mountain. After many years, the time to present the sculpture to the emperor finally arrived. Upon revelation of the sculpture, the emperor was dismayed to see, not an image of himself, but a figurine of a flock of birds. Naturally the artist was called to account for the apparent lack of deference to the emperor and nature of the commission. He explained that he had not found the emperor's likeness within the jade but instead had found the image of birds. Pursuit of a scientific investigation is quite analogous to the myth.

The study for my thesis began with the idea that the receptor for NGF would be crystallized and its structure determined. It was quickly realized that in order to maximize the possibilities of success, other neurotrophin receptors and even neurotrophins should be crystallized. After the passage of more than 3 years the proteins had been expressed but no diffracting crystals for any receptor or neurotrophin had been obtained (this study is not contained within the following thesis). This situation caused many difficulties for me and came close to terminating the entire thesis. Fortunately a change of concept resulted in a new study, which has led me to a different interpretation of the interaction of neurotrophins and their receptors than that previously espoused. Hence, like the sculptor, I did not find the structure that was originally sought, but from the trials and tribulations of the study a different and in many ways an equally interesting (if not beautiful) result was obtained.

There have been many individuals with whom I have interacted and who have influenced me over the duration of this thesis study. Firstly I would like to thank my wife Siu Lan who has endured stoically these difficult years and who has been my greatest source of encouragement. Without her, this thesis study would have terminated, without success, years ago. I should also like to thank my mother, Eileen, for her support and whose suffering with Parkinson's disease provided me with the initial incentive to pursue development of molecular solutions for human diseases. Without attempting to apportion any degree of direct influence or contribution to the study, the following individuals are now acknowledged for their help and encouragement:
Chin Shou Huang, Connie Jimenez, Deb Hall, Ken Neet, Ljubica Ivanisevic, Louis Reichardt, Martin Spencer, Pat Sullivan, Peter Hwang, Rainer Marksteiner, Rainer Schneider, Robert Fletterick, Ted Baker, Uri Saragovi, Vladimir Basus and William Mobley. I should like to thank Ted for originating the study and looking at the early drafts I submitted. In particular I should like to thank Pat for carefully reading the final thesis submission and making appropriate comments. Uri has been very supportive of my efforts and has reviewed, prior to submission, the papers resulting from this study.

Finally I would like to thank David Zarling, Pangene Corporation, Eric Hnath and Affinity Sensors. Eric provided much information for the initial phases of the kinetics study and assistance in the checking of data. Affinity Sensors provided, without charge, the biosensor instrumentation necessary to conduct the kinetics study of the interactions of the neurotrophins and their receptors. David provided laboratory space and funding at Pangene Corporation to conduct the kinetics experiments and, in addition, dangled a salary and a fascinating scientific project in front of me, as an incentive to complete the thesis. I might mention that these past two years I have had the good fortune to begin an oncology project at Pangene. The project is, unlike the thesis, proceeding well and has influenced my concepts of small molecule mimetics of proteins, as well as serving to overcome some of the lingering negative effects of the thesis study. Many of the kinetics techniques learned in the thesis study now form the foundations for the development of small molecule inhibitors of DNA repair enzymes, the basis of Pangene's oncology program. Perhaps, in the end it has all been worthwhile.

TABLE of CONTENTS

Abstract.....i
Acknowledgements.....iii
Table of Contents.....v
List of Figures.....viii
List of Tables.....xi
Appendix.....xii
Abbreviations.....xiii

TABLE OF CONTENTS

CHAPTER 1 Neurotrophins and Their Receptors

1.1 Introduction 1
1.2 The Structure of NGF 2
1.3 Basic Residues 3
1.4 Aromatic Residues 4
1.5 Carboxyl Group Modifications 5
1.6 Summary of NGF Residues Implicated in Receptor Binding 5
1.7 Brain Derived Neurotrophic Factor (BDNF) 7
1.8 Neurotrophin-3 (NT-3) 7
1.9 The Trk Receptor 8
1.10 The Immunoglobulin Domains and NGF Binding 14
1.11 The Immunoglobulin-like Domains of TrkA, TrkB and TrkC 17
1.12 A Crystal Structure of NGF and the Immunoglobulin Domain of TrkA 18
1.13 The TrkB Receptor 21
1.14 The Leucine Rich Domain and BDNF Binding 22
1.15 The Immunoglobulin-Like Domains and Neurotrophin Binding 25
1.16 The TrkC Receptor 27
1.17 Neurotrophin Binding Domains of TrkC 27

1.18 The p75 Receptor 28
1.19 Rational for the Thesis Research 32

CHAPTER 2 Trk Receptors, Expression and Purification

2.1 Introduction and Aims 34
2.2 Expression of Proteins in *P. pastoris* with the Vector pPICZαA 41
2.3 Construction of Expression Vectors 41
2.4 Cloning Techniques Following PCR 43
2.5 Transformation of *P. pastoris* strain X33 with trk/pPICZαA 49
2.6 Large Scale Protein Production and Purification 51
2.7 Purification by Ion Exchange Chromatography 53
2.8 Purification of Trk Protein 53
2.9 Protein Expression Results 59
2.10 Expression of Trk Proteins in *E. coli*. 61
2.11 Expression of MBP-fusion Proteins 61
2.12 Expression of Trk Protein Domains as His-tagged Proteins in *E. coli*. 65
2.13 Protein Expression 65
2.14 Protein Quantification 67
2.15 Identification of Recombinant Proteins 67
2.16 Mass Spectrometry 67
2.17 Western Blotting 71
2.18 Nerve Growth Factor Purification 79
2.19 Summary 80

CHAPTER 3 Ultracentrifuge Studies

3.1 Introduction 82
3.2 Methods 85
3.3 Data Analysis 85
3.4 Results 86
3.5 Summary 92

CHAPTER 4 Kinetics

4.1	Introduction	94
4.2	The IAsys Biosensor	94
4.3	Coupling of Trk Proteins to the IAsys Surface	98
4.4	Immobilization Chemistry of Trk Proteins to IAsys Biosensor Surface	100
4.5	Control of Non-Specific Interactions	101
4.6	Binding Data Collection	102
4.7	Definitions of Kinetics Terminology	104
4.8	Data Analysis and Error Propagation	106
4.9a	The Interactions of NGF with TrkA Proteins	113
4.9b	The Interactions of BDNF with TrkB Proteins	122
4.9c	The Interactions of NT-3 with TrkC Proteins	129
4.10	A Comparison of Neurotrophin-Receptor Interaction Studies	131
4.11	Summary	133

CHAPTER 5 Discussion

5.1	Introduction	139
5.2	Recombinant Proteins, Native Proteins and Crystal Structures	140
5.3	Binding Studies and Controls	142
5.4	Binding Data and Trk Receptor Structure	143
5.5	Previous In Vivo and In Vitro Studies of Trk Receptors and Neurotrophins	144
5.6	Protein Immobilization and Kinetics Data	147
5.7	Biosensor Kinetics	148
5.8	Biphasic Kinetics of the NGF-TrkA Interaction	150
5.9	Previously Observed Biphasic Kinetics of the NGF-TrkA Interaction	151
5.10	Neurotrophins and Receptor Structure Influence Kinetics	151
5.11	Mass Transport and Biosensor Kinetics	153
5.12	Biphasic and Monophasic Kinetics Observed by Biosensor	154
5.13	Biosensor Kinetics and Accuracy of Data	154
5.14	The Second TrkA LRR Domain and Ligand-Binding	155
5.15	TrkB and TrkC Biosensor Kinetics	155
5.16	An Hypothesis of Receptor and Ligand Interaction	157

5.17 Multivalency and Structure Changes of Receptor and Ligand 158
5.18 The Effect of Charged Residues on Neurotrophin-Receptor Interactions 160
5.19 Interactions of Trk Receptors and Accessory Proteins 160
5.20 Trk Receptor Ligand-binding Domains; a Role for the LRR Domain 164
5.21 Summary 165

REFERENCES 170

APPENDIX 181

LIST OF FIGURES

CHAPTER 1

Figure 1.1 NGF Structure of NGF 6
Figure 1.2 Model of neurotrophin binding to Trk receptors 9
Figure 1.3 TrkA receptor subdomains 10
Figure 1.4 C-terminal immunoglobulin-like domains of the Trk proteins 17
Figure 1.5 The NGF binding domains of TrkA C-terminal domain 19
Figure 1.6 Interaction regions of NGF with d2 of TrkA 20
Figure 1.7 Interaction Regions of TrkA and NGF 21

CHAPTER 2

Figure 2.1 Trk receptor structure 36
Figure 2.2 Map of pPICZαA 41
Figure 2.3 PCR products for human and rat TrkA extracellular domains 44
Figure 2.4 Agarose gels of the restriction enzyme digests of plasmid DNA 45
Figure 2.5 Gel showing digest of ligated DNA 46

Figure 2.6 Digests of ligated trkA and vector 47
Figure 2.7 Restriction digests of rat TrkA/pPICZαA 48
Figure 2.8 Restriction digests of human TrkA/pPICZαA plasmids 49
Figure 2.9 Expression of TrkA in *P. pastoris* 51
Figure 2.10 First purification step for Trk proteins expressed in yeast 56
Figure 2.11 Second purification step for Trk proteins expressed in yeast 57
Figure 2.12. Third purification step for Trk proteins expressed in yeast 58
Figure 2.13 A coomassie stained SDS-gel of TrkA extracellular domain 60
Figure 2.14 A coomassie stained SDS-gel of the TrkB extracellular domain 60
Figure 2.15 A coomassie stained SDS-PAGE gel of TrkA MBP-fusion proteins 63
Figure 2.16 A coomassie stained SDS-PAGE gel of TrkB MBP-fusion proteins 63
Figure 2.17 Gel of His-tagged protein expression in *E. coli*. 66
Figure 2.18 MALDI-TOF analysis of an MBP-fusion protein 69
Figure 2.19 SDS-PAGE and electrotransfer for the Western Blots 72
Figure 2.20 Antibody control gels 73
Figure 2.21 Western blot of TrkA MBP-fusion proteins 74
Figure 2.22 Western blot of TrkA MBP-fusion proteins 74
Figure 2.23 Western blot of TrkA MBP-fusion proteins 75
Figure 2.24 Western blot of TrkB MBP-fusion proteins 75
Figure 2.25 Western blot of TrkB MBP-fusion proteins 76
Figure 2.26 Western blot of TrkB MBP-fusion proteins 76
Figure 2.27 Western blot of TrkC MBP-ED protein 77
Figure 2.28 Western blot of TrkA and TrkB proteins expressed in *P. pastoris* 77
Figure 2.29 A coomassie stained gel of purified NGF 80

CHAPTER 3

Figure 3.1 Absorbance and statistical data TrkA ED 87
Figure 3.2 Absorbance and statistical data TrkA Ig-like Domain 87
Figure 3.3 Absorbance and statistical data TrkA Ig-like Domain 88

CHAPTER 4

Figure 4.1 The arrangement of the IAsys 97
Figure 4.2 Immobilization chemistry 100
Figure 4.3 Buffer experiment 101
Figure 4.4 IAsys plot showing typical association/dissociation data 102
Figure 4.5 Association curves 106
Figure 4.6 Association rate 107
Figure 4.7 Binding rate fit 108
Figure 4.8 Dissociation rate fit 108
Figure 4.9 Association rate of neurotrophins for Trk proteins 111
Figure 4.10 Dissociation rate of neurotrophins 111
Figure 4.11 Bar plot of TrkA-NGF reaction data 119
Figure 4.12 Association rates of individual TrkA domains 120
Figure 4.13 Dissociation rates of individual TrkA domains 121
Figure 4.14 Bar plot of TrkB-BDNF reaction data 126
Figure 4.15 Association rates of individual TrkB domains 127
Figure 4.16 Dissociation rates of individual TrkB domains 128
Figure 4.17 Bar plot of TrkC-NT-3 reaction data 130

CHAPTER 5

Figure 5.1 Hypothetical Model for Trk-Neurotrophin interactions 163

LIST OF TABLES

CHAPTER 1

Table 1.1 Binding data of NGF, BDNF and NT-3 binding to p75 receptor 29

CHAPTER 2

Table 2.1 TrkA extracellular domains expressed as MBP-fusion proteins 37
Table 2.2 TrkA extracellular domains expressed as His-tagged proteins 37
Table 2.3 TrkA full-length extracellular domain expressed in yeast 38
Table 2.4 Synthetic human TrkA peptide 38
Table 2.5 TrkB extracellular domains expressed as MBP-fusion proteins 38
Table 2.6 TrkB extracellular domains expressed as His-tagged proteins 39
Table 2.7 TrkB full-length extracellular domain expressed in yeast 39
Table 2.8 Synthetic human TrkB peptide 39
Table 2.9 TrkC extracellular domains expressed as MBP-fusion proteins 40
Table 2.10 TrkB full-length extracellular domain expressed in yeast 40
Table 2.11 Synthetic human TrkB peptide 40
Table 2.12 Expression level of purified Trk proteins 59
Table 2.13 Approximate expression levels of the MBP-fusion proteins 64
Table 2.14 Mass Spectrometry of MBP-fusion protein tryptic digests 70

CHAPTER 3

Table 3.1 Approximate molecular weights of Trk and neurotrophin proteins 89
Table 3.2 Protein solution stoichiometry 90

CHAPTER 4

Table 4.1 Protein immobilization levels on the biosensor surface 99
Table 4.2 TrkA LRR2 synthetic peptide, association and dissociation rates 113

Table 4.3 TrkA MBP-LRR2, association and dissociation rates 113
Table 4.4 TrkA MBP-LRR, association and dissociation rates 114
Table 4.5 TrkA MBP-C1LRR12, association and dissociation rates 114
Table 4.6 TrkA MBP-LRR23C2, association and dissociation rates 114
Table 4.7 TrkA MBP-C1LRR, association and dissociation rates 115
Table 4.8 TrkA MBP-LRRC2, association and dissociation rates 115
Table 4.9 TrkA Ig-like domain, association and dissociation rates 116
Table 4.10 TrkA Ig-like domain, association and dissociation rates 116
Table 4.11 TrkA MBP-ED, association and dissociation rates 117
Table 4.12 TrkA ED (*P. pastoris*), association and dissociation rates 117
Table 4.13 TrkA ED (insect cells), association and dissociation rates 117
Table 4.14 Values of the equilibrium dissociation constant for TrkA proteins 118
Table 4.15 TrkB LRR2 synthetic peptide, association and dissociation rates 122
Table 4.16 TrkB MBP-C1LRR, association and dissociation rates 122
Table 4.17 TrkB MBP-LRRC2, association and dissociation rates 123
Table 4.18 TrkB MBP-C1LRRC2, association and dissociation rates 123
Table 4.19 TrkB MBP-Ig-like domain, association and dissociation rates 124
Table 4.20 TrkB MBP-ED, association and dissociation rates 124
Table 4.21 TrkB ED (*P. pastoris*), association and dissociation rates 125
Table 4.22 Values of the equilibrium dissociation constant for TrkB proteins 125
Table 4.23 TrkC LRR2 synthetic peptide, association and dissociation rates 129
Table 4.24 TrkC MBP-ED, association and dissociation rates 129
Table 4.25 Values of the equilibrium dissociation constant for TrkC proteins 129
Table 4.26 A comparison of the equilibrium binding constants 132

APPENDIX

NGF sequence 181
BDNF sequence 181
TrkA (rat) sequence 182
TrkA (human) sequence 183
TrkB (rat) sequence 184
TrkB (mouse) sequence 185
TrkB (human) sequence 186
TrkC (rat) sequence 187

TrkC (human) 188
Neurotrophin Domains I-VII 190
Molecular Weights of MBP-fusion proteins 191
Charged Residues on the surfaces of neurotrophins 192

ABBREVIATIONS

Relevant Abbrevaitions to material in the text are given within the body of the material and in footnotes.

K_D	Equilibrium Dissociation Constant
µM	Micromolar
mM	Millimolar
nM	Nanomolar
K_D	Equilibrium Dissociation Constant
K_{off}	Dissociation Rate
K_{on}	Association Rate
BDNF	Brain Derived Growth Factor
CNS	Central Nervous System
MBP	Maltose Binding Protein
NGF	Nerve Growth Factor
NTF	Neurotrophic Factor
NT-3	Neurotrophin-3
PNS	Peripheral Nervous System
Trk	Receptor for NTF's

CHAPTER 1 NEUROTROPHINS AND THEIR RECEPTORS

1.1 Introduction

Neurotrophic Factors (NTFs) are proteins that appear to be necessary for the survival and development of neurons. These molecules are found throughout the mammalian peripheral and central nervous systems. Target neurons synthesize and release NTF's, which are then taken up by specific receptors on projecting neurons. Cell survival, growth and differentiation are demonstrated actions associated with NTFs. In the developing nervous system regulation and refinement of synapses by NTFs model the precise series of projections that constitute the mature nervous system (Barde 1988, Cowan et al. 1984, Hefti et al. 1989, Roback et al. 1992). Neuronal and synaptic plasticity, as well as neuronal survival, appear to be other activities associated with these molecules (Hefti 1986, Williams et al. 1986, Krommer et al. 1987, Roback et al. 1992, Thoenen 1995). Because of their diverse actions in the promotion of neuronal survival, NTF's have been considered for some time as possible therapies for such neurodegenerative disorders as Alzheimer's, Huntington's and some forms of Parkinson's diseases (Yuen and Mobley 1996).

One significant problem associated with the application of neurotrophins as a therapy, is molecular size. The blood-brain barrier prevents administration of neurotrophins orally or intravenously and hence they can only be dispensed by intracerebroventricular infusion, which carries a significant risk of infection and pericannular tissue necrosis. A possible solution to this problem is development of small molecule mimics of specific neurotrophins; molecules small enough to cross the blood-brain barrier. In order to develop these small molecules, a number of studies are presently underway to elucidate the structures of the neurotrophins, their receptors and the interactions between them. A number of NTF's have been identified and these include nerve growth factor (NGF), brain-derived neurotrophic factor (BDNF), neurotrophin-3 (NT-3), neurotrophin-4/5 (NT-4/5), ciliary neurotrophic factor (CNTF), glial cell line-derived neurotrophic factor (GDNF) and fibroblast growth factor (FGF).

Distinct neuronal populations are acted upon by different neurotrophins. All neurotrophins appear to act upon neurons through receptors, particularly those found at the axon foot. Specific receptors have been identified for NGF, BDNF and NT-3. These receptors contain a tyrosine kinase functional element that phosphorylates accessory proteins to activate signal transduction pathways within the neuron, upon the binding of an appropriate neurotrophin. In particular the receptors for NGF, BDNF and NT-3 are designated as TrkA, TrkB and TrkC respectively. There exists some promiscuity in receptor binding by neurotrophins; for example, NT-3 will bind with lowered affinity to both TrkA and TrkB. In addition to TrkA, NGF will bind with lowered affinity to another receptor, namely, p75 as will both BDNF and NT-3 (Kaplan et al. 1991, Klein et al. 1991, Thoenen 1991, Ip et al. 1993, Raffioni 1993, Dechant et al. 1994, Klein 1994, Huang and Reichardt 2003).

Signaling pathways are assumed to activate a cascade of events that promote cell survival and growth (Kaplan and Miller 2000). Recent experiments suggest that in addition to initiation of an intra-cellular signaling pathway, the neurotrophin receptor is internalized. After internalization, the receptor-neurotrophin complex is transported to lysosomes where lowered pH induces separation, followed by the recycling of the receptor to the cell surface. Some evidence exists to suggest that neurotrophin molecules are transported by microtubules to the cell body where they may mediate their actions (Grimes et al. 1996).

1.2 The Structure of NGF

NGF purified from mouse submandibular glands has been crystallized and an X-ray structure obtained with a resolution of 2.3 Å (McDonald et al. 1991). The topology of NGF shows that the molecule consists of seven β-strands, which contribute to three antiparallel pairs of twisted β-strands with the extended structure locked by a "cysteine knot" of three disulfide bridges (McDonald et al. 1991). Several regions of the structure show little or no electron density. These poorly defined regions include residues 1-10 (amino terminus) and residues 112-118 (carboxy terminus). These two regions are susceptible to proteolysis, are flexible and solvent accessible. Several regions that are also poorly defined include residue 43 and residues 76-79. An average temperature factor of 34 $Å^2$, indicates a flexible structure (McDonald et al. 1991). Two protomers

assemble about a two-fold axis to form the NGF dimer. The long axes of the two protomers are approximately parallel and their flat faces are in contact at the dimer interface. Protomer contacts are generally hydrophobic and are localized to three regions (McDonald et al. 1991).

1.3 Basic Residues

A clustering of positively charged residues occurs close to and around the β-hairpin Asp30-Lys34 of NGF. This region may have a role in binding NGF to the acidic p75 receptor (Radeke et al. 1987). At the "top" of the molecule, is a cluster of 4 of the 8 lysine residues found in NGF (murine). Of this lysine cluster, Lys32 is conserved in all NGF's (except platyfish) and Lys34 is conserved in all NGF's (except snake and mastomys), but neither is conserved in BDNF or NT-3. Other basic residues are also highly conserved. For example Lys25 is conserved in all neurotrophins except NT-5. In NT-5, Lys25 is replaced by an arginine, which forms a hydrogen bond to the buried Glu55. Lys95 is not well conserved. Other lysines, Lys57, Lys74 and Lys115 (not defined in the crystal structure) are all well conserved in the neurotrophin family.

Substitution of individual lysine residues has shown that Lys32, Lys34 and Lys95 are probably involved in interactions with p75 (Ibanez et al. 1992), as determined by binding studies with cells that express p75, TrkA (or both) and neurite differentiation in PCI2 cells. NGF (murine) contains 7 arginine residues that are well conserved in the neurotrophin family and generally found on the surface of the molecule. In mouse NGF, Arg69 is hydrogen bonded to Asp16 and also forms a hydrogen bond to the conserved Thr91. Modification of these two arginine residues resulted in significant loss of biological activity that could only be partially reversed, indicating that the arginine residues in question are buried within the molecule (Ibanez et al. 1992).

Two arginines, namely those at positions 69 and 100 are involved in internal hydrogen bonding to Asp16 and Thr91 respectively. Site directed mutants of Arg100 and Arg103 whose side chain hydrogen bonds to the carbonyl of Asp30, have been made (Ibanez et al. 1990). From mutation studies, these arginine residues appear to play a structural role and are also directly involved in receptor interactions. Two of the four histidine residues

found in NGF (murine), are located in the first 8 residues of the N-terminus. Since the N-terminal region of NGF is not visible in the crystal structure, the effect of changing these histidines on the conformation of the N-terminus, are indeterminable. The residue His75 (conserved in all neurotrophins except *Xenopus*) is found on the surface of the molecule and is hydrogen bonded to Asp72 (conserved in all neurotrophins). While this histidine residue is likely to stabilize the molecule, the effect site that directed mutations of surface residues have on stability, is probably minimal (Eriksson et al. 1987, Heinz et al. 1993) and hence the contribution to the structure of NGF by His75, is difficult to assess.

Chemical modification of histidine residues results in loss of binding of NGF to rabbit superior cervical ganglia (Dunbar et al. 1984), without apparent conformational change, as judged by fluorescence spectroscopy. These results and the reversibility of the effects of chemical modification, suggest that one or both histidines are involved in receptor binding. Ibanez et al. (1993). Studies have shown that His84 is a constituent of the TrkA binding region of NGF and that Glu84 in BDNF is an element of the TrkB binding region of BDNF. Replacement of His75 or His84 with alanine, results in decreased affinity for TrkA. However, the H75A mutant shows a 5-fold increase in affinity for p75 (Woo and Neet 1996). Simultaneous replacement of both His75 and His84 with alanine was neither additive nor synergistic. Circular dichroism spectra and weakened self-association of the mutants, suggest that His75 and His84 may be involved in the stability, dimerization and/or folding of NGF (Woo and Neet 1996). Chemical modification of histidine residues, His4 and His8 in the H75A/H84Q double mutant resulted in abolishing neurite outgrowth, binding to both p75 and TrkA and phosphorylation of TrkA in PCl2 cells. These results suggest that at least His75 and His84, if not all histidines, although located in three distinct regions, contribute to the maintenance of functional sites necessary for the receptor binding and activity of NGF (Woo and Neet 1996).

1.4 Aromatic Residues

Aromatic residues found in mouse NGF include 2 tyrosine residues and 3 tryptophan residues all well conserved within the neurotrophin family. Adjacent to the dimer interface, Tyr52 is involved in aromatic packing and makes contact with Phe101 of the other protomers. In each protomer, Tyr79 packs against Val111, but is in a position to interact with the N-terminus of the second protomer. The environment of Tyr79 is not well

defined in the crystal structure. Chemical modification of the tyrosine residues does not affect receptor binding or biological activity. All 3 tryptophan residues are involved in aromatic stacking at the dimer interface.

Site directed mutagenisis of NGF tryptophan residues was used to produce mutants (Drinkwater et al. 1991). These mutants retained full biological activity but showed a substantial decrease in binding to p75. It is possible that the mutations result in alterations of the subunit interface, a possible binding region for p75. Additional site directed mutants in which each tryptophan was replaced by phenylalanine, showed full biological activity and receptor binding (Ibanez et al. 1990), suggesting that the native NGF structure tolerates aromatic residue replacement.

1.5 Carboxyl Group Modifications

NGF (murine) has 12 side chain carboxyl groups, from Asp and Glu acid side chains, but none appear to be directly involved in receptor binding. There are three Asp residues with known structural roles; Asp16 (side chain) hydrogen bonds to Arg69, Asp72 (side chain) hydrogen bonds to His75 and Asp30, which stabilizes the 30-34 loop. One residue, Glu55 which hydrogen bonds to Lys25 plays a structural role in the molecule and is conserved in all neurotrophins. Chemical modifications of 4-5 of the 12 carboxyl groups has no effect on receptor binding or biological activity, suggesting that carboxyl groups do not play an important role in receptor binding. Ibanez et al. (1990, 1992) constructed mutants in which Asp 24, Asp 30 and Glu 30 were replaced with alanine residues. A 75% reduction in receptor binding and biological activity was found for the first mutant (Asp 24), however, little effect on receptor binding or biological activity was observed for the second and third mutants.

1.6 Summary of NGF Residues Implicated in Receptor Binding

A number of amino acids, in particular, residues 1-11, 21-25, 28-38, 40-49, 53-54, 72, 75, 76, 79-88, 93-99 and 102, have been implicated in determining the receptor specificity and the biological activity of NGF (Ibanez 1994, 1995, 1998, 2002, Ibanez et al. 1990,

1991, 1993, Bradshaw et al. 1994, Woo et al. 1995, Woo and Neet 1996, Guo et al. 1996, Saragovi et al. 1998, Woo et al. 1998). So many residues appear to be involved that it may be hypothesized that overall conformation of the NGF molecule is more important for binding and activity, than short "active site" like elements (Ibanez et al. 1993, Prof. W. C. Mobley, Stanford University, personal communication).

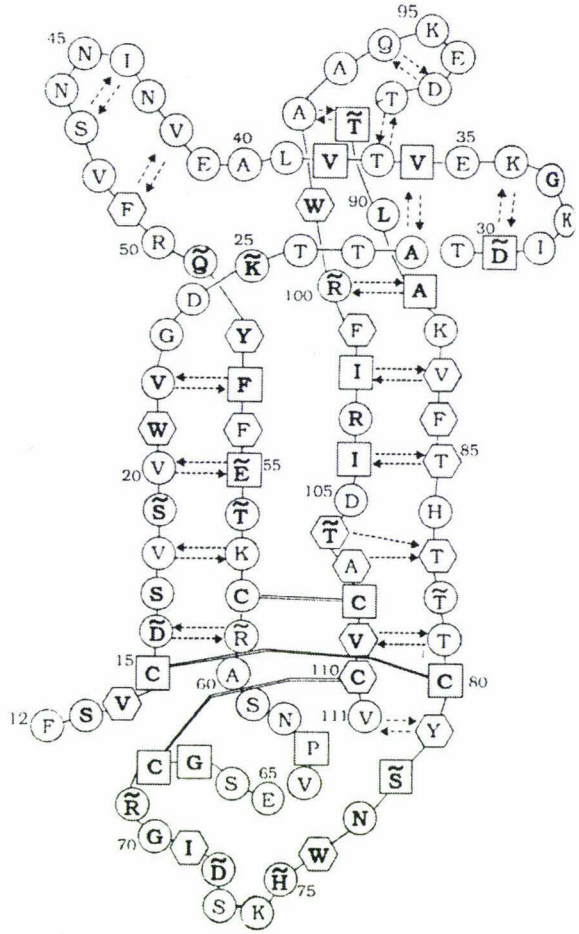

Figure 1.1 The amino acid structure of NGF. From McDonald et al. 1991.

Resides shown in bold, represent those conserved in all NGF and NGF related sequences. Squares represent buried residues in the β-NGF subunit, with a side chain solvent accessibility of < 7%. Hexagons represent residues involved in the dimer interface. The amino acid sequence of β-NGF is given in Appendix I.

1.7 Brain Derived Neurotrophic Factor (BDNF)

BDNF is a 120 amino acid polypeptide that has approximately 50% identity to NGF at the primary structure level. Biological responses to BDNF are mediated by the TrkB receptor, which like TrkA is a tyrosine kinase linked second messenger system. A number of TrkB transcripts encode truncated proteins that have no tyrosine kinase domains, which suggests that the binding of BDNF to TrkB receptors may or may not result in signaling events. BDNF also binds to the low affinity receptor, p75. The importance of BDNF and TrkB in the developing nervous system is evident in the extensive loss of sensory neurons in mice in which the genes for BDNF or TrkB are disrupted. In TrkB deficient mice, there is a loss of spinal cord and facial motor neurons (Yuen and Mobley, 1996). Unlike NGF, no crystal structure has been published of the BDNF homodimer, however the structure of a BDNF/NT-3 heterodimer, has been solved to a resolution of 2.3 Å. Compared with NGF only a few amino acids have been identified as being important in binding to the TrkB receptor; these include: residues 26-35, 45-49, 79-88, Lys95, Lys96, Arg97 (Ibanez 1995).

1.8 Neurotrophin-3 (NT-3)

As with NGF and BDNF, NT-3 has a specific tyrosine kinase receptor (TrkC) to which it binds with high affinity. The low affinity receptor for NGF and BDNF, p75 also binds NT-3. NGF and BDNF bind with high affinity to TrkA and TrkB respectively, however, NT-3 also binds, but with diminished affinity to both TrkA and TrkB. All neurotrophins bind as homodimers to their receptors. Both NT-3 and TrkC are widely expressed in the Central and Peripheral Nervous Systems (Barbacid 1994). An X-ray structure of NT-3 has been published (Butte et al. 1998). Residues implicated in binding to the TrkC receptor include: Arg8, Glu10, Tyr11, Asp15, Thr22, 39-48, Tyr51, Glu54, Arg56, Lys80, Gin83, Arg103 (Ibanez 1995).

Alignment of the sequences of NGF, BDNF and NT-3 show that there are seven regions of high sequence variation, namely, the N and C-termini and the regions I-IV[1] (Ibanez et al. 1991, Robinson et al. 1995). Of these variable regions, only two result in large structural differences between the protomers of NGF, BDNF and NT-3 (Robinson et al. 1995). Region I of BDNF differs

[1] See Appendix II for definitions of these regions.

from the same region of NGF and NT- 3 by having a two amino acid insertion as a result of formation of a turn of an α-helix (Robinson et al. 1995). In BDNF, region III has no sequence insertions or deletions, but does include a stretch of 3_{10} helix. Superposition's of the α-carbon backbone structure of the neurotrophin molecules shows that NT-3 is structurally similar to NGF. For BDNF and NGF, there is a root mean square correlation of 1.22 Å (Robinson et al. 1995). In the BDNF/NT-3 heterodimer, the 2-fold axis of NGF is for the most part retained.

Neurotrophin residues implicated in Trk binding do not form a spatially distinct cluster on each protomer. In the dimeric form, variable regions I and V of one protomer are in close proximity to variable region II of the other protomer. Both protomers may contribute to each receptor-binding site (Ibanez et al. 1992, Robinson et al. 1995).

1.9 The TrkA Receptor

Neurotrophin receptors are believed to act and have a domain structure as depicted below (Figure 1.2 and Figure 1.3). The neurotrophin-binding domain remains controversial at this time with a number of studies suggesting that neurotrophin binding is possible to either the Leucine Rich Region or Immunoglobulin-like domains.

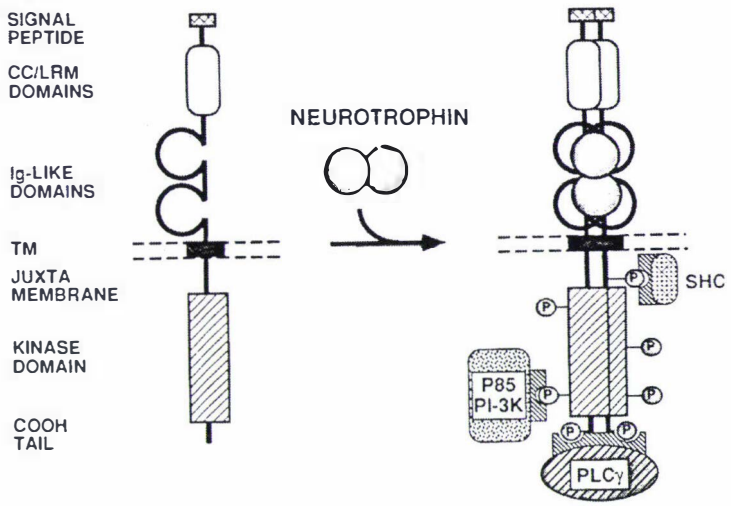

Figure 1.2 A model of neurotrophin binding to and activation of Trk receptors. From Barbacid 1994.

The receptor consists of a cysteine rich cluster (designated as CC in the diagram), a Leucine Rich Motif (designated as LRM), two immunoglobulin-like domains (Ig-like), a short transmembrane domain (TM) and an intracellular kinase domain. Upon binding neurotrophin, the Trk receptor dimerizes, autophosphorylation of Tyr residues occurs. This event is followed by the binding of intracellular downstream signaling proteins such as PLCγ, PI-3 kinase, P85 and SHC, which bind to the phosphotyrosines (Huang and Reichardt 2003).

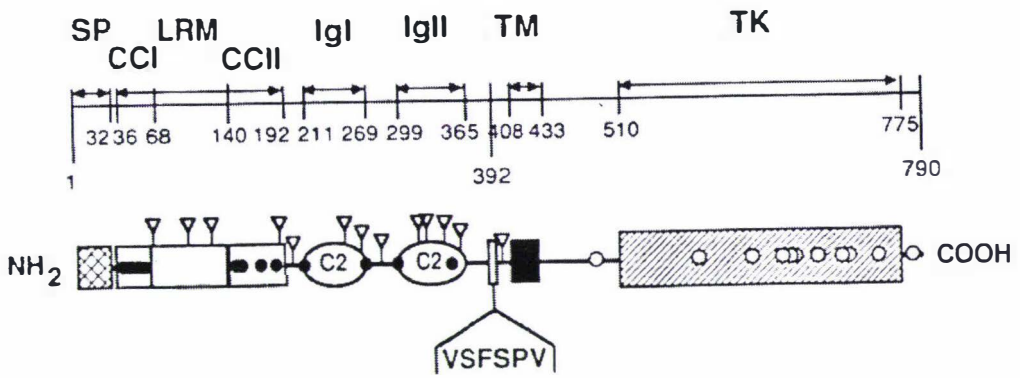

Figure 1.3 TrkA receptor subdomains. From Barbacid 1994.

As shown in Figure 1.2, Trk receptors consist of various domains. These domains include; the signal peptide (SP), two cysteine clusters (CCI and CCII), the leucine-rich motifs (LRM), two Ig-like-like regions (IgI and IgII), the transmembrane region (TM) and the tyrosine kinase region (TK). Six amino acids (VSFSPV) are found only in the neuronal-specific isoform of the receptor. Putative N-linked glycosylation sites are indicated by inverted triangles. Filled circles represent cysteine residues in the extracellular domain. Open circles represent cysteine residues in the intracellular domain. Closed circles represent Tyr residues in the extracellular domain. The amino acid residue numbers flanking each structural motif correspond to the nonneuronal Trk receptor. Sequences and structural domains for all Trk receptors are provided in Appendix I.

Two isoforms of 790 and 796 amino acids are presently known for the high affinity tyrosine kinase receptor for NGF (Martin-Zanca et al. 1989, Barker et al. 1993, Barbacid 1994). Both Trk A receptor isoforms have the structure of typical tyrosine kinase cell surface receptors, in that they consist of a signal peptide, an extracellular region that interacts with NGF (and NT-3), a single transmembrane domain and a cytoplasmic region that includes the catalytic tyrosine kinase domain (Meakin and Shooter 1992, Barbacid 1994). The two isoforms differ in the extracellular domain, in that, near the transmembrane region, there is a difference in the 6 amino acid residues, VSFSVP (Barbacid, 1994). Cells of neuronal origin primarily express the 796 amino acid isoform, while cells of non-neuronal origin express the truncated 790 amino acid form (Barker and Shooter 1994, Barbacid 1994).

A number of distinct regions are found in the extracellular domain. These include, three tandem repeats of 24 residues flanked by two cysteine clusters (CCI and CCII). Two immunoglobin like domains (Ig1 and Ig2) are located between the second cysteine cluster and the transmembrane domain. The receptor spans the cell membrane with a short sequence of 25 residues. Features unique to the cytoplasmic domain of the neurotrophin receptors include T647 instead of the alanine residue in the highly conserved HRDLAARN kinase motif found in many other tyrosine kinase receptors (Barbacid 1994). High affinity neurotrophin receptors differ from other tyrosine kinases in their kinase domains by having a tryptophan residue, W722. This residue occurs in place of the tyrosine found in the WEXXXXXXXPY sequence and P766 is replaced in the CWXXXXXXRP sequence near the C-terminus of the kinase domain (Barbacid 1994). A short carboxy-terminal tail of 15 amino acids includes a conserved tyrosine residue (Martin-Zanca et al. 1989, Barbacid, 1994).

The leucine rich domain has three leucine rich repeats (LRR's) that are short sequence motifs typically consisting of 24 residues. A number of proteins that have diverse function and cellular locations have been shown to contain LRR's. From the consensus sequences of many proteins that contain the LRR motif, the general arrangement LRR's suggests that they are usually present in tandem and the number of this motif ranges from one, as found in platelet glycoprotein, to 30, found in chaopin (Kobe and Deisenhofer 1994). The crystal structure of the porcine ribonuclease inhibitor protein (RI), which contains 15 alternating LRM's of 28 or 29 residues, has been determined (Kobe and Deisenhofer 1991). In the RI protein, the LRR structure consists of units, arranged such that they form a parallel β-sheet with one surface exposed to solvent. In addition, the protein adopts an unusual globular shape.

It has been suggested that the structure of the LRR's in RI is representative of the LRR motif in other proteins (Kobe and Deisenhofer 1991). Those residues that play a key structural role in RI, in particular those that cluster around the β-strand region are conserved throughout the LRR superfamily. While the LRR's found in RI are among the largest found in the superfamily, it is possible that shorter repeats in other proteins may adopt a similar conformation. The amino terminal structural repeat in RI contains only 25 residues but displays the same conformation as that found in longer repeats (Kobe and Deisenhofer 1991, 1994). In contrast to the structure of RI, a recent LLR has been reported in a protein from the microorganism Azobacter vinelandii. This protein, LRR variant, has a novel fold consisting of alternating 3_{10}-helices arranged in a right handed superhelix and having a complete absence of any β-sheet (Peters et al. 1996).

All three Trk receptors contain 3 LRR's consisting of 24 residues each and hence may adopt the conformation seen in the N-terminus of RI. Many proteins that contain the LRR motif also have homologous regions flanking the LRR domain. These homologous regions are characterized by four similarly spaced cysteines in a stretch of about 20 amino acids for the amino-terminal flanking region and about 50 amino acids flanking the carboxyl-terminal flanking region (Rothberg et al. 1990, Fischer et al. 1991, Kobe and Deisenhofer 1994).

All LRR containing proteins appear to be involved in protein-protein interactions or transduction pathways (Kobe and Deisenhofer, 1994). It is therefore possible that the LRR provides a structural motif for the number of specific molecular interactions. The non-globular shape of the motif may facilitate protein binding to LRR's because the large surface area may result in more protein-protein interaction and increased affinity. A large surface area may interact readily with small globular proteins. The neurotrophin structure, as determined for the NGF homodimer, a BDNF/NT-3 heterodimer and an NT-3 homodimer, is relatively compact and somewhat globular and hence may interact with the extensive LRR surface of a Trk receptor. Protein binding by a LRR may be facilitated by the large exposed surface of the parallel β-sheet structure. In the interior of proteins, parallel β-sheet structure is common and helices and other parallel β-sheet pack against them. For LRR containing proteins, it has been proposed that the binding of a ligand to the LRR substitutes for the packing interaction of interior β -sheet (Kobe and Deisenhofer 1994).

NGF binding to the LRR's and Ig-like domains of TrkA has been studied by expression of these two distinct regions along with the entire extracellular domain and variations of the LRR, in *Escherichia coli* (Windisch et al. 1995a, b, c). The proteins were expressed as recombinant maltose binding MPB-TrkA fusion proteins. Binding assays utilizing iodinated NGF were conducted and rates of association and dissociation were measured with the entire extracellular domain, the three LRRS, various combinations of the LRR's and the two Ig-like-like domains. In this study the complete extracellular domain has an equilibrium dissociation constant $K_D = \sim 10^{-9}$ M. The Ig-like domains however, showed no binding of NGF. The complete LRR region (three 24 residue repeats, L1, L2 and L3) including the flanking cysteine regions, showed a $K_D = \sim 10^{-9}$ M. Deletion of the flanking cysteine regions had no effect on binding NGF and this construct had the same K_D as the protein encompassing the three LRR's and flanking cysteine regions. Two proteins, (1) N-terminal cysteine (CI) through the second LRR (L2) and (2) C1[2] to the center of L2 both showed the same K_D as the entire extracellular domain. Two additional proteins (1) C-

[2] Depicted as CI in Figure 1.3

terminal cysteine (C2)[3] through L2[4] and (2) C2 to the center of L2 had the same K_D as the entire extracellular domain. These results suggest that the equilibrium dissociation constant for NGF binding to TrkA can be accounted for neurotrophin binding to the second LRR (L2) only (Windisch et al. 1995a, b, c). Binding measurements of NGF to the L2 protein showed the same K_D as measured for the entire extracellular domain.

In a study of the binding of BDNF to the nine MBP-fusion proteins (Windisch et al. 1995a), produced for TrkA, none showed detectable BDNF binding. For four TrkA fusion proteins, the entire extracellular domain, the two immunoglobin like domains, C1L1-3C2 and L1-3, no binding of NT-3 was observed. In addition to the extracellular domains of TrkA, the entire extracellular domain, the two Ig-like-like domains and the domain encompassing the three LRR's and flanking cysteine regions (C1L1-3C2) of TrkB were expressed in *E. coli* as maltose fusion proteins. Binding studies with these TrkB derivatives showed no binding of BDNF to the immunoglobin domain protein. BDNF did bind to the C1L1-3C2 and the entire extracellular domain proteins with a $K_D \sim 1x10^{-9}$ M. No binding of NGF was observed for any of the TrkB proteins, however NT-3 binding was however observed with the C1L1-3C2 and entire TrkB extracellular domain proteins.

An alignment of L2 regions for mammalian TrkA and TrkB reveals the consensus sequence for this domain:

TrkA (rat)	TIVKSGLRFVAPDAFHFTPRLSHL
TrkB (rat)	TIVDSGLKFVAYKAFLKNGNLRHI

The two sequences are 54% identical and as a consequence only 11 residues seem to account for the ligand binding specificity seen for TrkA and TrkB (Windisch et al. 1995a, b, c). The results of this study suggest that the binding of neurotrophins to their receptors may be quite localized and at least require the second leucine repeat region of the receptor for binding. That the second LRR showed full NGF binding but no binding of BDNF or NT-3 suggests that this domain is able to exert neurotrophin-binding specificity.

Scatchard plot analysis of the equilibrium binding of NGF to the recombinant second LRR domain showed that the kinetics of association of the second LRR with NGF is complex, with apparent biphasic kinetics. At low NGF concentrations (0.4 to 5 pM), the relationship between the observed

[3] Depicted as CII in Figure 1.3
[4] The leucine rich region, LRR consists of 3 domains, referred to as L1, L2 and L3

association rate and ligand concentration is linear, resulting in a K_{on}[5] of ~$1x10^{7}$ M^{-1} s^{-1}. At ligand concentrations approaching the K_D (~$1x10^{-9}$ M), a situation of negative cooperativity occurred. This resulted in a linear relationship between the observed association rate and NGF concentration and in a second K_{on} of ~ $3x10^{5}$ M^{-1} s^{-1} (Windisch et al. 1995a, b, c). For the entire recombinant extracellular domain, similar complex association kinetics was seen and two K_{on} values of ~ $7x10^{6}$ M^{-1} s^{-1} and ~ $2x10^{5}$ M^{-1} s^{-1} were measured.

From studies of the LRR's and Ig-like-like domains of TrkA and of TrkB, it appears that the specific binding of NGF to the second LRR of TrkA is established. Binding studies of NGF to receptors expressed in whole cells provide a number of equilibrium dissociation constants that vary between ~$1x10^{-9}$ M and ~ $1x10^{-11}$ M depending upon the type of cell used. It is difficult to ascribe binding in whole cell studies to binding of neurotrophin to only one receptor. The surfaces of cells are poorly understood and characterized and it is difficult to understand why TrkA binding of NGF to TrkA expressed by one cell type should show dramatic differences from NGF binding to TrkA expressed by another cell type. Hence the binding of NGF to specific isolated domains of the Trk receptor, while admittedly an artificial system, seems to offer a means of determining which domains of the receptors may be involved in binding. In addition to binding studies with the isolated domains of TrkA, the second LRR of TrkA appears to be further implicated in NGF binding by experiments in which this peptide resulted in degradation of NGF dependent neurons in the rat brain (Windisch et al. 1995a, b, c).

1.10 The Immunoglobulin Domains and NGF Binding

Comparative sequence analysis of the conserved regions of the extracellular domain of TrkA shows the presence of a combination of cell adhesion motifs corresponding to the conserved regions (Schneider and Schweiger 1991). The three LRR's share significant sequence homology with the *toll* gene product of Drosophila that mediates specific cell adhesion events. An additional significant region found in the extracellular domain of the neurotrophin receptors, consists of two repeats of the immunoglobin-like C2 type. These repeats are similar to those found in the neural cell adhesion molecules (N-CAMs) and in platelet-derived growth factor receptor (PDGFR) tyrosine kinase family (Schneider and Schweiger 1991, Zaccaro et al. 2001). It has been suggested that the two Ig-like domains, because they are located in close the proximity to the

[5] For definitions of Kinetics terminologies, see Chap 4.

membrane, may interact with other membrane bound proteins; in particular the low affinity NGF receptor, p75 (Schneider and Schweiger 1991).

In a study of the Ig-like domains of TrkA maltose fusion protein expressed in *E. coli* and secreted into the periplasm, no binding affinity for NGF was observed, leading to a hypothesis that NGF interaction with the receptor could be accounted for by neurotrophin binding to the LRR of TrkA exclusively (Windisch et al. 1995a, b, c). More recently, a similar study (Holden et al. 1997) showed that the recombinant Ig-like domain, expressed in *E. coli* as an N-terminal His-tagged protein bound NGF with nM affinity. Studies using radiolabeled NGF (Holden et al. 1997) showed that the refolded protein bound NGF and inhibited the effects of NGF on A 875 cells *in vivo*. *In vivo* inhibitory effects were observed for the Ig-like domains both as isolated protein and when bound to NGF. These results suggest that the lack of NGF binding to the Ig-like domains in the earlier studies (Windisch et al. 1995a, b, c) was a consequence of the incorrect folding of the Ig-like domains during export to the periplasm (Holden et al. 1997).

At least two recent studies (Perez et al. 1995, Urfer et al. 1995) have implicated the Ig-like domains of the TrkA, TrkB and TrkC receptors in neurotrophin binding. Ten chimeric receptors were constructed in which both cysteine clusters flanking the LRR's and Ig-like domains, were exchanged between the TrkA and TrkB receptors (Perez et al. 1995). The chimeric receptors were expressed in 293 cells (human fetal kidney cell line) and the binding of radiolabeled NGF to the receptors was measured. In cells that expressed the chimeric receptor in which the N-terminal cysteine cluster of TrkB replaced the N-terminal cysteine cluster of TrkA, but retained the Ig-like domains of the TrkA receptor, almost identical binding of NGF was observed to that seen for native TrkA expressed in 293 cells. For the chimeric receptors in which the two Ig-like domains of TrkA were exchanged for the same domains of TrkB, NGF binding similar to that for native TrkA receptors was observed. These results suggest that neurotrophin affinity and specificity is inherent in and dependent only on, the Ig-like domains of the neurotrophin receptors. Other chimeric receptors had NGF binding that varied between zero and ~ 60% of that of the native TrkA receptor.

Those chimeric receptors, in which the cysteine clusters of TrkA and TrkB were interchanged while retaining the Ig-like domains of TrkB, when expressed in 293 cells, showed no NGF binding. Similarly, receptors with cysteine clusters and the N-terminal TrkA Ig-like domain interchanged with those of TrkB, showed no NGF binding ability. These results suggest that the

C-terminal Ig-like domain is responsible at least in part for NGF recognition and binding. One chimera, which retained the entire extracellular domain of TrkA and the intracellular domain of TrkB, showed less than 40% of the NGF binding ability of native TrkA (Perez et al. 1995, Urfer et al. 1995). However, since 293 cells are constitutively active and poorly characterized it is difficult to interpret the experimental results, which call into question the assignment of neurotrophin binding and specificity to the Ig-like domain.

Another series of Trk domain deletions and chimeric proteins, in which domain exchanges were made between TrkA, TrkB and TrkC, have been analyzed for binding of different neurotrophins and neurotrophin-dependent receptor activation (Urfer et al. 1995). All receptor variants were constructed as immunoadhesins in which the extracellular domains were fused to the Fc portion of a human antibody. These proteins were expressed in 293 cells and purified. In those chimeric receptors in which the Ig-like domain of TrkA was deleted, the binding of NGF was abolished. When the Ig-like domain of TrkA was expressed in NIH 3T3 cells, in the absence of the other extracellular domains, binding affinity similar to that seen with full-length receptors was retained (Urfer et al. 1995). For those TrkA proteins in which the first Ig-like domain was deleted, a 2.3-fold reduction was observed in NGF binding. In the TrkA deletion protein lacking the three LRR's and flanking cysteine clusters, no reduction was observed in NGF binding. These results suggest that the second Ig-like domain of TrkA is the high affinity binding site for NGF; however, saturation experiments with a TrkA variant lacking the first Ig-like domain resulted in detectable specific NGF binding indicating the possible presence of additional elements in the three LRR's and flanking cysteine clusters that interact with NGF (Urfer et al. 1995).

Regions of NGF and NT-3 thought to be involved in receptor binding, consist of residues in the β-strand bundle. In NGF, the proposed TrkA binding site includes the six N-terminal residues and certain loop residues, which are not involved in the binding of NT-3 to TrkC, suggesting that the surface interactions of NGF with TrkA are more extensive than those for NT-3 with TrkC (Urfer et al. 1995). When the extracellular region of TrkA encompassing the LRR's and flanking cysteines is deleted, NT-3 binding is diminished, while deletion of the second Ig-like domain does not completely abolish binding of NGF suggesting a more extensive NGF/TrkA surface interaction than for NT-3/TrkC (Urfer et al. 1995).

1.11 The Immunoglobulin-like Domains of TrkA, TrkB and TrkC

X-ray structures of the C-terminal Ig-like domains (d5) of TrkA, TrkB and TrkC have revealed something of how this region of the three receptors may bind their respective neurotrophins (Ultsch et al. 1999). These three domains share a 41-44 % sequence identity and consist of two β-sheets, ABED and GFCC'. A short helical segment is found in the loop connecting strands E and F (Figure 1.4). Each Ig-like domain crystallized as dimmers, but domain swapping also occurred and no interaction of NGF with the d5 region of TrkA was observed in *in vitro* studies (Ultsch et al. 1999, Wiesmann et al. 1999, Dr. Bart de Vos, Genentech, personal communication).

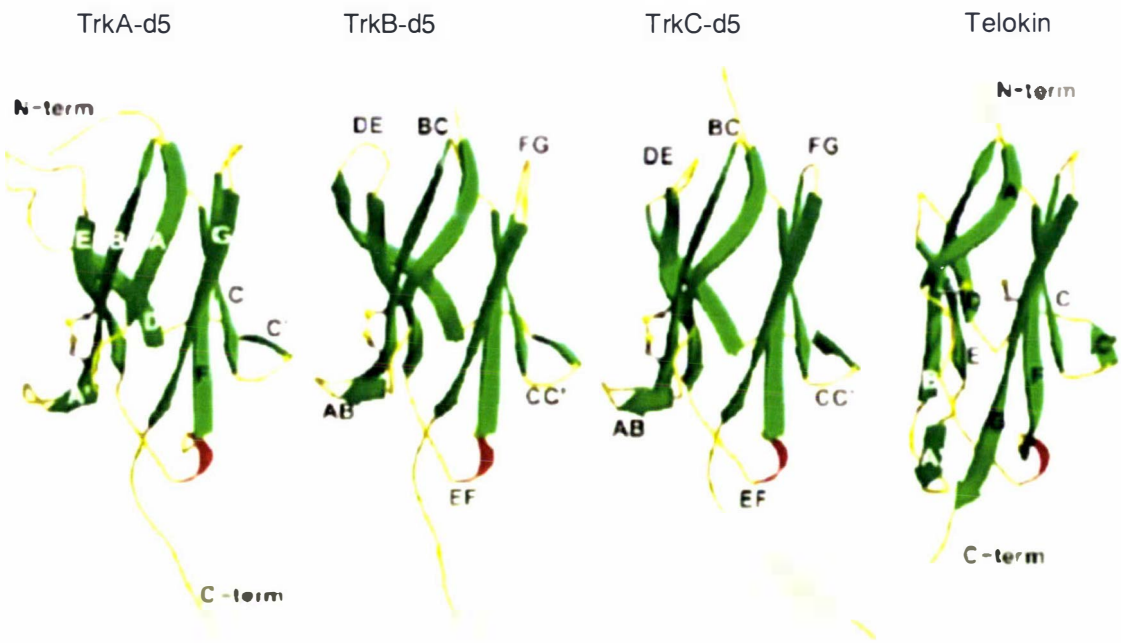

Figure 1.4 C-terminal Ig-like-like domains of the Trk receptors. From Ultsch et al. 1999.

The general structure of the d5 domains of the three receptors is similar to that found in the I-set of the immunoglobulin superfamily of transmembrane receptors and cell adhesion molecules (Ultsch et al. 1999). None of the recombinant d5 proteins, expressed in *E. coli*, were able to bind neurotrophins, a consequence of strand swapping and hence the refolded and crystallized proteins are considered to be dimeric artifacts (Ultsch et al. 1999).

Specificity of neurotrophin binding, a characteristic of the three Trk receptors, is at least partially explained by the three d5 structures. A hydrophobic pocket formed by residues on the exposed surface of the ABED sheet in TrkA accommodates the N-terminus of NGF. The disulfide bridge on the exterior of the Trk domain forms the bottom of this pocket while the side-chains of residues Val294, Met296, Pro302 and Leu333 form the walls of the pocket. The disulfide bridge is conserved in TrkB and TrkC but the residues forming the TrkA pocket walls are not. In TrkB, the residues found in the pocket are threonine, aspartic acid, proline and histidine replacing respectively those residues found in TrkA. These residues give rise to a hydrophilic pocket incapable of binding the hydrophobic N-terminus of NGF. In TrkC-d5, the side chains of Met 296 and Pro302 are replaced by arginine and glutamic acid, forming a salt bridge on top of the disulfide bridge and effectively filling the pocket (Ultsch et al. 1999).

1.12 Crystal Structure of NGF and the Immunoglobulin Domain of TrkA

A crystal structure of NGF complexed with the C-terminal Ig-like domain of TrkA has recently been published (Wiesmann et al. 1999). This structure (Figure 1.5, Figure 1.6) shows that the ligand receptor interface consists of two regions of similar size. One region consists of the central β-sheet core of the NGF homodimer and the loops formed by the C-terminal Ig-like domain (domain-5; d5) of TrkA. The second region is composed of the N-terminal region of NGF. These residues (2-9) are not seen in the original NGF structure (McDonald et al. 1991), presumably because they are disordered, however, in this complex the N-terminal region of NGF adopts a helical conformation and packs against the 'ABED' sheet (Figure 1.4) of the C-terminal Ig-like domain.

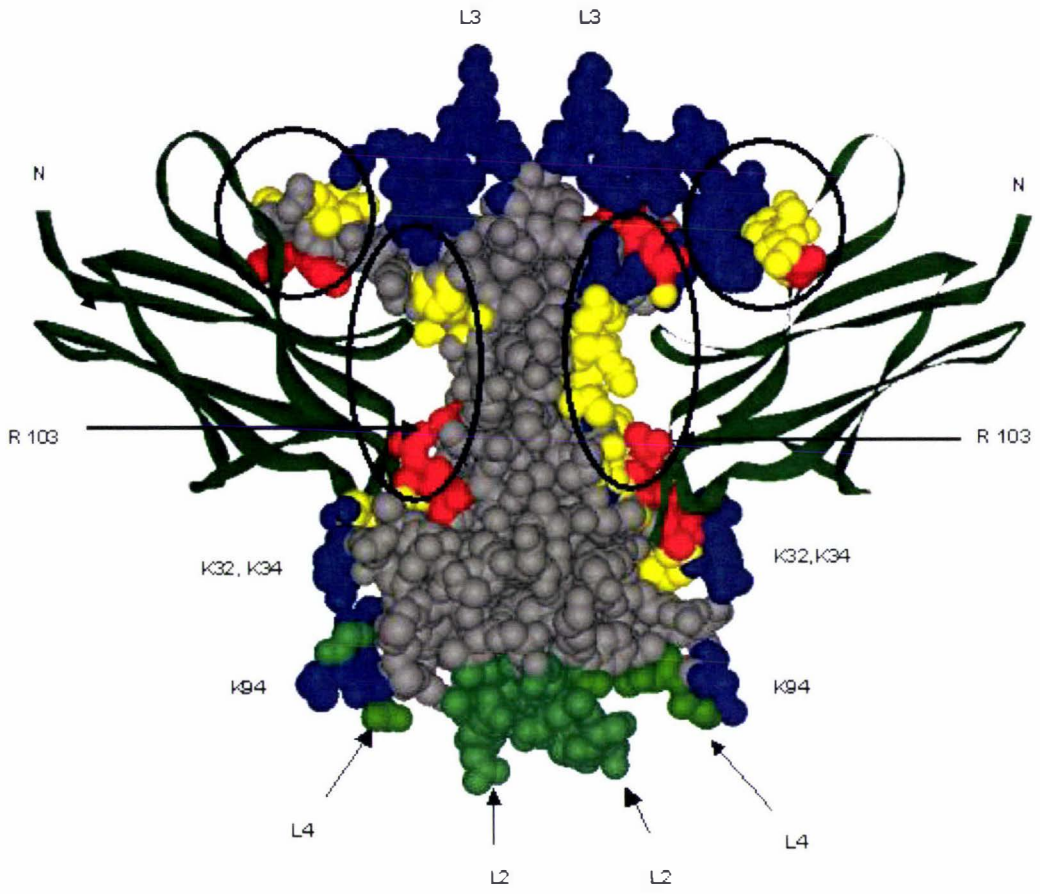

Figure 1.5 The NGF binding domains of TrkA C-terminal Ig-like-like domain. From Wiesmann et al. 1999.

In the space-filling model, the conserved and specificity regions of NGF are outlined with circles; ellipses denote the two symmetrical common regions. Regions of NGF believed to be in contact with the region of TrkA, C-terminal to d5 are denoted as L2 and L4. Residues of NGF that are in contact with d5, include those of the hairpin loop L1 and residues of the four β-strands that form the central region of the molecule. In particular, the strictly conserved residue found in all neurotrophins, Arg103 appears to be an important binding determinant in the interaction between NT-3 and TrkC (Wiesmann et al. 1999). The side chain of NGF stacks against the phenyl group of Phe327 of TrkA, forming a hydrogen bond with the carbonyl oxygen of Asn349 bond with the carbonyl oxygen of Asn349. Residues that make contact with d5 are red for the common region and green for those that confer specificity of interaction with the TrkA-d5 region are green.

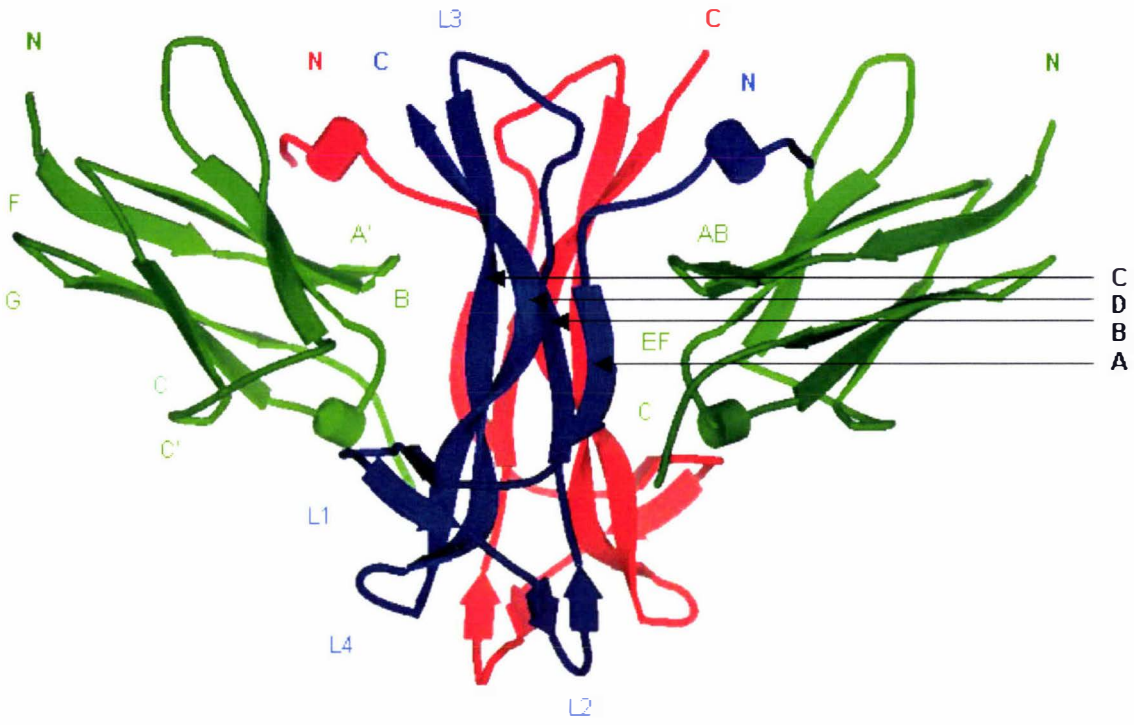

Figure 1.6 Interaction regions of NGF with d5 of TrkA. From Wiesmann et al. 1999.

The NGF monomers are red and blue, while the TrkA d5 region is green. The termini, some relevant loops and the secondary structure elements are labeled; loops L2 and L4 of NGF and the C-terminus of d5 (residue 382) point towards the membrane.

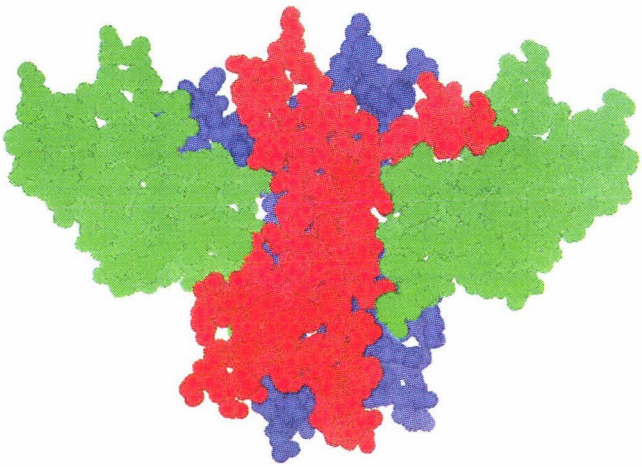

Figure 1.7 A space-filling model of the interaction regions of NGF with d5 of TrkA.

The NGF monomers are red and blue, while the TrkA d5 region is green. The model orientation is as shown in Figure 1.6. The molecular coordinates were obtained from the Protein Data Bank and the model produced with ViewerLite (Accelrys, San Diego).

1.13 The TrkB Receptor

The structural domains of the TrkB receptor are similar to those depicted for TrkA (Figure 1.2, Figure 1.3). These domains include; the signal peptide (SP), two cysteine clusters (CC), the leucine-rich motifs (LRM), two Ig-like-like regions (Ig), the transmembrane region (TM) and the tyrosine kinase region (TK). At least eight different transcripts of the *trk*B locus have been identified that encode two different types of receptor. The TrkB receptor, the high affinity receptor for BDNF, is a heavily glycosylated molecule of 821 amino acids. This receptor has an intracellular tyrosine kinase domain and is frequently designated as $TrkB^{TK+}$ to distinguish this isoform from those that lack a tyrosine kinase domain. A second class of TrkB receptors, designated as $TrkB^{TK-}$, has the same extracellular domain as $TrkB^{TK+}$ but lack the entire tyrosine kinase catalytic domain (Klein et al. 1990, Middlemas et al. 1991, Barbacid 1994). Two noncatalytic $TrkB^{TK-}$ receptor isoforms have been identified and are expressed in adult murine brain at comparable levels to $TrkB^{TK+}$ (Klein et al. 1990). The $TrkB^{TK+}$ receptor has a short

carboxy-terminal tail of 15 amino acids, which includes a conserved tyrosine residue (Klein et al. 1989).

1.14 The Leucine Rich Domain and BDNF Binding

As with the TrkA receptor, the extracellular domains of TrkB consists of a LRR flanked by cysteine clusters and two Ig-like domains. Overall identity between the extracellular domains of TrkA and $TrkB^{TK+}$ is 57%, with the most homologous regions between the two receptors found in the two LRR's and the second Ig-like domain (Schneider and Schweiger 1991). A number of studies have implicated the LRR domain of $TrkB^{TK+}$ as the binding site for BDNF. Five recombinant MBP-TrkB fusion proteins were expressed in *E. coli*, purified and utilized in binding studies with radiolabeled NGF and BDNF (Windisch et al. 1995a). The five fusion proteins expressed were (1) the entire extracellular domain (residues C21-E417), (2) the LRR and two flanking cysteine clusters (construct C1L1-3C2, residues L61-L132), (3), the three LRR's without the cysteine clusters (construct LRR, residues T72-L143), (4) the second LRR (construct L2, residues T86-109) and (5) the 2 Ig-like domains (residues S187-E417). Of these five domains, the complete extracellular domain and the C1L1-3C2 domain have a measured K_D for BDNF of ~ $1x10^{-9}$ M (virtually identical to the same domains of TrkA for NGF within experimental error. These same two domains bind NT-3 with a K_D of ~ $1x10^{-9}$ M (Windisch et al. 1995a), a value similar to those obtained in experiments with cells ectopically expressing TrkB (Soppet 1991, Denchant et al. 1993, Windisch et al. 1995c).

The complete LRR motif without the flanking cysteines binds BDNF, NT-3 and NT-4. Binding measurements of BDNF and NT-3 to the isolated second LRR resulted in essentially the same K_D as measured for the entire extracellular domain and also showed an affinity for NT-4. None of the TrkB fusion proteins showed an affinity for NGF. The isolated Ig-like domain showed no measurable BDNF, NT-3 or NT-4 binding. It appears from this study that TrkB neurotrophin binding can be isolated to the LRR region.

Failure to see such high binding affinities (i.e. K_D's ~ 10^{-11}M) for BDNF and NT-3 with the isolated extracellular domain and subdomains of TrkB may be due to isolation of the receptor from the cellular environment. It is possible that upon binding of a neurotrophin, a conformational change occurs within the receptor in the cellular environment, resulting in the transfer of ligand from the

second LRR to a high affinity binding site (Windisch et al. 1995c). High affinity binding may require additional membrane proteins or extracellular matrix components, for example, proteoglycans, which may only be present in the correct stoichiometric values in neurons for which high affinity has been measured (Windisch et al. 1995c). Intact signal transduction pathways have been suggested as requirements for generation of high affinity binding sites (Raffioni et al. 1993). The low affinity receptor for NGF, BDNF, NT-3 and NT-4/5 has been suggested as a component, together with a Trk receptor, in forming the high affinity receptor complex (Meakin and Shooter 1992).

Association and dissociation kinetics of the second LRR of TrkB binding with BDNF and NT-3 have revealed something of the complex nature of the interaction. Binding on-rates occur faster than ~ $3x10^5$ M^{-1} s^{-1} expected for a K_D of ~ $1x10^{-9}$ M (Rodriguez-Tabar and Barde 1988, Windisch et al. 1995c). The association kinetics measurements gave K_{on} values of $2.7x10^7$ M^{-1} s^{-1} for BDNF and 3.3 $7x10^7$ M^{-1} s^{-1} for NT-3 corresponding with the kinetics of the high BDNF and NT-3 receptors (Rodriguez-Tabar and Barde 1988, Windisch et al. 1995c). These results imply that a high affinity BDNF and NT-3 binding site is associated with the second LRR and that a complex mechanism may be involved in the association of neurotrophins with their receptors. Dissociation measurements for the second LRR gave half-lives of ~ 41.5 minutes for BDNF and ~ 19.5 minutes for NT-3; similar results to those obtained using whole cells (Rodriguez-Tabar and Barde, 1988, Rodriguez-Tabar et al. 1992, Windisch et al. 1995c). In studies of dissociation of BDNF from DRG neurons and dissociation of NT-3 from sensory neurons (Rodriguez-Tabar and Barde 1988, Rodriguez-Tabar et al. 1992), no biphasic behavior was observed.

Contrary to these results, biphasic dissociation behavior for BDNF and NT-3 was observed with the recombinant TrkB extracellular domain and subdomains (Windisch et al. 1995c). Steady state binding experiments corroborated the result and assigned neurotrophin binding to the 24 residue second LRR of TrkB (1995c).

A synthetic peptide corresponding to the second LRR of TrkB was shown to bind BDNF (Windisch et al a, b). Binding affinities of BDNF for the peptide were comparable with the affinity of NGF for the second LRR of TrkA. A similar binding study for NT-3 and NT-4 showed that these neurotrophins bind to the second LRR of TrkB, but with less affinity than BDNF. Since BDNF, NT-3 and NT-4 all bind to the second LRR of TrkB, it appears as though this domain represents a

strong and complex binding site for all three neurotrophins (Windisch et al. 1995a, c). Only 11 residues of the second LRR appear to be responsible for specific neurotrophin recognition.

Three isoforms of murine TrkB have been isolated and used in binding studies of BDNF, NT-3 and NT-4 (Ninkina et al. 1997, Dr. N. Ninkina, St. Andrews University, private communication). All three isoforms have deletions in the extracellular domain while retaining the two Ig-like motifs. Of the three isoforms, variant 1 lacked the first and second LRR's while retaining the flanking cysteine clusters. Variant 2 lacked all three LRR's but retained the flanking cysteine clusters and variant 3 lacked both cysteine clusters and the three LRR's. None of these three TrkB isoforms shows affinity for BDNF, NT-3 or NT-4 when compared with wild type TrkB used as a control. These results point to the importance of the LRR's, in particular the first two, in binding neurotrophins, at least for TrkB, and further supports the lack of neurotrophin binding to Ig-like domains, as reported by Windisch et al. (Windisch et al. 1995a, b, c).

High affinity binding associated with a small region of a large protein is not without precedence. The X-ray crystal structure of the complex between human growth hormone and the extracellular domain of its receptor (hGHpb) revealed that only about 30 side chains of the receptor and ligand make contact (Clarkson and Wells 1995). In the case of hGHpb, alanine-scanning experiments have revealed that a central hydrophobic core dominated by two tryptophans accounts for more than three-quarters of the binding free energy. Less important, generally hydrophilic and partially hydrated residues surround the "functional" epitope. Only a small and complementary set of contact residues exhibits binding affinity.

Mutational analysis of antibodies (Hawkins et al. 1993, Kelley and O'Connell 1993) and protein antigen complexes (Davies et al. 1990, Jin et al. 1992, Wilson and Stanfield 1993) has shown that typically only 14 to 21 residues are in contact and that only 3 to 10 side chains can account for most of the binding energy (Clarkson and Wells 1995). These results are supportive of theoretical studies that predict that only a few interactions in protein-protein binding, may be important for tight binding (Novotny et al. 1989). Hence assignment of high binding affinity for neurotrophins to the small 24 residue second LRR may not be unreasonable.

1.15 The Immunoglobulin-Like Domains and Neurotrophin Binding

Five chimeric receptors have been constructed in which the extracellular domains of human TrkB and TrkC were interchanged. These domains were fused to the Fc portion of a human antibody and expressed in the human fetal kidney cell line 293 as an immunoadhesion (Urfer et al. 1995). The following chimeras were constructed: chimera 1, consisted of the first 47 residues of TrkB, encompassing the first cysteine cluster, exchanged for the same region of TrkC. Chimera 2, consisted of the three LRR's of TrkB interchanged with the same region of TrkC. Chimera 3, consisted of the second cysteine cluster of TrkB interchanged with the same region of TrkC. Chimera 4, consisted of the N-terminal Ig-like domain of TrkB exchanged for the same domain of TrkC. Chimera 5, consisted of the C-terminal Ig-like domain of TrkB exchanged for the same domain of TrkC. Competition and saturation binding assays were performed with the chimeric proteins and the complete extracellular domains of TrkB and TrkC (also expressed as immunoadhesions).

Both TrkB and TrkC bind NT-3, with high affinity for TrkC and reduced affinity for TrkB (Urfer et al. 1994). If TrkB and TrkC utilize the same structural elements for neurotrophin binding, then a particular TrkB/TrkC chimera would be expected to have reduced, but not complete loss of binding affinity for NT-3 (Urfer et al. 1995). All chimeric proteins were assayed for BDNF and NT-3 binding. Competitive displacement assays with BDNF and TrkB resulted in an IC_{50} of 20.7 ± 2.8 pM, while TrkC showed no BDNF binding. Chimera 5 binds BDNF with an IC_{50} of 16.7 ± 1.5 pM, a similar affinity to that displayed by TrkB. In saturation binding experiments, TrkB and chimera 5 have K_D values of 10.4 ± 1.6 pM and 10.9 ± 2.3 pM respectively. All other TrkB/TrkC chimeras and domain deletions of TrkC showed no binding and this suggested that the individual TrkC domains did not contribute any repulsive effects. Hence the conclusion from these experiments is that the second Ig-like domain of TrkB specifies which neurotrophin, BDNF or NT-3, binds to the TrkB receptor.

All chimeric TrkB and TrkC receptors were assayed for NT-3 affinity to determine if structural elements of TrkB could prevent NT-3 binding. The TrkB immunoadhesin bound NT-3 with an affinity similar to that of TrkB expressed on NIH 3T3 cells (Escandon et al. 1994), but with a markedly reduced (11.0 ± 1.7 fold) affinity compared with the native TrkC receptor. Chimera 5 showed an almost identical loss of NT-3 affinity as TrkB while all the other chimeras were unaffected in their ability to bind NT-3. These binding studies suggest that the cysteine clusters,

the LRR's and the N-terminal Ig-like domain or elements within these domains, do not prevent NT-3 binding or participate in neurotrophin discrimination. Binding specificity for BDNF and NT-3 appears to reside only in the second Ig-like domain of the TrkB receptor (Urfer et al. 1995).

Another series of chimeric receptors in which the LRR's including flanking cysteine clusters and Ig-like domains of TrkA and TrkB were interchanged, were expressed in 293 cells and NGF binding was measured under equilibrium conditions to the chimeric protein (Perez et al. 1995). In these studies NGF bound to TrkB at 10% of the affinity of NGF for TrkA. For the chimera consisting of the TrkB protein with the second Ig-like domain of TrkB exchanged for the second Ig-like domain of TrkA, no NGF binding was observed. For the chimera consisting of the TrkB protein with the first Ig-like domain of TrkB exchanged for the first Ig-like domain of TrkA, no NGF binding was observed.

These results suggest that the Ig-like domains of the Trk receptors may be responsible for neurotrophin discrimination but this study does not assist in discriminating which Ig-like domain is responsible for neurotrophin identification. For the chimera consisting of the second Ig-like domain of TrkA exchanged for the second Ig-like domain of TrkB, no NGF binding was observed. This result suggests that the second Ig-like domain is responsible for neurotrophin discrimination, but since no chimera was studied in which the first Ig-like domain of TrkA is replaced with the same domain of TrkB, it is difficult to assess the role of the Ig-like domains in determining which neurotrophin binds to a particular receptor.

A study of the binding of NGF to recombinant Ig-like domains of TrkA expressed in *E. coli* (Holden et al. 1997) showed that the neurotrophin binds with nM affinity to the domain previously shown to have no NGF affinity (Windisch et al. 1995a, b, c). In contrast to the experiments of Windisch et al. (1995a, b, c) the Ig-like domain protein was purified from inclusion bodies and refolded prior to binding studies.

1.16 The TrkC Receptor

The structural domains of the TrkB receptor is similar to that depicted of TrkA (Figure 1.2 and Figure 1.3). At least four TrkC isoforms constituting two classes of receptor are known and all have the same structural form as the TrkA and TrkB receptors. The extracellular domains of the three receptors have approximately 53% identity while the intracellular tyrosine kinase domains share an approximate 87% identity (Barbacid 1994). All four isoforms share an extracellular domain of 430 amino acids but differ in the number of residues (14, 25, 39) that follow the conserved YSTDYYR motif, which includes the two tyrosine (Y711, Y712) residues. These residues have been identified as the presumed autophosphorylation site (Lamballe et al. 1993, Tsoulfas et al. 1993, Valenzuela et al. 1993, Barbacid 1994). As with the TrkB receptor, a second noncatalytic class of TrkC receptor, similar to $_{TrkB}{}^{TK-}$, is known. These receptors have the same extracellular and transmembrane domains as the catalytic TrkC receptor, however they lack the tyrosine kinase domain. Four different $_{TrkC}{}^{TK-}$ receptors have been identified; all have the first 74 cytoplasmic residues identical to those of the juxtamembrane region of the catalytic TrkC receptors. Residues beginning with 529 are derived from four dissimilar alternatively spliced exons (Tsoulfas et al. 1993, Valenzuela et al. 1993, Barbacid 1994).

1.17 Neurotrophin Binding Domains of TrkC

In contrast to the TrkA and TrkB receptors, few studies have been made of the cysteine clusters, LRR's, Ig-like domains and permutations of these domains of TrkC to determine their respective binding and discriminatory abilities for NT-3 and other neurotrophins. Expression of the extracellular domain and subdomains of TrkC as maltose fusion proteins in *E. coli* has been reported to be highly toxic to the bacterium (Windisch et al. 1995a). Few expression systems have been identified to reliably produce correctly folded Trk receptors and as a result, studies of the extracellular domains of TrkC tend to be of a very limited nature to date.

Chimeric proteins consisting of domain exchanges between TrkC and regions of both TrkA and of TrkB were fused with the Fc portion of a human antibody and expressed as an immunoadhesin (Urfer et al. 1995). Five chimeras consisting of domains of TrkC replacing the same domain of TrkB were expressed. The following domains of TrkB were exchanged for those of TrkC: (1) N-terminal cysteine cluster, (2) the LRR, (3) C-terminal cysteine cluster, (4) N-terminal Ig-like domain and (5) the C-terminal cysteine cluster. Of these chimeric proteins, all but chimera 5

showed a binding affinity for NT-3, $IC_{50mut}/IC_{50wt} < 3$, when compared with wild type TrkC. Chimera 5 showed essentially no affinity for NT-3 and had an $IC_{50mut}/IC_{50wt} > 40$. Only chimera 5, which consists of the entire TrkB extracellular domain with the TrkC C-terminal Ig-like domain of TrkC replacing that of TrkB, showed an ability to bind BDNF ($IC_{50mut}/IC_{50wt} < 3$), compared with wild type TrkB. None of the chimeric TrkC/TrkB proteins showed any measurable binding of NGF. Only one chimeric protein was made with TrkA and TrkC and consisted of the C-terminal Ig-like domain of TrkA replacing the same domain of TrkC. It showed essentially no ability to bind NT-3 ($IC_{50mut}/IC_{50wt} > 40$). However, this same protein showed the same ability to bind NGF as wild type TrkA ($IC_{50mut}/IC_{50wt} < 3$).

In addition, seven subdomains of the TrkC extracellular domain were also expressed as immunoadhesins in 293 cells. The seven TrkC proteins in this study consisted of the following domain deletions: (1) N-terminal cysteine cluster, (2) entire LRR motif, (3) C-terminal cysteine cluster, (4) N-terminal Ig-like motif, (5) C-terminal Ig-like motif, (6) all extracellular domains except the C-terminal Ig-like domain and (7) all extracellular domains except the two Ig-like domains. Only construct 5, the protein consisting of the entire TrkC extracellular domain except the C-terminal Ig-like motif bound NT-3 or BDNF. All the other proteins bound NT-3 with wild type TrkC affinity ($IC_{50mut}/IC_{50wt} < 3$). These results suggest that the Ig-like domains are required for high affinity neurotrophin binding for TrkA, TrkB and TrkC receptors and that the C-terminal Ig-like domain is required to discriminate between neurotrophins and hence specifies which neurotrophin binds to a particular receptor (Urfer et al. 1995).

1.18 The p75 Receptor

The NTF's NGF, BDNF and NT-3 all bind with lowered affinity (when compared with their ability to bind to TrkA, TrkB and TrkC respectively), to another receptor, namely p75, a 75 kD protein that mediates programmed cell death in neurons that have been deprived of NTF's (Lee et al. 1992, 1994, Rabizadeh et al. Barrett and Bartlett 1994, Barrett 2000, Yano and Chao 2000, Huang and Reichardt 2003). This receptor consists of a single polypeptide chain of approximately 400 amino acids with an extracellular domain and a short cytoplasmic domain separated by a single transmembrane domain. Four negatively charged cysteine rich regions or loops in the extracellular domain appear to be required for NGF binding (Yan and Chao 1991, Baldwin et al. 1992, Meakin and Shooter, 1992). The p75 NGF receptor is a member of a family of related

proteins that include tumor necrosis factor receptors (TNFRI and TNFRII) and the Fas antigen receptor. The p75 receptor does not have sequence homology with the Trk receptors.

Binding assays for receptors, with both high and low affinity, expressed on chick embryonic sensory neurons, have been made with NGF (Sutter et al. 1979), BDNF (Rodriguez-Tebar and Barde 1988) and NT-3 (Rodriguez-Tabar et al. 1992). A summary of the binding data of NGF, BDNF and NT-3 to both the high affinity receptors and p75, is given in Table 1.1.

Table 1.1 The characterization of NGF, BDNF and NT-3 receptors on chick embryonic sensory neurons by binding assays. From Meakin and Shooter (1992).

Two classes of NGF receptors were originally distinguished on chick embryonic sensory neurons by binding and kinetics measurements (Sutter et al. 1979). The major population of receptors have a K_D of 10^{-9} M, while a minor receptor population have a K_D of 10^{-11} M. These receptors are respectively known as low (LNGFR) and high (HNGRF) affinity receptors. The rates of association of neurotrophin to both types of receptor are similarly rapid, however, they differ in that the rate of dissociation is slow for the HNGRF and fast for the LNGFR. Subsequent studies have identified LNGFR as p75 and the HNGFR as TrkA. The binding data are from Sutter et al. 1979, Kow et al. 1979 and Burris et al. 1991.

	NGF	BDNF	NT-3
K_D of high affinity binding (M)	$2.3x10^{-11}$	$1.7x10^{-11}$	$1.8x10^{-11}$
Number of receptors per neuron	1000-3000	230	11000
K_D of low affinity binding (M)	$1.7x10^{-9}$	$1.3x10^{-9}$	$0.8x10^{-9}$
Number of receptors per neuron	23000-45000	3200	39000

While the K_D value is essentially identical for the binding of NGF, BDNF and NT-3 to p75, the association and dissociation rates differ significantly, possibly as consequence of differences in the structure of the neurotrophins or differences in conformational changes that may occur on ligand binding (Ernfors et al. 1990, Rodriguez-Tebar et al. 1992, Meakin and Shooter 1992, Bradshaw et al. 1994). TrkA has a very slow association rate with a K_{on} of $8x10^5$ M^{-1} s^{-1} (at 4ºC) and a very slow dissociation rate, suggestive of high affinity. Conversely, p75 has fast association and dissociation rates characteristic of a low affinity for NGF. Since these binding properties for the two receptors are observed in both neural crest derived and non neuronal cells, it appears that the on and off rates are characteristic of the receptors and not of cellular environment (Chao and Hempstead 1995). Co-expression of p75 and TrkA results in a 25-fold increase in the ligand on rate, suggesting that both p75 and TrkA contribute to the formation of a high affinity binding site for NGF (Chao and Hempstead 1995).

Expression of p75 both with Trk receptors and independently of TrkA, TrkB or TrkC is widespread in many cell types, including Schwann cells, motor neurons and cerebellar Purkinje cells (Chao and Hempstead 1995). While many studies have established the importance of the Trk family of receptors in the promotion of neurite outgrowth and cell survival, there exists little evidence of particular roles for p75. Receptor levels in responsive neurons indicate that TrkA expression is limited while that of p75 is higher; a ten-fold difference for example in mRNA levels in neonatal sympathetic ganglia (Chao and Hempstead 1995). NGF shows both high and low affinity binding sites in sensory and sympathetic neurons and PC12 cells. In these cells, a small percentage of high affinity NGF binding sites have been detected with these sites being assigned to TrkA and low affinity binding sites to p75 (Klein et al. 1991, Jing et al. 1992, Chao and Hempstead 1995). Responsive neurons appear to have 10-30% of the total binding of neurotrophin at high affinity sites (K_D ~10^{-11} M), while the remaining binding occurs at low affinity sites (K_D ~10^{-9} M). Under conditions in which p75 is expressed in excess with respect to TrkA, a similar number of high affinity binding sites are observed. Only low levels of expression of p75 compared with TrkA (1:10 ratio) appears to result in a lowering in the number of high affinity NGF binding sites (Jing et al. 1992, Chao and Hempstead 1995). These results suggest that the ratio of p75 to TrkA is important in the high affinity binding of NGF. Other neurotrophins, for example NT-3 appears to have few (1-2% of total binding) high affinity binding sites when interacting with TrkC (Chao and Hempstead 1995).

Expression levels for p75 and TrkA influences the number of low and high affinity binding sites for NGF in PC12 cells. High levels of TrkA result in an increased number of both low and high affinity

sites, while decreased levels of p75 or inhibition of NGF binding to p75 leads to a reduction of both low and high affinity binding sites (Weskamp and Reichardt 1991, Benedetti et al. 1993, Chao and Hempstead 1995). For a number of two-site binding receptors, for example interleukin-2, interleukin-6 and CNTF, the low affinity site is ten times more abundant than the high affinity site *in vivo* (Chao and Hempstead 1995).

Interaction of p75 with TrkA appears to influence cell survival (Casaccia-Bonnefil et al. 1999). Antibodies to p75 have no effect on the ability of NGF to promote cell survival and neurite outgrowth (Weskamp and Reichardt 1991, Chao and Hempstead 1995). A number of NGF mutants that do not bind to p75 but that do bind to TrkA, are capable of promoting cell survival, suggesting that Trk receptors may be able to function independently of p75 (Ibanez et al. 1992). Confusing the role of p75 in cell survival, are results of a study in which induction of TrkA autophosphorylation and c-fos mRNA in PC12 cells is influenced by the binding of NGF to p75. These effects are reduced by a monoclonal antibody directed against an extracellular epitope of p75 (Barker and Shooter 1994, Chao and Hempstead 1995).

A number of studies suggest that p75 and TrkA interact to form a high affinity neurotrophin receptor. Another possible role for p75 is that of recruitment of NGF from the environment and passage of the bound neurotrophin to its appropriate Trk receptor. Studies of mutant PC12 cells that do not express p75 suggest that p75 acts as a ligand-recruiting molecule since only in the presence of p75 are K_{on} values of ~ 10^7 M^{-1} s^{-1} observed (Mahadeo et al. 1994). Two models, neither of which reflects the measured stoichiometry of p75 and Trk receptors, have been suggested for p75-TrkA interactions. The first model proposes that NGF rapidly binds to p75 thus increasing the local concentration of neurotrophin in the vicinity of the Trk receptor (Mahadeo et al. 1994). In this model there is no direct interaction of p75 and the Trk receptor. A second model suggests that a direct interaction occurs between p75 and the Trk receptor resulting in a conformational change in the Trk receptor in the absence of ligand (Chapman and Kuntz 1996, Shamovsky et al. 1999, Neet and Campenot 2001).

Conformational change of the Trk receptor is hypothesized to result in an increased ligand on rate and hence formation of a high affinity binding site (Meakin and Shooter 1992, Wolf et al. 1995, Chao and Hempstead 1995, Neiderhauser et al. 2000). Both models require dimerization of Trk molecules following neurotrophin binding. Direct measurement of the interaction of p75 and Trk receptors has not been directly demonstrated, although one study utilizing recovery of

fluorescence after photobleaching suggests that TrkA immobilizes p75, in the absence of ligand, but only if the cytoplasmic domains of p75 and TrkA are intact (Wolf et al. 1995, Chao and Hempstead 1995). Another study utilizing fluorescent antibodies, appears to have established an interaction between p75 and TrkA receptors on the surfaces of cells (Wolf et al. 1998).

While argument by analogy must be used with caution, particularly when comparing prokaryotic and eukaryotic systems, a study of intracellular signaling by the *E. coli* aspartate receptor Tar (Tatsuno et al. 1996, Gardina and Manson 1996), having only one cytoplasmic domain per dimer, offers some suggestion as to the possibility for signaling by a heterodimer of TrkA/p75 and also of full length and truncated isoforms of TrkB and TrkC. To date no heterodimers of full length and truncated Trk receptors have been documented, however a controversial complex of p75 and TrkA has been reported (Wolf et al. 1995). Current models hypothesize that transmembrane signaling is accomplished by dimerization of the receptors upon binding of a ligand, or by changing the orientation of one monomer with respect to the other in an already existing dimer.

1.19 A Rationale for the Thesis Research

At the beginning of the 21st century, humanity has entered an era when average life expectancy has increased from approximately 50 years in the 19th century to 70-80 years. With the advent of modern medicine, many of the diseases that once afflicted mankind have now been eliminated or are controllable. Increasingly, the diseases and consequences of advanced age have become apparent. In particular, Alzheimer's and other neurological disorders are placing an escalating burden on the medical costs of communities worldwide (Kandel et al. 2000). Research to develop new and effective therapies for neurological diseases has become progressively more important.

Neurotrophins as a treatment for Alzheimer's and Parkinson's diseases especially, has been one approach in the development of new therapeutics. However, peptides as therapeutics do present a number of difficulties (Kandel et al. 2000, Williams and Lemke 2002). Small molecule mimetics of neurotrophins has been the quest of many international research efforts (Ibanez 1998). However, controversy still remains as to which domain or domains of the Trk receptors, a neurotrophin binds. The research conducted for this thesis has been undertaken in an attempt to further delineate the neurotrophin binding domain(s) of their receptors. By defining the interaction

domains, it is hoped that further progress may me made in the development of peptide and small molecule mimetics of the neurotrophins.

It is increasingly clear that accessory proteins such as p75 and intracellular proteins play important roles in the binding of neurotrophins to Trk receptors and of resulting biological activity. Because this thesis study was necessarily conducted in a non-biological environment, i.e. in the absence of p75 and accessory proteins known to bind to Trk receptors, it is impossible to equate the observations made in this authors research, with the reality of neurotrophin-Trk interactions in human neurons.

To date only one neurotrophin exhibits real potential as a therapy for neurological disorders, namely, GDNF, while NGF and BDNF have exhibited little or no therapeutic value in clinical trials. New methods for peptide delivery to the Central Nervous System via the nasal mucosa, (Gozes et al. 2000, Liu et al. 2001) may however overcome the need to develop small molecule mimetics of the neurotrophins and eliminate the difficulties associated with administration of NGF and other NTF's. Ultimately stem cell therapies may prove to be more effective than molecular treatments for neurological disorders. Thus the effort to determine the binding behavior of NTF's to Trk receptors may ultimately have proven to be only an interesting exercise in an ongoing scientific quest for new treatments to eliminate some of the more insidious afflictions of humankind.

CHAPTER 2 Trk RECEPTORS, EXPRESSION AND PURIFICATION

2.1 Introduction and Aims

The aim of this thesis project was to establish the neurotrophin binding domains of the Trk receptors. To conduct this study, a number of regions of the extracellular domains of TrkA, TrkB and TrkC, were produced in both prokaryotic and eukaryotic expression systems. A biosensor study of the binding of neurotrophins to the various extracellular domains of the respective Trk receptor was then undertaken. Although not intended to be exhaustive in terms of establishing absolute binding constants for each neurotrophin and respective receptor subdomains, the experimental design was sufficient to firmly determine neurotrophin binding to proposed ligand binding regions of each receptor.

A number of studies of the interactions of the neurotrophins with Trk receptors have been undertaken. Both *in vivo* and *in vitro* studies, have led to the identification of two distinct and reportedly exclusive, ligand-binding domains on the receptors. In particular, *in vitro* binding studies (Windish et al. 1995a, b, c) and *in vivo* studies (Ninkina 1997) have identified the leucine rich motif (abbreviated as LRR) of all three Trk receptors as the neurotrophin-binding domain. Conversely, *in vitro* (Holden et al. 1997, Wiesmann et al. 1999, Robertson et al. 2001) and in *vivo* studies (Urfer et al. 1995, 1998, Kojima et al. 1999), have identified the immunoglobulin-like domain (abbreviated as Ig1+Ig2) as the exclusive ligand-binding domain of the neurotrophin receptors.

An attempt was made to express a number of Trk proteins as C-terminal His-tagged proteins in *E. coli*. Expression systems were designed such that these proteins would cover the same residues as proteins expressed as MBP-fusion proteins in an earlier study (Windisch et al. 1995a). MBP-fusion protein expression constructs used in a previous study (Windisch et al. 1995a, b, c) were obtained[1] and these proteins were expressed for kinetics and other neurotrophin-receptor

[1] A gift of Prof. Rainer Schneider, University of Innsbruck, Austria.

studies. Justification for the choice of domain expressed as MBP-fusion proteins has been detailed previously (Windisch et al. 1995a, b, c).

Full-length Trk receptor extracellular domains were expressed as C-terminal His-tagged proteins in *Pichia pastoris* for this study. These proteins provide a set of controls, for comparison with those proteins expressed in *E. coli* (Windisch et al. 1995a). Native Trk proteins possess several post-translational modifications (Martin-Zanca 1989, Watson et al. 1999, Neet and Campenot 2001). The design of the expressed proteins was determined by the perceived need to retain the cysteines, N-terminal to the leucine rich region and both Immunoglobulin-like domains. Each construct was designed to terminate close to the recognized transmembrane domain. In addition, the TrkA proteins were designed to terminate on the same residue, namely, threonine, two residues (for *Rattus norvengicus*) before the first transmembrane residue. The TrkB and TrkC extracellular domains are several amino acids longer than the TrkA proteins and these constructs were designed to be of similar length to TrkA and terminate one residue (for TrkB, *Rattus norvengicus*) before the transmembrane domain. All the extracellular residues of the full-length TrkA and TrkB proteins are included in the *E. coli* constructs.

Three TrkA proteins[2] from an external source (Prof. Uri Saragovi, McGill University) were obtained to provide a control for potential problems with protein expression and purification technique, as well as providing controls for kinetics and related studies. In addition, three synthetic peptides, representing the smallest identified neurotrophin-binding domains (Windisch et al. 1995a, b, c), were produced. With these proteins, an extensive kinetics study of the neurotrophin-receptor interaction was possible. Further, physical properties of the proteins in solution, were assessed by ultracentrifugation.

[2] Ig-like domain expressed in *E. coli* and *P. pastoris*. Full-length extracellular domain expressed in insect cells.

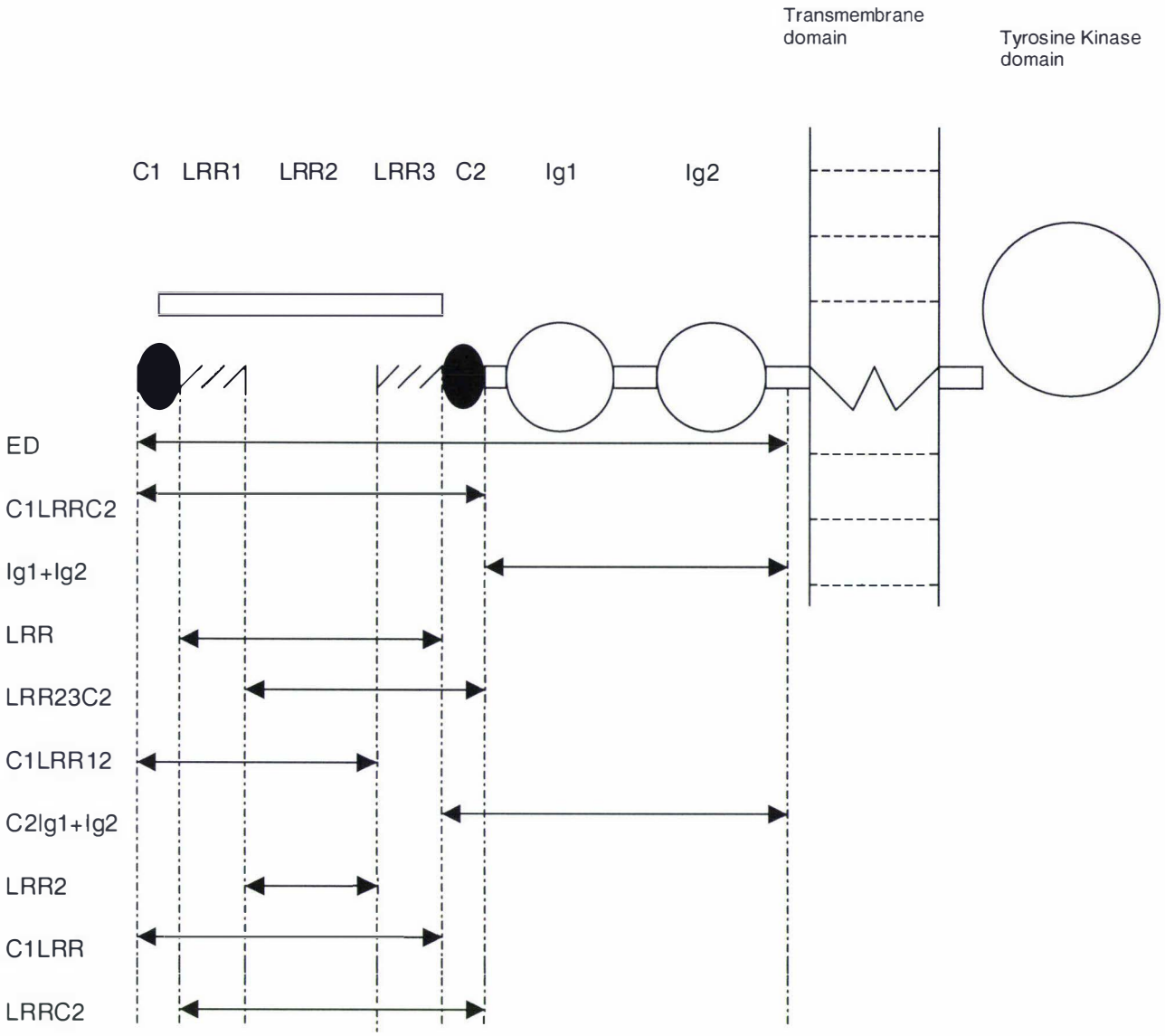

Figure 2.1 Trk Receptor Structure Adapted from Windisch et al. (1995a).

Potential neurotrophin binding regions showing the domains expressed as MBP-fusion and His-tagged proteins. The extracellular domain of the Trk receptor consists of two cysteine rich regions (C1 and C2) that are N and C terminal to the Leucine rich domain (LRR) respectively. The LRR domain is considered to consist of 3 individual regions (LRR1, LRR2 and LRR3). Two immunoglobulin-like domains (Ig1 and Ig2) complete the defined regions of the extracellular domain.

ED....Extracellular Domain Ig1+Ig2....Complete Immunoglobulin-like domain LRR....Leucine Rich Domain C1 and C2.... N and C terminal cysteine rich regions respectively LRR2....Protein expressed as an MBP-fusion protein and produced as a synthetic peptide

Table 2.1 TrkA extracellular domains expressed as MBP-fusion proteins. The Trk extracellular domains are shown in Figure. 2.1, while the particular residues, expression system and protein tag are shown below.

Domain[3]	Residues	Species	Expression System	Tag
ED	Cys^{36}-Glu^{416}	Rat	*E. coli*	MBP
C1LRR	Cys^{36}-Pro^{196}	Rat	*E. coli*	MBP
C1LRR12	Cys^{36}-Leu^{120}	Rat	*E. coli*	MBP
LRR	Tyr^{72}-Leu^{143}	Rat	*E. coli*	MBP
LRR23C2	Thr^{97}-Pro^{196}	Rat	*E. coli*	MBP
LRRC2	Tyr^{72}-Pro^{196}	Rat	*E. coli*	MBP
Ig1 + Ig2	Ser^{197}-Glu^{416}	Rat	*E. coli*	MBP
Ig1 + Ig2C2	Ser^{197}-Glu^{416}	Rat	*E. coli*	MBP
LRR2	Thr^{97}-Leu^{120}	Rat	*E. coli*	MBP

Table 2.2 TrkA extracellular domains expressed as His-tagged proteins. These proteins failed to express and hence could not be used in any subsequent studies.

Domain	Residues	Species	Expression System	Tag
ED	Cys^{36}-Glu^{416}	Rat	*E. coli*	His
C1LRR	Cys^{36}-Pro^{196}	Rat	*E. coli*	His
LRRC2	Tyr^{72}-Pro^{196}	Rat	*E. coli*	His
Ig1 + Ig2C2	Ser^{197}-Glu^{416}	Rat	*E. coli*	His
LRR2	Thr^{97}-Leu^{120}	Rat	*E. coli*	His

[3] The molecular weights for all TrkA, TrkB and TrkC MBP-fusion proteins expressed for this project are tabulated in the appendix.

Table 2.3 TrkA full-length extracellular domain expressed in yeast.

Domain	Residues	Species	Expression System	Tag
ED	Cys^{36}-Glu^{416}	Rat	*P. pastoris*	His
ED	Cys^{36}-Tyr^{414}	Human	*P. pastoris*	His

Table 2.4 Synthetic human TrkA peptide. This peptide representing the 24 residues of the second leucine rich repeat of human TrkA, was synthesized with a 6-His C-terminal tag; purity > 95% as determined by MALDI mass spectroscopy (Boston Biomolecule).

Domain	Residues	Species	Expression System	Tag
LRR2	Thr^{97} – leu^{120}	Human	synthetic	His

Table 2.5 TrkB extracellular domains expressed as MBP-fusion proteins. The Trk extracellular domains are shown in Figure 2.1 while the particular residues, expression system and protein tag are shown below.

Domain	Residues	Species	Expression System	Tag
ED	Cys^{32}-Glu^{424}	Mouse	*E. coli*	MBP
C1LRR	Cys^{32}- Pro^{185}	Mouse	*E. coli*	MBP
LRRC2	Leu^{72} - Pro^{198}	Mouse	*E. coli*	MBP
C1LRRC2	Cys^{32} - Pro^{198}	Mouse	*E. coli*	MBP
LRRC2	Leu^{72}-Pro^{198}	Mouse	*E. coli*	MBP
Ig1 + Ig2	Ser^{181} - Glu^{424}	Mouse	*E. coli*	MBP

Table 2.6 TrkB extracellular domains expressed as His-tagged proteins. These proteins failed to express and hence could not be used in any subsequent studies.

Domain	Residues	Species	Expression System	Tag
ED	Cys^{36}-Glu^{424}	Rat	*E. coli*	His
C1LRRC2	Cys^{36} - Pro^{197}	Rat	*E. coli*	His
Ig1 + Ig2	Arg^{187} - Glu^{424}	Rat	*E. coli*	His

Table 2.7 TrkB full-length extracellular domain expressed in yeast.

Domain	Residues	Species	Expression System	Tag
ED	Cys^{36}-Arg^{424}	Rat	*P. pastoris*	His

Table 2.8 Synthetic human TrkB peptide. This peptide representing the 24 residues of the second leucine rich repeat of human TrkB, was synthesized with a 6-His C-terminal tag; purity > 95% as determined by MALDI mass spectroscopy (Boston Biomolecule).

Domain	Residues	Species	Expression System	Tag
LRR2	Thr^{97} – Ile^{120}	Human	synthetic	His

Table 2.9 TrkC extracellular domains expressed as MBP-fusion proteins. The Trk extracellular domains are shown in Figure 2.1 while the particular residues, expression system and protein tag are shown below.

Domain	Residues	Species	Expression System	Tag
ED	Cys^{36}-Thr^{416}	Rat	*E. coli*	MBP

Table 2.10 TrkC full-length extracellular domain expressed in yeast.

Domain	Residues	Species	Expression System	Tag
ED	Cys^{36}-Thr^{416}	Rat	*P. pastoris*	His

Table 2.11 Synthetic human TrkC peptide. This peptide representing the 24 residues of the second leucine rich repeat of TrkC, was synthesized with a 6-His C-terminal tag; purity > 95% as determined by MALDI mass spectroscopy (Boston Biomolecule).

Domain	Residues	Species	Expression System	Tag
LRR2	Val^{97} - Pro^{120}	Human	synthetic	His

2.5 Expression of Proteins in *P. pastoris* with the Vector pPICZαA

Expression of Trk proteins was undertaken in the yeast *P. pastoris*, by cloning cDNA encoding the extra-cellular domains for TrkA (both rat and human), TrkB (rat) and TrkC (rat), into the expression vector pPICZαA (Invitrogen). The vector pPICZαA permits expression of the recombinant protein containing a myc epitope (useful in following protein expression by Western blot) and a polyhistidine tag capable of binding divalent cations (e.g. Ni^{2+}). Both the myc epitope and polyhistidine tag are C-terminal to the recombinant protein.

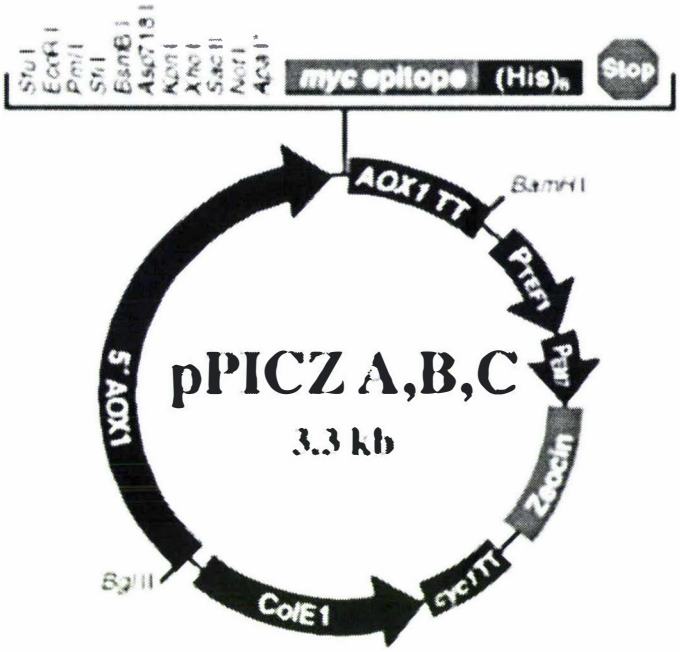

Figure 2.2 Map of pPICZαA (Invitrogen *P. pastoris* protein expression system manual).

2.3 Construction of Expression Vectors

All four Trk cDNA's were amplified by PCR to provide sufficient DNA for cloning into the expression vector pPICZαA. The TrkA (human and rat) N and C-terminal oligonucleotides were produced at 0.05μM quantity, the Trityl group was removed and the oligonucleotides purified by

HPLC to 0.5 OD scale (Operon Technologies). Both N and C-terminal oligonucleotides for TrkB and TrkC were supplied by Prof. Louis Reichardt (Howard Hughs Institute, San Francisco). Human TrkA template DNA was supplied by Prof. Uri Saragovi (McGill University), while rat TrkA, TrkB and TrkC template DNA was provided by Prof. Louis Reichardt.

TrkA human N-terminal 5'-AGA GAA TTC TGC CCC GAT GCC TGC TGC CCC CAC-3'

TrkA human C-terminal 5'-AGA CTC TAG ACC TGT TTC GTC CTT CTT CTC CAC CGG GTC-3'

TrkA rat N-terminal 5'-AGA GAA TCC TGT CGT GAG ACC TGC TGT CCC GTG GGC-3'

TrkA rat C-terminal 5'-AGA CTC TAG ACC TGT TTC GTC CTT CTT CTC CAC TGG GTC-3'

For both human and rat TrkA oligonucleotides, the N-terminal was designed to incorporate an EcoRI site, while the C-terminal oligonucleotide incorporates an XbaI site. This design permitted direct ligation of the PCR product into the same sites in the expression vector pPICZαA .

TrkB rat N-terminal 5'-AGA GAA TTC TGC CCC ATG TCC TGC AAA TGC-3'

TrkB rat C-terminal 5'-AGA CTC TAG ACC CTC CCG ATT GGT TTG GTC AGC AAC ATC-3'

For the TrkB construct, the N-terminal oligonucleotide was designed to incorporate an EcoRI site, while the C-terminal oligonucleotide incorporates an XbaI site, thus allowing direct cloning of the PCR product into the same sites in pPICZαA.

TrkC rat N-terminal 5'-AGA AGC GGC CGC TGC CCT GCA AAT TGT GTC TGC AGC AAG ACT-3'

TrkC rat C-terminal 5'-AGA CTC TAG ACC AGT GTC TTC CTC TGG TTT GTG GGT CAC AGT-3'

The N-terminal oligonucleotide for the TrkC construct includes an XbaI site, while the C-terminal oligonucleotide incorporates a NotI site, permitting direct cloning of the PCR product into these sites in pPICZαA.

All PCR solutions consisted of a total of 100µl of the following components:

65.5µl H_2O

65.5 5 µl of each of the N and C-terminal oligonucleotides (10 µM each)

3 µl of 50 mM $MgCl_2$

1 µl of 1 ng/µl of the DNA template

10 µl of 2 mM dNTP

10 µl of 10x PCR buffer

0.5 µl Taq polymerase (BRL)

The following PCR conditions using an Ericomp thermal cycler were employed to give the final PCR products.

Cycles (30)	1' at 94ºC	2' at 94ºC	2' at 72ºC
Last cycle	1' at 94ºC	2' at 50ºC	10' at 72ºC

2.4 Cloning Techniques following PCR

All techniques for the cloning of the four Trk extra-cellular domains expressed in *P. pastoris*, are illustrated by the following protocols for the two TrkA protein expression systems. Only the restriction enzymes used to digest pPICZαA for insertion of the PCR product and subsequently, to confirm that the correct constructs for TrkB and TrkC were ligated into pPICZαA, are different. An aliquot of DNA from each PCR reaction vial was run on a 1% agarose gel in TAE buffer together with an appropriate DNA standard (Figure 2.3). All PCR products ran on the gel at ~ 1.2 kB, the expected size for the DNA representing the extra-cellular domains of the four Trk receptor proteins. All PCR products (1µl of the 100µl reaction mixture) were ligated into the pCR2.1 vector (Invitrogen) at 15°C overnight following the protocols for the TA cloning kit (Invitrogen). Taq polymerase has a nontemplate-dependent activity, which adds a single deoxyadenosine (A) to the 3' ends of PCR products.

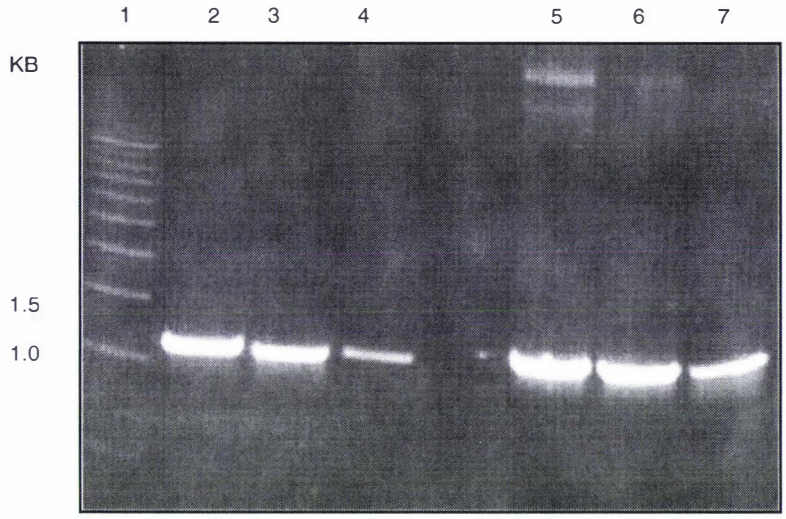

Figure 2.3 PCR products for human and rat TrkA extracellular domains.
Lane 1 is the 500bp standard (BioRad). Lanes 2, 3 and 4 show the PCR product for human TrkA. Lanes 5,6,7 show the PCR product for rat TrkA. The expected size for the cDNA for both constructs is ~ 1.2kB and it can be seen that this is the size of the DNA obtained. Essentially the same results were obtained for the PCR products of TrkB rat and TrkC rat extracellular domains.

The linearized pCR2.1 vector has a single 3' deoxythymidine (T) residue, thus allowing efficient ligation of the PCR insert into the pCR2.1 vector. Following ligation, INVαF' competent *E. coli* cells (Invitrogen) were transformed by heat shock with the new construct trk/TA vector. The transformed *E. coli* was plated onto an LB[4] plate containing 100 μg/ml of ampicillin and Xgal[5] at a concentration of 40 mg/ml of medium. After growing at 37°C overnight, 10 white colonies of each construct were selected and grown overnight in 5ml of LB containing 100 μg/ml of ampicillin. DNA was extracted from each overnight culture using a Rapid Pure Mini Prep kit (RPM kit, BIO101). All DNA was digested by restriction enzymes, EcoRI/XbaI (all restriction enzymes and reaction buffers were from New England Biolabs) for the two TrkA constructs, EcoRI/ XbaI for the TrkB construct and XbaI/ NotI for the TrkC construct to confirm the presence of the correctly sized insert (e.g. Figure 2.3). After enzymatic digestion (typically overnight), each reaction mixture was

[4] Luria Broth

[5] 5'-Bromo-4-chloro-3-indolyl- [beta] -D-galactopyranoside $C_{14}H_{15}BrClNO_6$

run on a 1% agarose gel to determine which DNA was of the appropriate size to be inserted into pPICZαA (Figure 2.4).

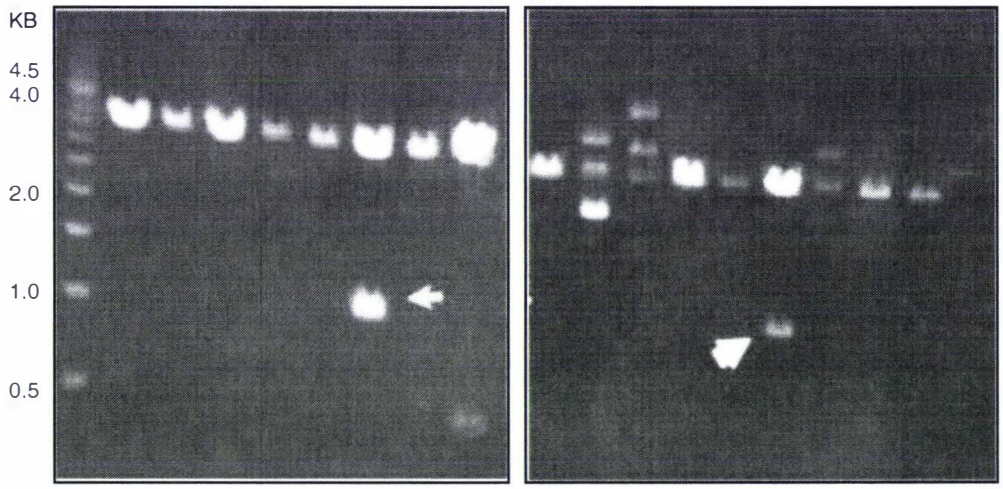

Figure 2.4 Agarose gels of the restriction enzyme digests of the plasmid DNA from the PCR constructs. Arrows indicate the correct size cDNA insert. Gel (a) is human TrkA while Gel (b) is rat TrkA. One colony from each analysis had the correct sized insert.

The expression vector was digested with the appropriate restriction enzymes for the insertion of the Trk DNA into pPICZαA. An enzymatic digest of one trkA/TA construct (for each of the four Trk proteins), identified as having the correctly inserted trk cDNA, was heated at 65°C for 20 min to heat inactivate the restriction enzymes. An overnight ligation at 15°C of 1μl of the digested pPICZαA vector and 1μl the digest of trk/TA construct was performed in a 10 μl total reaction volume. After ligation, 1μl of the reaction mixture was used to transform competent DH5α *E. coli* (prepared by the $CaCl_2$ method; Sambrook, Fritsch, Maniatis, 2nd edition, 1.82). The transformed *E. coli* was plated on LB plates containing 100 μg/ml of ampicillin and grown at 37°C overnight. Fifteen colonies from the plate were selected and grown overnight at 37°C in 5 ml of LB containing 100 μg/ml of ampicillin.

DNA was prepared from each of the overnight cultures by Rapid Pure Miniprep (RPM). DNA of an appropriate size, namely, 4.8 kB (1.2 kB trk cDNA+3.6 kB for pPICZαA) were then digested with EcoRI/Xbal in the case of the two trkA/ pPICZαA constructs, the trkB/ pPICZαA construct and

XbaI/NotI for the trkC/pPICZαA construct. All digests were run on a 1% agarose gel together with an appropriate DNA standard. The gel was stained with ethidium bromide, visualized with UV and photographed. Gels of the digested trkA/pPICZαA constructs for human and rat are shown below. Essentially the same results were obtained for the constructs trkB/ pPICZαA and trkC/pPICZαA (Figure 2.5 through Figure 2.8).

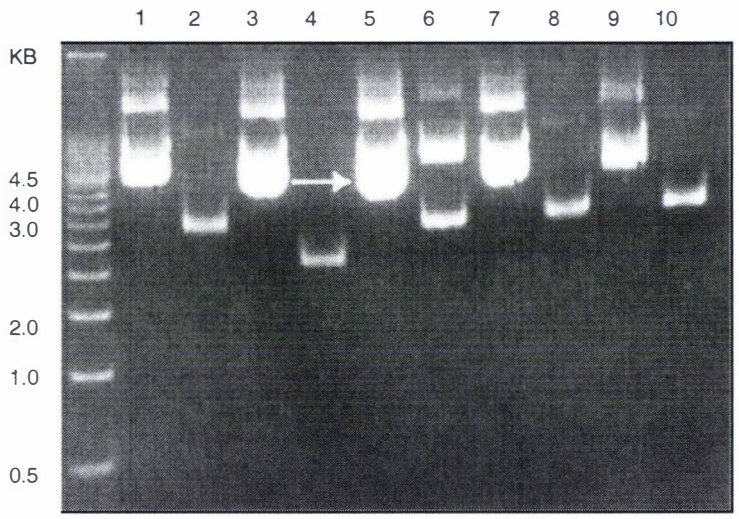

Figure 2.5 This gel shows digests of the ligated DNA of trkA (human) cDNA and of pPICZαA. The purified DNA from 5 *E. coli* colonies shows a plasmid of the expected size (indicated by an arrow) for the construct trkA/pPICZαA for human TrkA.

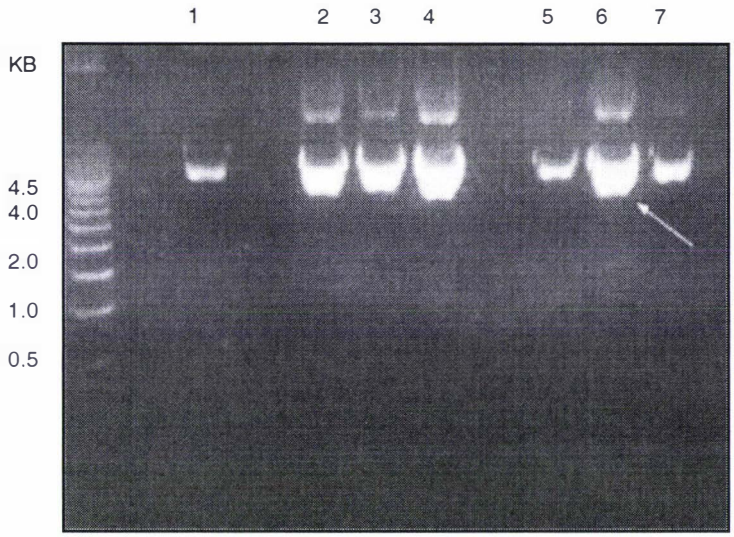

Figure 2.6 This gel shows digests of the ligated DNA of trkA (rat) cDNA and of pPICZαA. The purified DNA from 6 of the *E. coli* colonies shows a plasmid of the expected size for the construct trkA/pPICZαA for rat TrkA.

In the case of the trkA/pPICZαA constructs, additional digests of the DNA with EcoRI/XbaI, EcoRI/BamHI, and EcoR1/HindIII were made to further confirm that the correct cDNA had been cloned into the expression vector. No additional digests were made for the trkB/ pPICZαA and trkC/pPICZαA since the observed bands on the gels were identical to those obtained in a previous cloning by Louis Reichardt of these two trk cDNA's, using the same PCR products and similar protocols. DNA sequencing subsequently confirmed that the constructs contained the correct sequences.

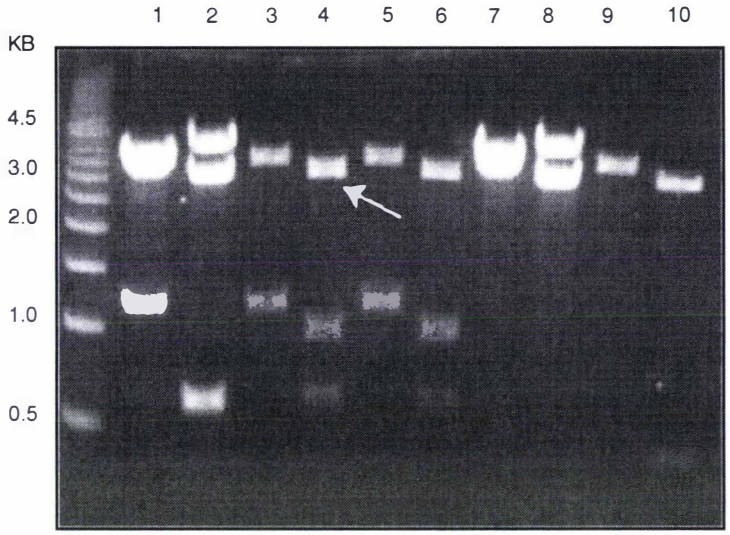

Figure 2.7 Restriction digests of rat TrkA/pPICZαA plasmids. The agarose gel above shows the EcoRI/Xba/BamHI restriction enzyme digest of purified DNA from colonies of *E. coli* transformed with the rat construct trkA/pPICZαA. Lanes 1, 4 and 6 show DNA of the size corresponding to trkA. These colonies were picked and grown in LB for maxiprep purified DNA for sequencing and transformation of *P. pastoris*.

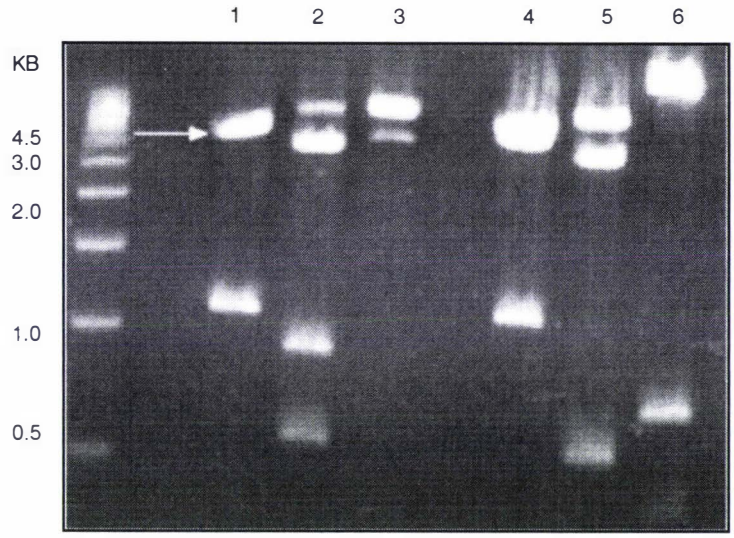

Figure 2.8 Restriction digests of human TrkA/pPICZαA plasmids. The agarose gel above shows the EcoRI/Xba/BamHI restriction enzyme digest of purified DNA from colonies of *E. coli* transformed with the human construct trkA/pPICZαA. Lanes 1 and 4 show DNA of the size corresponding to trkA and these colonies were picked and grown in LB for maxiprep purified DNA for sequencing and transformation of *P. pastoris*.

2.5 Transformation of *P. pastoris* strain X33 with trk/pPICZαA

Expression constructs were transformed into the *P. pastoris* strain X33. This is a wild-type Pichia strain that permits selection with the antibiotic Zeocin and exhibits large-scale growth. Transformation of X33 with all four trk/pPICZαA constructs followed the protocols in the EasySelect™ P., expression kit (Invitrogen). Briefly, ~2 μg of each trk/pPICZαA construct (from an RPM preparation) was linearized by digestion overnight with the restriction enzyme PmeI. Following digestion, the linearized DNA was precipitated with ethanol (Sambrook, Fritsch, Maniatis 2nd edition, E12) to reduce the digestion volume from 50 μl to 5 μl for transformation. Competent X33 cells were prepared following the protocol in the EasySelect™ Pichia expression kit manual. Transformed X33 was plated in two aliquots of 50 and 150 μl on YPDS[6] plates

[6] Growth medium: composition details may be found in the Invitrogen Pichia protein expression manual: 2% tryptone, 1% yeast extract, 2% glucose, 1 M sorbitol, 2% agar.

containing Zeocin at 100 μg/ml of medium. The plates were incubated at 30°C until colonies (~30) were observed (3-4 days in each case).

Ten colonies of each transformant were selected and grown in 5 ml of BMGY[7] medium containing Zeocin at 25 μg/ml of medium for 18 hr at 30°C. At the end of the initial growth period, the cells were gently centrifuged, the BMGY medium poured off and replaced with MM medium containing 25 μg/ml of Zeocin. After introduction of the cells into MM, a 100 μl aliquot was taken from each culture; this was designated as the uninduced protein sample and was stored at -70°C. Growth of all cultures was continued at 30°C with shaking for 96 hr. Every 24 hr, absolute methanol was added to a concentration of 5% of the total culture volume and a 100 μl aliquot was taken, centrifuged and stored at -70°C for analysis of protein expression. An SDS-PAGE gel was run of all the timed samples. The gel was silver stained and examined for protein expression. Only 2-3 clones of each of the four constructs showed the presence of the putative Trk protein. One colony for each was chosen for large-scale protein production trials.

Overnight cultures of all four Trk constructs (from the best expressing clones) were grown overnight in 100 ml of BMGY medium containing 25 μg of Zeocin. After reaching an OD_{600} of ~ 2, the yeast cells were removed by centrifugation and then transferred to 100 ml of MM medium containing 25 μg of Zeocin. These cultures were grown for 96 hr as previously described. After completion of the incubation period, SDS-PAGE gels were run and proteins visualized by silver staining. From the gels, it was clear that for the TrkA human protein, induction could be continued, at least through 96 hr with little or no degradation of protein (Figure 2.9). For rat TrkA, protein expression could be continued up to 48 hr with few degradation products being observable (Figure 2.9). After 48 hr, degradation products increase dramatically, rising to ~ 50% after 72 hr. The same observations were made for the TrkB and TrkC proteins. Hence it appears that the most viable protein expression period is 96 hr for human TrkA and 48 hr for rat TrkA, rat TrkB and rat TrkC.

[7] BMGY is a medium for growth of bacteria. : yeast extract, 10 g/L; meat peptone, 20 g/L; 100 mM potassium phosphate buffer pH 6.0; yeast nitrogen base without amino acids, 13.4 g/L; biotin, 400g/L; glycerol, 10ml/L.

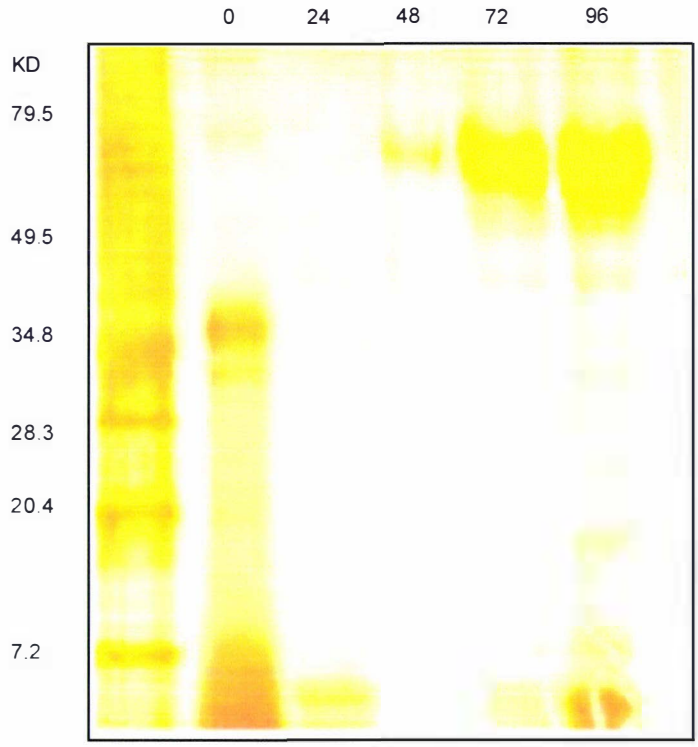

Figure 2.9 Expression of TrkA in *P. pastoris*. Above is shown a silver stained 4-20% gradient gel (Biorad) of the timed expression of TrkA (rat). Expression is indicated before induction (time = 0) and at 24, 48, 72 and 96 hr after induction. The expressed protein runs at ~ 70 kD on the gel. Some unknown contaminants are observed before induction; possibly medium proteins that were degraded with time, or metabolized by the yeast during growth.

2.6 Large scale protein production and purification

In order to obtain sufficient protein for further studies, 3 liters of culture were produced for each of the four Trk proteins. Production techniques followed the same methodology of the smaller (100 ml) cultures and optimal growth times for each protein were those established for the smaller trial cultures.

Initial purification techniques sought to exploit the C-terminal His-tag on each protein and the affinity of the tag for a Ni^{2+} chelating column. All trials of this purification method utilized the

QIAexpress Ni-NTA protein purification system (Qiagen). Since the TrkB and TrkC proteins were available for purification before the two TrkA proteins, only these two proteins were used in testing the viability of purification by chelating column. After 48 hr of growth, the yeast cells were separated by centrifugation (4000 x g) from the medium containing the recombinant protein. The 3 liters of medium was concentrated to ~ 500 ml using a spiral-wound cartridge (5000 MW cutoff) concentrator (Amicon). This system was used to exchange the supernatant into 20 mM Tris/HCL pH 8.0 (at room temperature) containing 150 mM NaCl, by addition of the buffer after the supernatant volume had been reduced to ~ 200 ml. Four rounds of concentration and buffer exchange were made for each protein.

Further concentration to 50 ml was achieved using a miniplate concentrator (Amicon). All concentrations were performed at 4°C. A disposable Poly-Prep column (BioRad) was packed with 1 ml of Ni-NTA agarose resin (Qiagen) and equilibrated with 20 column volumes of 20 mM Tris/HCL pH 8.0 containing 300 mM NaCl and 0.1% Tween-20. Concentrated supernatant (5 ml) was added to the column. Non-specifically bound protein was eluted from the column with the addition of 20 column volumes of 20 mM Tris/HCL pH 8.0 containing 300 mM NaCl and 0.1% Tween-20. After this wash procedure, specifically bound protein was eluted from the column by the addition of 1 ml aliquots of 20 mM Tris/HCL pH 8.0 containing 100 mM NaCl and various concentrations of imidazole (Sigma). One ml fractions that eluted from the column were collected and stored on ice for further analysis. Imidizole concentrations varied from 10 mM to 600 mM. A final wash with 0.1% SDS was used to remove all remaining protein from the column. All collected fractions were concentrated in microcon microconcentrators of 3000 mW cutoff (Amicon). Concentrated fractions were run on a 4-15% SDS-PAGE gel together with a 10-200 kD protein standard.

It was clear from SDS-PAGE gels, that while the His-tagged protein could be eluted from the Ni-NTA agarose resin with imidizole, contaminant proteins consisting of ~ 50% of the total protein, eluted together with the Trk protein. These results suggested that purification of the His-tagged Trk proteins would be difficult, if not impossible by chelating columns[8] (Blanc et al. 1998). In addition, these results suggest that the six histidines required for specific binding to the resin, may be folded up against the body of the protein[9], thus preventing strong specific binding of

[8] Difficulties with purification of His-tagged proteins is well documented on Internet molecular biology sites.

[9] Note taken from the Qiagen His-tag protein purification manual.

protein to the Ni cations coordinated to the resin. It is generally accepted that six free histidines are required for strong binding to the chelating column.

2.7 Purification by ion exchange chromatography

In an attempt to increase the yield of Trk proteins expressed in *P. pastoris*, growth of the four transformants undertaken in a Bioflo 3000 Bioreactor (New Brunswick Scientific). An initial starter culture was grown overnight by adding 10 µl of freezer stock of each transformant to 25 ml of BMGY (Invitogen) medium containing 50 µg of Zeocin. The initial starter culture was added to 500 ml of BMGY and then grown to an OD_{600} of 2. The final culture was centrifuged (3000xg) and the resulting pellet suspended in 50 ml of BMMY (Invitrogen), which was then re-suspended in 2 L of BMMY in the bioreactor vessel. Absolute methanol was added to the medium at a rate of 10 ml/hr throughout the growth period. The temperature was maintained at 30°C while the medium pH was allowed to drop from 6.0 at the time of inoculation, to a pH of ~4 at the end of 72 hr.

2.8 Purification of Trk protein

After 72 hr of growth, the medium was centrifuged (3000xg) to remove cells and the remaining supernatant was applied at a flow rate of 20 ml/min with a peristaltic pump, to a 2 cm x 50 cm column of S-sepharose anion exchange resin (HS column, Pharmacia), pre-equilibrated to pH 4.0 with 20 mM citrate buffer (Figure 2.10). On completion of the application of the supernatant, the column was connected to a BioCAD SPRINT perfusion chromatography system (PerSeptive Biosystems) and then washed with 20 mM citrate buffer pH 4.0 at a flow rate of 10 ml/min to remove non-specifically bound protein. Specifically bound protein was eluted from the column with a two-step gradient of 500 and 2000 mM NaCl (in 20 mM citrate buffer pH 4.0) over 30 min at a flow rate of 10 ml/min. The protein eluted with 500 mM NaCl was dialyzed in 20 mM Tris/HCL pH 8.0 (3 x 2 liters).

After exchanging into 20 mM Tris/HCl pH 8.0 buffer, the protein was applied at a flow rate of 5 ml/min to an HQ Poros cation exchange column (PerSeptive Biosystems) equilibrated with the same buffer (Figure 2.11). Non-specifically bound protein was removed from the column with a 20

mM Tris/HCl pH 8.0 buffer wash. Specifically bound protein was eluted from the column with a two-step gradient of NaCl, 600 and 1000 mM in 20 mM Tris/HCL, pH 8.0. SDS-gel analysis of the protein that did not bind to the column, together with eluted specifically bound protein, indicates that the protein assumed to be the Trk receptor, was eluted within the 600 mM NaCl fraction. The flow through fraction did not stain with Coomassie brilliant blue dye, indicating that while this fraction has high 260 and 280 nm absorbance, it probably consists of molecules originating from the growth medium.

Preferential binding of highly negatively charged medium molecules provides an explanation for the inability of both nickel and copper chelating chromatography to directly purify Trk protein from the growth medium. A 1 ml chelating column (Pharmacia) was charged with 100 mM $CuCl_2$, attached to a BioCAD FPLC (Applied Biosystems) and then equilibrated with 20 mM Tris/HCl pH 7.4, 500 mM NaCl at a flow rate of 1 ml/min. The 600 mM NaCl fraction eluted from the cation exchange column (peak 2, Figure 2.11) was applied to the chelating resin at a flow rate of 1 ml/min and protein contaminants were removed from the column by a step gradient of ammonium chloride. Specifically bound His-tagged protein was eluted from the column with 50 mM EDTA dissolved in the same equilibration buffer. Following elution from the chelating column, contaminating $CuCl_2$, NaCl and EDTA was removed from the protein by several rounds of buffer exchange (20 mM Hepes pH 7.4) in a Vivaspin concentrator (10 kD cutoff). Concentrated protein was stored at -80°C.

Figures 2.10, 2.11 and 2.12 show typical elution profiles for the purification of a recombinant Trk ED on HS, HQ and chelating columns, respectively. This procedure yielded a single band of each protein on an SDS-PAGE gel. Figure 2.13 and Figure 2.14 show human TrkA ED and human TrkB respectively, as typical examples of the results of the purification protocol. It was noted that the Trk ED preparations migrate as a slightly diffuse band and this may be due to microhetrogeneity in glycosylation.

Table 2.12 summarizes the yields of the Trk ED proteins obtained from *P. pastoris*. Two types of *P. pastoris* strains[10] were used to express the Trk proteins; namely, Mut^+ and Mut^S. With the

[10] Pichia Strains. There are two genes in *P. pastoris* that code for alcohol oxidase, *AUG1* and *AUG2* (alcohol utilizing gene) (Raymond et al. 1998). The *AUG1* gene appears to be responsible for the majority of alcohol oxidase activity in the cell. The *AUG1* gene has been isolated and a

exception of the TrkB rat ED, the best results were obtained with the expression method using the Mut^+ strain. The final yields varied widely from 0.03 to 70.3 mg/L. The reasons for these differences were not investigated further. This protocol of anion exchange (Poros Perspective Biosystems HS resin), cation exchange (Poros Perspective Biosystems HQ column) and chelating columns (Pharmacia) proved the most consistent purification protocol for purifying Trk proteins expressed in *P. pastoris*.

---

plasmid-borne version of the *AUG1* promoter is used to drive expression of the gene of interest encoding the desired heterologous protein (Raymond et al. 1998). The nucleotide sequence of *AUG2* is about 83% identical to *AUG1* and strains with an *aug1* genotype grow slowly on methanol. This slow growth on methanol allows isolation of Mut^S strains (Raymond et al. 1998). Loss of the *AUG1* gene and thus a loss of most of the cell's alcohol oxidase activity, results in a strain that is phenotypically Mut^S (Methanol utilization slow) and exhibits poor growth on methanol medium. Mut^+ (Methanol utilization plus) refers to the wild type ability of strains to metabolize methanol as the sole carbon source. Identifying the Mut phenotype of a *P. pichia* transformant may help to optimize growth conditions. (From Invitrogen *P. pastoris* expression manual).

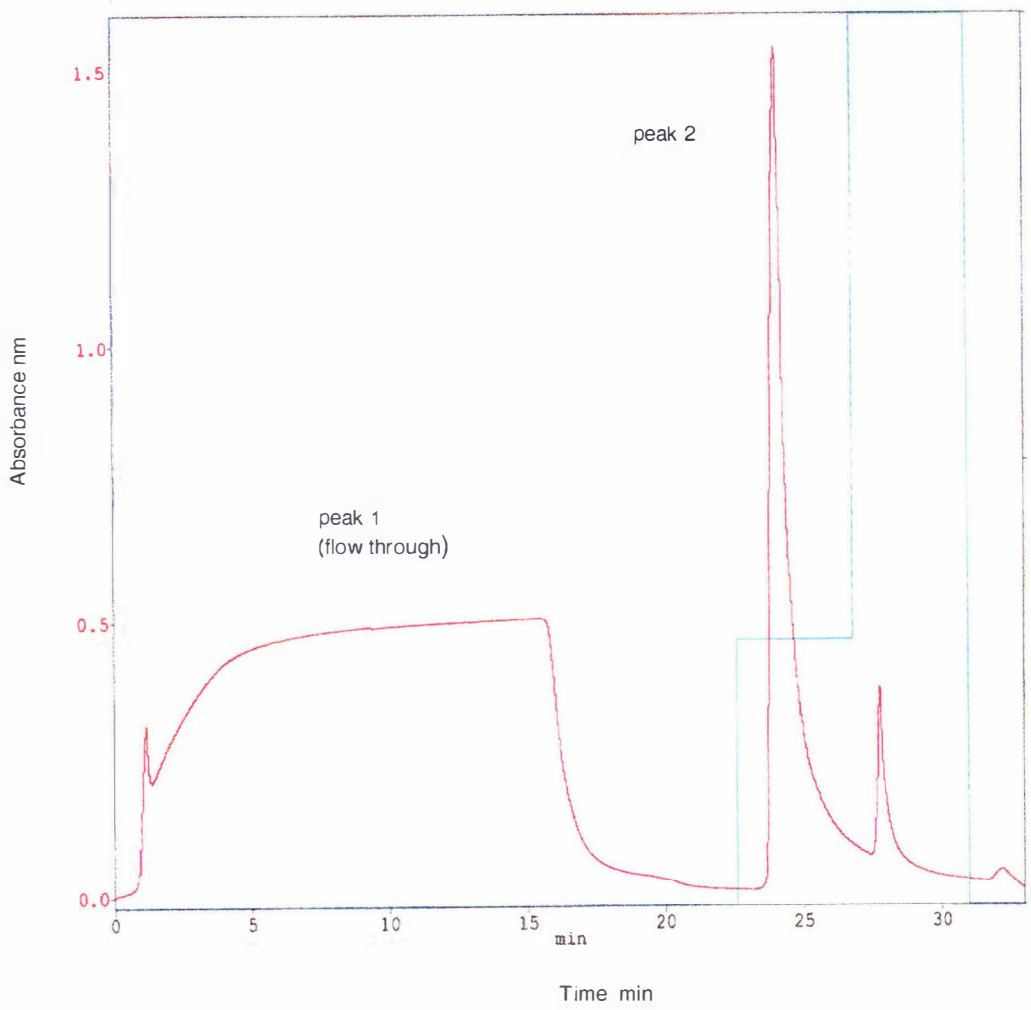

Figure 2.10 The Trk proteins expressed in *P. pastoris* were purified in a three-step process. The first purification step consisted of elution of the protein from an anion exchange column. Medium containing the *P. pastoris* expressed protein was applied to the column pre-equilibrated to pH 4.0 with 20 mM citrate buffer. Bound protein was removed from the column with a two-step NaCl gradient (500 and 2000 mM). A typical elution profile for the His-tagged Trk protein (human), from the anion exchange column is shown above. Peak 1, probably consists of medium molecules that have high absorbance at 280 nm, but do not stain with Coomassie blue on an SDS-PAGE gel. Peak 2 contains the purported Trk protein (as determined by SDS-PAGE gel) eluted with 500 mM NaCl, between ~ 23 and ~ 27 mins. A minor contaminant is removed from the column by 2000 mM NaCl at ~ 28 min. The NaCl step gradient is shown by the blue trace. Protein found in peak 2 was dialyzed in 20 mM Tris/HCl pH 8.0, 500 mM NaCl before application to the cation exchange column.

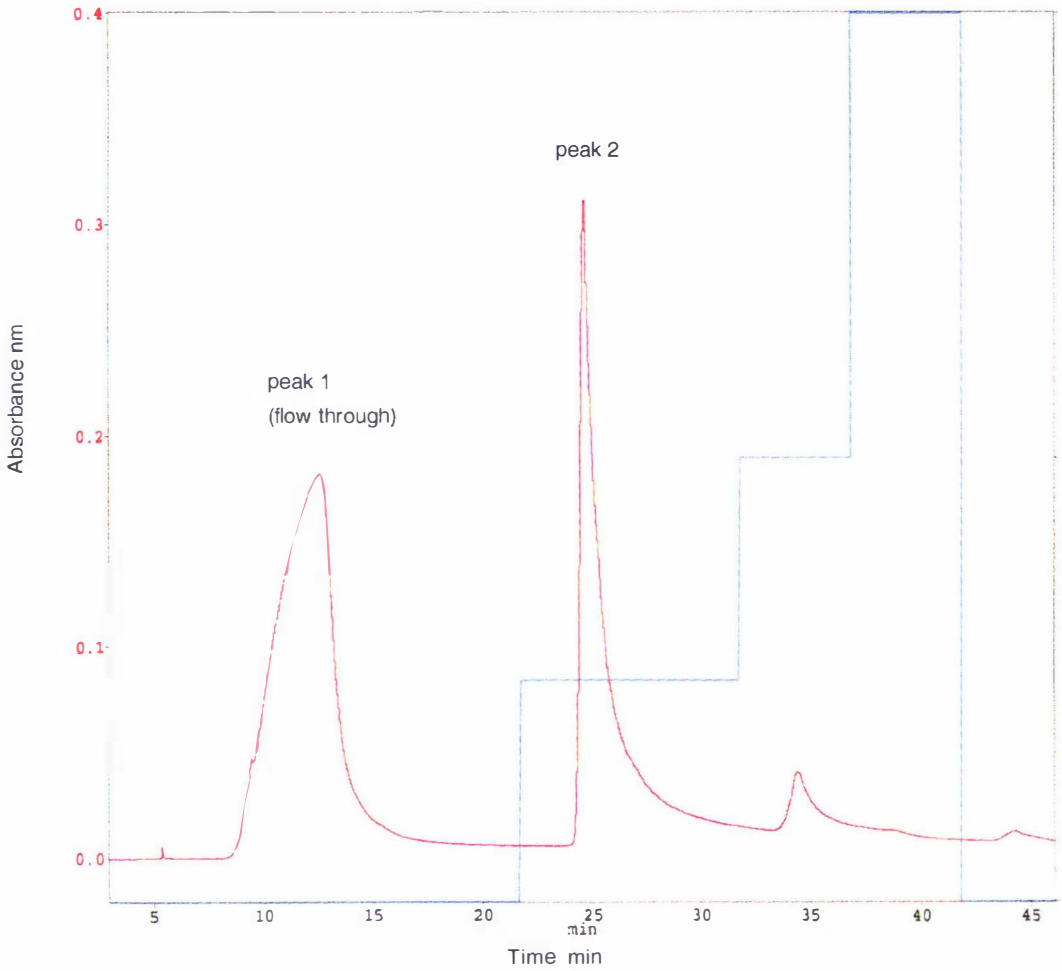

Figure 2.11 The second step in the Trk protein purification, consisted of elution from a cation exchange column. Protein eluted from the anion exchange column in peak 2 (Figure 2.10), was dialyzed in 20 mM Tris/HCl pH 8.0, 500 mM NaCl and loaded on the column as described above. Proteins were eluted from the column with a step gradient of NaCl (600, 1000, 2000 mM) in 20 mM Tris/HCl pH 8.0. A typical elution profile for the His-tagged Trk protein from the cation exchange column is shown above. Peak 1, probably consists of medium molecules that have high absorbance at 280 nm, but do not stain with Coomassie blue on an SDS-PAGE gel. Peak 2 contains the purported Trk protein eluted with 600 mM NaCl between ~ 22 min and ~ 30 min. A minor contaminant protein is removed from the column at ~ 35 min by 1000 mM NaCl. No further contaminants were removed when the NaCl gradient was raised to 2000 mM at ~ 37 min. Protein from peak 2 was dialyzed into 20 mM Tris/HCl pH 7.4, 500 mM NaCl and then applied to a metal chelating column after the procedures described above. Peak 3 is a minor contaminant eluted with 1000 mM NaCl. The NaCl step gradient is shown by the blue trace.

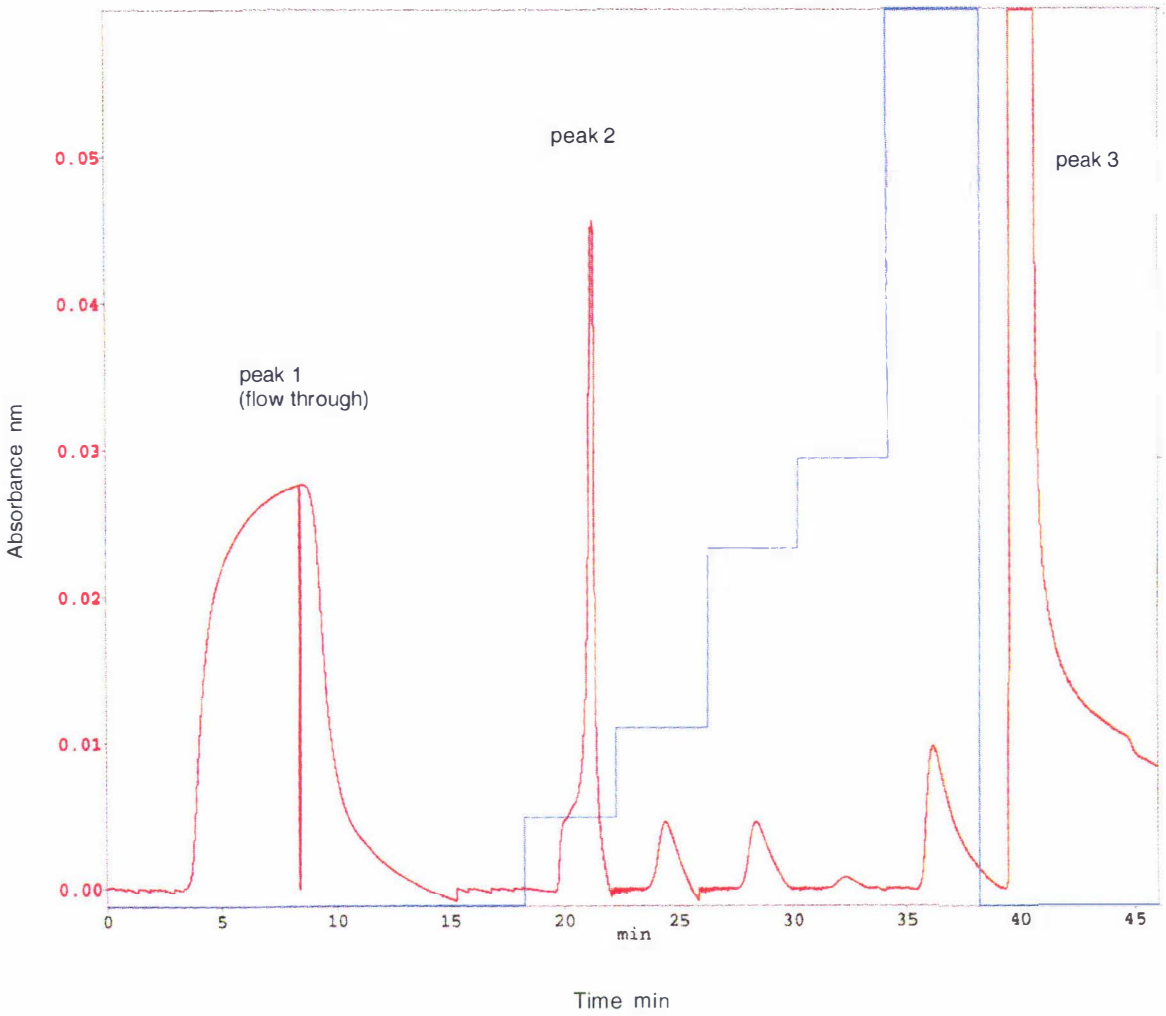

Figure 2.12 The third step in the purification of the His-tagged Trk proteins expressed in *P. pastoris* consists of a chelating column equilibrated in 20 mM Tris/HCl pH 7.4, 500 mM NaCl. Protein from peak 2 (Figure 2.11) was dialyzed into 20 mM Tris/HCl pH 7.4, 500 mM NaCl and loaded on the chelating column. A Step gradient of NH_4Cl (200, 400, 800, 1000, 2000 mM) was used to remove contaminating proteins from the Trk protein. Peak 1, consists of molecules (medium) that have high absorbance at 280 nm, but do not stain with Coomassie blue on an SDS-PAGE gel. Peak 2 and subsequent small peaks eluted between ~ 20 min and ~ 38 min, are minor contaminants. At ~ 37 min the column was washed with 20 mM Tris/HCl pH 7.4, 500 mM NaCl. Protein was eluted from the column with 50 mM EDTA in 20 mM Tris/HCl pH 7.4, 500 mM NaCl. Peak 3 contains the purported Trk protein, eluted from the column with EDTA. The NH_4Cl_2 step gradient is shown by the blue trace. NaCl and EDTA were removed from the protein by several rounds of buffer exchange (20 mM Hepes pH 7.4).

2.9 Protein Expression Results

Table 2.12 Expression levels of purified TrkA, TrkB and TrkC proteins produced in *P. pastoris*. The protein expression level was determined as described in section 2.14. The protein yield is given in mg/L of growth medium.

Construct	Yield
TrkA human Mut+	0.07
TrkA human Muts	no expression
TrkA rat Mut+	3.00
TrkA rat Muts	no expression
TrkB rat Mut+	0.05
TrkB rat Muts	70.3
TrkC rat Mut+	0.30
TrkC rat Muts	0.03

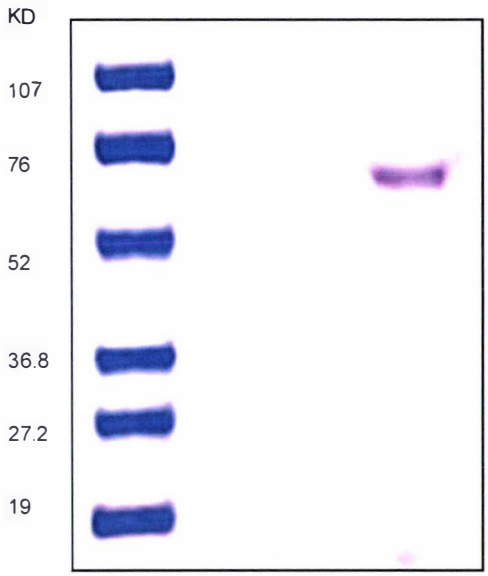

Figure 2.13 A Coomassie stained SDS-gel of TrkA extracellular domain (rat) expressed in *P. pastoris*. The protein runs as a slightly diffuse band; possibly a consequence of the protein being heterogeneously glycosylated.

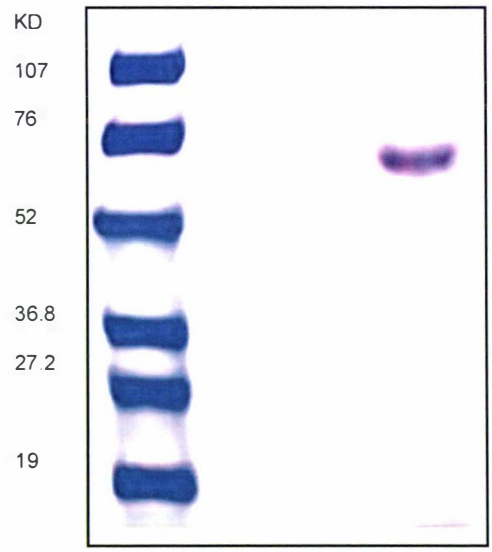

Figure 2.14 A Coomassie stained SDS-gel of the TrkB extracellular domain (rat) expressed in *P. pastoris*. The protein runs as a slightly diffuse band; possibly a consequence of the protein being heterogeneously glycosylated.

2.10 Expression of Trk proteins in *E. coli*

Expression of the complete extra-cellular domain and sub-domains of TrkA, TrkB and TrkC in *E. coli* was attempted using cDNA extracellular domain constructs provided by Dr. Rainer Schneider (University of Innsbruck). These constructs have been described previously (Windisch et al. 1995a, b, c) and are all expressed as maltose binding protein-fusion proteins (MBP-fusion proteins) in the expression vector pMAL-p2 (New England Biolabs) using the *E. coli* strain M15. Although binding studies have been conducted using the MBP-fusion proteins, only the equilibrium-binding constant could be determined by the method employed. With newly available biosensor techniques, it seemed feasible to attempt to measure affinity and dissociation constants for the fusion proteins and compare these data with the values obtained from the Trk extracellular domain proteins produced in *P. pastoris*.

Initial attempts to express the MBP-fusion proteins in M15[11] were unsuccessful, with the exception of the Ig-like domain of TrkA. All subsequent expression of the fusion proteins was undertaken using the *E. coli* strain BL21(DE3) (Novagen). All MBP-fusion protein constructs used in this study are listed in Tables 2.1, 2.5 and 2.9.

2.11 Expression of MBP-fusion Proteins

Competent BL21(DE3) *E. coli* (Novagen) was prepared by the $CaCl_2$ method (Sambrook, Fritsch, Maniatis, 2nd edition, 1.82). The *E. coli* was transformed by heat shock with each plasmid containing cDNA representing the different domains of the Trk receptors and grown on LB plates containing ampicillin (200 ug/ml) at 37°C overnight. A single colony was selected and grown in 50 ml of rich medium[12] containing ampicillin (200 ug/ml), overnight at 37°C. The initial 50 ml inoculum was added to 1000 ml of rich medium containing ampicillin (200 ug/ml) equilibrated to 30°C overnight in a 4-liter flask. Growth of the trk transformed BL21(DE3) was monitored at short intervals until the absorbance at 600 nm reached ~0.3. At this time, IPTG was added to a final concentration of 0.5 mM and growth was continued with vigorous agitation for a further 90 min.

---

[11] The expression vector used by Prof. Rainer Schneider.

[12] 10 gm Tryptone, 5 gm Yeast Nitrogen base, 5 gm NaCl, 2 gm glucose in 1000 ml of water

After 90 min the supernatant was centrifuged and the resulting cell pellet was resuspended in 20 ml of 20 mM Tris/HCL pH 7.4 containing 200 mM NaCl, 1mM EDTA and 1 mM PMSF. The resuspended cells were lysed by passage (3x) through a French press and centrifuged at 10,000xg for 30 min. A 1 ml bed volume amylose (New England Biolabs) column (2 cm diameter) was equilibrated with 20 column volumes of the lysis buffer. Centrifuged supernatant was diluted with the lysis buffer to a total volume of 50 ml and applied at a flow rate of ~0.5 ml/min to the amylose column at 4°C.

After loading the supernatant onto the resin, non specifically bound proteins were eluted by washing the column with ~150 ml of the lysis buffer (NaCl to 500 mM) at a flow rate of ~0.5 ml/min. Additional multiple 5 ml aliquots of the lysis buffer were added to the column after the initial wash and the level of protein and nucleic acids eluted was monitored by collecting 0.5 ml fractions and measurement of absorbance at 280 nm and 260 mm respectively. When the 280 nm absorbance reached a level less than 0.001, specifically bound protein was eluted from the amylose resin by the addition of 5 ml aliquots of the lysis buffer containing 20 mM maltose (Sigma). The eluate was collected in 0.5 ml fractions and those fractions with a 280 nm absorbance > 0.1 were pooled.

After a measurement of the 260 nm and 280 nm absorbance of the pooled protein, the sample was concentrated in a vivaspin 15 (10 kD cutoff) concentrator (Vivascience). Maltose removal and buffer exchange was achieved by addition of aliquots (10 ml total) of 20 mM Hepes pH 7.4 followed by further concentration. Figure 2.15 and Figure 2.16 show an SDS-PAGE analysis of the purified MBP-fusion proteins of TrkA and TrkB respectively. The apparent molecular weights of the purified proteins are consistent with the calculated values (i.e., MPB plus the Trk domain). The yield of the MBP-fusion proteins ranged from 0.03 mg/L for the full length TrkB extracellular domain, to 10 mg/L for TrkA immunoglobulin-like domain. In most instances the yield was less than 0.5 mg/L, but in all instances, sufficient protein was produced for subsequent studies.

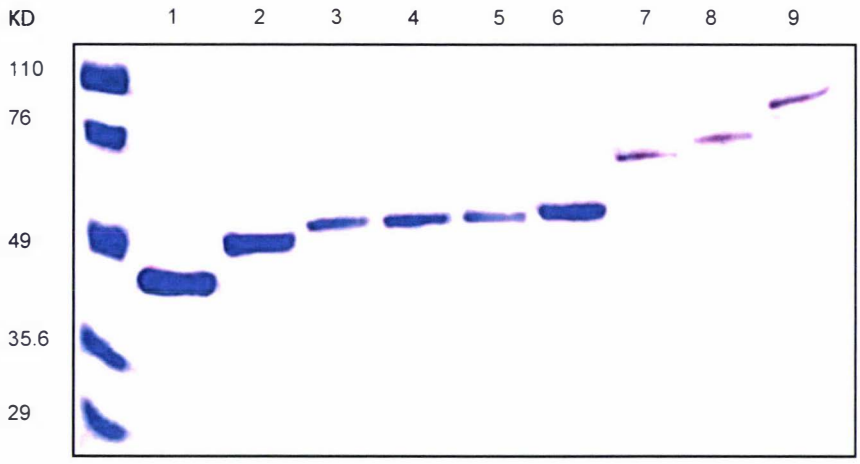

Figure 2.15 A Coomassie stained SDS-PAGE gel of the MBP-fusion proteins, shows the TrkA MBP-fusion proteins after purification. Above is shown a 10% gel (Biorad) of TrkA MBP-fusion proteins. Lane 1 is MBP2[13] (New England Biolabs). Lane 2 is LRR, lane 3 is C1LRR12, and Lane 4 is LRR23C2. Lane 5 is C1LRR. Lane 6 is LRRC2. Lane 7 is the Ig-like domain. Lane 8 is the Ig-like domain with the C-terminal cysteine rich region. Lane 9 is the ED. It appears from overloaded gels, that each protein approaches 95% in purity.

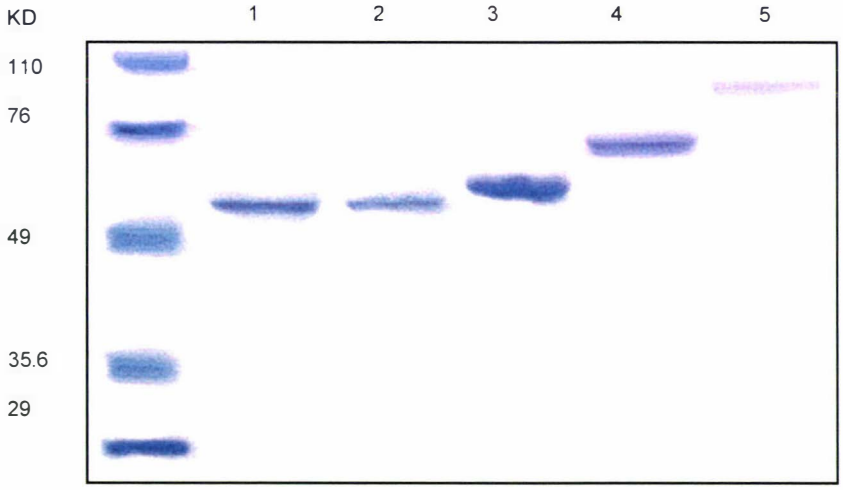

Figure 2.16 A Coomassie stained SDS-PAGE gel of the MBP-fusion proteins, shows the TrkB MBP-fusion proteins after purification. Lane 1 is C1LRR, Lane 2 is LRRC2, and Lane 3 is C1LRRC2. Lane 4 is the Ig-like domain. Lane 5 is the full length ED.

[13] MBP2 is attached to the N-terminus of all MBP-fusion proteins expressed for this study.

Table 2.13 Approximate expression levels of the MBP-fusion proteins per liter of culture. The yield is given in mg/L of culture.

Construct	Yield
TrkA LRR2	0.65
TrkA LRR	0.42
TrkA C1LRR	0.15
TrkA LRRC2	6.25
TrkA C1LRR12	1.42
TrkA LRR23C2	0.13
TrkA Ig	0.04
TrkA IgC2	10.25
TrkA ED	0.13
TrkB C1LRR	0.07
TrkB LRRC2	0.05
TrkB C1LRRC2	0.08
TrkB Ig	0.06
TrkB ED	0.03
TrkC ED	0.03

2.12 Expression of Trk protein domains as His-tagged proteins in *E. coli*

Various domains of TrkA[14], TrkB[15] and TrkC[16] were constructed as His-tagged proteins in an attempt to improve protein yield and for ease of purification. Construction of expression vectors followed the same techniques as described for the production of the *P. pastoris* expressed proteins. The expression vector used for all constructs was pET15b (Novagen) and the cDNA was cloned into the BamHI, Xbal sites.

2.13 Protein Expression

A 100 ml overnight growth (at 37°C) of a colony representing each protein was induced with IPTG to a concentration of 0.2 mM and allowed to grow for 2 hr. After this time, the cells were pelleted and re-suspended in 2 ml of 20 mM Hepes pH 7.4 containing 150 ug/ml of PMSF. After sonication and centrifuging, the pellet was re-suspended in 100 µl of SDS-polyacrylamide gel electrophoresis sample buffer and boiled for 5 min. This fraction constituted the insoluble protein. The supernatant from the sonicated cells constituted the soluble protein fraction. For each construct, an SDS-PAGE gel of uninduced *E. coli* protein was run, together with the insoluble and soluble proteins obtained after induction.

From SDS-PAGE gels it was clear that none of the proteins express well, if at all, in either as soluble or insoluble protein fractions (Figure 2.17). Qualitative measurements of the soluble fractions of the TrkA domains were made using the IAsys Biosensor (see Chap 4 for details of the methods). Binding of a molecular species from the supernatants to immobilized NGF on the IAsys biosensor surface, suggested that some of the extra-cellular Ig-like and LRR domains were present in solution. Attempts to increase soluble proteins for these three domains, by growth at different temperature (30 °C) and by induction at both low and high OD_{600}, failed to improve the yields of soluble proteins.

---

[14] Expression vector design by A Bates and Chin Shou Huang, UCSF.

[15] Expression vectors constructed by Shaun Lott , Massey University.

[16] Expression vector design by A Bates and Chin Shou Huang, UCSF.

By SDS-PAGE gels, the only Trk receptor domain that expresses well as His-tagged proteins is the Ig-like domain for TrkA and TrkB. As reported previously, the Ig-like domain was essentially found only in the insoluble inclusion bodies (Holden et al. 1997, Dr. Shaun Lott, Massey University, private communication). These recombinant proteins were not studied further.

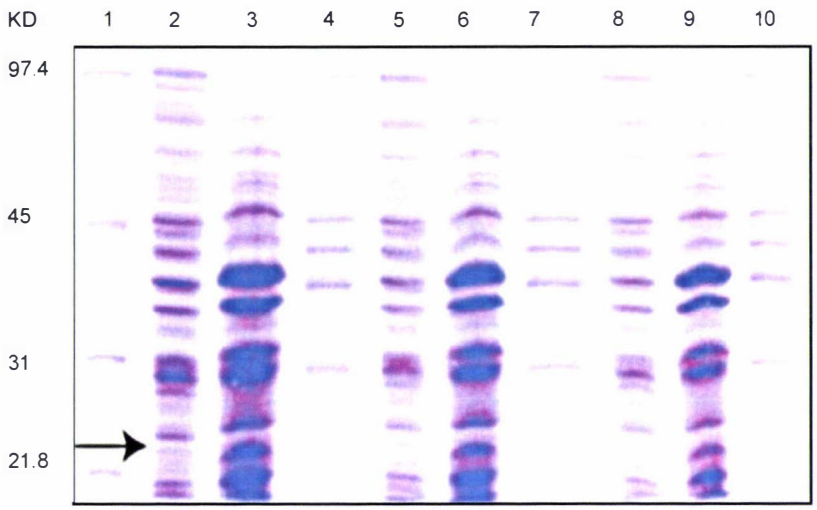

Figure 2.17 A 12% Coomassie stained gel showing expression of the TrkA, TrkB and TrkC His-tagged Ig-like domain proteins in *E. coli*. Lane 1, MW standard (BioRad). Lane 2 is an uninduced TrkA culture. Lane 3 is insoluble fraction TrkA. Lane 4 is soluble fraction TrkA. Lane 5 is uninduced TrkB culture. Lane 6 is insoluble fraction TrkB. Lane 7 is soluble fraction TrkB. Lane 8 is uninduced TrkC culture. Lane 9 is insoluble fraction TrkC. Lane 10 is soluble fraction of TrkC. The arrow indicates the induced protein bands in Lanes 3, 6 and 9.

2.14 Protein Quantification

The quantity of all proteins expressed in this study was determined by running a known amount of each protein preparation on a 4-20% SDS-gel (BioRad) together with known amounts of BSA. Each gel was stained with Sypro orange stain (BioRad) and then scanned with a phosporimager (Fuji). A curve was plotted from the BSA standards and the quantity of each Trk protein was then determined by comparison with the standard curve using MacBas software (Fuji).

2.15 Identification of Recombinant Proteins

Because the MBP-fusion proteins have MBP attached to the N-terminus of the Trk proteins, simple N-terminal sequencing and molecular weight determination by either SDS-PAGE gel or mass spectroscopy was deemed to provide a poor method to confirm the identification (Prof. E. N. Baker, Auckland University, private communication)[17]. Mass spectroscopy of trypsin digested MBP-fusion proteins, followed by a data-bank search for the expected peptides from trypsin digests of TrkA, TrkB and TrkC proteins, provided a more accurate method for confirming the identity of the expressed proteins. This technique for identification of unknown proteins, known as "peptide mapping" provides a method of identifying N-terminal blocked proteins and for those proteins where the N-terminal sequence of even a significant number of residues fails to uniquely identify a given protein (Wilkins et al. 1998). Western blotting was also used to confirm identity of the recombinant proteins.

2.16 Mass Spectroscopy

[17] Since the MBP-fusion protein is in essence a single protein composed of two parts, viz., the non neurotrophin binding domain (MBP) and the neurotrophin binding domain (Trk), each construct is in reality a single protein. Because the DNA representing each MBP-Trk construct was sequenced to confirm the fusion protein, then identification of the MBP domain of each construct is in reality, sufficient to identify each Trk protein. Further verification of correct protein identity comes from the molecular weight determination of some proteins by ultracentifuge, sequencing and by specific activity with appropriate neurotrophin. Hence protein identification was conducted more extensively in this thesis than usually undertaken.

Using a standard laboratory protocol of the Mass Spectroscopy Laboratory UCSF, the recombinant proteins were prepared for mass spectroscopy analysis. MBP-fusion proteins were elecrtrophoresed on a 4-15% SDS gel to separate the MBP-fusion protein from even minor contaminants. Approximately 4 µg of each protein was applied to the gel. After electrophoresis, the gels were stained with R350 Coomassie blue (Pharmacia) for 20 min, followed by destaining. The band corresponding to the expected molecular weight for each protein was cut from the gel, crushed in a small aliquot of water, added to a 0.5 ml siliconized tubes (PGC Scientific), vortexed for 10 min at room temperature and then centrifuged. After two water washes, the gel fragments were pelleted by centrifugation. A series of washes of the gel with 25 mM ammonium bicarbonate in 50% ACN[18] and vortexing removed the Coomassie stain from the gel fragments. After bleaching, the final buffer wash was removed and the gel dried in a Speedvac (Savant). Sequencing grade modified trypsin (Promega) digest solution was prepared by dissolving 25 ng/µl of trypsin in 25 mM NH_4HCO_3. This solution was added to just cover the dried gel. Following vortexing and centrifugation, digestion was allowed to proceed at 37°C for four hr.

Peptides from the digest were recovered by multiple extractions from the gel with 50%ACN/5%TFA[19]/H_20. After the digest period, the supernatant was removed and replaced with HPLC grade H_20 (100 µl). The supernatant was retained in a clean eppindorf. After vortexing (10 min) and sonication (10 min) the supernatant was removed and pooled with the supernatant from the digest. The pooled supernatant fractions were lyophilized to ~50 µl in a Speedvac. Each concentrated peptide supernatant was stored at -20°C for mass spectroscopy.

Mass Spectroscopy of digested Trk protein was undertaken by MALDI[20] mass spectrometry (Voyager-DE STR; Applied Biosystems). A sample (1 µL) of each digest was mixed with an equal volume of matrix (2,5-dihydroxybenzoic acid, in 20% ACN/1% TFA (10 mg/ml)) and applied to the sample plate of the mass spectrometer. A mass spectrum of each digest was collected and the masses of all peaks entered into a database of trypsin-digested proteins (Protein Prospector, UCSF). Collected spectra were also compared with expected mass peaks from a theoretical digest of the appropriate MBP-fusion protein (Protein Prospector, UCSF). Correct identification of

---

[18] Acetonitrile

[19] Trifluoroacetic acid

[20] Mass spectra and protein identification were both undertaken by Connie Jimenez, Pharmaceutical Chemistry Department/Mass spectrometry Laboratory, UCSF.

each protein was judged on the basis of at least 2 peaks of the mass spectrum being assignable to the appropriate Trk protein and 2 peaks assignable to MBP.

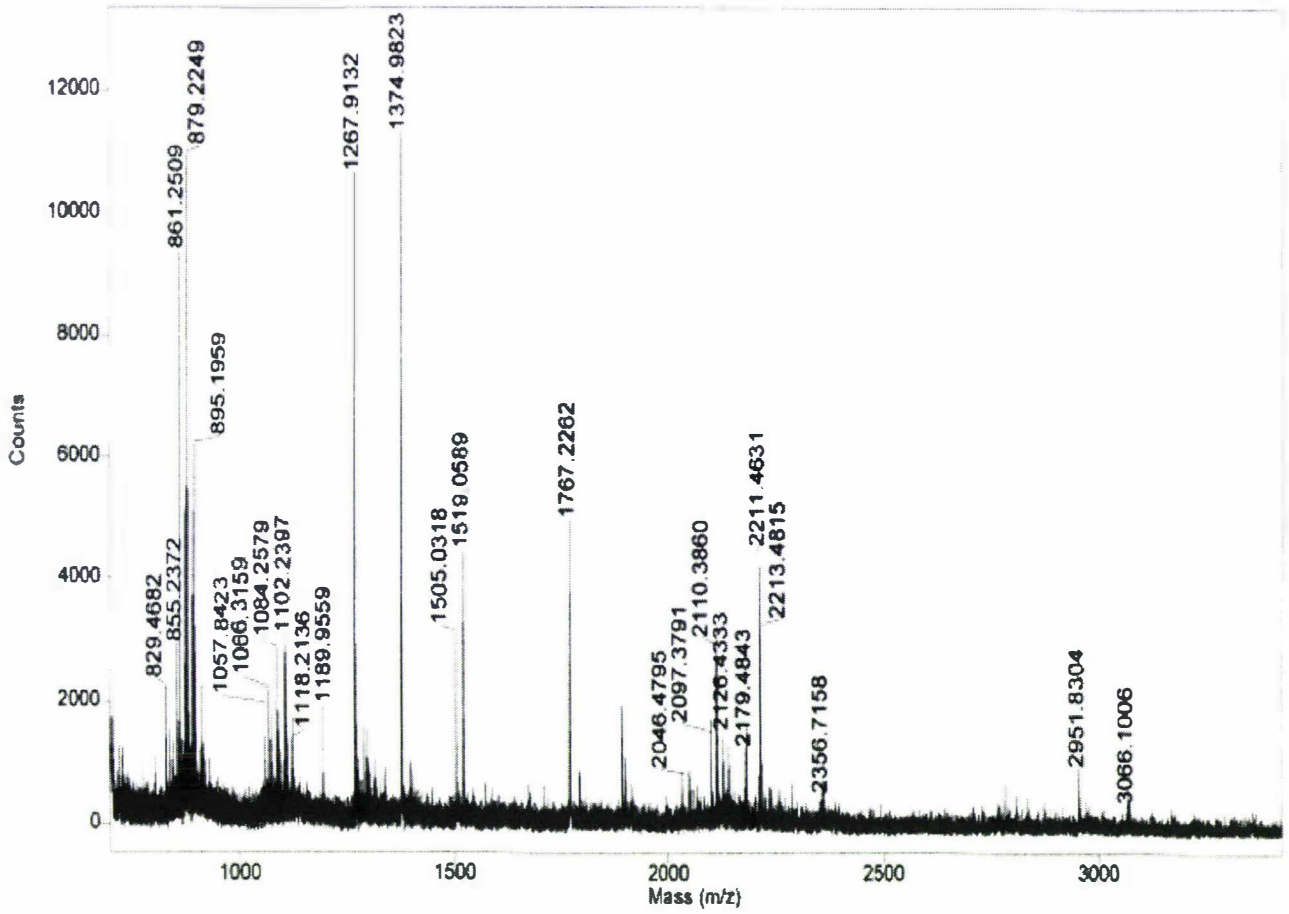

Figure 2.20 MALDI-TOF analysis of an MBP-fusion protein (TrkA MBP-LRRC2). Peaks denoted by "t" arise from digestion of the Trk protein; while peaks denoted "m", arise from MBP. The remaining peaks are assignable to MBP, Trk and from trypsin cleavage within the full length MBP-Trk fusion protein.

Table 2.14 Mass spectroscopy of trypsin digests was used to identify *E. coli* expressed MBP-Trk fusion proteins and the His-tagged proteins produced in *P. pastoris*. A minimum of two identifiable MBP and two identifiable Trk mass peaks was used for protein identification. Mass peaks arise from enzymatic digestion of sites within MBP, Trk protein and the full length MBP-fusion protein. A number of readily identifiable mass peaks arising from the trypsin digest of each protein are shown.

Protein	Peaks from MBP	Peaks from Trk protein	Peaks from the full length fusion protein
TrkA LRR2	1007.8163, 1571.9922 2055.9887	873.6744, 1854.9877 2268.2601	915.6001, 1076.5910 1818.0054
TrkA LRR	966.5507, 1092.6102 1540.0055	1073.6013, 1899.0544 2573.5101	932.6100, 1073.7044 1423.8441
TrkA C1LRR	937.5100, 1130.1102 1816.9915	932.4988, 1007.1255 1771.0553	845.4956, 1150.1006 2031.0006
TrkA LRRC2	1767.2262, 1057.8423 2356.7158, 2179.4843	1519.0589, 1505.0318 1519.0589	1189.9559, 2179.4843, 2213.4815
TrkA C1LRR12	1189.8637, 2110.2570 2213.3314, 1891.3007	1289.7548, 1767.0763 1404.8599, 1563.9357	2213.3314, 2126.3070 1066.1941, 1058.3903
TrkA LRR23C2	886.4544, 1428.8111 2446.3444	1405.4412, 2260.4347	1057.5322, 1556.7194, 1892.4122
TrkA Ig	959.5382, 1236.7000 1817.0432	960.1239, 2043.1210 2300.7012	816.9993, 1130.3112 1444.6129
TrkA IgC2	1057.8438, 2110.4097, 2213.4649	959.7129, 1941.3935 2545.3213	893.1889, 1439.9285 1891.4487
TrkA ED	966.6004, 1236.7649 1771.0046	1073.6812, 1404.9124 2171.2003	903.5003, 1065.7101 1843.0033
TrkB C1LRR	886.5112, 968.5201 1539.9164, 1890.0122	918.5428, 1341.7155	937.5129, 1032.6175
TrkB LRRC2	1077.1239, 1388.6012 2143.4321	1583.9137, 1820.1037 2127.0978	938.0553, 1092.5417 1460.6639
TrkB C1LRRC2	1129.4987, 1423.8114 2538.3055	832.9943, 1430.2110 1722.9155	1007.6444, 1281.7437
TrkB Ig	1129.6017, 1445.5983 2712.7547	1241.8321, 1513.5438	1275.6145, 1614.9216 1960.876
TrkB ED	1007.3987, 2394.2134 2416.7144, 2949.8912	827.1246, 1687.1375 2631.4752	832.6014, 1190.5219 1623.9104
TrkA ED (P.pastoris)	–	845.4859, 1171.6710 1941.0494, 2043.1071	–
TrkB ED (P.pastoris)	–	1032.5981, 1272.7391 1445.6018, 2251.1924	–

2.17 Western Blotting

In addition to identification by mass spectrometry, further proof of the correct identification for each recombinant protein was undertaken by subjecting each protein to Western blotting using a suite of antibodies (Figure 2.19 through Figure 2.28). Western blotting was conducted using the standard protocols established by the manufacturers of each Western blotting kit used (e.g. ECL or Vector Laboratories). To further increase the stringency of each antibody for its recombinant protein, the antibodies were applied to the membrane blot (PVDF, Amersham) of all proteins in TBST[21] with NaCl, increased from the standard 150 mM to 600 mM. In order to eliminate potential damage to antibody epitopes by stripping, individual SDS-PAGE gels were run for each antibody used in this study. Primary antibodies were used at a 1:1000 dilution, while secondary antibodies were diluted to 1: 5000.

Approximately 1-3 µg of the Trk proteins was used in all Western blotting experiments. This level of protein was sufficient to verify the transfer of protein to the PVDF membrane by staining with Ponceau S.

Because of very limited quantities of the recombinant protein, antibody controls were tested first and independent of the Trk proteins. If the antibodies that were used in identifying the recombinant proteins interacted with MBP, then there would have been little point in using them for identification of the recombinant Trk proteins. The control gels are shown in Figure 2.19 and Figure 2.20. Blotting controls consisted of maltose binding protein (MBP, New England Biolabs), BSA (Sigma), mouse IgG (Zymed), TrkA (Uri Saragovi) and TrkB (*P. pastoris*) run on an SDS gel and blotted to nitrocellulose membrane (Amersham). The membrane was stained with Ponceau S (Sigma) to provide evidence of protein transfer. The control proteins were then subjected to each primary Trk antibody in order to test for non-specific interactions between the control proteins and the antibodies.

The control Western blot shows that the interactions of the antibodies with the Trk proteins were specific. The antibody controls show that the MBP region of each fusion protein is not recognized by any antibody specific to Trk protein epitopes. In addition, the antibody to MBP does not recognize any Trk protein epitope. As expected, the mouse IgG is recognized by all antimouse primary and secondary antibodies.

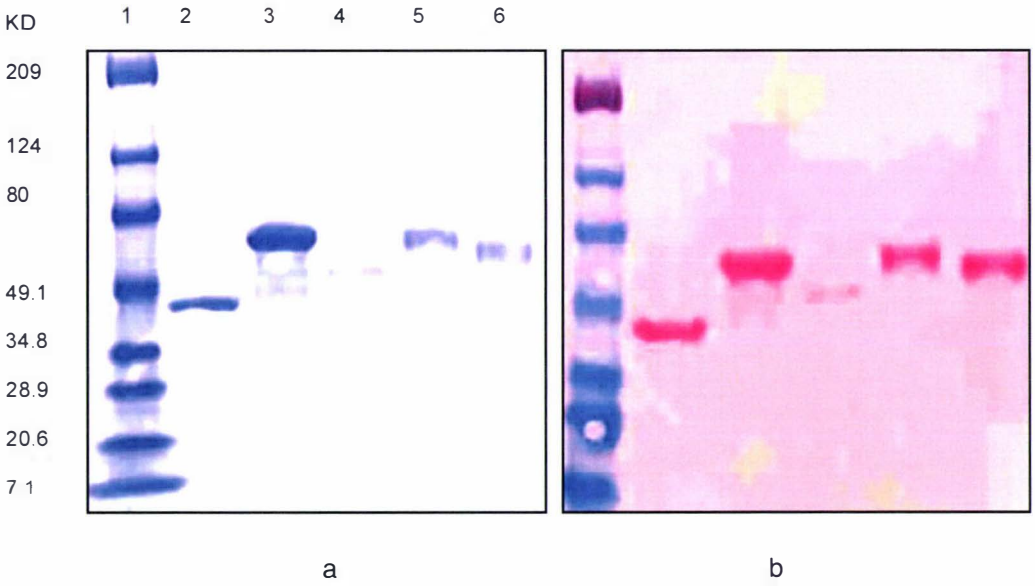

Figure 2.19 SDS-PAGE and electrotransfer for the Western Blots. (a) is a Coomassie stained gel (4-15%, BioRad) of the control proteins and (b) is a Ponceau S (Sigma) stained membrane after electrotransfer. Four Western blots were made to probe with the individual antibodies used to identify the various Trk proteins expressed for this study. In (a), lane 1 is a molecular weight standard (BioRad), lane 2 is MBP, 3 is BSA, lane 4 is mouse IgG, lane 5 is TrkA (Uri Saragovi) and lane 6 is TrkB (*P. pastoris*). In (b) the molecular weight and lane designations designations are the same as for (a). The levels of protein loaded on the Coomassie and Western blot gels was the same and all gels were run at the same time and at identical voltages.

[21] Tris buffered saline solution

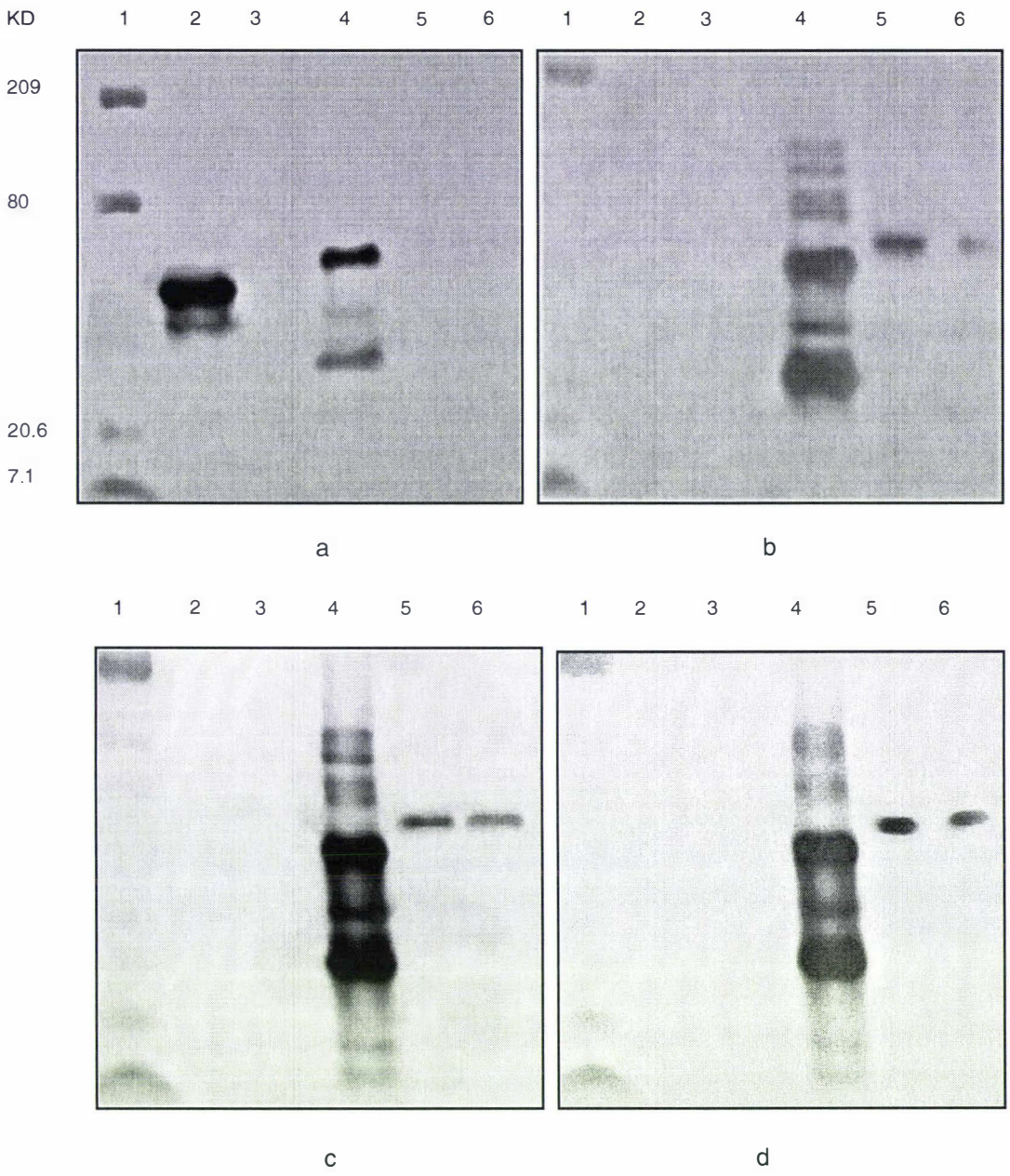

Figure 2.20 Antibody control gels. Western blots of the control proteins shown in Figure 2.19. Western blot (a) shows the interaction of the MBP antibody with the control proteins. (b) shows the interaction of the Trk polyclonal antibody (Uri Saragovi) with the control proteins. (c) shows the interaction of the Trk monoclonal antibody (Zymed) with the control proteins. (d) shows the interaction of the myc antibody (Invitrogen) with the control proteins. Lane designations are identical to those of Figure 2.19.

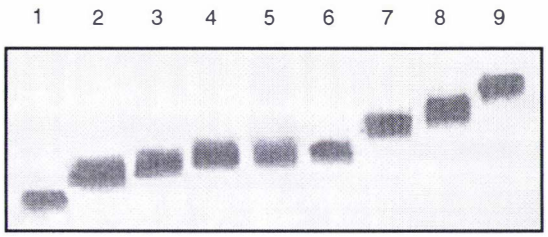

Figure 2.21 Western blot of TrkA MBP-fusion proteins probed with a polyclonal antibody to MBP Lane 1 MBP, lane 2 LRR, lane 3 C1LRR, lane 4 LRR23 C2, lane 5 C1LRR, lane 6 LRRC2, lane 7 Ig-domain, lane 8 C2Ig-domain and lane 9 is ED. A pre-stained molecular weight standard (BioRad) was run on all the gels. This gel is directly comparable with that in Figure 2.15 as each gel was run at the same time and are the identical proteins.

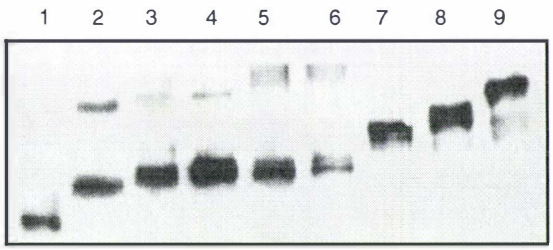

Figure 2.22 Western blot of TrkA MBP-fusion proteins probed with a polyclonal antibody to the ED of TrkA (Uri Saragovi). The lanes were loaded as for Figure 2.15. This gel is directly comparable with that in Figure 2.15 as each gel was run at the same time and are the identical proteins.

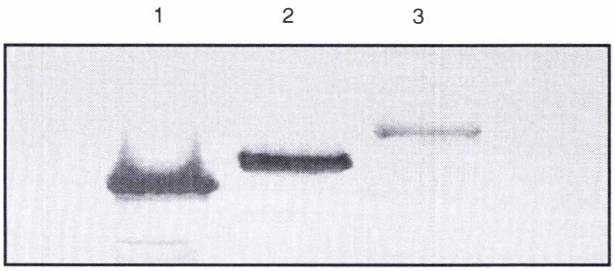

Figure 2.23 Western blot of TrkA MBP-fusion proteins probed with a polyclonal pan-Trk antibody[22] (Zymed Laboratories). Lane 1, Ig-domain, lane 2 C2Ig-domain and lane 3 ED. This antibody detected the Ig-like domains but gave a barely detectable signal with the LRR domains of TrkA. This gel is directly comparable with that in Figure 2.15 as each gel was run at the same time and are the identical proteins.

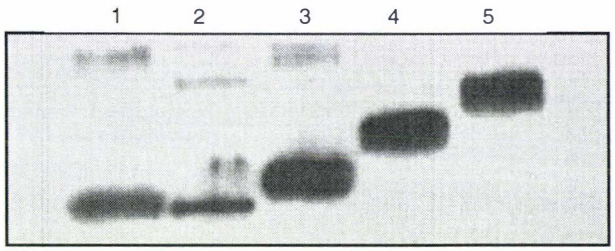

Figure 2.24 Western blot of TrkB MBP-fusion proteins with a polyclonal antibody to MBP (Santa Cruz). Lane 1 C1LRR, lane 2 LRRC2, lane 3 C1LRRC2, lane 4 Ig-like domain and lane 5 is the ED. This gel is directly comparable with that in Figure 2.16 as each gel was run at the same time and are the identical proteins.

22 This antibody was made to the extracellular domain of TrkB, but also reacts with epitopes in the extracellular domains of both TrkA and TrkC and may be used for immunoblotting of both proteins (Zymed Laboratories technical information).

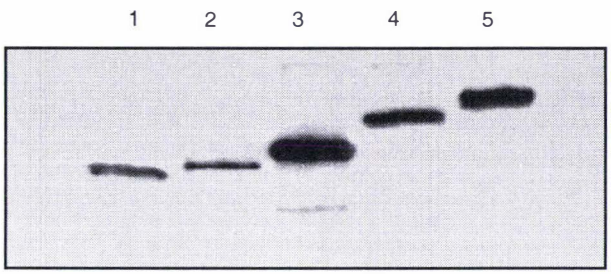

Figure 2.25 Western blot of TrkB MBP-fusion proteins with a polyclonal pan-Trk antibody (Zymed Laboratories). Lane 1 C1LRR, lane 2 LRRC2, lane 3 C1LRRC2, lane 4 Ig-like domain and lane 5 is the ED. This gel is directly comparable with that in Figure 2.16 as each gel was run at the same time and are the identical proteins.

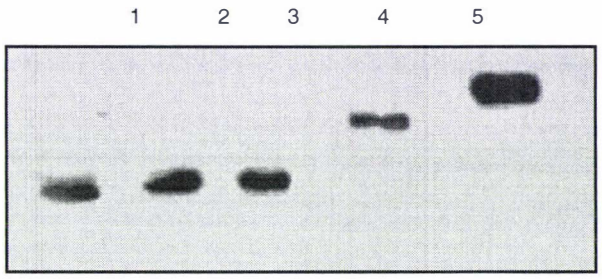

Figure 2.26 Western blot of TrkB MBP-fusion proteins with a polyclonal TrkB antibody (Santa Cruz). Lane 1 C1LRR, lane 2 LRRC2, lane 3 C1LRRC2, lane 4 Ig-like domain and lane 5 is the ED. This gel is directly comparable with that in Figure 2.16 as each gel was run at the same time and are the identical proteins.

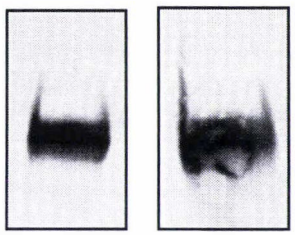

Figure 2.27 (a) Western blot of TrkC ED, MBP-fusion protein, with a polyclonal antibody to MBP (Santa Cruz). (b) Western blot of TrkC ED MBP-fusion protein, with a polyclonal pan-Trk antibody (Zymed Laboratories).

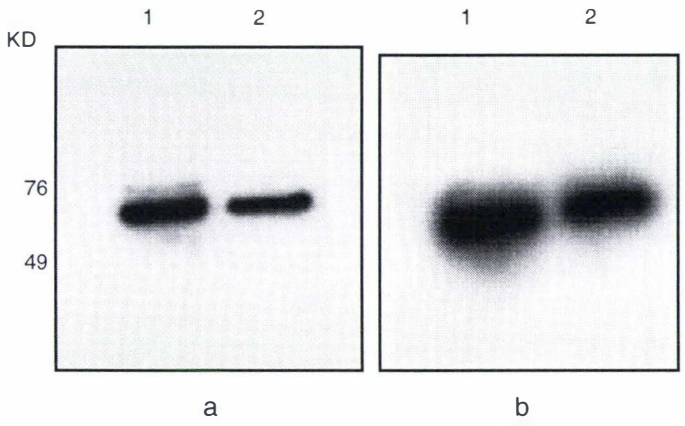

Figure 2.28 (a) Western blot of His-tagged extracellular domains of TrkA and TrkB proteins expressed in *P. pastoris* and probed with a polyclonal pan-Trk antibody (Zymed Laboratories). Lane 1 is TrkA and Lane 2 is TrkB. (b) Western blot of His-tagged extracellular domains of TrkA and TrkB proteins expressed in *P. pastoris* and probed with a monoclonal myc antibody (Invitrogen). Lane 1 is TrkA and Lane 2 is TrkB. The myc epitope is retained near the C-terminal of each recombinant protein.

A suite of antibodies for MBP and against epitopes of the extracellular domains of TrkA, TrkB and TrkC, Figure 2.19 through Figure 2.28, provides evidence for the presence of Trk protein in all MBP-fusion constructs. Antibodies also provide evidence for the expression of Trk His-tagged proteins expressed in *P. pastoris* and purified using the protocol described in section 2.10.

In instances where the MBP-fusion proteins were analyzed with an antibody to MBP (Figure 2.22 and Figure 2.24), some extraneous bands that do not run at the expected molecular weight of the expressed MBP-fusion proteins are observed. These bands are not directly interpretable, but may result from aggregation of protein on the gel. Detection of proteins by antibodies is orders of magnitude more sensitive than Coomassie stained gels (ng versus µg respectively). On Coomassie stained gels the purified proteins appear to be free of contaminating protein; however no purification protocol can completely eliminate all minor contaminants. Hence, contaminants not detectable on the protein gels (Figure 2.15 and Figure 2.16) may be detected by the antibody to MBP. Other antibodies used in this analysis do not detect the presence of contaminating proteins. Each Trk protein runs as a slightly diffuse band on a protein gel (Figure 2.13 and Figure 2.14), possibly as a consequence of the heterogeneity of molecular weight, caused by glycosylation. This molecular weight heterogeneity is seen for Trk proteins expressed in mammalian-like protein expression systems and is attributable to sugar residues (Prof. Ken Neet, University of Chicago, private communication).

Supplementary data that serves to identify the recombinant proteins produced for this study come from both sequencing and kinetics. The MBP-fusions proteins, TrkA, LRR, C1LRR, C2Ig and ED were N-terminal sequenced[23]. Sequencing correctly identified the MBP located at the N-terminal of each protein. The kinetics data indicate that each Trk protein interacted specifically with its appropriate neurotrophin. No binding of NGF, BDNF or NT-3 was observed with MBP by biosensor analysis, confirming the observation of Windisch et al. (Windisch et al. 1995a). Insulin growth factor[24] (IGF) a small protein not expected to interact with the Trk proteins was tested for binding to all Trk proteins immobilized on the biosensor surface. No Trk-IGF interactions were observed, even at mM IGF concentrations. All recombinant MBP-fusion proteins had been previously identified, sequenced and the characteristic behavior of these proteins on gels was provided for this study (Dr. Rainer Marksteiner, University of Innsbruck, private communication).

---

[23] Sequenced at Massey University.

[24] Provided by Dr. Martin Spencer, Laboratory of Growth and Development, Davies Medical Center, San Francisco. The protein was > 95% pure.

2.18 Nerve Growth Factor Purification

NGF for the studies of the interaction of with Trk receptors was purified from mouse submaxillary glands (Pel-freeze). A technique, well established in the Mobley laboratory (UCSF/Stanford)[25] to produce NGF for both the laboratory and for supply to Promega, was followed. Approximately 40 gm of Swiss Webster type (more than 60 days old), mouse submaxillary glands, was homogenized in 200 ml of cold water in a blender for 2 min. The homogenate was centrifuged for 60 min at 10000 x g. The supernatant was then dialyzed in 3500 MW cut-off tubing, for 20 hr, against 20 mM sodium phosphate buffer, pH 6.8. Four changes of buffer were made throughout the dialysis period. The dialyzed supernatant was shaken with CM52 beads (Whatman), equilibrated in 20 mM sodium phosphate buffer at pH 6.8, for 3 hr and then poured into a glass gravity column. Sodium phosphate buffer (20 mM, pH 6.8) was flowed through the column until the OD_{280} fell below 0.5. The eluant was dialyzed for 20 hr, against four changes of 0.25 mM sodium phosphate buffer, pH 6.8.

Following dialysis, PMSF was added to a final concentration of 0.1 M and the supernatant was acidified with 0.5 M sodium acetate buffer, pH 4.0. The supernatant was centrifuged at 10000 x g for 30 min and then applied to CM52 beads (in a glass gravity column) equilibrated in 50 mM sodium acetate buffer, pH 4.0 containing NaCl to 0.4 M. After loading the dialyzed supernatant, 50 mM sodium acetate buffer, pH 4.0, 0.4 M NaCl, was run through the column until the OD_{280} fell below 0.01. Three column volumes of sodium phosphate buffer (50 mM, pH 4.0) was run through the column to remove the NaCl, followed by 50 mM Tris/HCl buffer, pH 9.0, until the OD_{280} fell below 0.01. Nerve growth factor was eluted from the column with a gradient (0-0.4 M) of NaCl in 50 mM Tris/HCl buffer, pH 9.0. Elution was followed by absorbance at 280 nm and pooled fractions of OD_{280} greater than 0.1 were dialyzed against 4 liters of 0.2% acetic acid, concentrated in a 3000 MW cut-off centricon (Millipore) and stored in aliquots at -85°C. Approximately 6 mg of NGF was obtained from this purification.

An ultracentrifuge analysis, established the molecular weight of the purified NGF as 24374 Daltons, which compares well with a molecular weight of 24398 Daltons, (also established by ultracentrifugation) for the commercially available BDNF (Amgen) used in these studies. Figure 2.29 shows an SDS-PAGE analysis of the NGF preparation.

[25] Mobley W. C., et al. 1976 Biochemistry 15, 5543.

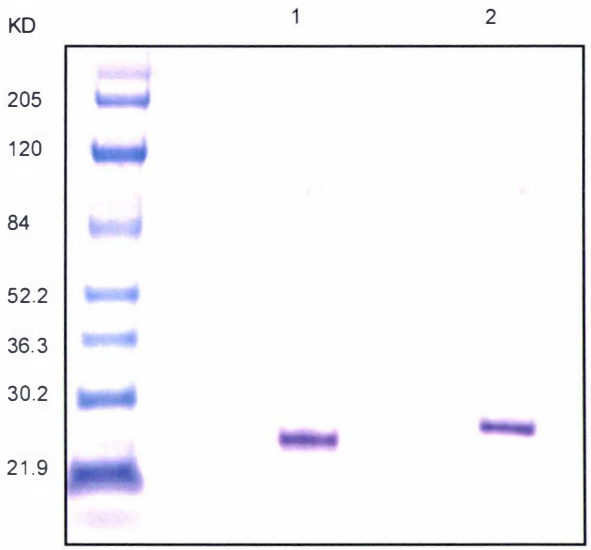

Figure 2.29 A Coomassie stained SDS-PAGE gel of the purified NGF (lane 1). For comparison BDNF (Regeneron) is shown in lane 2. Non-denaturing 4-20% SDS-PAGE gel (BioRad).

2.19 Summary

Expression of TrkA (rat) and TrkB (rat) ED proteins appears to be feasible in the yeast *P. pastoris*. Reasonable expression yields (> 3 mg/L) were obtained for both proteins. Both TrkA (human) and TrkC (rat) were expressed at very low levels. A simple purification scheme was established for the purification of the His-tagged TrkA and TrkB proteins produced in *P. pastoris*; however, the initial expectation that a chelating column alone would be sufficient for a one step purification method, proved to be unfounded.

Several constructs of TrkA, TrkB and TrkC extracellular domains were expressed in *E. coli* as MBP-fusion proteins. Only one domain (TrkA MBP-Ig) expressed well in the *E. coli* strain used by Windisch et al. (1995a). A different *E. coli* species (BL21(DE3), Novagen) was used in this study to obtain usable yields of the proteins for later studies. The expression levels of all proteins appear to be an order of magnitude lower than that obtained by Rainer Schneider. This may be a consequence of the methods used for growing the bacteria, induction of expression, the *E. coli* species used and of a different measurement technique for total protein.

Experiments to find optimal growing conditions for *E. coli* expression of the MBP-fusion proteins were conducted (Prof. Rainer Schneider, University of Innsbruck, private communication). In order to achieve optimal growth conditions, protein expression needs to be followed at different growth temperatures, for different medium, for different concentrations of IPTG used to induce protein production and for different growth periods after induction. It is unlikely that all these conditions were met by following the protocols for the *E. coli* species used in the study by Windisch et al. (1995a, b, c). Why little protein could be expressed by following the protocols (and *E. coli* species) of Windisch et al. remains unknown. However, protein was obtained at levels sufficient for the completion of the proposed studies and this dictated the criterion on which further trials of the optimization of protein expression levels ceased. Attempts to obtain highly purified protein undoubtedly resulted in low yield, but quality rather than quantity was more important for the proposed studies.

Expression of many of the TrkA, TrkB and TrkC proteins produced as MBP-fusion proteins, was attempted in *E. coli* with an expression vector that resulted in a His-tag at the C-terminus of the recombinant protein. No reasonable levels of soluble protein were obtained for any of the His-tagged proteins. It appears that the presence of either a large soluble protein such as MBP, in the case of the Trk MBP-fusion proteins, or glycosylation on the 13 potential glycosylation sites of the Trk proteins produced in *P. pastoris*, is required for soluble protein production. Removal of the MBP from the Trk fusion proteins, results in loss of solubility (Prof. Rainer Schneider, University of Innsbruck, private communication). Furthermore, additional attempts to produce the MBP-fusion constructs as His-tagged proteins resulted in negligible or no soluble protein production (Prof. Rainer Schneider, University of Innsbruck, private communication)[26].

[26] Further attempts to express the Trk receptors (full length and domains) as His-tagged proteins ceased based upon this communication.

CHAPTER 3 ULTRACENTRIFUGE STUDIES

3.1 Introduction

Interaction between the Trk receptor proteins and their ligands may be investigated by sedimentation-diffusion studies using ultracentrifugation (Glasel and Deutscher 1995). Sedimentation equilibrium may be utilized to measure molecular masses over a wide range, from that of small molecules, such as sucrose, to the large molecular masses of viruses. Such interaction studies are nondestructive and can thus be used to determine the behavior of proteins under normal solution conditions. Analytical ultracentrifugation is able to discriminate between simple heterogeneity and reversible interactions between protein molecules. Since the technique is able to distinguish between self-association of proteins to form discrete polymers (dimers, tetramers etc) and heteroassociation, in which different proteins interact to form a complex, the method is suitable for determining the molecular weights and solution stoichoimetry of the recombinant Trk proteins and neurotrophins.

An analytical ultracentrifuge is a high-speed centrifuge with an optical system that permits observation of the position of sedimenting boundaries as a function of time. By analyzing, at equilibrium, the concentration distribution of molecules that are self-associating, hetero-associating, dissociating or non-interacting, it is possible to obtain molecular mass averages as a function of concentration and position in the ultracentrifuge sample cell. Analysis of the concentration distribution by curve fitting to various molecular models, or by dependence of the molecular mass averages on concentration, allows the molecular masses of the proteins comprising the system, to be obtained.

For an interacting system, it is possible to obtain the stoichiometries and equilibrium constants of the interacting proteins. The sum of the forces acting on a macromolecule suspended in a buffer is zero and the molecule is at rest (ignoring Brownian motion), until a centrifugal force field is applied. In the centrifugal force field, the molecule accelerates in the direction of the applied force, until the frictional resistance from the solvent equals the centrifugal force. At this time, the

sum of the forces acting on the molecule is again zero; the molecule ceases to accelerate and continues to move with uniform motion. The centrifugal force Fc (dynes/mole) is the product of the mass of the molecule corrected for its buoyancy in water or other solvent and of the centrifugal acceleration $\omega^2 r$, where ω is the angular velocity (radians/sec) and r is the distance between the molecule and the center of rotation for the centrifuge.

$$F_c = M_2(1-v_2\rho)\,\omega^2 r \qquad 1$$

The molar mass M_2 is the mass of the biomolecule (grams/mole), v_2 is the partial specific volume of the molecule (cm^3-g) and p is the density of the solution (g/cm^{-3}). The frictional force F_f (dynes/mole) is determined by the relationship:

$$F_f = N f dr/dt \qquad 2$$

Where f is the frictional coefficient of the sedimenting molecule (dynes-sec/cm) and N is Avogadro's number. When the system reaches equilibrium, $F_c = F_f$ and then:

$$N f dr/dt = M_2(1-v_2\rho)\omega^2 r \qquad 3$$

By defining the sedimentation coefficient, s as the velocity per unit centrifugal force, then:

$$s = dr/dt/\omega^2 r = M_2(1-v_2\rho)/N_f \qquad 4$$

For molecules in a solution, a boundary forms between the molecules as they sediment and the buffer left in the supernatant. As the boundary progresses down the sample cell, it spreads by diffusion while at the same time, the concentration of the region centrifugal to the boundary (the "plateau region"), decreases with time. Since the rate of movement of the boundary is approximately proportional to time and the rate of spreading of the boundary from diffusion is approximately proportional to the square root of time, then resolution will increase with time, irrespective of diffusion. Molecular concentration is observed to decrease in the plateau region as a consequence of dilution that occurs as the sedimenting molecules move into the increasingly larger volume in the sector shaped sample cell. The frictional coefficient, f, may be written as:

$$f = RT/ND \qquad 5$$

Where D is the diffusion coefficient (cm^2/sec) and T is the absolute temperature (Kelvin). From equations 4 and 5, the Svedberg relationship may be written:

$$s/D = M_2(1-v_2\rho)/RT \quad (6)$$

where s is the sedimentation coefficient in units of seconds or Svedbergs. By determining s and D, it is possible to estimate the molecular mass of a protein. A mathematical description of the time dependence of molecular concentration during sedimentation in a cylindrical reference frame is give by the Lamm equation (Cantor and Schimmel 1980). At equilibrium, when no further changes in concentration is occurring, then:

$$\partial c/\partial t = r^{-1}\partial/\partial r[r(J_s + J_d) = 0 \quad (7)$$

where J_s and J_d are the fluxes due to sedimentation and diffusion respectively and may be described by:

$$J_s = \omega^2 rsc \quad (8)$$

$$J_d = -D(\partial c/\partial r) \quad (9)$$

where $\partial c/\partial r$ is the concentration gradient and D is the diffusion coefficient (cm^2sec^{-1}). At equilibrium, the flux due to sedimentation transport equals that due to diffusion transport, then:

$$D(\partial c/\partial r) - \omega^2 rsc = 0 \quad (10)$$

From equation 6 and 10:

$$d\ \ln(c)/d(r^2/2) = \omega^2 s/D = M_2(1-v_2\rho)\omega^2/RT \quad (11)$$

The slope of the plot of ln[c(r)] against $r^2/2$, where c(r) is the equilibrium concentration distribution, gives the molecular mass M_2 of the macromolecule within the sample cell. If this plot curves upward, then the molecular system in the cell is polydisperse and the tangent to the curve gives a mass average (Mw) of the molecular species present providing that all the macromolecules present have the same partial specific volume. If the plot curves downward, indicating that the molecular weight decreases with increasing concentration, then the solution is non-ideal and the molecular weight exhibits concentration dependence.

3.2 Methods

Sedimentation-equilibrium experiments of all recombinant Trk proteins and neurotrophins were performed using an Optima XL-A ultracentrifuge with scanning uv/vis capabilities (Beckman Coulter). The scanning uv/vis detection system provides sensitivity for low concentration studies and selectivity for optimizing detection based on the analytes maximum absorbance. A 12 mm double-sector sample cell with quartz windows was used. A total of nine protein samples and nine buffer (20 mM Hepes pH 7.4, 150mM NaCl) controls were measured simultaneously during each sedimentation-equilibrium experiment. The total volume of sample loaded into each cell was 110 µl and the quantity of protein added to each cell was adjusted with 20 mM Hepes pH 7.4 to give an absorbance of between 0.2 and 0.4 at 280 nM, corresponding to a protein concentration of ~ 0.3 to 0.6 mg/ml[1].

A preliminary experiment in which absorbance was measured as a function of wavelength, showed that maximum absorbance was recorded at 220 nM and this wavelength was used for all subsequent measurements. Initial rotor speed was 8000 rpm with subsequent increases to 15000 rpm over a period of 96 hours. Equilibrium was judged to have been achieved when only single boundaries were observed for the sedimentation velocity profiles. Sedimentation equilibrium data was collected at three speeds (8000, 10,000 and 15,000 rpm), at 25ºC. The partial specific volume of each protein, based upon the amino acid composition of each protein, was calculated with Sedenterp software[2] (Laue et al. 1992, Zhong et al. 2002) and data analysis was performed with Origin 4.01 software (Microcal).

3.3 Data Analysis

The utracentrifuge data was analyzed by plotting the protein absorbance (at a particular radius) versus the radius, i.e., the distance of the sample cell from the center of rotation. The software used for this analysis (Origin 4.01) is supplied with the utracentrifuge, by its manufacturer

---

1 The protein concentration in mg/ml may be estimated by [protein] = 1.5 A_{280}-0.75A_{260} where A_{280} and A_{260} refer to the absorbance at 280 and 260 nm respectively Protein Methods, Bollag DM & Edelstein SJ, pub. by Wiley-Liss.

2 This program is available from J. Philo at Amgen, Thousand Oaks, California.

(Beckman Coulter). The software plots the Absorbance versus radius data (e.g. Figure 3.1) at the completion of each centrifuge run. A perfect fit for the estimate of the molecular weight of a given protein is indicated by the red line intersecting the data point curve, all along the curve (Origin utracentrifuge data analysis manual). The accuracy of the fit may be estimated by observation of the pattern of the residuals. Residuals are calculated by subtracting the absorbance of the fitted curve from the absorbance data as a function of radius. A good fit of the data to the fitted curve is indicated by random scattering of an equal number of residual data points above and below the curve. Residual patterns with systematic variation from the fitted curve may indicate non-ideality or the presence of an aggregating system (Origin utracentrifuge data analysis manual).

3.4 Results

Typical ultracentrifuge absorbance data is shown in Figure 3.1, 3.2 and 3.3 below. The absorbance data for all proteins studied by ultracentrifuge (Table 3.1) shows the same standard as these examples.

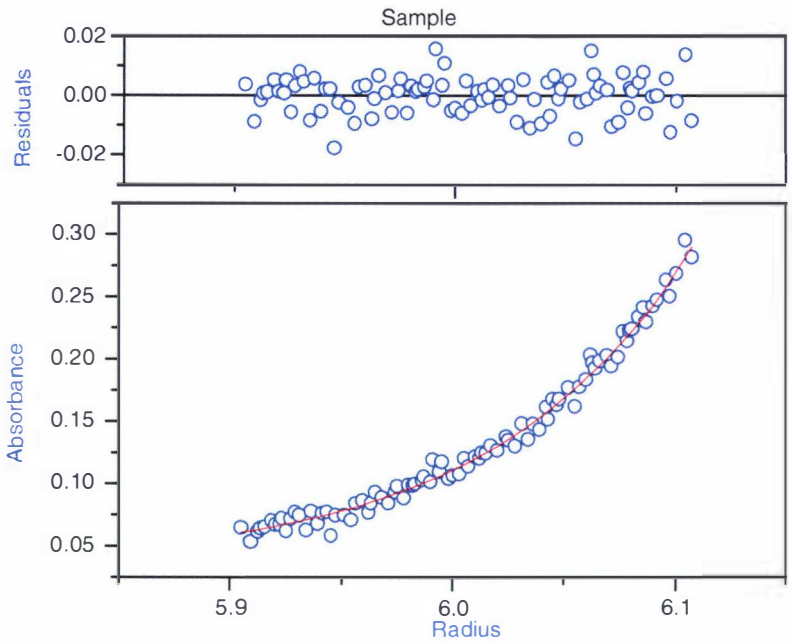

Figure 3.1 Absorbance and statistical residual data generated in the utracentrifuge for the TrkA ED human recombinant protein expressed in insect cells (Prof. Uri Saragovi, McGill University).

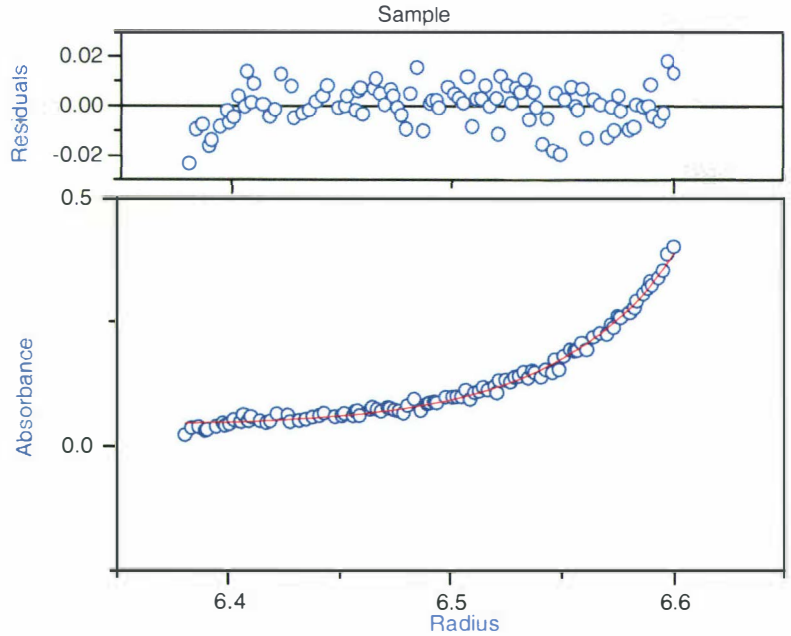

Figure 3.2 Absorbance and statistical residual data generated in the utracentrifuge for the TrkA Ig-like domain recombinant protein expressed in *P. pastoris* (Prof. Uri Saragovi, McGill University).

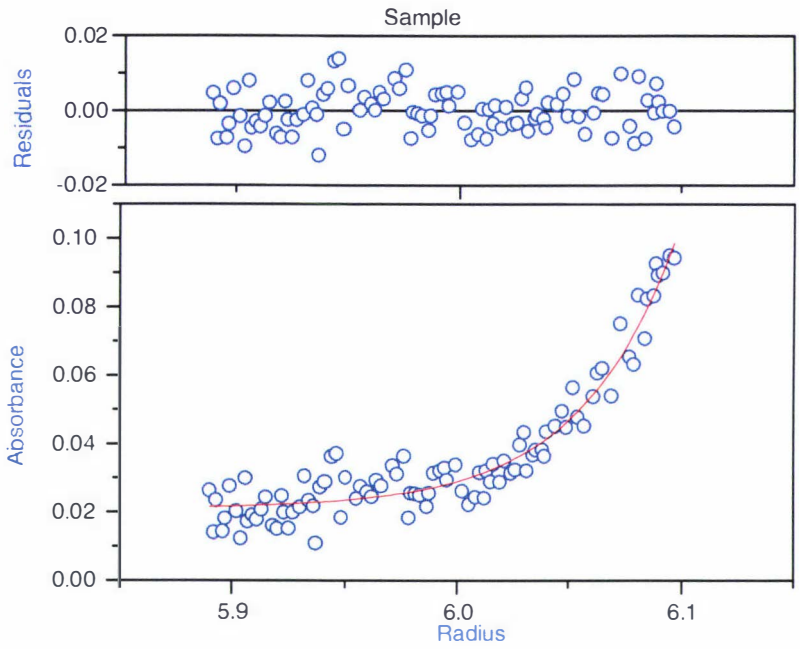

Figure 3.3 Absorbance and statistical residual data generated in the utracentrifuge for the TrkA Ig-like domain recombinant protein expressed as an MBP-fusion protein in *E. coli*.

Table 3.1 Approximate molecular weights of Trk and neurotrophin proteins as determined by ultracentrifuge. The calculated molecular weights (based on amino acid composition) of each protein studied by ultracentrifuge are shown, together with their model molecular weights as determined by the ultracentrifuge study. The MW's are given in Daltons.

Protein	Monomer MW	Dimer MW	Model MW
NGF	13,538	27,076	24,374
BDNF	13,909	27,818	24,398
ED (TrkA) Insect cells	43,000 Unglycosylated	86,000	68,942
Ig-like (TrkA) (P. pastoris)	60,000	120,000	108,300
LRR2 (TrkA) MBP-fusion	45,410	90,820	90890
C1LRR (TrkA) MBP-fusion	60,781	121,562	117,000
Ig-like (TrkB) MBP-fusion	68,883	137,766	143,400

Table 3.2 Protein solution stoichiometry determined by Origin 4.01 software (Microcal). * Expressed as MBP-fusion protein in *E. coli*. ** Expressed in *P. pastoris*.

Protein	Solution Stoichoimetry
NGF	dimer
BDNF	dimer
ED (TrkA)*	monomer
Ig-like (TrkA)**	dimer
Ig-like (TrkB)*	dimer
C1LRR (TrkA)*	dimer
LRR2 (TrkA)*	dimer

The ultracentrifuge study showed self-association of NGF monomers in solution. This NGF was purified, as described previously, from mouse submaxilary glands. From the ultracentrifuge data at 15000 rpm, the model fit shows that the NGF forms a dimer of MW 24,374 daltons, less than the expected MW of 27,076 daltons. The dimeric state is consistent with the reported solution structure of NGF (McDonald et al. 1991).

The ultracentrifuge study also showed the self-association of BDNF monomers in solution. This BDNF is human recombinant protein expressed in *E. coli* (Amgen). From the data at 15,000 rpm, the model fit shows that the BDNF forms a dimer of MW 24,398 daltons, less than the expected MW of 27,818 daltons. A MW of 27,273 daltons was reported by Amgen from the ultracentrifuge analysis of BDNF. Human recombinant TrkA ED protein, expressed in insect cells is highly

glycosylated (Prof. Uri Saragovi, McGill University, personal communication, Woo et al. 1998). From the ultracentrifuge data at 15,000 rpm, the model fit shows that the ED has a MW of 68,942 daltons. Since the calculated MW of the protein is approximately 43,000 daltons in an unmodified form, it was concluded that the protein exists in solution as a monomer and approximately 26,000 daltons can be attributed to glycosylation of the 13 potential glycosylation sites.

Self-association of TrkA LRR domain molecules (C1LRR) appears to occur in solution. This is rat recombinant MBP-fusion protein expressed in *E. coli*. From the ultracentrifuge data at 15,000 rpm, the model fit showed that the C1LRR domain formed dimers of MW 117,000 daltons in solution. The fusion protein has a calculated MW of approximately 60,781 daltons; hence the MW for the supposed dimer is slightly lower than might be expected.

It appears that the TrkA second LRR domain (LRR2) molecules also self-associate in solution. This is rat recombinant MBP-fusion protein expressed in *E. coli*. From the ultracentrifuge data at 15,000 rpm, the model fit shows that the LRR2 domain molecules appear to be dimers of MW 90,890 daltons in solution. The fusion protein has a MW of approximately 45,410 daltons; hence the MW for the supposed dimer is close to that expected.

A monomer of TrkB MBP- Ig protein has a theoretical MW of approximately 68,883 daltons, based on amino acid composition. The ultracentrifuge data at 15,000 rpm showed that the Ig-like domain molecules have a MW of 143,400 daltons in solution, close to that expected for the calculated MW of a dimer. For the TrkB, rat Ig-like domain, expressed as an MBP–fusion protein in *E. coli*, the molecules appear to self-associate to form a dimer in solution.

Like the TrkB Ig-like domain, the human recombinant TrkA Ig-like domain also appears to self-associate in solution. Because this protein was expressed in *P. pastoris*, it is possible that this domain, having a number of potential glycosylation sites, has sugar residues covalently linked to it. The ultracentrifuge data at 15,000 rpm fits a model in which the protein has a molecular weight of 108,300 daltons. The purified TrkA Ig-like domain run on an SDS-PAGE gel shows the presence of a single band of ~55 KD. The protein contains ~25 kD of carbohydrate post-translational modifications (Prof. Uri Saragovi, McGill University, personal communication, Saragovi et al. 1998, Woo et al. 1998). The full-length ED appears to have approximately 20-25 kD of post-translational modifications by the ultracentrifuge analysis; however it is not possible to

assign the glycosylation to either the LRR or the Ig-like domains exclusively as this analysis was beyond the scope of the study. If all the glycosylation of the ED is due to the Ig-like domain, then, conceivably by this conjecture, the weight of the Ig-like domain alone, is approximately 55 kD and hence the MW determined by the centrifuge for this domain would suggest that this protein exists as a dimer in solution.

3.5 Summary

Analysis of the ultracentrifuge data, allowed for the testing of models of momomer or multimer formation of the Trk and neurotrophin proteins in solution. Two variables, namely the molecular weight and partial specific volume of each protein, calculated from sequence information, together with the variation of radius with absorption, form the basis of model prediction. Molecular weights from the models are approximate, but are of sufficient accuracy to permit the stoichiometry of the proteins in solution, to be determined.

This utracentrifuge study permitted assessment of the stoichoimetry, in solution, of the proteins investigated. In this study, all TrkA proteins, with the exception of the complete ED, appear to form dimers in solution. The TrkA ED, for an unknown reason, appeared by this analysis to remain in monomeric form in solution. It is possible that the high level of glycosylation keeps this protein in solution as monomers. If the MBP of the fusion proteins is removed, all of these proteins become insoluble and precipitate (Prof. Rainer Schneider, University of Innsbruck, private communication). It appears that the Trk proteins require some modification in the form of glycosylation or MBP to remain soluble. A high level of glycosylation of the ED may cause steric hindrance and prevent association in the absence of neurotrophin.

Analysis of NGF and BDNF gave consistent results, despite their quite different sources and means of purification. In addition, the MW for BDNF (Amgen) obtained in this study, is similar to that obtained by ultracentrifugation and reported by Amgen. That the molecular weights differ by approximately 10% is probably due to the quality of the ultracentrifuges used in the two studies, rather than technique. The closeness of the two BDNF MW's provides a check of technique and data analysis methodology used in this study.

TrkB Ig-like domain gave excellent data, but the TrkB C1LRRC2 domain gave no absorbance at 280 nm. Consequently no ultracentrifuge data was collected for this protein. For other TrkB proteins, too little material was available for the ultracentrifuge study.

All TrkA and TrkB proteins listed above were centrifuged with their respective neurotrophin. Although a difference in MW between the Trk-neurotrophin and Trk protein alone was discerned, the available analysis software proved inadequate in analyzing a mixed species in solution. Hence the data did not conclusively support the formation of Trk-neurotrophin complexes and this analysis was ultimately abandoned. Consequently the ultracentrifuge analysis was only used to support the formation in solution of dimeric forms of appropriate MW for the LRR and Ig-like domains of the Trk proteins.

This result does have implications for the analysis of the proteins immobilized to the biosensor surface. It would appear that the LRR and Ig-like domain proteins may immobilize as dimers on the biosensor surface and hence may act in a fashion envisioned for the Trk receptor on a cell surface. These constructs however represent quite artificial entities and as such cannot be reasonably employed to explain Trk receptor phenomena *in vivo*. That the TrkA ED did not appear to dimerize in solution is perplexing and implies that the protein immobilizes to the biosensor surface as monomers. If however the density of the monomers on the biosensor surface is sufficiently large, it is possible that neurotrophin may bind to two close monomers, resulting in a dimeric receptor and hence produce a facsimile of the situation of the Trk receptor on a cell surface. Additionally, it is possible that this result implies that the Trk receptors exist as monomers on a cell surface, only forming a dimer on the binding of neurotrophin.

CHAPTER 4 KINETICS

4.1 Introduction

Surface Plasmon Resonance (SPR) biosensors are increasingly becoming the preferred method of studying macromolecular interactions. SPR permits the molecular interactions to be studied in real time and without the use of detection labels (Cook et al. 1997, Malmquist and Karlsson 1997, Lipshultz et al. 2000, Myszka et al. 2000, McDonnel 2001). The ability to analyze interactions in real time enables the collection of data, not only on the affinity of the ligand for its receptor, but also on the kinetics of the interaction. Prior to the introduction of SPR biosensors, biomolecular interaction analysis was limited to binding partners with suitable spectroscopic properties such as fluorescent tags or other labels, or of a suitably positioned tryptophan residue that confers a useful fluorescence spectra (Malmquist and Karlsson 1997). The research described in this thesis, is the most extensive study of the interactions of the kinetics of the interactions between Trk receptors and neurotrophins, conducted to date.

4.2 The IAsys Biosensor

Real time quantitative analysis of the interactions of all recombinant Trk proteins with neurotrophins was undertaken with an IAsys biosensor (Affinity Sensors). In using the IAsys biosensor, one of the reactant molecules is coupled to a surface and an evanescent field is used to monitor changes in refractive index, caused by molecular interactions occurring within a few hundred nm of the sensor surface (Cush et al. 1993). Electromagnetic waves undergo refraction upon crossing the boundary between two mediums. The refractive index (n) of the medium (which determines the speed of the wave) and the angles of refraction (θ) are related by Snell's law; $n_1 \mathrm{Sin}\theta_1 = n_2 \mathrm{Sin}\theta_2$.

On traveling from a medium of high refractive index to a medium of low refractive index, the angle θ_2 increases relative to θ_1. At a particular angle of incidence θ_c (critical angle), the angle of the exiting wave θ_2, is 90º and the refracted wave is directed along the interface between the two mediums. At incident angles greater than θ_c, the incident wave is no longer transmitted through the second medium and is completely reflected (total internal reflection). The electric field associated with the electromagnetic radiation penetrates into the low refractive index medium, where it dies away exponentially. The distance (Z_o) that this "evanescent field" penetrates depends upon n_1, n_2 and the incident angle.

When the incident wave is totally internally reflected, the evanescent field is sensitive to changes that occur only within the distance Z_o (the distance the field penetrates) of the interface; bulk medium changes that occur beyond Z_o are not detectable. The IAsys utilizes a waveguide (a region of high refractive index bounded on either side by a low refractive index medium), to constrain the incident electromagnetic wave to total internal reflections at the low refractive index boundaries. Wave guidance only occurs when the "round trip" reflection is an integral multiple of 2π and for a thin waveguide; this condition is met by only one angle between θ_c, and 90º. Light propagation within the waveguide occurs at one reflection angle (θ_{guide}) and this angle is exquisitely sensitive to changes in the refractive index n_1. Small changes in n_1 result in large changes in θ_{guide}. Changes in n_1 may for example result from a biomolecular interaction event. Prism coupling is used to introduce laser light into the thin waveguide and to measure changes in θ_{guide}.

The IAsys biosensor uses a high refractive index prism to introduce light into the waveguide. Provided the prism is situated close to the waveguide surface, a light ray is totally reflected off the prism face parallel to the waveguide surface. If the distance between the prism face and the waveguide is similar to $\sin\theta_{guide}$, then while most of the light is reflected, some is able to continue uninterrupted in the direction of the original light beam. If the waveguide and the prism have the same refractive index, then the two angles, θ_{guide} and θ_p, (where θ_p is the reflection angle in the prism) are related by Snell's law; $n_{guide}\sin\theta_{guide} = n_p\sin A\,\theta_p$. A plot of the intensity of the light propagated within the waveguide versus the prism angle θ_p shows a sharp peak corresponding to the propagation angle θ_{guide}. In order to use the resonant mirror principle for measurement of biomolecular interactions, the prism is coated with a low refractive index coupling layer (~100 nm thick), forming a gap between the prism and waveguide.

The prism forms the base of a stirred cuvette used to contain the reactants. During the measurement of an interaction event, light reflected from the inside of the resonant mirror is measured as a function of the incident angle. With the exception of light incident at $\theta_{guide,}$ light is totally reflected at the prism, coupling-layer interface. At resonance, the incident light propagates down the waveguide and within the coupling layer through the evanescent field. Because the angle of excitation at resonance is sensitive to changes at the sensing surface, interactions at the surface may be monitored by changes in the excitation angle. Changes in the excitation angle are measured by arbitrary units, referred to as reaction units (RU's) and are measured as “arc secs”.

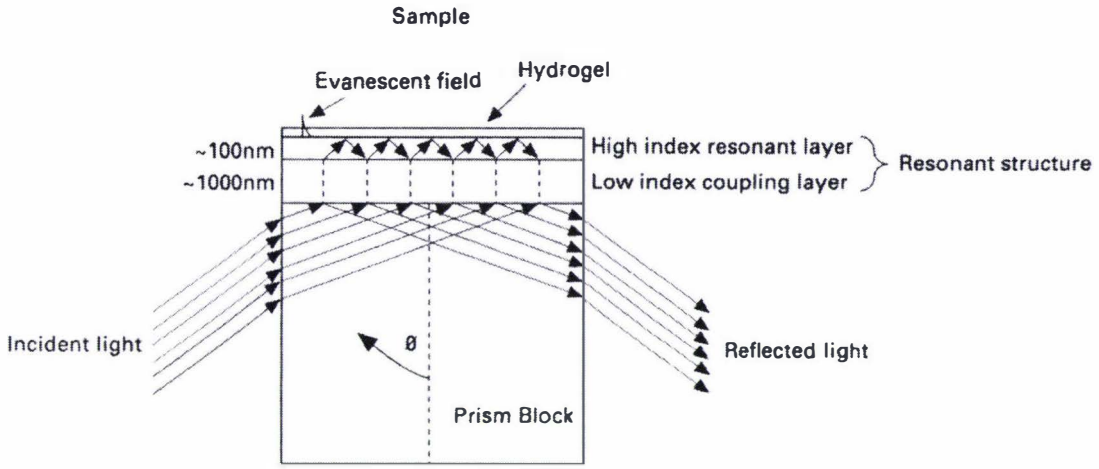

a

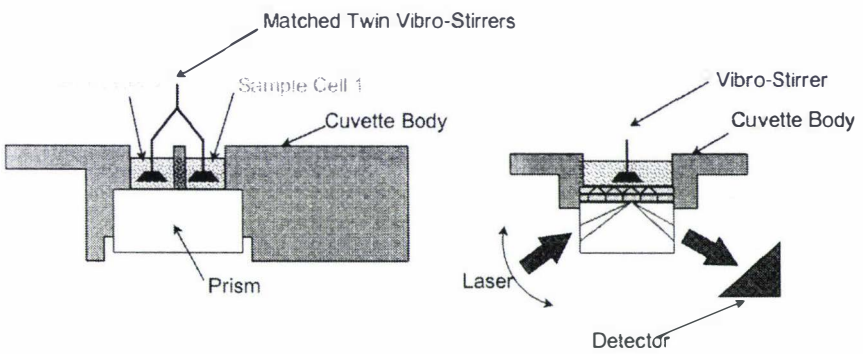

b

Figure 4.1 The arrangement of the IAsys biosensor surface and the components of the sensing system. (a) shows the prism that forms the base of stirred cuvette cell. This surface of the prism (exposed to the liquid in the cuvette) is coated with carboxymethyl dextran, to which the Trk proteins are covalently attached. (b) shows the arrangement of the cuvette itself and the stirring mechanism.

4.3 Coupling of Trk Proteins to the IAsys Surface

Immobilization of the MBP-fusion proteins was achieved through the carboxylate groups of the carboxymethyl dextran (CMD) surface of a IAsys cuvette and the primary amino groups (N-terminal and Lysine residues) of the Trk proteins, using 1-ethyl-3-(3-dimethylaminopropyl) carbodimide (EDC) and N-hydroxysuccinimide (NHS) chemistry and protocols (Affinity sensors).

The EDC/NHS chemistry (Figure 4.2) is shown below. After completion of the EDC/NHS activation of the surface of the reaction cuvette, 20 mM ammonium acetate pH 4.2 buffer was added to the reaction cell (the choice of immobilization buffer was dictated by the pI of the proteins, all of which have pI's ~ 5). Protein was then added to the cell and allowed to form covalent bonds with the activated carboxymethyl dextran. The level of protein immobilized never exceeded 3500 arc secs, well below the maximum level of 10,000 arc secs where spurious surface effects may be experienced (Affinity Sensors). When an adequate level of immobilization was achieved, the remaining activated CMD groups were blocked by the addition of 1 M Tris/HCl pH 8.

The synthetic His-tagged peptides representing the second LRR domain of TrkA, TrkB and TrkC were immobilized to the biosensor surface using an antibody to the His-tag (a gift of Affinity Sensors). The antibody was covalently attached to the cuvette surface with EDC/NHS chemistry.

Table 4.1 Protein immobilization levels (in arc secs) on the biosensor surface. A level of protein immobilization between 100 and 5000 arc secs will provide appropriate surface conditions for kinetics measurements (Dr. Eric Hnath, Affinity Sensors, personal communication).

Protein	Level
TrkA domains	
LRR2 synthetic peptide	850
MBP-LRR2	660
MBP-LRR	1050
MBP-C1LRR12	1320
MBP-LRR23C2	1438
MBP-C1LRR	1680
MBP-LRRC2	578
Ig-like (glycosylated)	990
Ig-like (unglycosylated)	736
MBP-ED	988
ED (*P. pastoris*)	493
TrkB domains	
LRR2 synthetic peptide	3200
MBP-C1LRR	790
MBP-LRRC2	1920
MBP- C1LRRC2	725
MBP-Ig	1095
MBP-ED	1021
TrkC domains	
LRR2 synthetic peptide	1200
MBP-ED	950

4.4 Immobilization Chemistry of Trk Proteins to IAsys Biosensor Surface

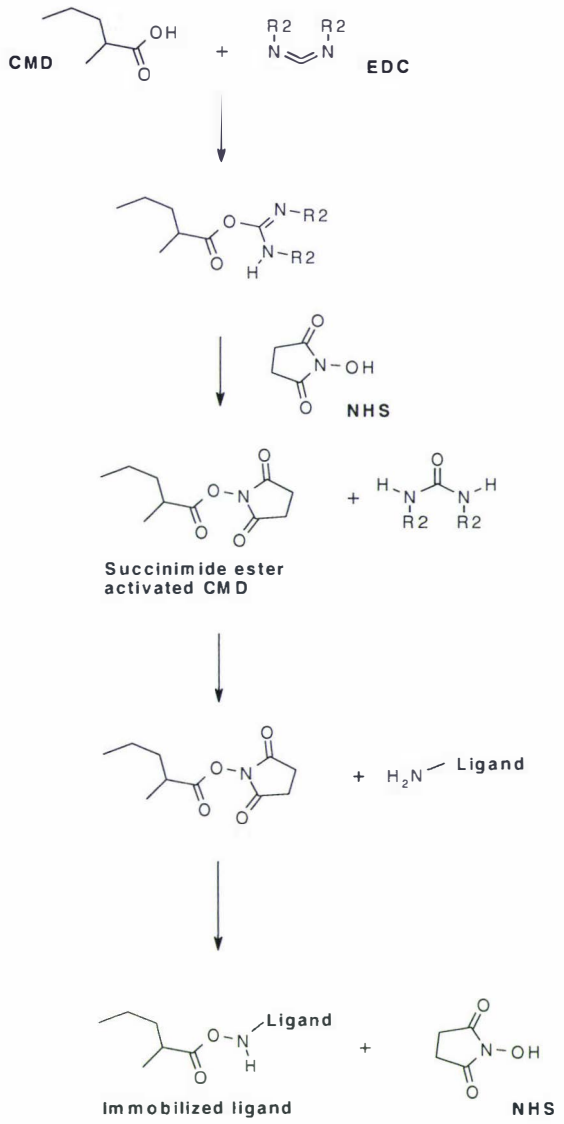

Figure 4.2 The immobilization chemistry used in covalently linking Trk proteins to the biosensor cuvette surface.

4.5 Control of Non-Specific Interactions

Non-specific interactions of neurotrophin with the biosensor surface or with the Trk proteins, was controlled by addition of NaCl, at a concentration of 150 mM and of Tween-20 at a concentration of 0.01%, to the reaction buffer. The method of determining the level of salt to add to the reaction buffer is shown in Figure 4.3.

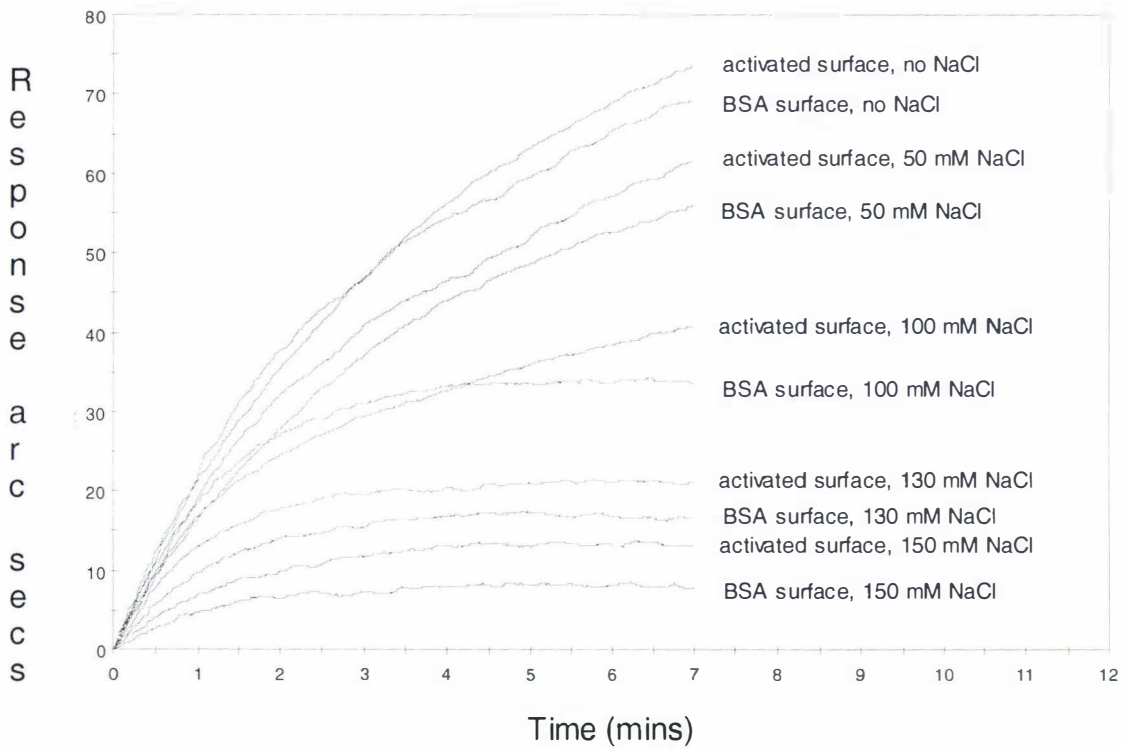

Figure 4.3 To determine the concentration of salt to be added to reaction buffers, sufficient to prevent non-specific interactions with the biosensor surfaces, NGF at a concentration 10 fold higher than the highest concentration used in the binding studies, was allowed to react with the two surfaces of an IAsys cuvette. Both surfaces were activated with the EDC/NHS chemistry used to immobilize Trk proteins on the biosensor surface. On one surface, BSA (~ 600 arc secs) was immobilized. No protein was immobilized on the second surface. Neurotrophin was allowed to react with both surfaces, in aliquots of the reaction buffer containing varying concentrations of NaCl. From the plot above, approximately 5-10 arc secs of the apparent reaction with either surface can be attributed to bulk

refractive index change, upon the addition of neurotrophin to the reaction wells. As shown, 150 mM of NaCl in the reaction buffer eliminated all non-specific interaction of NGF with the cuvette surface. Similar results were obtained for BDNF and NT-3 in buffer containing 150 mM NaCl. The neutotrophins showed no affinity for immobilized MBP (New England Biolabs), as previously reported (Windisch et al. 1996a).

4.6 Binding Data Collection

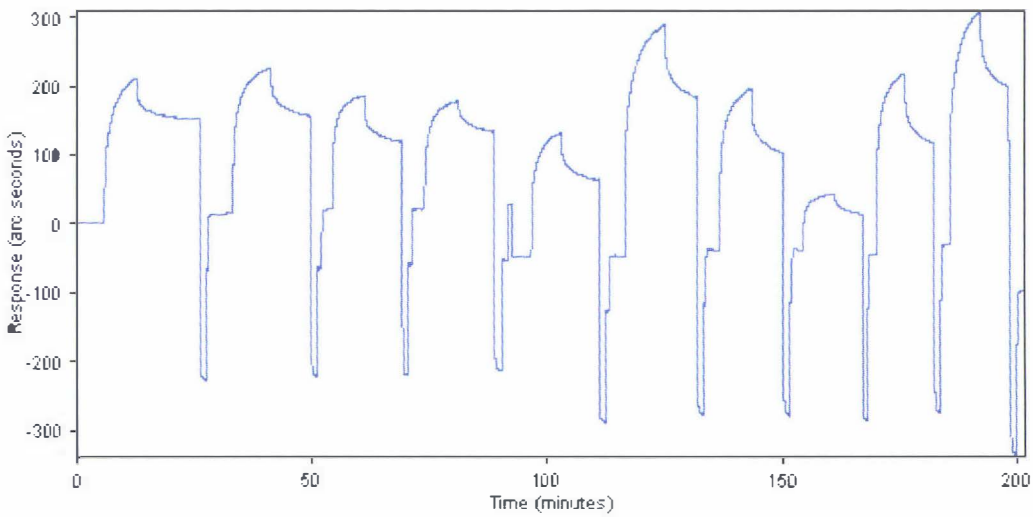

Figure 4.4 A typical set of association and dissociation data generated from the biosensor study of neurotrophin binding to an immobilized Trk protein[1].

An example of the binding and dissociation response from the IAsys biosensor during the collection of a set of binding/dissociation data is shown in Figure 4.4 (TrkA MBP-C1LRR at 15ºC). Rising curves result from the binding of neurotrophin to immobilized Trk protein. Neurotrophin of a known concentration (~ 1nM to ~ 5 µM) was added as a 5 µl aliquot with a 10 µl Hamilton syringe, to 50 µl of buffer (10 mM Hepes pH 7.4, 150 mM NaCl, 0.01% Tween 20) in the cuvette. Descending curves result from dissociation of bound neurotrophin from the Trk

[1] This data set was amongst the first collected and will be used throughout this chapter to illustrate various points and explanations of data collection and analysis.

protein after the buffer containing neurotrophin was removed from the reaction cuvette and replaced with fresh buffer. The almost vertical response from the instrument results from the removal of the buffer from the reaction cuvette and replacement with 10 mM HCl. This ensured complete removal of any neurotrophin that remained bound to the receptor after the dissociation event and prior to the addition of a new neurotrophin concentration. Following equilibration in fresh buffer, a new association/dissociation reaction data set was collected. Typically, association/dissociation reaction rates were measured for 10 different neurotrophin concentrations.

Reaction rates were measured at 3 different temperatures for each Trk protein; 15, 25 and 37ºC. All buffers contained 150 mM NaCl. Initial experiments to determine the binding of the neurotrophins to activated carboxymethyl dextran (CMD) surfaces without immobilized Trk protein, showed that 150 mM NaCl was an essential component of all buffers if electrostatic interaction between neurotrophin and the CMD surface was to be completely eliminated. Failure to eliminate such non protein-protein interactions would have severely compromised the accurate determination of the binding and dissociation constants for the Trk-neurotrophin interactions.

Different neurotrophin concentrations were added to the reaction cuvette in random order, that is, the concentrations did not follow a low to high pattern throughout the binding assay. Neurotrophin concentrations in the reaction cuvette varied from ~ 1200 nM to ~ 5500 nM (for NGF interactions with TrkA proteins) after dilution from stock solutions. Intermediate concentrations were prepared by serial dilution from an initial stock solution. Each concentration was further analyzed by UV spectroscopy and the concentration determined by the absorbance at 280 nm using the extinction coefficient for each neurotrophin at this wavelength[1]. The neurotrophin concentrations used ensured a response of >50 arc secs for the lowest concentration, thus increasing the accuracy of the data analysis. Stirrer speed was maintained at 80% of maximum throughout all experiments to eliminate mass transport effects. The reaction temperature in the cuvette varied by < 0.3ºC of the set temperature throughout each experiment.

[1] NGF = 8250 M^{-1} cm^{-1} BDNF = 6400 M^{-1} cm^{-1} NT-3 = 7680 M^{-1} cm^{-1} at 280 nm

4.7 Definitions of Kinetics Terminology

The interactions between neurotrophin and Trk receptor were analyzed by plotting the measured on-rate constant, k_{on} obtained from association analysis at a number of neurotrophin concentrations, versus neurotrophin concentration. From such plots, the equilibrium dissociation constant, K_D may be determined for each Trk protein-neurotrophin interaction. A single example of this type of analysis is shown in Figures 4.5 through 4.8. Because of limitations in the quantity of neurotrophins available for this study, only one K_D for each Trk protein, at three different temperatures, could be determined.

Association occurs on addition of ligate at a defined concentration to the IAsys reaction cuvette. On the surface of the cuvette, a putative ligand is immobilized. The association curve obtained is the net response between association and dissociation events. Monophasic association occurs when the response, on addition of ligate, increases in an exponential manner, with only one distinguishable phase. The quantity of complex formed in time t, namely $[CL]_t$ is given by:

$$[CL]_t = [CL]_{eq}[1-\exp(-k_{on}t)] \quad (1)$$

where $[CL]_{eq}$ is the concentration of the complex at equilibrium, L is the ligand and k_{on} is the pseudo first order rate for the molecular interaction.

$$k_{on} = k_{ass}[L] + k_{diss} \quad (2)$$

where k_{ass} is the derived association rate constant obtained from the slope of the plot of k_{on} versus concentration of sample. Similarly, k_{diss} is the derived dissociation constant obtained from the intercept of the plot of k_{on} versus concentration of sample.

Hence k_{on} varies with ligand concentration. The instrument response R (measured in arc secs), is proportional to the mass of bound ligate, resulting in:

$$R_t = (R_{eq} - R_0)[1 - \exp(-k_{on}t)] + R_o \quad (3)$$

In this relationship, R_t is the instrument response at time t, R_{eq} is the maximal instrument response and R_o is the initial instrument response value. These instrument response values are obtained experimentally and hence the single unknown, k_{on} at a particular concentration of ligate (e.g., neurotrophin), is derived. Multiple determinations of k_{on} for the Trk-neurotrophin

interaction were obtained by carrying out repeat association measurements at various concentrations[3] of neurotrophin.

Equation (3) is in the form of a straight line and hence a plot of the values of k_{on} derived from a complete (6-10 measurements) interaction experiment, against the ligate concentration at which they were conducted, allows k_{ass} and k_{diss} to be estimated. The gradient of the line gives $k_{ass,}$ while the y-axis intercept allows the value of k_{diss} to be estimated (Figure 4.6). The dissociation constant values often have large errors associated with them, a consequence of the difficulty in accurately estimating the intercept values for lines that intersect the y-axis at shallow angles.

Experimentally derived association curves having an immobilized ligand and soluble ligate are often not well described by simple monophasic kinetics. In these situations, two distinguishable association phases are noticeable. Such biphasic kinetics may be considered to be the sum of two distinct association processes, each of which has an apparent association rate constant, described by the relationship:

$$R_t = A[1 - \exp(-k_{on(1)}{}^{t)})] + B[1 - \exp(-k_{on(2)}{}^{t})] + R_0 \quad (4)$$

Where A and B represent the two phases of the association and $k_{on(1)}$ and $k_{on(2)}$ are the respective, apparent association rates.

In practice, the association curves obtained for each ligate concentration are fitted to both theoretical monophasic and biphasic association curves. From this analysis, the best fit of the association data, to either monophasic or biphasic kinetics is determined.

Once the molecular complex has been formed, it will eventually dissociate into its components, namely immobilized ligand and free ligate. Simple monophasic dissociation is described by the exponential relationship:

$$R_t = R_0 \exp(-k_{diss} t) \quad (5)$$

[3] Typically only 6 concentrations of ligate are used to determine association curves and to estimate the equilibrium dissociation constant for a molecular interaction. For all Trk-neurotrophin interactions, k_{on} was determined at 10 different concentrations of neurotrophin, in order to reduce the errors in the estimate of the dissociation constant.

The amount of complex at time t, namely R_t, is dependent on the initial complex concentration R_0 and the dissociation rate constant k_{diss} As with biphasic association, biphasic dissociation having two phases A and B, is described by two dissociation constants $k_{diss(1)}$ and $k_{diss(2)}$ such that:

$$Rt = Aexp(-k_{diss(1)}{}^{t}) + B(-k_{diss(2)}{}^{t}) \qquad 6$$

4.8 Data Analysis and Error Propagation

A total of 10 association and dissociation curves were obtained for each neurotrophin-Trk receptor interaction. Association curves for one reaction are shown in Figure 4.5.

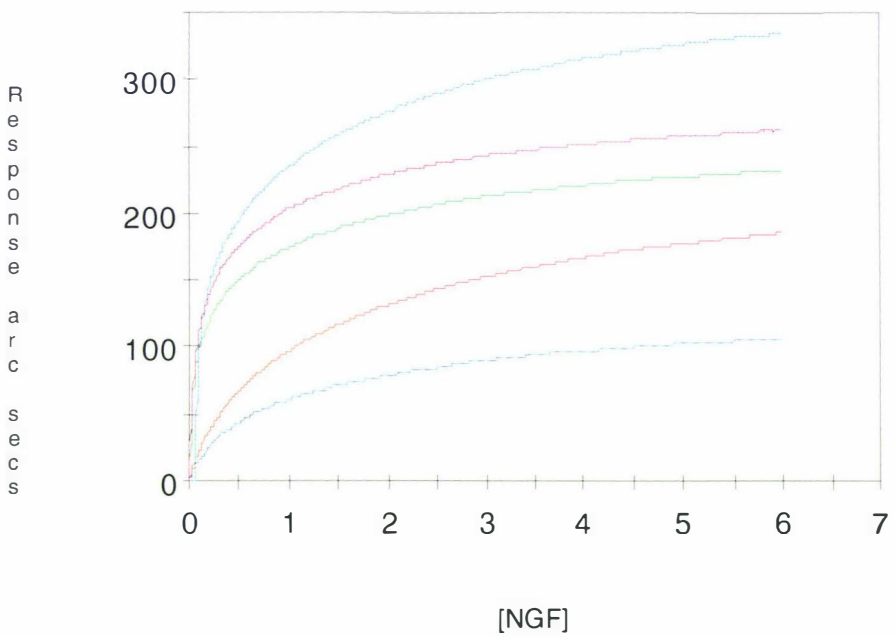

Figure 4.5 Association curves for the reaction of NGF with TrkA MBP-C1LRR recombinant protein at 15°C. The full set of association and dissociation curves for this reaction is shown in Figure 4.3. Only 5 of the 10 association curves are shown for clarity.

The association rates for each reaction at a particular neurotrophin concentration are plotted against the neurotrophin concentration. This results in a data plot, as shown in Figure 4.6. From a least squares fit to the data, the association rate constant k_{ass} is obtained. The data analysis software (Affinity Sensors) returns a report of the slope of the fitted line, an error and the correlation coefficient. For all interaction studies, the correlation coefficient was better than 0.98, indicating a good fit of the data.

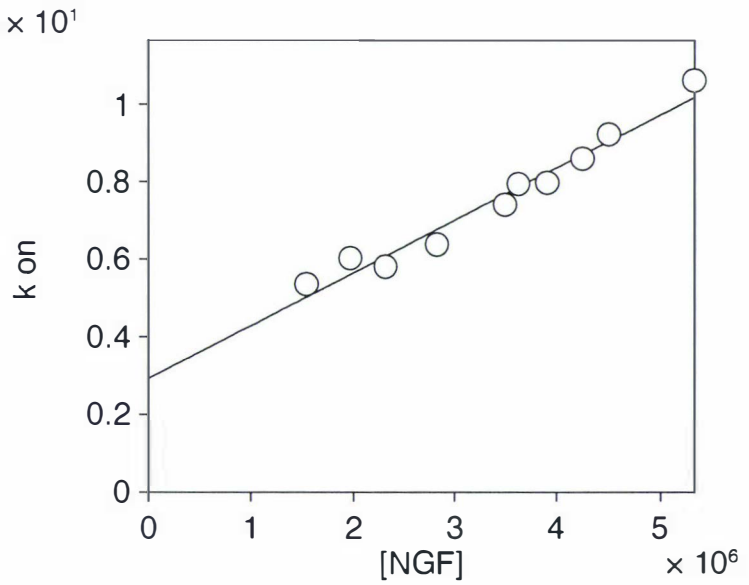

Gradient = 13594.4 ± 859.596 Corr Coeff = 0.982479

Figure 4.6 The association rate K_{ass} is determined by plotting the neurotrophin concentration versus, K_{on}, the rate at which the neurotrophin interacts with the immobilized Trk protein. The slope of the least squares fit to the data is the association rate (data collection shown in Figure 4.4). The interaction of NGF with TrkA MBP-C1LRR at 15^{0}C is shown above. The gradient and correlation coefficient report is copied from the analysis software report.

Each association (Figure 4.4) and dissociation curve may be fitted to a theoretical monophasic or biphasic association or dissociation equation. The quality of the fit of the theoretical curves to the actual data is judged by the excellence of the overlay to each binding, or dissociation curve, as shown in Figure 4.7 and Figure 4.8, respectively.

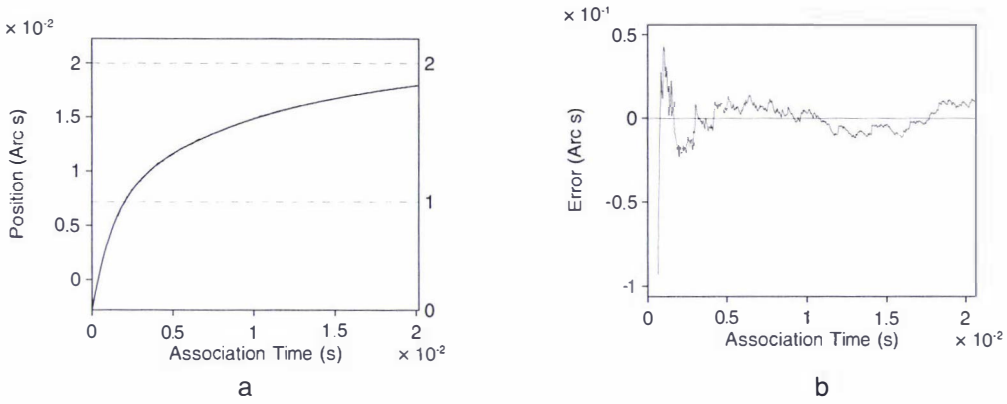

Figure 4.7 The quality of the fit of a binding rate equation to the association data is shown in (a). The theoretical fit it seen as a red line, overlaying the binding curve (red line does not transfer from the data analysis software to an external document). Further judgment of the quality of the data fit to the association rate theoretical model is made by examination of a plot of the error about the line, as shown in (b). This Figure shows data analysis of a single binding curve from Figure 4.5.

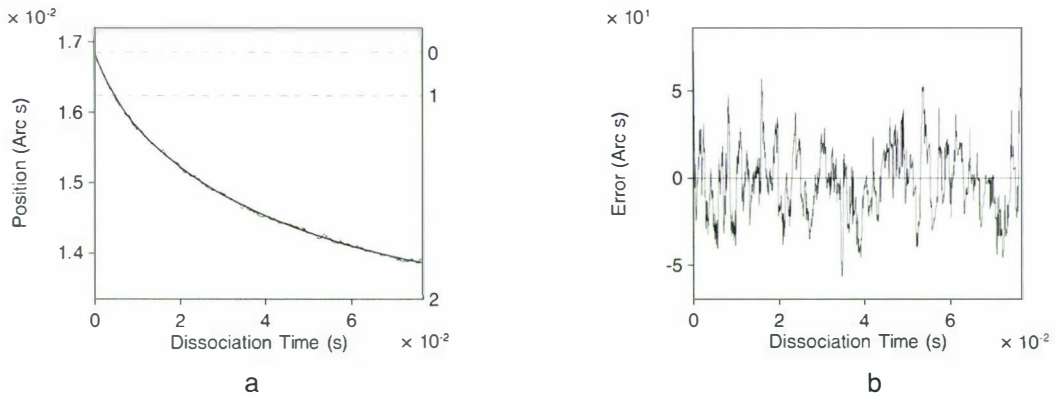

Figure 4.8 The quality of the fit of a dissociation rate equation to the dissociation data is shown in (a). The theoretical fit it seen as a red line, overlaying the binding curve (red line does not transfer form the data analysis software to an external document). Further judgment of the quality of the data fit to the dissociation rate theoretical model is made by examination of a plot of the error about the line, as shown in (b). This Figure shows data analysis of a single dissociation curve from Figure 4.4.

The observed association of NGF for all TrkA proteins, may be best described by fitting, to the binding data, an equation of the form:

$R_t = A(1-\exp^{-k_{on(1)}t}) + B(1-\exp^{-k_{on(2)}t})$, where R_t is the instrument response at time t and A is the extent of the first phase, having an apparent "on-rate" defined as $k_{on(1)}$. B is the extent of the second phase having an apparent "on-rate" of $k_{on(2)}$.

The dissociation event is described by an equation of the form:

$R_t = R_0\exp(-k_{diss}t)$, where R_t is the amount of complex formed at time t and is dependant on the initial complex concentration R_0. The dissociation constant for the complex separating into its component proteins is given by k_{diss}. The dissociation of NGF from all TrkA proteins used in the biosensor study is monophasic.

The association and dissociation events for the interaction of NGF with the recombinant and synthetic proteins, representing different ED regions of the TrkA receptor, are tabulated below (Tables 42 through 4.14).

The equilibrium dissociation constant is calculated from the relationship:

$$K_D = k_{diss}.\ k_{ass}^{-1}$$

The association of NGF with all TrkA proteins was observed to be biphasic, the tabulated kinetics below, show only a single association rate, K_{ass}. Only monophasic dissociation was observed. The dissociation constant K_{diss} is shown in the Tables (Tables 4.4 through 4.14). The equilibrium dissociation constant (K_D) is shown and is calculated from the values of K_{ass} and k_{diss}. It is difficult to assign a second equilibrium dissociation constant, given that monophasic dissociation does not permit the unambiguous calculation of the constant.

A method of calculating the K_{ass} and k_{diss} values for an interaction of NGF with a TrkA protein, involves fitting a binding curve through the data shown in Figure 4.5. This method appears,

from previous data analysis attempts, to return an average value for the two equilibrium dissociation constants that describe biphasic protein association interactions. Hence, while the slower association rate is reasonably obtained by this method, the faster association rate is poorly described. Consequently, a best estimate for one K_{ass} was determined to provide a single K_D.

While the rate k_{on}, for the interaction of a neurotrophin with a Trk protein, varies with the concentration of neurotrophin, the dissociation rate k_{diss} will not change (except within experimental error). The association data was fitted to obtain only the fastest k_{on} rate for the interactions of NGF with all TrkA recombinant proteins, allowing the estimate of k_{ass}, as illustrated in Figure 4.7a. The dissociation rate, k_{diss}, for the reactions is obtained from the mean of the 10 dissociation curves (Figure 4.4 and Figure 4.8) for each interaction. The percentage error in the value of k_{ass} and the percentage error in the value of k_{diss} (standard deviation) are added to provide an error in the value of the equilibrium dissociation constant, K_D, for each neurotrophin-Trk protein interaction.

From the tabulated equilibrium dissociation (K_D) data for each reaction of a neurotrophin with a particular Trk protein (Table 4.2 through Table 4.25), it is seen that the values for the K_D's at 3 different temperatures, are the same within the error estimates. In particular, the association and dissociation rates increase with temperature, as illustrated in Figure 4.9 and Figure 4.10, respectively. Many molecular interaction rates display this relationship, as described by the Arrhenius equation (Atkins 1986) and has been seen for protein-protein interactions studied by biosensors (Oddie et al. 1997). The increase in K_{ass} and k_{diss} with temperature, is not influenced by any potential mass transport effects since increasing temperatures raise the diffusion coefficient of the protein in solution (Oddie et al. 1997).

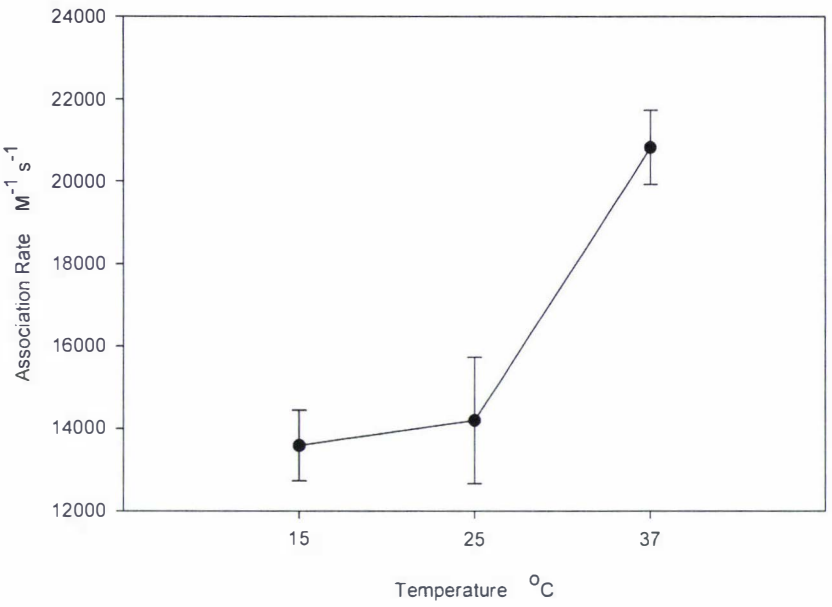

Figure 4.9 The association rate of neurotrophins for Trk proteins, increases with temperature. The data shown above is for the interaction of NGF with TrkA C1LRR (Figure 4.4).

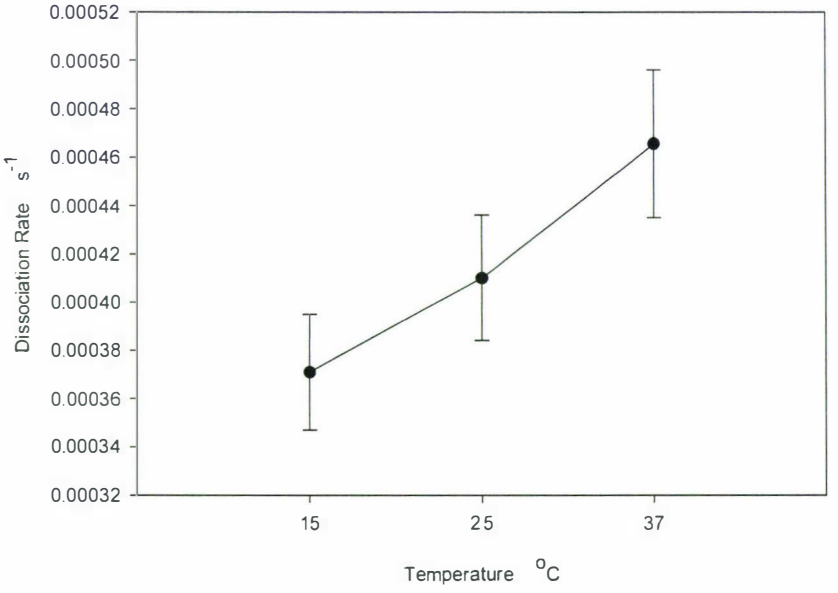

Figure 4.10 The dissociation rate of neurotrophins for Trk proteins, increases with temperature. The data shown above is for the interaction of NGF with TrkA C1LRR (Figure 4.4).

The observed association of BDNF for all TrkB proteins and of NT-3 for TrkC proteins, can be described by fitting, to the binding data, an equation of the form:
$R_t = R_{eq}(1-\exp^{-k_{on}t})$, where R_t is defined above, R_{eq} is the equilibrium response and k_{on} is the apparent "on-rate" for a given ligand concentration. Hence the association of BDNF for all TrkB recombinant proteins is described by a monophasic association event.

The dissociation event is described by an equation of the form:
$R_t = R_0\exp(-k_{diss}t)$, where R_t is the amount of complex formed at time t and is dependant on the initial complex concentration R_0. The dissociation constant for the complex separating into its component proteins is given by k_{diss}. The dissociation of BDNF from all TrkB proteins used in the biosensor study is monophasic.

The association and dissociation events for the interaction of BDNF with the recombinant and synthetic proteins, representing different ED regions of the TrkB receptor, are tabulated below (Table 4.15 through Table 4.25).

4.9 Results

4.9 a The interactions of NGF with TrkA Proteins

Table 4.2 TrkA LRR2 synthetic peptide. The measured association and dissociation rates for the synthetic peptide.

°C	$k_{ass(1)}$ M^{-1} s^{-1}	k_{diss} s^{-1}	K_D nM
15	5044 ± 320	3.7553e-4 ± 3.5589e-5	74.5 ± 11.8
37	5670 ± 292	3.8543e-4 ± 2.8262e-5	68 ± 8.5

Table 4.3 TrkA MBP-LRR2. The measured association and dissociation rates for the recombinant protein LRR2.

°C	$k_{ass(1)}$ M^{-1} s^{-1}	k_{diss} s^{-1}	K_D nM
15	10842 ± 1062	2.6059e-4 ± 3.0003e-6	24 ± 2.6
25	15051 ± 1124	3.5506e-4 ± 2.23929e-6	22.9 ± 1.9
37	16346 ± 1164	3.1563e-4 ± 1.1529e-5	19.3 ± 2.1

Table 4.4 TrkA MBP-LRR. The measured association and dissociation rates for the recombinant protein LRR.

°C	$k_{ass(1)}$ M^{-1} s^{-1}	k_{diss} s^{-1}	K_D nM
15	10731 ± 1612	2.7202e-4 ± 1.4577e-5	25.4 ± 5.2
25	11769 ± 1039	2.5325e-4 ± 2.9861e-6	21.5 ± 2.2
37	12317 ± 1404	2.8657e-4 ± 1.5863e-5	23.3 ± 4

Table 4.5 TrkA MBP-C1LRR12. The measured association and dissociation rates for the recombinant protein C1LRR12.

°C	$k_{ass(1)}$ M^{-1} s^{-1}	k_{diss} s^{-1}	K_D nM
15	12582 ± 1353	3.5549e-4 ± 4.0196e-5	28.3 ± 6.2
25	14966 ± 1399	2.7886e-4 ± 1.2902e-5	18.6 ± 2.6
37	15842 ± 1512	4.1805e-4 ± 1.6425e-5	26.4 ± 3.6

Table 4.6 TrkA MBP-LRR23C2. The measured association and dissociation rates for the recombinant protein LRR23C2.

°C	$k_{ass(1)}$ M^{-1} s^{-1}	k_{diss} s^{-1}	K_D nM
15	14181 ± 731	4.4739e-4 ± 3.3256e-5	31.6 ± 4
25	14974 ± 1560	3.3995e-4 ± 2.6057e-5	22.7 ± 4
37	16103 ± 1504	4.0688e-4 ± 5.8339e-6	25.2 ± 2.7

Table 4.7 TrkA MBP-C1LRR. The measured association and dissociation rates for the recombinant protein C1LRR.

°C	$k_{ass(1)}$ M^{-1} s^{-1}	k_{diss} s^{-1}	K_D nM
15	13594 ± 860	3.7087e-4 ± 2.3972e-5	27.3 ± 3.5
25	14202 ± 1535	4.1008e-4 ± 2.5978e-5	28.9 ± 5
37	20825 ± 902	4.6555e-4 ± 3.0535e-5	22.4 ± 2.4

Table 4.8 TrkA MBP-LRRC2. The measured association and dissociation rates for the recombinant protein LRRC2.

°C	$k_{ass(1)}$ M^{-1} s^{-1}	k_{diss} s^{-1}	K_D nM
15	14494 ± 1511	3.6405e-4 ± 4.6693e-5	25.1 ± 5.8
25	15978 ± 680	3.5491e-4 ± 1.5650e-5	22.2 ± 2
37	16290 ± 1542	4.66176e-4 ± 8.4163e-6	28.6 ± 3.2

Table 4.9 TrkA Ig-like domain (glycosylated). The measured association and dissociation rates for the recombinant protein Ig-like domain. Protein expressed in *P. pastoris* and provided by Prof. Prof. Uri Saragovi, McGill University, McGill University.

°C	$K_{ASS(1)}$ M^{-1} S^{-1}	K_{DISS} S^{-1}	K_D nM
15	8878 ± 1297	1.3165e-4 ± 8.8277e-6	14.8 ± 3.2
25	11029 ± 1264	1.6575e-4 ± 2.9817e-5	15 ± 4.4
37	13457 ± 1431	1.6902e-4 ± 1.4781e-5	12.6 ± 2.4

Table 4.10 TrkA Ig-like domain (unglycosylated). The measured association and dissociation rates for the recombinant protein Ig-like domain. Protein expressed in *E. coli* and provided by Prof. Uri Saragovi, McGill University.

°C	$k_{ass(1)}$ M^{-1} s^{-1}	k_{diss} s^{-1}	K_D nM
15	7260 ± 1213	5.7519e-5 ± 4.0334e-6	8 ± 1.9
25	14185 ±1806	1.6614e-4 ± 1.9742e-5	12 ± 1.7
37	15783 ± 810	1.9309e-4 ± 3.9415e-5	12 ± 3

Table 4.11 TrkA MBP-ED. The measured association and dissociation rates for the recombinant protein ED domain.

°C	$k_{ass(1)}$ M^{-1} s^{-1}	k_{diss} s^{-1}	K_D nM
15	12055 ± 1168	1.9028e-4 ± 2.7892e-5	15.8 ± 3.9
25	15606 ± 1179	2.0565e-4 ± 1.7915e-5	13.2 ± 2.2
37	16962 ± 1698	2.3934e-4 ± 3.3898e-5	14.1 ± 3.4

Table 4.12 TrkA ED (*P. pastoris*). The measured association and dissociation rates for the recombinant protein ED domain.

°C	$k_{ass(1)}$ M^{-1} s^{-1}	k_{diss} s^{-1}	K_D nM
15	14795 ± 1930	2.0164e-4 ± 2.8375e-5	13.6 ± 3.7
25	15180 ± 1425	2.3097e-4 ± 2.1834e-5	15.2 ± 2.9
37	18228 ± 565	2.1280e-4 ± 2.9469e-5	11.7 ± 2

Table 4.13 TrkA ED (insect cells). The measured association and dissociation rates for the recombinant protein ED domain. Protein provided by Prof. Uri Saragovi, McGill University.

°C	$k_{ass(1)}$ M^{-1} s^{-1}	k_{diss} s^{-1}	K_D nM
15	11490 ± 1648	2.4757e-4 ± 2.9488e-5	15.8 ± 2.5
25	17673 ± 1524	2.3989e-4 ± 1.8092e-5	13.6 ± 2
37	18329 ± 2094	3.3128e-4 ± 1.1995e-5	18 ± 2.7

Table 4.14 Values of the equilibrium dissociation constant (K_D), for the interaction of NGF with recombinant and synthetic TrkA proteins, over the temperature range of 15-37 °C.

TrkA Protein	K_D nM
LRR2 synthetic peptide	71.3 ± 4.6
MBP-LRR2	22.1 ± 2.5
MBP-LRR	23.4 ± 2.0
MBP-C1LRR12	24.4 ± 5.1
MBP-LRR23C2	26.5 ± 4.6
MBP-C1LRR	26.2 ± 3.4
MBP-LRRC2	25.3 ± 3.2
Ig-like (glycosylated)	14.1 ± 1.3
Ig-like (unglycosylated)	10.7 ± 2.3
MBP-ED	14.4 ± 1.3
ED (P. pastoris)	13.5 ± 1.8
ED (insect cells)	15.8 ± 2.2

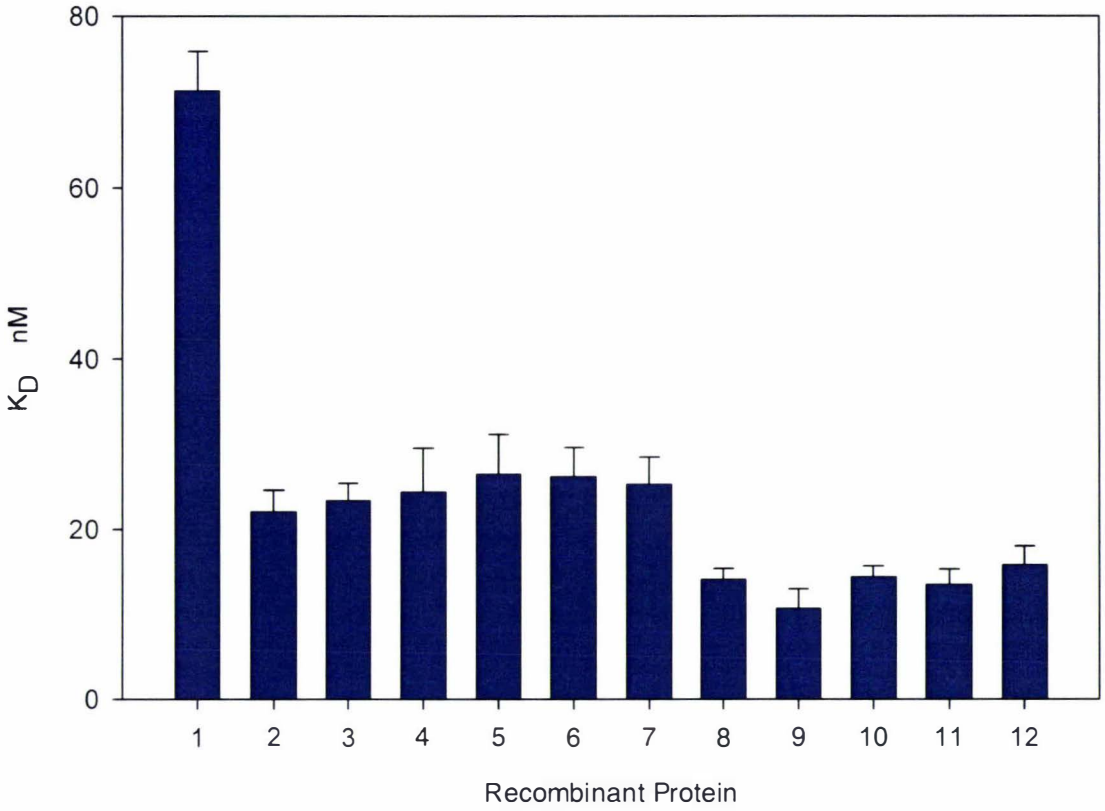

Figure 4.11 The mean and standard deviations of the equilibrium dissociation constants for the interactions of NGF with the TrkA, recombinant proteins and synthetic peptide for the temperature range 15-37 °C

Recombinant Protein

1.....LRR2 synthetic peptide

2.....MBP-LRR2

3.....MBP-LRR

4.....MBP-C1LRR12

5.....MBP-LRR23C2

6.....MBP-C1LRR

7.....MBP-LRRC2

8.....Ig-like domain (glycosylated)

9.....Ig-like domain (unglycosylated)

10.....MBP-ED

11.....ED (*P. pastoris*)

12.....ED (insect cells)

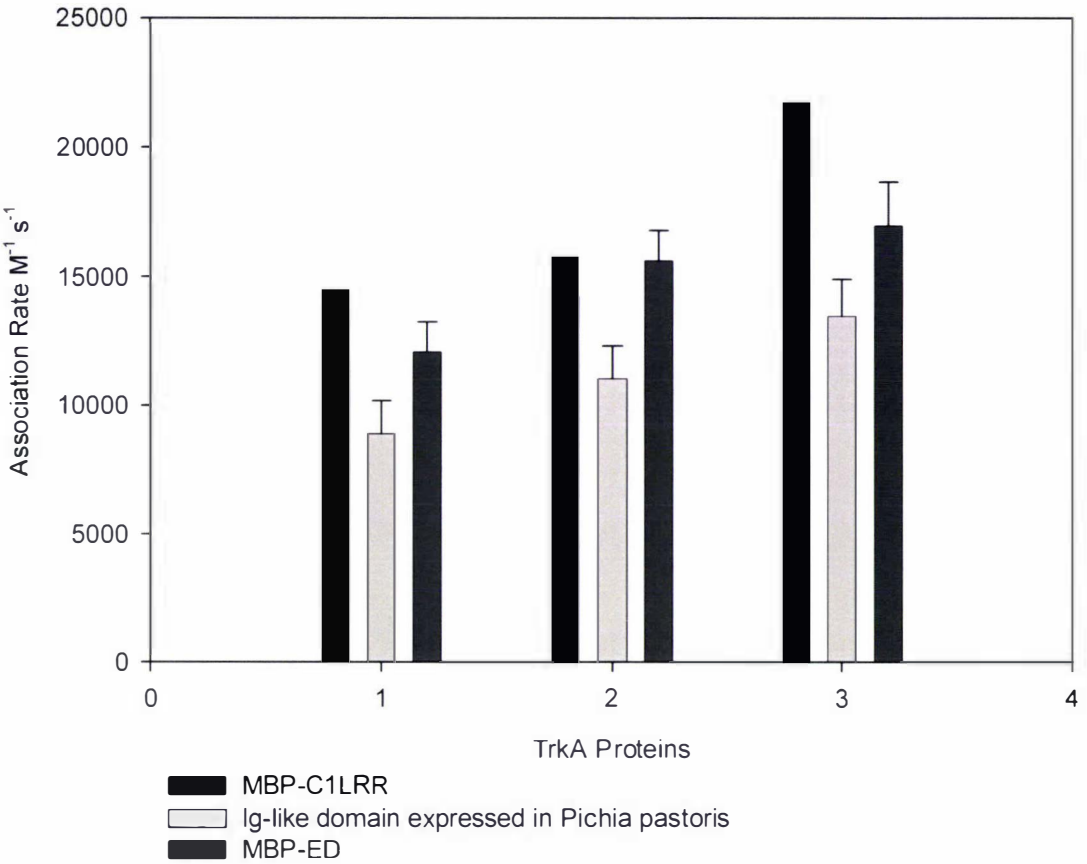

Figure 4.12 The association rates of the individual TrkA domains are essentially the same as for the complete ED domain of TrkA at the 3 temperatures at which measurements are made. The data set denoted as 1, corresponds to association rates at 15°C, set 2 corresponds to association rates at 25°C and set 3 corresponds to association rates at 37°C.

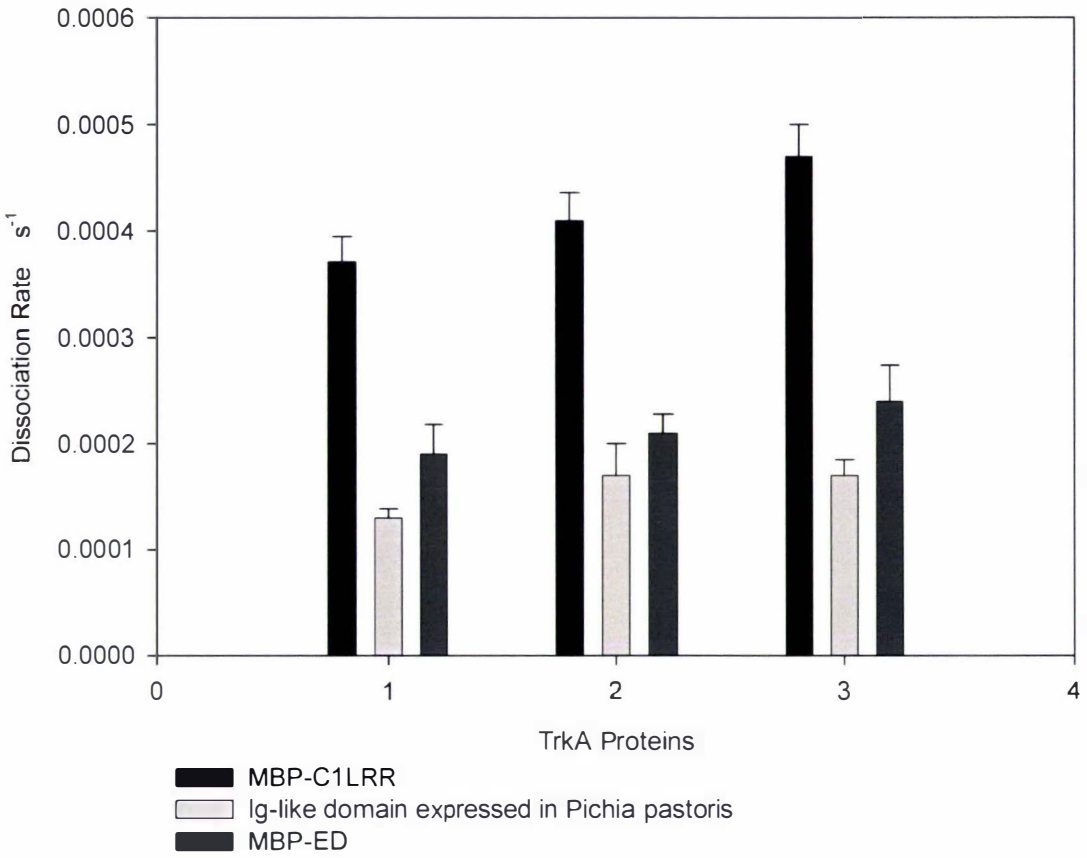

Figure 4.13 The dissociation rates of the individual TrkA domains are essentially the same at 15°C, 25°C and 37°C. The LRR domain has a lower affinity for NGF (at all three temperatures) than either the Ig-like domain or the ED domain. The data set denoted as 1, corresponds to dissociation rates at 15°C, set 2 corresponds to dissociation rates at 25°C and set 3 corresponds to dissociation rates at 37°C.

4.9 b The interactions of BDNF with TrkB Proteins

Table 4.15 TrkB LRR2 synthetic peptide. The measured association and dissociation rates for the synthetic peptide.

°C	k_{ass} M^{-1} s^{-1}	k_{diss} s^{-1}	K_D nM
15	42292 ± 4901	1.6307e-3 ± 2.0935e-4	38.6 ± 9.4
25	54606 ± 3656	1.7514e-3 ± 1.8730e-4	32.1 ± 5.6
37	60397 ± 5543	1.8290e-3 ± 2.4480e-4	30.3 ± 6.8

Table 4.16 TrkB MBP-C1LRR. The measured association and dissociation rates for the recombinant protein C1LRR.

°C	k_{ass} M^{-1} s^{-1}	k_{diss} s^{-1}	K_D nM
15	45106 ± 7274	6.4964e-4 ± 9.3974e-5	14.4 ± 4.4
25	81968 ± 6612	1.3982e-3 ± 3.4988e-4	17.1 ± 5.7
37	88684 ± 5387	1.8608e-3 ± 4.7135e-4	21 ± 6.6

Table 4.17 TrkB MBP-LRRC2. The measured association and dissociation rates for the recombinant protein LRRC2, are tabulated above. The dissociation data for the set of measurements at 15°C was very poor, with the consequence that the dissociation curves could not be fitted well; hence the unusually large error in the estimate of the dissociation rate.

°C	k_{ass} M^{-1} s^{-1}	k_{diss} s^{-1}	K_D nM
15	42802 ± 5757	7.3489e-4 ± 4.1679e-4	17 ±12
25	71000 ± 8031	1.4754e-3 ± 2.5603e-4	20.8 ± 6
37	74895 ± 2808	1.5885e-3 ± 4.3782e-4	21.2 ± 6.6

Table 4.18 TrkB MBP-C1LRRC2. The measured association and dissociation rates for the recombinant protein C1LRRC2.

°C	k_{ass} M^{-1} s^{-1}	k_{diss} s^{-1}	K_D nM
15	28898 ± 693	4.8266e-4± 2.6648e-5	16.7 ± 1.3
25	74798 ± 6535	1.4541e-3 ± 2.1816e-4	19.4 ± 4.6
37	95355 ± 9889	2.0915e-3 ± 9.1297e-5	21.9 ± 3.2

Table 4.19 TrkB MBP-Ig-like domain. The measured association and dissociation rates for the recombinant protein Ig-like domain.

°C	k_{ass} M^{-1} s^{-1}	k_{diss} s^{-1}	K_D nM
15	38824 ± 3844	7.3553e-4 ± 2.3317e-5	19 ± 2.5
25	88443 ± 4566	1.2156e-3 ± 1.9684e-4	13.7 ± 2.9
37	101390 ± 10726	1.5592e-3 ± 7.6620e-5	15.4 ± 2.4

Table 4.20 TrkB MBP-ED. The measured association and dissociation rates for the recombinant protein ED domain.

°C	k_{ass} M^{-1} s^{-1}	k_{diss} s^{-1}	K_D nM
15	52089 ± 3088	6.2608e-4 ± 1.7253e-4	12 ± 4
25	94241 ± 7341	7.0685e-4 ± 1.2800e-4	7.5 ± 1.9
37	133520 ± 3297	1.0080e-3 ± 7.2353e-5	7.6 ± 0.7

Table 4.21 TrkB ED (*P. pastoris*). The measured association and dissociation rates for the recombinant protein ED domain, expressed in *P. pastoris*.

°C	k_{ass} M^{-1} s^{-1}	k_{diss} s^{-1}	K_D nM
15	58603 ± 6879	7.3877e-4 ± 1.4004e-4	12.6 ± 3.9
25	100038 ± 6618	8.9154e-4 ± 5.6568e-5	8.9 ± 1.2
37	122308 ± 12306	1.5914e-3 ± 3.0546e-4	13 ± 3.8

Table 4.22 Values of the equilibrium dissociation constant (K_D), for the interaction of BDNF with recombinant and synthetic TrkB proteins, over the temperature range of 15-37 °C.

TrkB Protein	K_D nM
LRR2 synthetic peptide	33.7 ± 4.4
MBP-C1LRR	17.5 ± 3.3
MBP-LRRC2	19.7 ± 2.3
MBP- C1LRRC2	19.3 ± 2.6
MBP-Ig	16.0 ± 2.7
MBP-ED	9.0 ± 2.6
ED (P. pastoris)	11.5 ± 2.3

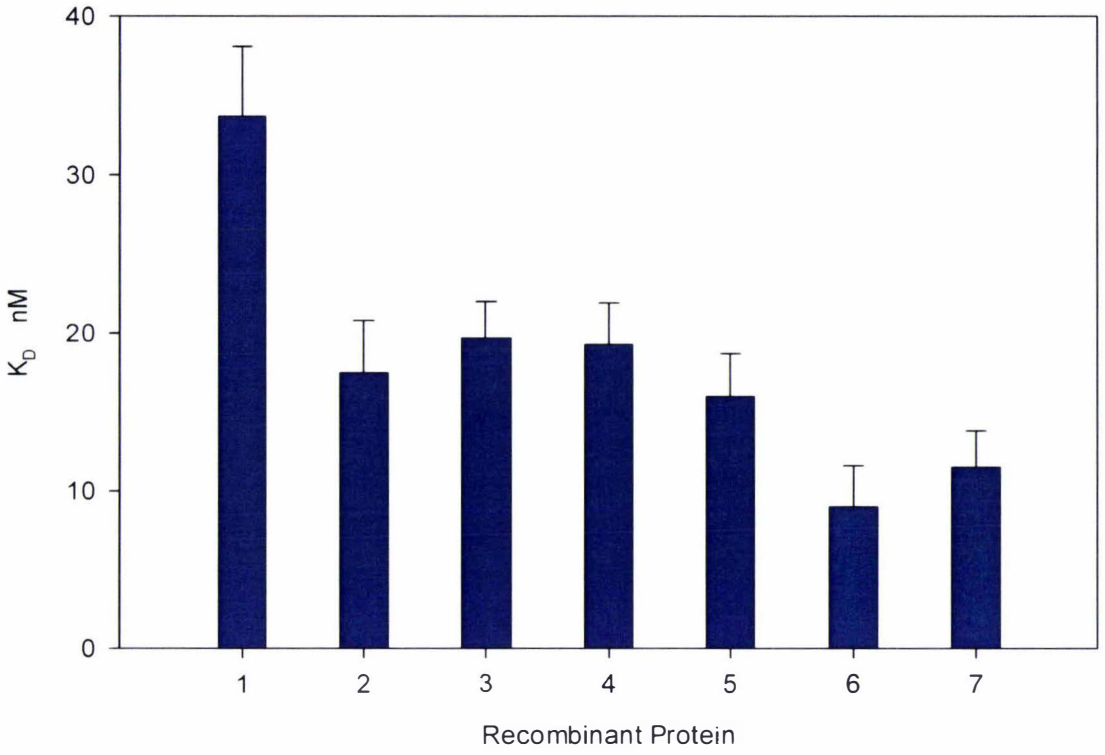

Figure 4.14 The mean and standard deviations of the equilibrium dissociation constants for the interactions of BDNF with the TrkB, recombinant proteins and synthetic peptide for the temperature range 15-37 °C.

1.....LRR2 synthetic peptide

2.....MBP-C1LRR

3.....MBP-LRRC2

4.....MBP-C1LRR2

5.....Ig-like domain (unglycosylated)

6.....MBP-ED

7..... ED (*P. pastoris*)

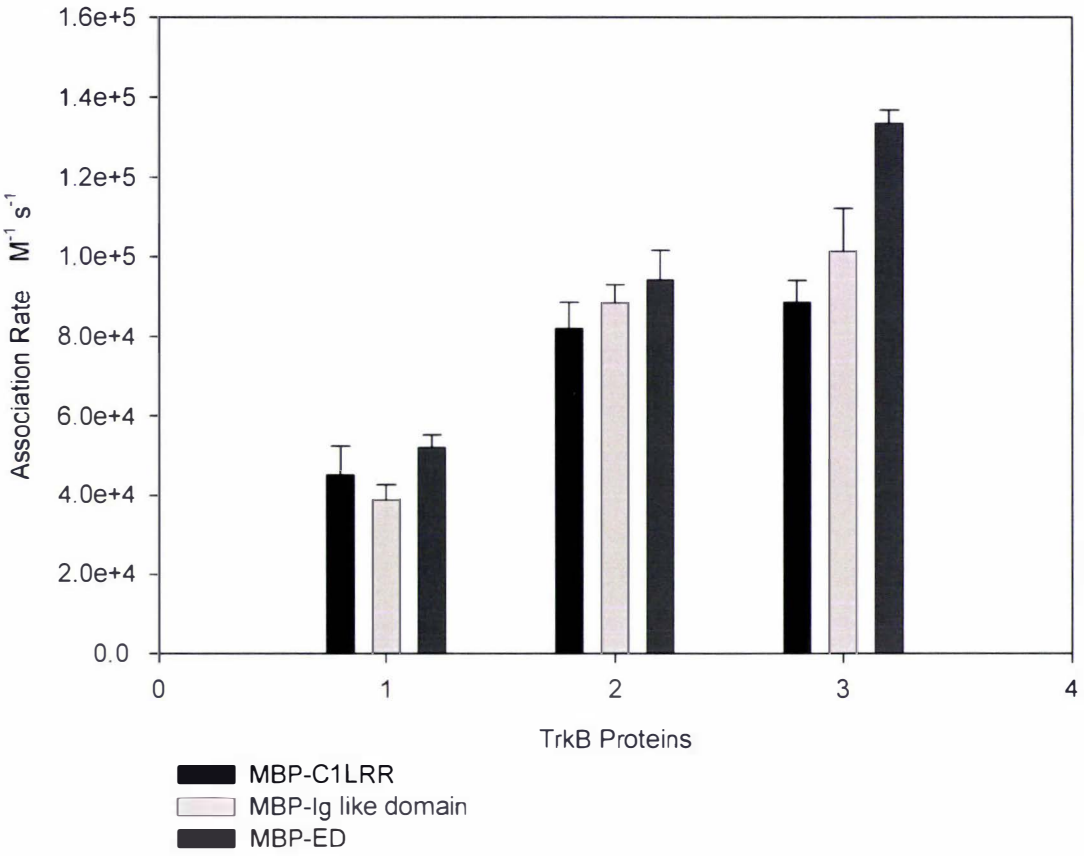

Figure 4.15 The association rates of the individual TrkB domains are essentially the same as for the complete ED domain of TrkB at the 3 temperatures at which measurements are made. The data set denoted as 1, corresponds to association rates at 15°C, set 2 corresponds to association rates at 25°C and set 3 corresponds to association rates at 37°C.

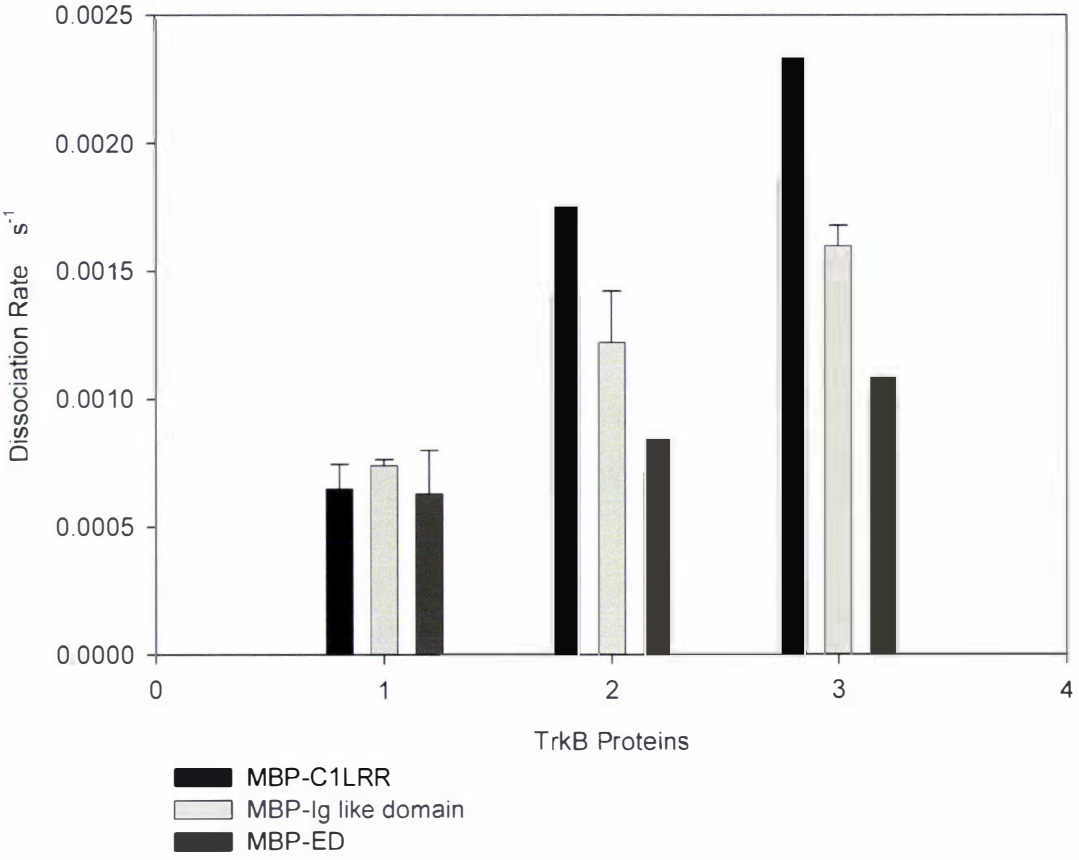

Figure 4.16 The dissociation rates of the individual TrkB domains are essentially the same as for the complete ED domain of TrkB at 15°C at which measurements are made. For 25°C and 37°C, the dissociation rates indicate that the complete ED domain has greater affinity for BDNF than either of the individual LRR and Ig-like domains. The data set denoted as 1, corresponds to dissociation rates at 15°C, set 2 corresponds to dissociation rates at 25°C and set 3 corresponds to dissociation rates at 37°C.

4.9 c The interactions of NT-3 with TrkC Proteins

Table 4.23 TrkC LRR2 synthetic peptide. The measured association and dissociation rates for the synthetic LRR2 peptide.

°C	k_{ass} M^{-1} s^{-1}	k_{diss} s^{-1}	K_D nM
15	33880 ± 3343	3.3557e-4 ± 8.9324e-5	9.9 ± 3.6
25	47190 ± 3582	5.5738e-4 ± 9.4018e-5	11.8 ± 2.9

Table 4.24 TrkC MBP-ED. The measured association and dissociation rates for the recombinant protein ED domain.

°C	k_{ass} M^{-1} s^{-1}	k_{diss} s^{-1}	K_D nM
15	27266 ± 1762	1.0406e-4 ± 9.4438e-6	3.8 ± 0.6
25	57385 ± 2432	1.4276e-4 ± 3.4905e-5	2.5 ± 0.7

Table 4.25 Values of the equilibrium dissociation constant (K_D), for the interaction of NT-3 with recombinant and synthetic TrkC proteins, over the temperature range of 15-25 °C.

TrkC Protein	K_D nM
LRR2 synthetic peptide	10.9 ± 1.3
MBP-ED	3.2 ± 0.9

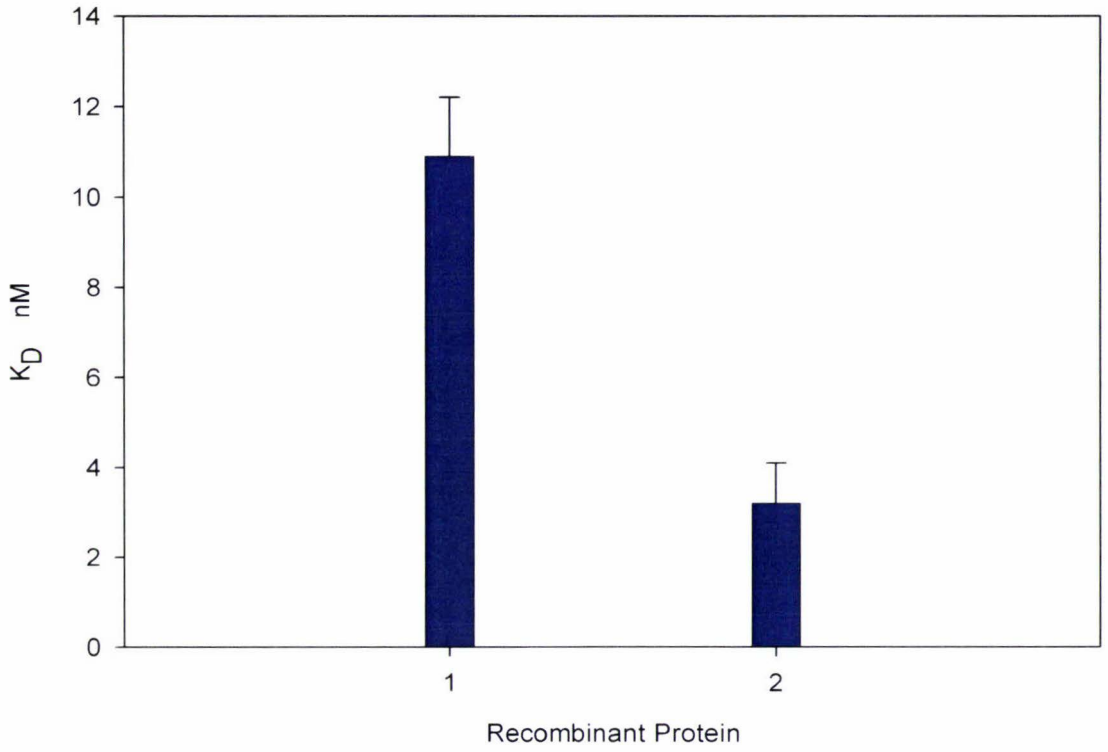

Figure 4.17 The mean and standard deviations of the equilibrium dissociation constants for the interactions of NT-3 with the TrkC, recombinant proteins and synthetic peptide for the temperature range 15-25 °C.

Recombinant Protein

1.....LRR2 synthetic peptide

2.....MBP- ED

4.10 A Comparison of Neurotrophin-Receptor Interaction Studies

In addition to the thesis study, to date 3 biosensor studies of the interactions of Trk proteins with neurotrophins have been reported. Only the interactions of TrkA with NGF have been studied by SPR biosensors and these may be directly compared with the study reported in this thesis. In addition, a series of equilibrium binding constants have been measured for the interaction of NGF with TrkA MBP-fusion proteins and BDNF with the TrkB MBP-fusion proteins used in this study. The K_D's reported for all studies may be compared directly. Each K_D is reported in nM.

- Study 1 Thetis Study.
- Study 2 Windisch et al. (1995a).
- Study 3 Woo et al. (1998).
- Study 4 Robertson et al. (2001).

Studies 1, 3 and 4 were conducted using an SPR biosensor, while study 2 used a immobilized Trk protein and radio-labeled neurotrophin It should be noted that for study 4, no details of the experiment are provided and neither is an estimate of the error in the reported K_D. In general, it appears that the biosensor measured K_D's are an order of magnitude lower than those measured by gravity column and labeled neurotrophin. For Studies 1 and 4, the K_D measured for the TrkA Ig-like domain are comparable within the experimental error of Study 1. For Study 1 and 3, the K_D measured for the TrkA ED domain is different by an order of magnitude, perhaps as a consequence of experimental technique (discussed in Chap. 5).

Table 4.26 A comparison of the equilibrium binding constants for the interaction of NGF with different extracellular domains of TrkA and of BDNF with TrkB extracellular domains, expressed in different cell types for 4 different studies.

Protein	Expression system	Study 1	Study 2	Study 3	Study 4
TrkA LRR2	*E. coli*	22.1 ± 2.5	1.33 ± 0.36	_____	_____
TrkA C1LRR12	*E. coli*	24.4 ± 5.1	0.84 ± 0.30	_____	_____
TrkA LRR23C2	*E. coli*	26.5 ± 4.6	1.15 ± 0.25	_____	_____
TrkA LRR	*E. coli*	23.4 ± 2.0	0.97 ± 0.22	_____	_____
TrkA Ig-like	*E. coli*	10.7 ± 2.3	no binding	_____	11.8 ± ?
TrkA Ig-like	*P. pastoris*	14.1 ± 1.3	_____	_____	_____
TrkA C1LRRC2	*E. coli*	_____	1.09 ± 0.24	_____	_____
TrkA ED	*E. coli*	14.4 ± 1.3	1.29 ± 0.20	_____	_____
TrkA ED	*P. pastoris*	13.5 ± 1.8	_____	_____	_____
TrkA ED	*Insect cells*	15.8 ± 2.2	_____	2.92 ± 0.75	_____
TrkB C1LRR	*E. coli*	17.5 ± 3.3	1.16 ± 0.23	_____	_____
TrkB LRRC2	*E. coli*	19.7 ± 2.3	_____	_____	_____
TrkB C1LRRC2	*E. coli*	19.3 ± 2.6	1.09 ± 0.24	_____	_____
TrkB Ig-like	*E. coli*	16.0 ± 2.7	_____	_____	_____
TrkB ED	*E. coli*	9.0 ± 2.6	0.93 ± 0.17	_____	_____
TrkB ED	*P. pastoris*	11.5 ± 2.3	_____	_____	_____

4.11 Summary

As with all SPR biosensor studies, the immobilization of a protein to the surface of the cuvette (or chip surface in the case of BIAcore instruments) is the most critical component of the experimental design. Failure to appreciate the effects of high levels of protein immobilization can lead to specious kinetics results. An additionally important component of the experiment design is the method in which the protein is immobilized. Covalent attachment of an antibody to the protein in question is often a route of choice. By this method, capture of the target protein by the immobilized antibody orients the protein away from the biosensor surface. Other methods of attachment may be used, such as the protein amino groups. However care must be taken to ensure that any method of immobilization must not occlude the ligand-binding domain. In reality, no method can be devised to ensure this and only ligand binding to the target protein can be used to show the functioning of the ligand-target interaction. It is for this reason that it is probably better to consider the biosensor as a qualitative rather than quantitative tool to show molecular interactions, rather than attempting to use then to define absolute kinetics parameters.

Initially for the study of the MBP-fusion proteins, a monoclonal antibody against MBP (New England Biolabs) was attached to the carboxymethyl dextran of a IAsys cuvette. The antibody was used to capture MBP-fusion proteins. Despite the anticipated simplicity of Trk protein immobilization by this method, a small but measurable interaction between NGF and the antibody was detectable, negating the suitability of MBP antibodies for immobilizing MBP-fusion proteins. A similar binding of NGF to anti-His antibody negated the suitability of antibodies for immobilizing His-tagged proteins produced in *P. pastoris*.

For the synthetic His-tagged TrkA, TrkB and TrkC peptides representing the second LRR domain of the three receptors, immobilization to the CMD surface was accomplished by first immobilizing an antibody to a 4-histidine sequence. This antibody proved to have a very slow dissociation rate and did not bind neurotrophin. This antibody was hence quite suitable for the kinetics study of the synthetic peptides.

Protein amino groups have a number of features that make them suitable for immobilizing proteins; in particular Є-amino groups are both charged and hydrophilic. These groups are usually found projecting from the surface of proteins and are able to be covalently linked to the CMD surface with little possibility of denaturation, thus preserving the native conformation of the immobilized protein. Lysine residues occur with an average frequency of 5.7% in proteins (McCaldon and Argos 1988) and thus represent a relatively high proportion of the total amino acids of any protein. Lysine residues are generally found to be well distributed over the surface of proteins and for this reason, immobilization via these groups is less likely to introduce steric hindrance which may occur with immobilization through less abundant amino acids.

To determine the suitability of this immobilization technique, MBP was immobilized on one cell surface (150 arc secs immobilized) and TrkA MBP-LRR (295 arc sees immobilized) was immobilized to the second cell of the double cell cuvette. Addition of various concentrations of NGF (1 nM to 5 μM) indicated that the equilibrium dissociation constant for the MBP-TrkA LRR protein appeared initially to be high nM and hence was similar to that measured for this construct by immobilization to amylose resin (Windisch et al. 1995a). It appears that immobilization of the MBP-fusion proteins through amino groups does not block the ligand binding site. NGF showed no binding to the immobilized MBP.

With most recombinant Trk proteins, there appears to be some small variation of the dissociation constant with temperature. These variations may be intrinsic to the different Trk protein domains. Equally possible is some complex biosensor surface effects, although the latter is probably less likely, given that no such effects have been reported for biosensors. In general, biosensor measurement of the kinetic parameters of biomolecular interactions is conducted at 20-25ºC (Dr. Eric Hnath, Affinity Sensors, private communication) and not at lower or higher temperatures as used in this study. Measurement of Trk protein-neurotrophin kinetics was made at the instrument default temperature of 25ºC immediately after immobilization of each Trk protein on the biosensor surface. Before kinetics measurements at 15 and 37ºC, the biosensor cuvette was stored at 4ºC for periods of 24-48 hours and this may have contributed to some degradation of the protein surface, resulting in loss in protein activity and variability in the observed kinetics. Degradation of the protein surface, especially at 37ºC, throughout the long period of data collection, may also have occurred, with obvious consequences for accuracy in the kinetics data.

The limited number of measurements made is adequate to determine the interactions of neurotrophin with any Trk protein domain at a specific temperature, although inadequate to accurately determine the K_D of the interaction. Hence, variation in the K_D between the LRR TrkA domain proteins for example, should not be interpreted as changes in neurotrophin affinity, brought about by the presence or absence of flanking cysteines that are N and C-terminal to the full-length LRR domain. The absolute effects of other modifications on neurotrophin affinity, such as the presence or absence of one or more regions of the full-length LRR domain, should similarly not be interpreted from the measured K_D's. The number of binding curves obtained, namely 10 for each Trk protein, is adequate to show neurotrophin binding and to estimate an error in each equilibrium dissociation constant.

The measurements made are sufficient to show specific neurotrophin binding to both LRR and Ig-like domains, of both TrkA and TrkB. In another biosensor study in which 3 K_D's (n=3) were measured for the ED domain of recombinant TrkA (Woo et al. 1998), the error in the estimate for the equilibrium dissociation constant was 26%. This level of error would suggest that even if more than one K_D measurement was made for each Trk protein, it is unlikely that any real differences in neurotrophin affinity that is a consequence of modifications, of for example, the LRR domain of TrkA or TrkB, would be detected. A further example of the large errors often associated with biosensor measurements of equilibrium dissociation constants, may be seen in an IAsys study of the biomolecular interactions of the DNA repair enzyme, Rad51A (De Zutter and Knight 1999). The binding constants calculated from four repeated binding experiments, resulted in errors of 5-30%.

For any given Trk-neurotrophin interaction; $\Delta G = -RT\ln K_D$, where R is the gas constant and T the absolute temperature. The effect of temperature on the equilibrium dissociation constant is described by the relationship:

$\ln K_D = \Delta H(T)\,(RT)^{-1} - \Delta S(T)R^{-1}$

Both enthalpy and entropy are functions of temperature and may vary widely with temperature changes for protein-protein interactions (Hinz 1983, Lauffenburger and Linderman 1993), thus complicating the analysis of the Trk-neurotrophin interaction at different temperatures. While receptor-ligand binding processes are generally exothermic ($\Delta H < 0$), many are driven primarily by positive entropy changes; $\Delta S > 0$ (Klotz 1985, Limbird 1986, Lauffenburger and Linderman 1993). If the entropic term dominates, only small changes in equilibrium binding will occur with temperature. Since the equilibrium dissociation constants for all neurotrophin-Trk interactions is essentially constant for all three temperatures at which kinetics measurements are made, it

seems reasonable to conclude that entropy, rather than enthalpy dominates in these interactions.

For all TrkA proteins, the rate of association is initially high, resulting in a low K_{D1}. A second, considerably lower rate of association results in a K_{D2}, considerably greater than K_{D1}. It is possible that electrostatic attraction between the TrkA protein and NGF is initially significant. With binding of NGF, a structural rearrangement of the receptor protein may occur, resulting in lowered charge attraction between receptor and neurotrophin. The consequence of this rearrangement may be a reduced rate of association and biphasic kinetics. As with a previous study (Windisch et al. 1995a), no interaction of NGF with the MBP-Ig like domain was observed. However, the interaction was observed between this domain and NGF, when the domain was expressed in *P. pastoris* and insect cells.

The association and dissociation rates for neurotrophins interacting with their respective receptor, show a general increase with temperature. Dissociation rates at physiologically relevant temperatures, show that dissociation rate of neurotrophin from Trk recombinant protein is in the order of LRR domain > Ig-like domain > ED domain. This suggests that neither LRR domain nor Ig-like domain have the complete neurotrophin binding capabilities of the intact ED domain. It is possible however, that this order of dissociation rate is a consequence of protein folding or of immobilization to the biosensor surface.

All TrkB and TrkC proteins show an association rate for their respective neurotrophin, significantly greater than that exhibited by the TrkA proteins. This may be a consequence of high electrostatic attraction between receptor and neurotrophin, without structural rearrangement of the receptor upon ligand binding. As with the interaction of NGF with the TrkA ED domain, the TrkB glycosylated ED domain, resulting from expression of the protein in *P. pastoris,* does not show a lower BDNF association rate, when compared with the unglycosylated, *E. coli* expressed protein. This suggests that glycosylation[4] plays no role in

[4] There are potentially 13-14 glycosylation sites on the ED of each Trk receptor. These proteins, when expressed in non-prokaryotic cell are always glycosylated. Only by estimating the molecular weight of each Trk ED from sequence data and comparing this to the molecular weight of each Trk when run on an SDS-PAGE gel, is it possible to estimate (if rather crudely) the level of glycosylation. All Trk proteins expressed in *P. pastoris* and insect cells

NGF binding to TrkA or BDNF binding to TrkB as suggested by the experiments of Windish et al. (1995a). The observed monophasic kinetics of the interaction of BDNF with TrkB may be a consequence of a lack of structural rearrangement of the receptor upon ligand binding and of an absence of steric hindrance effects (from attached sugar chains) on structural movements. In addition, structural changes in the neurotrophins upon binding to their respective receptor, may also contribute to the observed kinetics. If this is the situation, then possibly NGF undergoes greater structural rearrangements than BDNF or NT-3 upon binding to TrkA, TrkB or TrkC respectively.

Despite variability in the equilibrium binding constants with temperature, the data collected for each protein studied, clearly shows neurotrophin binding. In no instance is a binding interaction at one temperature eliminated by a variation of temperature. Of equal importance is the type of binding observed for each Trk receptor protein subset. Only biphasic kinetics is observed for all TrkA proteins, regardless of expression system, or experimental temperature. Only monophasic kinetics is observed for all TrkB and TrkC proteins; similarly invariant with temperature. Hence it is reasonable to conclude from the kinetics data, that proteins representing the LRR domain and proteins that represent the Ig-like domain, for both TrkA and TrkB receptors, bind neurotrophin at physiologically relevant temperatures. From this result, it is possible to conclude that previous *in vitro* studies that have identified only the LRR domain (Windisch et al. 1995a, b, c), or the Ig-like domain (Holden et al. 1997, Wiesmann et al. 1999), are open to interpretation. Neurotrophins, at least *in vitro*, bind to both domains of their respective receptor and not exclusively to one.

From the kinetics study of the three synthetic peptides of TrkA LRR2, TrkB LRR2 and LRR2 interacting with NGF, BDNF and NT-3 respectively, it is clear that the TrkA peptide binds with biphasic kinetics to NGF while the TrkB and TrkC peptides bind with monophasic kinetics to BDNF and NT-3. Charge distributions on the surface residues of NGF, BDNF and NT-3 (Appendix IV), produced with Grasp software (Nichols et al. 1991), show considerable differences in distribution on the surfaces of the proteins. From an NMR[5] study of the TrkA and TrkB peptides, the TrkA peptide is all random coil, while the TrkB peptide has significant α-helical secondary structure. It is possible that the dissimilar kinetics displayed by the two

---

show approximately 30-40 kD of sugar residues (Prof. Uri Sargovi, McGill University, Prof. Ken Neet, University of Chicago, personal communication).

[5] Spectra collected by Dr. Vladimir Basus , Department of Pharmaceutical Chemistry, UCSF.

peptides, arises from the difference in charge distribution on the surfaces of the neurotrophins, as well as the solution structure of the peptides. It is clear from the biosensor study that the neurotrophin-binding domain cannot be assigned exclusively to the second LRR domain of any of the Trk receptors. Rather, it appears that neurotrophin binding may occur over an extensive region of all neurotrophin receptors.

CHAPTER 5 DISSCUSSION

5.1 Introduction

By expressing a number of domains of the extracellular regions of the TrkA, TrkB and TrkC receptors in both prokaryotic and eukaryotic cells, the binding behavior of neurotrophins with their respective receptors was amenable to systematic investigation. Previous studies of the binding of neurotrophins to Trk receptors have been made using whole cells expressing Trk receptors on their surfaces and as recombinant proteins. In the majority of these studies, the binding of radiolabeled neurotrophins was used to establish the equilibrium binding constants of the neurotrophins to their receptor. While the equilibrium dissociation constant is a reasonable measure of the ligand-binding ability of the receptors and of the avidity of the interaction, this constant does not provide detailed information about the kinetics of interaction at the molecular level. Both the rate of interaction of the ligand-binding to (as measured by the binding rate constant, k_{on}) and dissociating from (as measured by the dissociation rate constant, k_{off}) the receptor are only readily determined using biosensors. The interaction of the recombinant Trk protein domains with their respective neurotrophin was studied in "real time" using a biosensor, thus providing an increased level of understanding of the interactions, not achieved in previous studies.

A number of *in vitro* and *in vivo* studies of the interactions of neurotrophins with their respective receptor have been undertaken, all of which have led to different postulates of how the interaction occurs. To a degree, each theory of the interaction has difficulties in explaining all observed data. For example, the observation that a mutant TrkB receptor lacking the LRR domain, when expressed on cell surfaces, does not bind BDNF (Ninkina et al. 1997) and has no biological function when exposed to BDNF, is in direct conflict with the crystal structure of BDNF bound to the Ig-like domain of TrkB (Banfield et al. 2001). In this instance, is the *in vivo* study more valid, since a biological system is employed in investigating the neurotrophin-receptor interaction, or is the isolated Ig-like domain, representing only a part of the receptor a valid description of the interaction of a neurotrophin with the Trk receptor? Unfortunately personal prejudices often dictate preference for a model resulting from such conflicting data. The research undertaken for

this thesis is presented as it was conducted and is not intended to be dogmatic in interpretation. Rather, previous studies are presented and a hypothetical model the may explain the conflicting data is offered. No single model may be adequate in describing the neurotrophin-receptor interaction and each may be merely a glimpse of reality.

5.2 Recombinant Proteins, Native Proteins and Crystal Structures

Recombinant proteins such as those produced for this study, have the potential to be misfolded and consequently possess structures quite unlike those of the proteins in their native state. Biophysical measurements, such as circular dichroism do not provide evidence of native conformation, only a measure of secondary structure. Since there is no native structure for comparison, no method will unambiguously confirm the native structure of the Trk proteins used in this study. Even an X-ray crystallography structure is not a measure of native protein conformation. Cyclosporin is known to adopt different structures depending on its environment at different locations within a cell (Zeder-Lutz et al. 1993, Altschuh et al. 1994).

It is becoming increasingly clear that protein motions are essential for protein function (Zavodszky 1998, Faber 1999). Some of the motions may be small structural adjustments while others are substantial (Faber 1999). These motions may be the consequence of interactions with other molecules, but equally may result from changes in the environment. Changes in the pH and hydrophobic nature of the microenvironment, can induce considerable structural plasticity in a protein structure (Faber 1999). The design of pharmaceutical drugs based upon crystal structures of target proteins is now beginning to provide a basis for an understanding of how protein structures in crystals often provides a poor understanding of the structure of a protein in its native environment (Yannawar et al. 1995, Xu et al. 1997, Faber 1999).

Hence it is unlikely that a protein adopts a truly native conformation (for example the Trk Ig-like domains) in the exotic, non-physiological conditions in which proteins crystallize. Such structures quite probably provide only a degree of native like conformation. Only the binding of neurotrophic factor to the Trk proteins is available to provide a measure of correct folding of the recombinant proteins used in this study, but this does not prove that they adopt the structure of the proteins expressed by neurons in the human brain.

Trk receptors and their sub-domains, when expressed as His-tagged constructs in *E. coli*, result in insoluble and biologically inactive proteins (Prof. Rainer Schneider, University of Innsbruck, personal communication, Allen et al. 1997, Wiesmann et al. 1999, 2000, Robertson et al. 2001). In all instances, the proteins were found in inclusion bodies and required refolding by dissolution in urea, followed by dialysis into an appropriate buffer, in order to gain the ability to bind neurotrophin. In contrast MBP proteins from diverse bacteria and archaea, when used as affinity tags in place of polyhistidine, shows a remarkable ability to enhance the solubility of its fusion partner (Fox et al. 2003). There appear to be no reported instances of biological inactivation of the partner of MBP fusion proteins, as a consequence of the production of a denatured product; i.e., all MBP-fusion proteins seem to be folded suitably and able to bind their appropriate ligand.

All Trk MBP-fusion proteins (with one exception) bound its appropriate neurotrophin, while none interacted with an inappropriate binding partner (IGF), even at mM concentrations. Only the Ig-like domain of TrkA showed no affinity for NGF, possibility a consequence of incorrect folding (resulting in a denatured protein), or occlusion of the neurotrophin binding site by MBP. It is possible that the MBP tag was too close to the NGF binding site on the TrkA Ig-like domain, resulting in a loss of ligand-binding activity. In this circumstance the protein is not exhibiting inactivity as a consequence of a non-native structure, nor is it the consequence of a denatured protein.

In this thesis study, a number of MBP-fusion proteins were expressed. No attempt was made to remove the N-terminal MBP tag, for two reasons. Firstly, the MBP provided a convenient method of attaching the Trk proteins to the biosensor surface so there was a significant probability of the protein being oriented away from the sensor surface, hence reducing the possibility of any region of the protein interacting with the surface. If the immobilized Trk protein interacted with the immobilization surface in any way, then there would be a distinct possibility for occlusion of the ligand-binding regions by the CMD surface of the biosensor.

A second reason for not removing the MBP tag was provided by the reported experiences of other researchers. Removal of tags from fusion proteins, e.g., MBP, GST and Thioredoxin can result in aggregation and precipitation of the fusion partner (Prof. Rainer Schneider, University of Innsbruck, personal communication, Dr. Steven Finkbeiner and Dr. Karl Weisgrabber, Gladstone Institute, personal communication, Stevens 2000). Affinity tags are removed by endopeptidases, which have many limitations, including the presence of peptide secondary cleavage site activities,

resulting in proteolytically damaged products (Stevens 2000). Successful cleavage of a protein from its tag may even require partial denaturation in order to successfully remove a tag from the protein of interest (Stevens 2000).

Insoluble, inactive His-tagged Trk proteins, may result from a lack a chaperones *in E. coli* that are needed for correct folding and production of soluble protein. MBP-fusion proteins remain in solution, as do the Trk proteins expressed in *P. pastoris*. If chaperones are not critical components in the correct folding of soluble Trk proteins, then it appears that large molecular components, such as oligosaccharides in the case of *P. pastoris*, or MBP, are necessary to prevent aggregation of neurotrophin receptors and their constituent domains. Quite possibly oligosaccharides and MBP may prevent the interaction of various amino acids on the surface of the Trk proteins, thus inhibiting aggregation.

5.3 Binding Studies and Controls

In the thesis study, a number of equilibrium binding constants for the LRR and Ig-like domains of both TrkA and TrkB were measured at three different temperatures (Tables 4.2 through 4.25). These measurements established that neurotrophins bind to both the LRR domain and the Ig-like domain of the Trk receptors. A total of 10 TrkA and 3 TrkB LRR domain constructs were produced in both eukaryotic and prokaryotic expression systems (Tables 2.1, 2.2, 2.3, 2.5, 2.6, 2.7, 2.9, 2.10). These constructs were tested for their ability to bind NGF and BDNF respectively.

Since neurotrophin binding was tested at three different temperatures, a total of 27 LRR and 9 Ig-like domain-binding measurements were made with the recombinant proteins. A total of 10 binding curves were obtained for each Trk protein at the given temperatures. Hence, >270 binding experiments were performed with the LRR domains and >90 binding experiments were performed with the Ig-like domains. With only one exception (the TrkA Ig-like domain expressed in *E. coli*), specific binding of neurotrophin to Trk proteins was observed in all instances.

Maintaining a high salt and detergent component in the reaction buffers ensured specificity of the interaction between neurotrophin and receptor construct. Before beginning binding studies, each neurotrophin was tested for non-specific interactions with the biosensor CMD surfaces. The two

surfaces of the biosensor were activated with the same chemistry used to immobilize the Trk proteins. One surface was left in an "activated" state, i.e., ready to immobilize Trk protein, while the second surface had BSA immobilized to it. Neurotrophins at 10x the highest concentration used in the binding studies was allowed to react with the biosensor surfaces, in reaction buffer containing various concentrations of NaCl. It was found that 150 mM NaCl in the reaction buffer eliminated all non-specific interactions with the two control surfaces. Buffers containing 150 mM NaCl were used for all subsequent binding studies.

In addition, each neurotrophin was tested for interaction with BSA and MBP. Insulin like growth factor (IGF), at mM concentrations, was tested for binding to all Trk proteins. In all instances, no interactions with BSA, MBP or IGF were observed. Even when tested in buffers containing salt concentrations of 0.5 M, neurotrophin interactions with Trk proteins were quite apparent.

For all Trk receptor domains, binding of neurotrophin was both evident and specific at 15 °C, 25 °C and 37 °C.

5.4 Binding Data and Trk Receptor Structure

Some variation of the equilibrium dissociation constants with temperature was noticeable with all synthetic and recombinant Trk proteins (Tables 4.2 through 4.25, Figure 4.11 through Figure 4.17). This variation has been noted previously (Neet and Campenot 2001) and should not be interpreted simply as a consequence of the experimental design or of the measurement technique used in this study. Within the LRR group, variation of the equilibrium dissociation constants was noted (Table 4.14). It may or may not be possible to interpret these variations as a consequence of the presence or absence of the cysteine rich regions that flank the LRR domains. Limited quantities of NGF, BDNF and NT-3 precluded the determination of more than one equilibrium dissociation constant for each LRR domain at each of three temperatures (Tables 4.15 through 4.25).

It would be inappropriate to interpret variations in the equilibrium dissociation constants of the Ig-like domains to the presence or absence of the cysteine rich regions that flank these domains (Tables 4.14 and 4.22). The presence or absence of sugar moieties that are found on the 13

putative glycosylation sites of the Trk receptors should not be invoked to interpret the variations in neurotrophin binding affinity, for the various proteins used in this study. Establishment of the variation of equilibrium dissociations constants with receptor modification by glycosylation was beyond the extent of this study and in fact, such a study has never been undertaken for the Trk receptors.

5.4 Previous *In Vivo* and *In Vitro* Studies of Trk Receptors and Neurotrophins

Although the kinetics of neurotrophin binding and dissociation from Trk receptors expressed on whole cells and with the isolated recombinant Trk proteins are undoubtedly not directly comparable, it is reasonable to view the set of recombinant proteins as a distinct entity and to make a comparison between these proteins. A significant number of conclusions relating to the neurotrophin binding regions of the Trk receptors have been derived from recombinant proteins; namely MBP-fusion proteins of TrkA and TrkB (Windisch et al. 1995a, b, c) and the *E. coli* expressed Ig-like domains of TrkA co-crystallized with NGF (Wiesmann et al. 1999, 2000) and of BDNF co-crystallized with TrkB (Banfield et al. 2001). A consequence of these studies in particular, has been to magnify the confusion over which of two potential ligand-binding domains of the neurotrophin receptors, actually binds the neurotrophin.

Equilibrium kinetic analysis with the TrkA and TrkB domains suggested that only the LRR region of the receptors was responsible for neurotrophin binding (Windisch et al. 1995a) and that the Ig-like domains do not bind neurotrophin. Only the LRR domain of the receptor showed affinity for neurotrophin, with an equilibrium dissociation constant similar to that measured for Trk receptors expressed on the surface of intact cells (Table 1.1). This thesis biosensor study, confirmed that the Ig-like domain of TrkA expressed as an MBP-fusion protein, showed no affinity for NGF. However, the same domain expressed as a His-tagged protein in *E. coli* and *P. pastoris*, showed significant affinity for NGF (Table 4.14).

These results suggest that the MBP-fusion construct of the Ig-like domain of TrkA was incorrectly folded during expression (Baneyx 1999, Wirtz and Steipe 1999, Wiesmann et al. 1999, 2000, Kurucz et al. 2000, Qiao et al. 2001). Evidence for the misfolding of Trk Ig-like domains is found in the crystal structure of TrkA, in complex with NGF (Wiesmann et al. 1999). In this structure, the

Ig-like domains have exchanged strands, resulting in protein that cannot bind NGF (Dr. Bart de Vos, Genentech, private communication, Wiesmann et al. 1999, 2000).

Conversely, the same domain for TrkB expressed as an MBP-fusion protein in a different *E. coli* species than that used for the original study (Windisch et al. 1995a), showed full activity in binding BDNF (Table 4.22). Binding kinetics using the biosensor, fully support the earlier conclusion that the LRR domain of the Trk receptors binds neurotrophins (Windisch et al. 1995a), and this domain has similar binding and dissociation kinetics to those observed for both the complete extracellular domain and the Ig-like domain. These results suggest that neurotrophins are able to bind to both the leucine-rich and Ig-like domains of TrkB with similar kinetics (Tables 4.15 through 4.22).

An X-ray crystallography study (Wiesmann et al. 1999, 2000) of the Ig-like domain co-crystallized with NGF has yielded a structure showing NGF bound to the C-terminal Ig-like domain (referred to as d5). During crystallization, the N-terminal Ig-like domain (referred to as d4) was lost from the expressed construct as a result of proteolysis. In addition to the loss of d4, domain swapping occurred, resulting in the interchange of the two d5 domains of the homodimeric receptor. One consequence of the domain interchange is a loss of neurotrophin binding; no binding of NGF to the TrkA protein used in the crystallization study was observed in kinetics studies (Dr Bart de Vos, Genentech, private communication, Wiesmann et al. 1999, 2000). In the final X-ray structure of NGF/d5, the two d5 regions are altered by molecular modeling software to produce a structure in which these regions are not interchanged.

Co-crystals of interacting biomolecules may be obtained if the interaction between the molecules is at least μM (Prof. E. N. Baker, Auckland University, private communication). Hence, if the affinity of the Ig-like domain for NGF is μM, then it is possible that the X-ray structure of the co-crystal of NGF and the Ig-like domain, is a reasonable model for the interaction of NGF with one ligand-binding region of TrkA.

Studies in which the domains of TrkA, TrkB and TrkC are interchanged to produce chimeric proteins, suggest that only the Ig-like domain of the receptors is exclusively responsible for neurotrophin binding (Urfer et al. 1995, Urfer et al. 1998, Wiesmann et al. 2000). These studies fail to appreciate the unknown effects of appending, for example, a TrkA domain to TrkB. It is

quite conceivable that such interchanged domains result in propagation of secondary and tertiary structural changes in the resulting homodimeric receptor. Such changes of the structure could quite conceivably alter a binding site for the neurotrophin in the leucine-rich domain, resulting in elimination of binding to this region, while binding is only observed to structurally unaffected Ig-like domains. An additional unknown is introduced into this study by the expression of each protein as immunohesins in which the extracellular domains of the Trk proteins are fused to the F_c portion of a human antibody. This construct results in the production of artificial dimers, which may further influence the binding of neurotrophin.

TrkB constructs with deletions in the extracellular domain, have been expressed in mammalian cells (COS-1) and studied for their ability to bind BDNF (Kojima et al. 1999). The six constructs consisted of (1) the entire Ig-like domain, (2) the C-terminal Ig-like domain and (3) regions of the N-terminal Ig-like domain. Only one mutant protein consisted of 17 residues of the LRR domain and all subsequent C-terminal residues. Those mutant proteins that included the complete Ig-like domain showed BDNF binding, comparable with wild-type TrkB, while those consisting of only the C-terminal Ig-like domain showed little affinity for the ligand.

The construct consisting of 17 residues of the LRR domain and all subsequent C-terminal residues shows approximately 60% of the affinity for BDNF, when compared to the wild-type protein. This result is inconsistent with studies, which claim that only the residues between the N and C-terminal Ig-like domain affect the affinity of the proteins for BDNF. It is inconsistent that the construct consisting of 17 residues of the LRR domain and all subsequent C-terminal residues showed a reduced binding affinity for BDNF. This result suggests that there is an unidentified problem with the experimental design.

In a study of the binding of BDNF to naturally occurring isoforms of TrkB (each lacking the intracellular tyrosine kinase domain) expressed on the surface of NIH 3T3 cells, the LRR domain of TrkB was shown to be essential for BDNF binding to the receptor (Ninkina et al. 1997). Those isoforms of TrkB having the entire Ig-like domain, but lacking the LRR domain showed no ability to bind BDNF. In addition, cells expressing these isoforms neither survive, nor undergo morphological transformation in response to neurotrophins. This study appears to be straightforward in the experimental design and clearly shows that BDNF binding is observed with the TrkB isoform that possess both the LRR and Ig-like domain. Unfortunately this study did not determine the equilibrium binding constants and hence it is not possible to assess any influence

that accessory proteins that bind to the intracellular domain, may have on the binding affinity of the receptor domains.

The essentially non-physiological environment in which the study is invariably conducted complicates an understanding of the binding of ligands to isolated recombinant receptor proteins. In addition, the expression vector system and cell type in which the protein is produced can affect the experimental results. These problems are illustrated by the study of the binding of neurotrophins to TrkA and TrkB recombinant proteins, expressed as MBP-fusion proteins (Windisch et al. 1996a). In this study, it is possible for incorrect folding of the Ig-like domain during protein expression (Wiesmann et al. 1999, 2000, Baneyx 1999, Wirtz and Steipe 1999, Neet and Campenot 2001). This domain may fold incorrectly as a consequence of the four cysteine residues found within this region (Baneyx 1999, Wirtz and Steipe 1999) and hence the possibility of disulfide bridge isomerization (Wiesmann et al. 1999, 2000, Neet and Campenot 2001). If the domain folded incorrectly, then it is possible that neurotrophin binding is inhibited or prevented, with the consequence that the Ig-like domain is interpreted as having no neurotrophin binding capability.

Conversely, the LRR domain contains no cysteines and although cysteine rich regions that may form disulfide bridges flank this domain, the LRR expressed as a recombinant protein has a reasonable probability of being correctly folded upon expression. It is clear from the binding activity of the TrkA Ig-like domain, expressed as a recombinant protein in eukaryotic cells (*P. pastoris*), that the cell in which the Trk protein is expressed, has a marked influence on its correct folding. A consequence of not investigating the folding of the MBP-Ig-like proteins may have led to the misinterpretation of the LRR as the only active neurotrophin-binding domain in the Trk receptors.

5.5 Protein Immobilization and Kinetics Data

One possible complication introduced into the interpretation of biosensor kinetics data, results from the unknown nature of the arrangement of immobilized protein on the biosensor surface, that could result in a heterogeneous system and receptor binding sites with different binding affinities for neurotrophin. It is assumed that the proteins are coupled to the biosensor surface in such a manner that the ligand-binding domains are not occluded. Heterogeneity of the

immobilized Trk protein may arise during the immobilization step if more than one coupling site is present on the Trk protein. Complex (biphasic) kinetics for the neurotrophin-Trk interaction could result from a heterogeneous surface. This problem may be eliminated by using an oriented Trk surface; in particular the MBP of each fusion protein provides this orientation. Since all TrkA proteins showed biphasic kinetics and all TrkB and TrkC proteins showed monophasic kinetics at similar levels of protein immobilization, it seems reasonable to conclude that heterogeneous Trk immobilization, does not account for the observed kinetics.

Only if a protein can be shown to bind its ligand, is it assumed that the immobilization has not affected ligand-binding epitopes. Argument by analogy is the only manner in which this situation may be addressed. Because the TrkB and TrkC proteins all showed monophasic binding kinetics, similar to those previously reported for *in vivo* and *in vitro* binding studies (Sutter et al. 1979, Cohen et al. 1980, Schechter and Bothwell 1981, Bernd and Greene 1984, Layer and Shooter 1983, Hosang and Shooter 1985, Woodruff and Neet 1986, Godfrey and Shooter 1986, Kaplan et al. 1991, Klein et al. 1991, Soppet et al. 1991, Rodriguez-Tebar et al. 1992), it is probable that the immobilization of the recombinant proteins to the biosensor surface in this study did not compromise the ligand-binding domains.

By analogy, the TrkA proteins quite probably immobilized in such a manner that NGF binding was unaffected. Additional confidence in the immobilization protocol for the TrkA proteins to the biosensor surface, is provided by the observation of similar biphasic kinetics to that obtained in previous *in vivo* and *in vitro* binding studies (Meakin and Shooter 1991, Meakin et al. 1992, Rodriguez-Tebar et al. 1992, Windisch et al. 1995a).

5.7 Biosensor Kinetics

None of the studies of isolated recombinant proteins or of the Trk receptors on the surfaces of eukaryotic cells appear to completely eliminate or support the claims of specific binding of neurotrophin to the LRR domain or the Ig-like domain exclusively. A systematic study of isolated, non chimeric recombinant TrkA, TrkB and TrkC proteins that are expressed in both prokaryotic and eukaryotic cells seems to have provided a reasonable approach for evaluating the relative affinities of the LRR and Ig-like domains for the neurotrophins (Tables 4.2 through 4.25). All studies of these proteins were conducted with the same methodology, that is, a series of kinetics

experiments were made in a microenvironment of identical pH, temperature and ionic strength. Real time kinetics data, collected over a short time span, reduces the possibility of protein degradation, while providing greater detail of the association and dissociation events than are possible from all previous studies of the Trk receptors.

The Biosensor system may also offer an additional advantage when compared with other assay systems for receptor-ligand studies. Although the receptors (or domains) are covalently linked to the surface, the ligand (neurotrophin) is unmodified and this eliminates a possible structural change that might be introduced by radiolabeling.

Biosensors do have the demonstrated ability to study complex interactions between biomolecules. Conformational changes that may accompany a protein-protein interaction have been observed by biosensor and have led to new theories for the mechanism of a given interaction (De Crescenzo et al. 2000). Biphasic kinetics observed for the interaction of Transforming Growth Factor α with the extracellular domain of the EGF receptor, have been interpreted as a receptor activation mechanism in which ligand binding results in a conformational-driven exposure of a dimerization site on the receptor (De Crescenzo et al. 2000).

From this thesis biosensor study, it appears reasonable to conclude that both the LRR and Ig-like domains of TrkA, bind NGF with similar affinity (Table 4.14, Figure 4.11). Similarly, the LRR and Ig-like domains of TrkB bind BDNF (Table 4.22, Figure 4.14). This study also indicated that the binding of the TrkA proteins with NGF is quite different to the binding of BDNF to the TrkB recombinant proteins and of NT-3 to the TrkC proteins. All the recombinant and synthetic TrkA constructs, bound NGF with biphasic binding kinetics. Monophasic kinetics was observed in the binding of BDNF to all TrkB proteins and in the binding of NT-3 to two TrkC proteins, both expressed and synthetic.

The observed association of NGF for all the TrkA proteins, is best described by fitting the binding data, an equation of the form:
$R_t = A(1-\exp^{-k_{on(1)}t}) + B(1-\exp^{-k_{on(2)}t})$, where R_t is the instrument response at time t and A is the extent of the first phase, having an apparent "on-rate" defined as $k_{on(1)}$. B is the extent of the second phase having an apparent "on-rate" of $k_{on(2)}$. This biphasic association of NGF for TrkA proteins is in contrast to the observed association of BDNF for all TrkB proteins and of NT-3, for

the limited number of TrkC proteins utilized in this study. The observed association of BDNF and NT-3 for their respective receptors and the different domains of their receptors, can only be described by fitting, the binding data, to an equation of the form:
$R_t = R_{eq}(1-\exp^{-k_{on}t})$, where R_t is defined above, R_{eq} is the equilibrium response and k_{on} is the apparent "on-rate" for a given ligand concentration. Hence, while biphasic association was observed for NGF binding to TrkA proteins, only monophasic association was observed for the association of BDNF and NT-3 for their respective receptors and receptor domains.

5.8 Biphasic Kinetics of the NGF-TrkA Interaction

The biphasic nature of the association of NGF with the TrkA proteins could be a consequence of either poor experimental design, or of actual physical processes in the binding of NGF to TrkA proteins. It is well established in biosensor analysis, that immobilization of high levels of protein can result in biphasic binding phenomena. For the IAsys instrument used in this study, biphasic binding may occur if proteins are immobilized at levels of ~ 10,000 arc secs (Affinity Sensors). Throughout this study however, protein immobilization levels never exceeded 3,200 arc secs and were usually ~ 1000 arc secs, well below the level at which spurious association effects might be expected to occur. In addition, the levels of immobilization of all TrkB and TrkC proteins were within 200 arc secs of the immobilization levels of all TrkA proteins.

On no occasion was biphasic association of ligand for TrkB or TrkC proteins, observed. This leads credence to the biphasic binding of NGF for TrkA proteins, being a "real phenomenon", rather than an experimental artifact. Further support for real binding phenomena lies in the observation of monophasic dissociation. For cells over expressing a given receptor and for overloaded biosensor surfaces, biphasic dissociation may result from the rebinding of dissociating ligand (Lai and Guyda 1984, Lauffenburger and Linderman 1993, Edwards et al. 1998, Luo et al. 2001). No biphasic dissociation was observed in any experiment, thus providing additional evidence for appropriate levels of immobilized Trk proteins.

If no independent *in vivo* or *in vitro* data existed for biphasic binding of NGF to TrkA, then other conditions, imposed by the biosensor itself, would need to be invoked to explain the bimodal kinetics observed. Artificial biphasic kinetics observed in some biosensor protein-protein interactions, have been explained on the basis of steric hindrance and conformational changes of

immobilized protein (Edwards et al. 1995). Biphasic kinetics could also be due to two distinct populations of immobilized TrkA resulting from the coupling chemistry. However it seems reasonable to accept the biphasic biosensor NGF-TrkA interactions, since they have been previously observed for Trk-neurotrophin interactions (Meakin et al. 1992, Windisch et al. 1995a).

5.9 Previously Observed Biphasic Kinetics of the NGF-TrkA Interaction

In a previous study of the binding of NGF to TrkA MBP-fusion proteins (Windisch et al. 1995a), complex biphasic association was noted, together with biphasic dissociation events. While biphasic association of NGF for all TrkA recombinant proteins was observed for the exhaustive biosensor study, no biphasic dissociation events were observed. The biphasic nature of the dissociation observed by Windisch et al. (1995a), may be explained by rebinding events occurring in the poorly stirred (gravity column) system in which the binding of radiolabeled NGF to immobilized TrkA proteins, was conducted. Such rebinding events may have been eliminated in the biosensor experiments, by a rapidly stirred environment in which the interaction of ligand and receptor proteins took place. Complex association events for NGF and TrkA proteins have also been reported previously (Meakin et al. 1992). The binding of NGF to TrkA expressed in COS cells showed biphasic association, with two clearly distinct association rates.

5.10 Neurotrophins and Receptor Structure Influence Kinetics

The apparent differences between the binding of NGF to TrkA and of BDNF and NT-3 to their respective receptors, may be due to differences in the neurotrophin residues involved in binding to Trk receptors, as well as the overall differences in structures. While many different residues of NGF, BDNF and NT-3 have been identified as having an influence on the binding of these neurotrophins to their respective receptor (Ibanez 1996, 1998), unlike BDNF and NT-3, the N-terminal residues 1-11 of NGF are important for the binding of NGF to TrkA (Mobley, unpublished observations, Urfer et al. 1994, Ibanez 1996, Kullander et al. 1997, Ibanez 1998). In the structure of the d5 domains of TrkA, TrkB and TrkC (Ultsch et al. 1999), a significant difference is noticeable when compared to the co-crystal structure of NGF-d5 domain of TrkA (Wiesmann et al. 1999, 2000).

In the co-crystal, the N-terminal domain of NGF lies in a hydrophobic pocket in the N-terminal region of d5 (Wiesmann et al. 1999, 2000). The same pocket in the d5 domain of TrkB is hydrophilic and cannot accommodate the N-terminal residues of BDNF. The d5 domain of TrkC has no binding pocket in which the N-terminal domains of NT-3 may bind. Thus it appears that the N-terminal residues of NGF bind to the TrkA receptor, almost as a distinct (when compared to BDNF and NT-3) region of the neurotrophin and well separated in distance from other amino acids of the neurotrophins, identified as receptor binding (or influencing) residues (Ibanez 1996, 1998, Wiesmann et al. 1999, 2000, Banfield et al. 2001).

A recent survey of the structures of protein-protein interactions in co-crystals (Chakrabarti and Janin, 2002), shows that contacts in which > 2000 $Å^2$ of surface area is buried, indicates the potential for structural changes upon the association of the binding partners. In the crystal structure of NGF-TrkA d5, 2220 $Å^2$ of surface area is buried. This, together with the high temperature factors of the structures of the NGF (McDonald et al. 1991) and NT-3 (Butte et al. 1997) homodimers, suggest that structural rearrangements may occur upon the binding of neurotrophin to Trk receptor. At the very least, a significant level of change must occur in the N-terminal region of NGF, which is too flexible to be seen in the NGF homodimer structure (McDonald et al. 1991), but is observed associated with the d5 domain of TrkA, in a co-crystal.

Biphasic binding of NGF to TrkA may result from an initial interaction of the N-terminal regions of NGF with TrkA binding domains, followed by the interaction of other regions of the neurotrophin with the receptor. Such an interaction would not occur for BDNF and NT-3 interactions with their receptors. An interaction of NGF to TrkA should be seen as a bimodal event with a biosensor, if such a binding of N-terminal, followed by association with additional NGF domains, takes place. Structural changes may also contribute to the biphasic nature of the interaction, namely, cooperative allostery.

Structural changes that may be too small to see in a crystal structure, can contribute significantly to the loss or increase of binding affinity between protein binding partners. Electrostatic interactions and hydrogen bonds contribute approximately 5 and 1 kcal of binding energy respectively. At 25°C, a free energy change of only 1.4 kcal/mol corresponds to a ten-fold increase in binding affinity. A free energy change of 7-12.6 kcal/mol, corresponds to a change in affinity from 10^5 to 10^9 M (Orengo et al. 1999, Regenmortel 2001). Hence it is reasonable to assume that even the loss of one hydrogen bond in the immobilization of the Trk proteins may

dramatically influence binding of neurotrophin. However, despite the less than predicable nature of the immobilization of Trk protein to biosensor surface, the inescapable hypothesis from the *in vitro* kinetics data is that binding does occur to more than the d5 domain of each receptor.

5.11 Mass Transport and Biosensor Kinetics

In a study by Woo et al. (1998), a BIAcore instrument (BIAcore) was used to measure the interaction of NGF with TrkA. No biphasic NGF-TrkA interactions were observed in this study. Problems of mass transport, inherent with the BIAcore, were appreciated and assessed, however the means of estimating the effects of mass transport were significantly different than those presently employed (Myszka 1999, Lipshultz et al. 2000, Laich and Sim 2001). BIAcore ligate flow rates are now typically 100 µl/min compared with 5 µl/min previously used. Consequently the effects of mass transport may have been underestimated. Mass transport effects with the BIAcore, have only recently been appreciated as contributing to erroneous assumptions of molecular interactions and estimates of binding constants (Cook et al. 1997, Schuck 1997, Myszka 1999, Lipshultz et al. 2000). It is quite conceivable that the equilibrium dissociation constant measured by Woo et al. (1998), reflects contributions from mass transport effects.

Techniques been developed to estimate mass transport effects with the BIAcore. These methods are quite different from those used to estimate mass transport effects in the study by Woo et al. (1998). Unlike the microfluidic liquid flow cells of the BIAcore, the IAsys biosensor is a stirred cell and as such, mass transport effects are considered to pose less of a potential problem in the estimate of macromolecule binding constants (Glaser 1993, Schuck 1996, Schuck and Minton 1996, 1997a, b, Cook et al. 1997, Schuck 1997, Myszka 1999, Lipshultz et al. 2000). It has been calculated that the stirred cell environment of the IAsys biosensor, corresponds to a flow rate of 8-10 ml/min in a BIAcore biosensor (Dr. Eric Hnath, Affinity Sensors, personal communication).

5.12 Biphasic and Monophasic Kinetics Observed by Biosensor

While the BIAcore study showed monophasic binding kinetics, the IAsys study shows that the interaction of NGF with the recombinant extracellular TrkA domain is biphasic. Biphasic binding kinetics was also observed in a study of the binding of NGF to TrkA (Windisch et al. 1995a). Similarly, biphasic interactions have been observed in *in vivo* binding of NGF to TrkA, expressed on the surface of COS cells (Meakin et al. 1992).

These results point to the *in vitro* kinetics of the interaction between NGF and TrkA proteins, observed in this biosensor study, being similar to those observed *in vivo*. If the interaction of NGF with TrkA data is reliable, then the interaction between BDNF and the TrkB proteins observed in this study may also be correct. These results suggest that there is a fundamental difference between the interaction kinetics of NGF-TrkA and of BDNF-TrkB.

5.13 Biosensor Kinetics and Accuracy of Data: Qualitative Protein-Protein Interaction Analysis with Biosensors

Equilibrium dissociation constants determined for the interactions of NGF with the recombinant TrkA proteins expressed for this study (Table 4.2 through Table 4.14), are insufficiently accurate to make clear distinctions between the effects of deletions of different residues on the binding to the LRR domains of the receptor (Tables 4.2 through 4.8). Similarly, no distinction may be made for the binding of BDNF to the TrkB recombinant LRR domain proteins (Table 4.15 through Table 4.22). Rather this study has established that neurotrophins interact with both LRR and Ig-like domains of the Trk receptors (Table 4.2 through Table 4.25, Figure 4.11, Figure 4.14, Figure 4.17).

The use of biosensors to demonstrate the interactions between molecules, without an extensive determination of the binding constants involved by repeated measurement (i.e. n >1), is well established. An example of such a methodology is found in the demonstration of the specific interaction between the eukaryotic initiation factors, eIF4A and eIF4B in yeast (Dominguez et al. 1999).

In a previous study of the interactions of domains of TrkA and TrkB with NGF and BDNF (Windisch et al. 1995a), no great differences could be established in the binding of neurotrophins to different LRR domains. Hence, any attempt to obtain equilibrium dissociation constants for the interactions, from multiple measurement of any given neurotrophin-Trk protein interaction, would ultimately prove unsuccessful. Because of the large errors associated with biosensor measurements of binding constants, multiple measurements of each K_D, would not serve to establish fundamental differences in neurotrophin affinity by any given receptor domain. Rather, a single set of stringently controlled measurements of the interaction between immobilized Trk proteins and their respective neurotrophin, was utilized to determine if interactions actually occur and to establish equilibrium dissociation constant for each interaction (Table 4.2 through Table 4.25).

5.14 The Second TrkA LRR Domain and Ligand-binding

It is interesting that the synthetic peptide representing the second LRR domain of TrkA (LRR2) exhibited biphasic kinetics on binding NGF. An NMR study of this peptide showed it to be all random coil (Prof. Vladimir Basus, UCSF, personal communication) and from the binding constants it is possible to hypothesize that the binding of NGF might follow an induced fit model, with initially weak binding of the neurotrophin, followed by an increased affinity for NGF subsequent to, or concurrent with, a structural change in the peptide or NGF. From the biosensor study it appears that the affinity of this peptide for NGF is approximately 33% of that exhibited by the complete LRR domain and 20% of that of the full-length extracellular domain of the TrkA receptor. The LRR domain expressed in *E coli* has an affinity for NGF that is lower than that for the intact extracellular domain. Hence, unlike the conclusion of the previous study (Windisch et al. 1995), it cannot be reasoned that the LRR2 is the unique binding domain of TrkA for NGF.

5.15 TrkB and TrkC Biosensor Kinetics

All TrkB proteins have a single equilibrium dissociation constant with values from ~ 9 nM to ~ 20 nM (Table 4.22, Figure 4.14). The fact that these constructs have equilibrium dissociation constants similar to those obtained for the extracellular domain of TrkB expressed on the

surfaces of whole cells engenders considerable confidence in the validity of the biosensor kinetics measurements for all three receptor proteins studied.

It might be expected that dissimilar techniques used to measure equilibrium dissociation constants for the Trk receptors might lead to some differences in their values. However, it would seem unreasonable to see differences of one to two orders of magnitude, unless some real differences in the binding kinetics is being measured, or the experimental technique is invalid.

Additionally, similar biosensor kinetics results for the recombinant TrkB and TrkC extracellular domains to those obtained in *in vivo* binding studies, suggest that the means of immobilizing the recombinant proteins to the biosensor surface, had little or no affect on the ligand-binding activity of the recombinant proteins (Tables 4.15 through 4.25, Figure 4.14, Figure 4.17). Unlike the synthetic LRR2 of TrkA, the same LRR2 peptides of TrkB and TrkC both show higher affinity for their respective neurotrophin; similar to that exhibited for the entire extracellular domain of the two receptors (Table 4.15 and Table 4.23, Figure 4.14, Figure 4.17). An NMR spectrum of the TrkB peptide showed a significant level of secondary structure in the form of short α-helix connected by random coil. These two peptides show only monophasic ligand-binding and it may be speculated that the high affinity binding of BDNF to the TrkB LRR2 is a consequence of the observed secondary structure of this peptide. It seems reasonable to conjecture than the TrkC LRR2 must have similar secondary structure to that of the TrkB peptide and does not resemble the random coil nature of the TrkA peptide. Kinetics data for the three synthetic LRR2 peptides suggests that this region of the three receptors is a binding "hot spot" for neurotrophin on the Trk surfaces.

A summary of the equilibrium binding constants obtained by different methodologies is presented in Table 4.26. One possible explanation for the differences between the measured binding constants, as determined by different *in vivo* and *in vivo* measurement, may be found in the effect that the ionic strength of the buffer used in an experiment may have on the measured K_D. The equilibrium dissociation constants observed for the interactions of NGF and BDNF with TrkA and TrkB respectively, using the IAsys Biosensor and also reported for the BIAcore study of the TrkA Ig-like domain (Robertson et al. 2001), are approximately an order of magnitude higher than observed by other means. Measurements of the association rates of the neurotrophins with their respective receptor appear to be markedly affected by the ionic strength of the buffers used in the experiments. The interaction rate of NGF and BDNF for their respective receptor was very dependent on the ionic strength of the buffer, implying the importance of electrostatic interactions in the neurotrophin-receptor interaction. A BIAcore biosensor study of the Thrombin-

Thrombomodulin interaction (Baerga-Ortiz et al. 2000) and for complement C4bC2 formation (Laich and Sim 2001) demonstrate the dramatic effect that solution ionic strength may have on protein-protein interactions in which electrostatics play a role. As small an increase as 50-100 mM in the buffer ionic strength, can readily change the equilibrium dissociation constant of a protein-protein interaction by an order of magnitude, or more. Hence, relatively small changes of the ionic strength of the buffers used in the various *in vivo* and *in vitro* experimental measurements of the neurotrophin-receptor interaction, may account for differences in measured values for the dissociation constants.

5.16 An Hypothesis of Receptor and Ligand Interaction

Hypotheses of the interactions of the neurotrophins with the Trk receptors may be formulated from the results of the kinetics experiments of this study. In particular, the interaction of the neurotrophins with both the LRR and Ig-like domains of the TrkA and TrkB receptor, suggests that the neurotrophin may bind to both domains of the intact receptor. This supposition leads to the possibility of neurotrophin binding to both domains simultaneously or binding to either single domain. The attendant consequence of either situation is a mixed receptor population at the cell surface; that is, at any given time, some fraction of the receptors will have neurotrophin bound to the LRR while some will have neurotrophin bound to the Ig-like domain.

What the biological consequences of this situation might be is open to speculation. For example, binding of neurotrophin might initially occur to the Ig-like domain followed by movement to the LRR domain; subsequent actions initiated by this event, such as conformational change of the receptor, may lead to receptor-ligand internalization or intracellular events such as phosphorylation and intracellular signaling.

An experiment designed to test the binding of NGF to the LRR while inactivating the binding activity of the Ig-like region of the intact extracellular segment of TrkA, proved inconclusive when NGF was found to bind to the antibody used to block NGF binding to this domain. Hence no kinetics experiment incontrovertibly supports the sequential binding of neurotrophin to the two-candidate ligand-binding domains of the Trk receptors.

5.17 Multivalency and Structure Changes of Receptor and Ligand

While the kinetics of ligand-binding to the Trk receptors suggests a mechanism for the interaction from the point of view of the receptor, the interactions should also be considered by interpreting potential behaviors of the neurotrophins. A second hypothesis of Trk-neurotrophin interaction may be made based on the binding of neurotrophin to two domains of the receptors. Neurotrophins may be considered to be multivalent ligands in that are able to undergo some structural change upon receptor binding. Because of the structural differences between the LRR and Ig-like domains, it is unlikely that the regions of the neurotrophins that bind to them are located in the same area of the ligand molecule. If this premise is correct, then the neurotrophins are multivalent ligands that bind to multivalent receptors.

From mutational analysis of neurotrophins, it appears that a large proportion of the surface of neurotrophins may interact with respective receptors (Neet and Campenot 2001). Hence it is reasonable to interpret the kinetics observed in this study as the binding of neurotrophin to the receptor LRR and Ig-like domains through different regions of the ligand molecule.

Additional support for neurotrophin structural changes being responsible for the biphasic binding observed for the TrkA receptor and monophasic binding observed for the TrkB and TrkC receptors, appears to be provided by the strictly monophasic dissociation of all neurotrophins from their respective receptor (Table 4.2 through Table 4.23). These observations suggest that on binding to the TrkA receptor, NGF undergoes structural changes that are observed as biphasic association kinetics. BDNF and NT-3 both exhibit monophasic association kinetics, suggesting that these molecules are relatively rigid and do not undergo large structural changes upon binding to TrkB or TrkC. Monophasic dissociation of the neurotrophins from their receptors can be explained on the basis, that on each receptor, the neurotrophin is structurally constrained and does not undergo domain movements upon dissociation.

Small synthetic peptides of less than 20 amino acids have been shown to exhibit biphasic kinetics when associating with a large enzyme molecule (Eto et al. 1999). These kinetics are interpreted as structural changes of the interacting molecules. Given that the TrkA synthetic peptide shows biphasic kinetics, while the TrkB and TrkC peptides both show monophasic association, it may be reasonable to conclude that neurotrophin domain movement provides a reasonable explanation

for the observed kinetics for all three receptors. A study of the interaction of Trk proteins with neurotrophins under conditions of varying ionic strength, suggest that domain movements do occur with NGF, BDNF and NT-3. It is probable that the domain movements of NGF are rapid and significant, compared with those for BDNF and NT-3.

A possible resolution to the confusion in ligand-binding domain assignment for Trk receptors and subsequent biological effects may be found in the "ligand paradox" (Kenakin and Onaran 2002). Studies of ligand-binding to the histamine H2 and other receptors show that ligand affinity and biological consequence (efficacy) need not be related (Ruffolo et al. 1979, Ganellin and Durant 1981, Ruffolo and Waddell 1983, Black 1996, Hestermann et al. 2000). This paradox can be explained on the basis of heterogeneity in receptor tertiary conformations. Since proteins are subject to constant local and regionally independent unfolding reactions (Woodward et al. 1982, 1993), different ligand-binding domains with dissimilar pharmacological consequences may result. Hence it is possible for a ligand to bind with nM affinity to a receptor domain but elicit no biological consequence, such as phosphorylation or internalization. Conversely a ligand with μM affinity for a particular region of the protein may produce such events (Kenakin and Onaran 2002).

Receptor function is more reasonably assigned to a probabilistic model of protein conformations. Thus the receptor function arises as a consequence of ligand-induced perturbation of the distribution of conformational states over conformational space (Kenakin and Onaran 2002). With this model the possibility of neurotrophin independently binding to the LRR and Ig-like domains, when expressed on the surfaces of cells becomes possible. Various biological and physical events may expose different regions of the Trk receptor to neurotrophin binding. Binding of neurotrophin to the LRR domain may produce completely different biological consequences to neurotrophin binding to the Ig-like domain. Hence, binding of neurotrophin to each of these different domains may or may not cause reception dimerization, phosphorylation or internalization, each event being completely independent consequences of ligand and domain interactions. Isolated domains expressed as MBP-fusion proteins may thus each bind neurotrophin without showing inhibition of phosphorylation in cell based assays. Binding of neurotrophins to Trk receptors thus may not be so readily determined by receptor phosphorylation and internalization studies.

5.18 The Effect of Charged Residues on Neurotrophin-Receptor Interactions

Charged residues have been shown, by mutagenisis studies, to affect the binding of NGF and GDNF to p75 (Urfer et al. 1994, Panayotatos et al. 1995, Ryden and Ibanez 1996, Ibanez 1998). Long range electrostatic forces are probably important in recruiting limiting quantities of neurotrophic factors available *in vivo* and localizing them at the cell membrane (Ibanez 1998). Replacement of positively charged residues by alanine, can eliminate binding of NGF and GDNF to p75 (Ibanez 1998). The co-crystal structure of TrkA d5 and NGF showed that regions of NGF interact with d5. Of particular importance are Arg 103, which is conserved in all neurotrophins (Wiesmann et al. 1999, 2000), His 4 and Arg347.

Since these charged residues play a role in the interaction of NGF with a single TrkA domain, it is reasonable to speculate that interactions with the region, C-terminal to d5 and other receptor domains, may also be influenced by charged residues in both neurotrophin and receptor. The dramatic affect on the binding of neurotrophin to receptor with different salt concentrations, demonstrate the effect of charged residues on the interactions of NGF and BDNF with their respective receptor.

5.19 Interactions of Trk Receptors and Accessory Proteins

From a model of the interaction between receptors in endosomes and a membrane associated accessory molecule (Linderman and Lauffenburger 1988), it is possible to postulate how the binding of neurotrophin to Trk receptors may be influenced by the intracellular domain of the receptors and accessory proteins. In this model, ligand free receptors have no affinity for an intracellular accessory protein. A monovalent intracellular domain accessory protein may cause aggregation of receptors with the consequent binding of neurotrophin. If the mobile Trk receptors bind a multivalent accessory protein, receptor aggregation can occur with the subsequent binding of a multivalent ligand. The affinity of the accessory protein for the complex will determine the probability of receptor-ligand interaction. A multivalent accessory protein has in this model, a higher avidity for receptor aggregates than for single receptors. Obviously, the converse scenario is equally plausible, that is, multivalent neurotrophins may cause the binding of a multivalent accessory protein.

Studies of the interactions of NGF, p75 and TrkA on cell surfaces (Ross et al. 1996, Wolf et al. 1998) have shown that the extracellular domain of TrkA is sufficient for interaction with p75. Both the transmembrane and intracellular domains of the receptor however have a significant influence on the interaction with p75 and the binding of NGF (Ross et al. 1996). Such results suggest that the high equilibrium dissociation constants measured by *in vivo* methods, may differ considerably from the equilibrium dissociation constants for recombinant proteins in which the intracellular domain of the proteins are absent. Furthermore, phosphorylation of multiple intracellular sites, influences the mobility (Wolf et al. 1998) and hence possibly, the binding of NGF to the receptor. In conclusion, all studies of the Trk receptors to date, point to a complex chain of events in the binding of neurotrophin to receptor. This interaction is influenced in many unknown ways, both by extracellular and intracellular proteins and their role in the Trk receptor-neurotrophin interaction remains to be clarified.

Recently, several new proteins that interact with the intracellular domain of TrkA and p75 have been identified. The protein ARMS has been shown to interact with significant affinity with both p75 and TrkA intracellular domains (Kong et al. 2001). Proteins such as ARMS may be able to associate with both p75 and TrkA, forming the proposed ternary complex, resulting in high affinity receptors or changes in receptor populations differing in their active conformations (Lindstrom-Lang and Schellman 1959, Kenakin 1996).

An hypothesis resulting from this study, is that both neurotrophins and their receptors have bivalent binding properties (Table 4.2 through Table 4.25). *In vivo* studies of the aggregation of neurotrophin, p75 and TrkA on the surface of cells (Ross et al. 1996, Wolf et al. 1998), suggests that NGF and the low and high affinity neurotrophin receptors, display behavior consistent with the bivalent nature of a ligand and receptor. NGF has been shown to associate with TrkA on the surface of cells, resulting in decreased mobility of the receptor with respect to mobility displayed in the absence of neurotrophin. In addition, p75 has been shown to aggregate with TrkA in the presence and absence of NGF (Ross et al. 1996). It is conceivable that a multivalent NGF ligand, achieves its high level of affinity, when measured *in vivo*, by binding to the receptor through more than one binding region on single Trk receptors. Such neurotrophin cross-linked receptors may result in a high affinity binding between ligand and receptor; higher than observed in biosensor studies. A consequence of this interaction would be formation of aggregates of the Trk receptor on the cell surface, with consequent loss of receptor mobility.

The results from the IAsys biosensor study, suggests a hypothetical mechanism of neurotrophin interaction with the Trk receptors. Consistent with the observed interaction of p75 and Trk receptor (Huber et al. 1995, Ross et al. 1996, Ross et al. 1998, Bibel et al. 1999); neurotrophin bound to the p75 receptor is passed to either the LRR or Ig-like receptor domain, followed by translation of the neurotrophin to the second neurotrophin binding region with consequential biological activity. Such a mechanism may account for the difference in the orientation of neurotrophin binding, with respect to the cellular membrane, suggested from theoretical models of p75 (Chapman and Kuntz 1995, Shamovsky et al. 1999) and of the orientation of NGF observed in the crystal structure of NGF bound to the C-terminal Ig-like domain of TrkA (Wiesmann et al. 1999, 2000). If passage of NGF from p75 to the LRR domain of the Trk receptor occurs first, it is possible that the orientation of NGF may be changed. In this reaction, the NGF molecule oriented with the N and C terminals towards the cell membrane is rotated, such that the ligand N and C terminals orient away from the membrane when bound to the LRR. Passage of NGF from the LRR to the Ig-like domain of TrkA could then occur with the attendant NGF orientation observed in the X-ray crystallography study (Wiesmann et al. 1999, 2000).

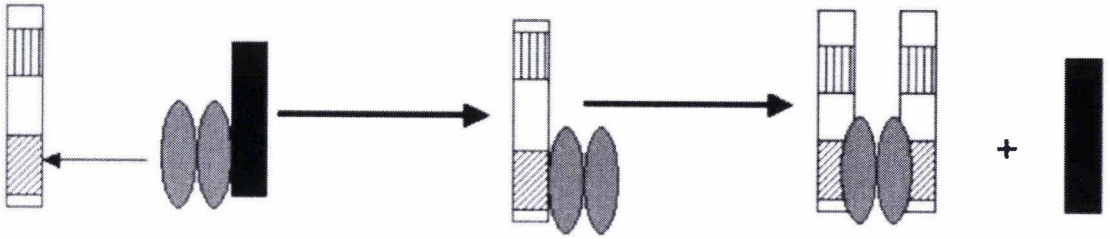

Model a

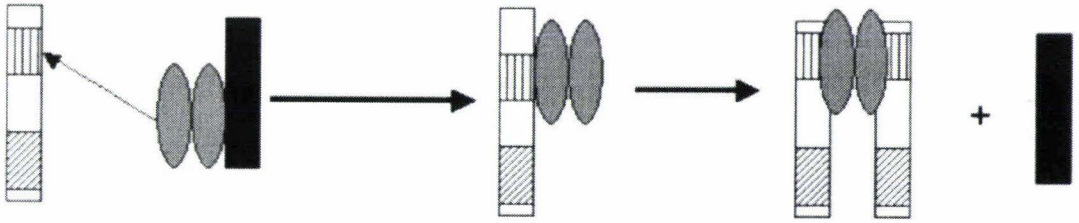

Model b

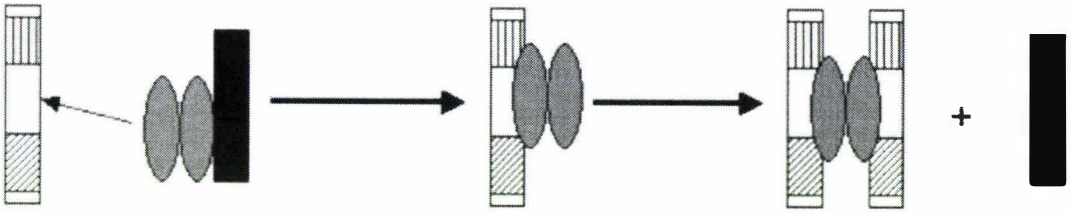

Model c

Figure 10.1 Hypothetical models for the interaction of the Extracellular Domains of Trk Receptors with Neurotrophins.

A number of models for the interaction are possible, all of which account to some degree, for reported *in vivo* and *in vitro* experimental results. In Models (a) and (b), the neurotrophin interacts exclusively with the Ig-like and LRR domains respectively, as observed for these two receptor regions in the IAsys biosensor study. It is believed that *in vivo*, p75 recruits neurotrophins and presents them to the Trk receptor, before the homodimer of the receptor forms, as depicted in these models. In model (c), the neurotrophin interacts with both Ig-like and LRR domains upon binding to the Trk receptor. It is also possible that the Trk receptors may exist as a cell surface mixture of models (a) and (b). In addition it is also conceivable that binding of neurotrophin occurs initially as depicted in Model (a) before a movement of bound neurotrophin from the Ig-like domain to the LRR domain, resulting in Model (b). It is quite probable, that intracellular accessory proteins may pay a significant role in neurotrophin-Trk interactions, however, this effect cannot be assessed from *in vivo* and *in vitro* experiments conducted to date and no attempt to depict the complex interactions are shown in the models.

5.20 Trk Receptor Ligand-binding Domains; a role for the LRR Domain

Based upon the results of the biosensor study and of many other studies, it is reasonable to postulate that the three principal ligand-binding "hot spots" of the Trk receptors, include both the d4 and d5 Ig-like domains and N-terminal regions encompassing the LRR domain. Further, these regions participate in neurotrophin binding and activation of Trk receptors. It is believed that the d5 domain is the main site binding cf NGF, BDNF and NT-3 (Wiesmann et al. 1999, 2000, Saragovi and Zaccaro 2002). The d4 site may, in some as yet undetermined fashion, bind neurotrophins, but act as an inhibitory site (Saragovi and Zaccaro 2002). The LRR domain also mediates NGF-TrkA functionality, but is postulated to do so *in vivo*, only when p75 is co-expressed on a cell surface (Zaccaro et al. 2001, Saragovi and Zaccaro 2002).

It is postulated that ligands bound to the activation "hot spots," are likely to be functional as agonists or antagonists of the Trk receptor and as such will assist in the screening and characterization of neurotrophin mimetics (Saragovi and Zaccaro 2002). Ligands that bind to d5, may be agonistic, while ligands that bind d4 may serve as antagonists of neurotrophin receptor

activity (Saragovi and Zaccaro 2002). Ligands that bind to the N-terminal LRR domains in the presence of p75, may serve to regulate receptor activity (Saragovi and Zaccaro 2002).

As with other models of neurotrophin interaction with its low and high affinity receptors, the proposed mechanism of Zaccaro et al. (2001) has its deficiencies. The model requires that the LRR domain be exposed on the surface of the receptor on binding neurotrophin. In the experiment by Zaccaro et al., the antibody did not interact with the LRR domain that should have been exposed if the proposed model is correct. This lack of detection was explained by the suggestion that the antibody does not interact with epitopes within the LRR domain. However, this same antibody (provided by Prof. Uri Saragovi, McGill University) readily and explicitly detects the LRR domain in all MBP-LRR proteins (Figure 2.22). Hence, if the model by Zaccaro et al. is correct, then the LRR surface is exposed and should have been detected by the antibody. That the LRR domain was not detected suggests that the proposed model resulting from the experiment is incorrect in some fashion.

5.21 Summary

In summary, the biosensor study shows that neurotrophins, at least *in vitro*, bind to the Trk receptors in multiple domains and not just the Ig-like domain as suggested previously. Complex biphasic association of NGF to TrkA, stands in contrast to the monophasic association of BDNF and NT-3 with TrkB and TrkC respectively. Instrument and protein limitations prevented a more detailed examination of the binding events much beyond the establishment of multiple neurotrophin binding domains. Binding to LRR and Ig-like domains in all three Trk receptors, is unaffected by temperature and appears to be real, at least within the limitations of the experimental system.

To conduct a more extensive study, namely repeated binding assays for each Trk protein utilized in the study, would not have been more informative. In an earlier study Windisch et al. (1995a), found that the standard deviation for 3-4 repeated experiments was in the range of 16-36% for the equilibrium dissociation constants. Multiple repeated binding experiments for a typical biosensor study, have errors of 20-40%, far exceeding the experimental error range necessary to determine accurately, binding differences between Trk receptor domains. The IAsys biosensor, while quite suitable for screening the interaction of biomolecules, shows significantly high standard deviations for repeated kinetics analysis. For example, the interaction of Rad51A with

DNA has been measured and reported with an error range of ~ 40% for 4 repeated experiments (De Zutter and Knight 1999).

The error range of the experiments does not permit a differentiation of the equilibrium dissociation constants between the bimodal interaction phases of the NGF interactions with the TrkA proteins. In addition, establishing the binding constants by *in vitro* assay is unlikely to provide a real measure of association, dissociation and equilibrium binding constants for Trk receptors at the membrane surface of neuronal cells in the human brain. Many complex issues are involved in interpreting *in vivo* binding from *in vitro* assays.

In vivo measurement has established that the equilibrium dissociation constants for the interactions of neurotrophins with their respective receptor, is within the range of 10^{-9} to 10^{-11} M (Sutter et al. 1979, Cohen et al. 1980, Schechter et al. 1981, Bernd and Greene 1984, Layer and Shooter 1983, Hosang and Shooter 1985, Woodruff and Neet 1986, Godfrey and Shooter 1986, Kaplan et al. 1991, Klein et al. 1991, Soppet et al. 1991, Rodriguez-Tebar et al. 1992). The biosensor study has established equilibrium dissociation constants for the interactions of neurotrophins with different domains of their receptors that range in value from approximately 3 to 25 nM. These values are 2 to 3 orders of magnitude higher than those measured *in vivo*. However, they are similar to measurements made for the interaction of NGF with the extracellular domain of TrkA (Woo et al. 1998). In a biosensor study of the interaction of NGF with the Ig-like domain of TrkA, a K_D of 11.8 nM was reported (Robertson et al. 2001), however, since no experimental details and no error estimate were given for the reported K_D, it is impossible to make a direct comparison between the data collected in the two studies. Many complex issues are involved in interpreting *in vivo* binding using an *in vitro* assay. Simple and often unknown changes in solution ionic strength have been shown to have dramatic influences on protein-interactions (De Crescenzo et al. 2000, Laich and Sim 2001) and hence direct comparison between experimental techniques and results is difficult at best.

The measurements of the interaction of the recombinant Trk proteins and their neurotrophins in this study were made *in vitro*. These data may not accurately reflect real affinity constants of the Trk-neurotrophin interaction *in vivo* (Table 4.2 through Table 4.25). However, it is reasonable to conclude that the biosensor study has shown that two distinct domains, namely, the LRR domain and the immunoblobulin-like domain of both TrkA and TrkB both bind NGF and BDNF respectively. If binding of neurotrophins to the LRR and Ig-like domains of the Trk receptors does

occur *in vivo*, then it is possible to resolve some of the conflicting binding data cited from many previous neurotrophin-receptor interaction studies (Neet and Campenot 2001).

Two crystal structures of NGF bound to a single Ig-like region of TrkA have been produced to date (Wiesmann et al. 1999, 2000, Robertson et al. 2001). One structure of BDNF bound to the Ig-like region of TrkB has also been reported (Banfield et al. 2001). These structures do not prove that other regions of the Trk receptors interact with neurotrophins (Neet and Campenot 2001). A significant consequence of neurotrophin binding to both LRR and Ig-like domains of the Trk receptors, is that crystallization of fragments of proteins in complex with a ligand, may well lead to erroneous conclusions of the functional characteristics of the proteins in the complex. A static picture of NGF bound to one domain of TrkA may lead to a lack of appreciation of a possible dynamic movement of neurotrophin between the LRR and Ig-like domains of the receptor.

NGF has a motif consisting of residues Val-48, Pro-49 and Gln96, situated in the top β-loop, together with a second motif consisting of residues Pro-5 and Phe-7 situated in the proximal part of the N-terminus. Together, these domains form two topographically distinct regions of NGF that have been shown to determine receptor specificity and activation (Kullander et al. 1997). The β-loop residues do not make any physical contacts with the d5 domain of TrkA in the NGF-d5 structure (Wiesmann et al. 1999, 2000). The residue, Phe-7 of NGF has been predicted to show a stereochemical fit to a domain of the LRR domain of TrkA (Kullander et al. 1997).

It is possible that these two distinct motifs bind to the LRR domain and the Ig-like domain of TrkA, but it is not possible to assign an NGF binding motif to either receptor domain. Specificity of NGF interactions with TrkA may well be determined by at least two distinct regions of NGF (Kullander et al. 1997).

The biosensor study showed that the LRR domain of TrkA, TrkB and TrkC, bind their respective neurotrophin with similar affinity and kinetics as the entire extracellular domain of the receptors (Table 4.2 through Table 4.25, Figure 4.11, Figure 4.14, Figure 4.17). It cannot be concluded, based upon cell competition studies with the synthetic peptides representing the central 24 residues of the LRR domain, that this region represents more than a binding "hot spot" for the neurotrophins on the surface of the receptors. It is possible for as few as 3 amino acids of a peptide to confer nM affinity for a receptor (Horwell 1995). However, since the binding affinity of the synthetic peptides is significantly weaker than the full-length LRR, it would appear that the

appropriate amino acids for nM affinity to the Trk receptor may not be contained in the 24 residue peptides.

No inhibition of cell survival was observed in a cell competition study using the synthetic peptides. The study appeared to show that the binding of neurotrophin to the ligand "hot spot" has no biological consequences. Conceivably, the observed binding of the LRR2 domain of the receptors to the neurotrophin actually represents the interaction of a small charged molecule (free of steric hindrance of the secondary and tertiary structure of the ED), to the neurotrophins. If this is indeed the situation, then the null results of the cell survival study with these peptides is more readily understandable.

The IAsys biosensor study of neurotrophins binding to their respective receptor showed that complex binding phenomena may occur in the interaction of neurotrophins with Trk receptors. A 2-binding site model has to be considered, as was found for the dimeric HGH and EPO receptors, that have two ligand-binding sites (Saragovi and Zaccaro 2002). An alternative model is that proposed for the TGF-beta type II interactions. In this case Trk and p75 would be receptor subtypes having overlapping ligand-binding sites at adjacent positions on the ligand surface (Saragovi and Zaccaro 2002).

It is essential that *in vivo* data take precedence in the interpretation of *in vitro* data, when investigating biological phenomena. The best designed biophysical experiments, must take into account any relevant biological experiments in explaining observed data and in formulating hypotheses. To this end, the observed biphasic nature of NGF to TrkA receptors, expressed on the surfaces of cells (Meakin et al. 1992), the monophasic binding of BDNF to TrkB receptors in cell based assays (Dechand et al. 1993) and the absence of binding of BDNF to isoforms of TrkB lacking the LRR domain (Ninkina et al. 1997), must be taken into account when interpreting the kinetics of neurotrophin binding to Trk proteins in the biosensor study. Biological experiments clearly support the biphasic nature of the interaction of NGF with TrkA proteins and also support the importance of the LRR domain in neurotrophin binding to their receptors.

As described above, no model for the binding of neurotrophins to their low and high affinity receptors is able to fully explain all the observed interactions in the many *in vivo* and *in vitro* studies that have been undertaken. Without exception, each model posses as many problems for the interpretation of the receptor-ligand interaction as it professes to explain. Hence the models

described in this thesis are only concepts in a pathway of discovery that will undoubtedly involve many iterative and novel approaches. Much more research and reflection will be needed for a full understanding of the Trk receptors and the interactions with their ligands.

If the development of therapies for Alzheimer's, Parkinson's and other neurodegenerative diseases is the goal, then the design of small molecule agonists and antagonists of the neurotrophins and their receptors remains an unfulfilled vision. While progress has been made in the understanding of the Trk-neurotrophin interactions and of the structures of these molecules, the design of small molecule mimics of the neurotrophins has, by comparison, been relatively measured. It remains to be seen if the screening of combinatorial chemical libraries, a pharmaceutical industry approach, together with the design of cyclic peptides and the production of monoclonal antibodies to receptors and ligands, the academic laboratory approach, will in time succeed in the elucidation of appropriate small molecule therapies for neurodegenerative diseases and cancers (Saragovi and Burgess 1999). If indeed the neurotrophins bind to two distinct domains on the receptor surface and if the receptor interaction domains on the neurotrophin are spatially distinct, then it seems unlikely that a single small molecule mimic of neurotrophin action is possible. Rather, it seems more likely that a cocktail of small molecules may offer the ultimate goal of a neurotrophin like molecule, sufficiently small enough to cross the blood-brain barrier.

REFERENCES

Atkins P.W., 1986, Physical Chemistry, 3rd Edition, W. H. Freeman and Co., Chapter 28.

Allen, S.J., S.H. MacGowan, S. Tyler, G.K. Wilcock, A.G. Robertson, P.H. Holden, S.K. Smith, and D. Dawbarn. 1997. Reduced cholinergic function in normal and Alzheimer's disease brain is associated with apolipoprotein E4 genotype. *Neurosci Lett.* 239:33-6.

Altschuh, D., W. Braun, J. Kallen, V. Mikol, C. Spitzfaden, J.C. Thierry, O. Vix, M.D. Walkinshaw, and K. Wuthrich. 1994. Conformational polymorphism of cyclosporin A. *Structure.* 2:963-72.

Baerga-Ortiz, A., A.R. Rezaie, and E.A. Komives. 2000. Electrostatic dependence of the thrombin-thrombomodulin interaction. *J Mol Biol.* 296:651-8.

Baldwin, A.N., C.M. Bitler, A.A. Welcher, and E.M. Shooter. 1992. Studies on the structure and binding properties of the cysteine-rich domain of rat low affinity nerve growth factor receptor (p75NGFR). *J Biol Chem.* 267:8352-9.

Baneyx, F. 1999. Recombinant protein expression in Escherichia coli. *Curr Opin Biotechnol.* 10:411-21.

Banfield, M.J., R.L. Naylor, A.G. Robertson, S.J. Allen, D. Dawbarn, and R.L. Brady. 2001. Specificity in Trk receptor:neurotrophin interactions: the crystal structure of TrkB-d5 in complex with neurotrophin-4/5. *Structure (Camb).* 9:1191-9.

Barbacid, M. 1994. The Trk family of neurotrophin receptors. *J Neurobiol.* 25:1386-403.

Barde, Y.A. 1988. What, if anything, is a neurotrophic factor? *Trends Neurosci.* 11:343-6.

Barker, P.A., C. Lomen-Hoerth, E.M. Gensch, S.O. Meakin, D.J. Glass, and E.M. Shooter. 1993. Tissue-specific alternative splicing generates two isoforms of the trkA receptor. *J Biol Chem.* 268:15150-7.

Barker, P.A., and E.M. Shooter. 1994. Disruption of NGF binding to the low affinity neurotrophin receptor p75LNTR reduces NGF binding to TrkA on PC12 cells. *Neuron.* 13:203-15.

Barrett, G.L. 2000. The p75 neurotrophin receptor and neuronal apoptosis. *Prog Neurobiol.* 61:205-29.

Barrett, G.L., and P.F. Bartlett. 1994. The p75 nerve growth factor receptor mediates survival or death depending on the stage of sensory neuron development. *Proc Natl Acad Sci U S A.* 91:6501-5.

Benedetti, M., A. Levi, and M.V. Chao. 1993. Differential expression of nerve growth factor receptors leads to altered binding affinity and neurotrophin responsiveness. *Proc Natl Acad Sci U S A.* 90:7859-63.

Bernd, P., and L.A. Greene. 1984. Association of 125I-nerve growth factor with PC12 pheochromocytoma cells. Evidence for internalization via high-affinity receptors only and for long-term regulation by nerve growth factor of both high- and low-affinity receptors. *J Biol Chem.* 259:15509-16.

Bibel, M., E. Hoppe, and Y.A. Barde. 1999. Biochemical and functional interactions between the neurotrophin receptors trk and p75NTR. *Embo J.* 18:616-22.

Black, j. 1996. A Personal View of Pharmacology. *Ann Rev Pharmacol Toxicol.* 36:1-33.

Bradshaw, R.A., J. Murray-Rust, C.F. Ibanez, N.Q. McDonald, R. Lapatto, and T.L. Blundell. 1994. Nerve growth factor: structure/function relationships. *Protein Sci.* 3:1901-13.

Butte, M.J., P.K. Hwang, W.C. Mobley, and R.J. Fletterick. 1998. Crystal structure of neurotrophin-3 homodimer shows distinct regions are used to bind its receptors. *Biochemistry.* 37:16846-52.

Cantor C.R., P.R. Schimmel, 1980, Biophysical Chemistry, W. H. Freeman and Co, Chap. 11.

Casaccia-Bonnefil, P., C. Gu, and M.V. Chao. 1999. Neurotrophins in cell survival/death decisions. *Adv Exp Med Biol.* 468:275-82.

Chakrabarti, P., and J. Janin. 2002. Dissecting protein-protein recognition sites. *Proteins.* 47:334-43.

Chao, M.V., and B.L. Hempstead. 1995. p75 and Trk: a two-receptor system. *Trends Neurosci.* 18:321-6.

Chapman, B.S., and I.D. Kuntz. 1995. Modeled structure of the 75-kDa neurotrophin receptor. *Protein Sci.* 4:1696-707.

Clarkson, T., and J. Wells. 1995. *Science.* 267:383.

Cohen, P., A. Sutter, G. Landreth, A. Zimmermann, and E.M. Shooter. 1980. Oxidation of tryptophan-21 alters the biological activity and receptor binding characteristics of mouse nerve growth factor. *J Biol Chem.* 255:2949-54.

Cook, J.P., A.J. Henry, J.M. McDonnell, R.J. Owens, B.J. Sutton, and H.J. Gould. 1997. Identification of contact residues in the IgE binding site of human FcepsilonRIalpha. *Biochemistry.* 36:15579-88.

Cowan, W.M., J.W. Fawcett, D.D. O'Leary, and B.B. Stanfield. 1984. Regressive events in neurogenesis. *Science.* 225:1258-65.

Cush, R., J. Cronin, W. Stewart, C. Maule, J. Molloy, and M. Goddard. 1993. *Biosensors and Bioelectronics.* 8:347.

Davies, D.H., C.M. Hill, J.B. Rothbard, and B.M. Chain. 1990. Definition of murine T helper cell determinants in the major capsid protein of human papillomavirus type 16. *J Gen Virol.* 71 (Pt 11):2691-8.

De Crescenzo, G., S. Grothe, R. Lortie, M.T. Debanne, and M. O'Connor-McCourt. 2000. Real-time kinetic studies on the interaction of transforming growth factor alpha with the epidermal growth factor receptor extracellular domain reveal a conformational change model. *Biochemistry.* 39:9466-76.

De Zutter, J.K., and K.L. Knight. 1999. The hRad51 and RecA proteins show significant differences in cooperative binding to single-stranded DNA. *J Mol Biol.* 293:769-80.

Dechant, G., S. Biffo, H. Okazawa, R. Kolbeck, J. Pottgiesser, and Y.A. Barde. 1993. Expression and binding characteristics of the BDNF receptor chick trkB. *Development.* 119:545-58.

Dechant, G., A. Rodriguez-Tebar, and Y.A. Barde. 1994. Neurotrophin receptors. *Prog Neurobiol.* 42:347-52.

Dominguez, D., M. Altmann, J. Benz, U. Baumann, and H. Trachsel. 1999. Interaction of translation initiation factor eIF4G with eIF4A in the yeast Saccharomyces cerevisiae. *J Biol Chem.* 274:26720-6.

Drinkwater, C.C., U. Suter, C. Angst, and E.M. Shooter. 1991. Mutation of tryptophan-21 in mouse nerve growth factor (NGF) affects binding to the fast NGF receptor but not induction of neurites on PC12 cells. *Proc R Soc Lond B Biol Sci.* 246:307-13.

Dunbar, J., G. Tregear, and R.A. Bradshaw. 1984. *J Prot Chem.* 3:349.

Edwards, P.R., A. Gill, D.V. Pollard-Knight, M. Hoare, P.E. Buckle, P.A. Lowe, and R.J. Leatherbarrow. 1995. Kinetics of protein-protein interactions at the surface of an optical biosensor. *Anal Biochem.* 231:210-7.

Edwards, P.R., C.H. Maule, R.J. Leatherbarrow, and D.J. Winzor. 1998. Second-order kinetic analysis of IAsys biosensor data: its use and applicability. *Anal Biochem.* 263:1-12.

Erickson, J., B. Goldstein, D. Holowka, and B. Baird. 1987. The effect of receptor density on the forward rate constant for binding of ligands to cell surface receptors. *Biophys J.* 52:657-62.

Ernfors, P., C.F. Ibanez, T. Ebendal, L. Olson, and H. Persson. 1990. Molecular cloning and neurotrophic activities of a protein with structural similarities to nerve growth factor: developmental and topographical expression in the brain. *Proc Natl Acad Sci U S A.* 87:5454-8.

Escandon, E., D. Soppet, A. Rosenthal, J.L. Mendoza-Ramirez, E. Szonyi, L.E. Burton, C.E. Henderson, L.F. Parada, and K. Nikolics. 1994. Regulation of neurotrophin receptor expression during embryonic and postnatal development. *J Neurosci.* 14:2054-68.

Eto, A., T.C. Saido, K. Fukushima, S. Tomioka, S. Imai, T. Nisizawa, and N. Hanada. 1999. Inhibitory effect of a self-derived peptide on glucosyltransferase of Streptococcus mutans. Possible novel anticaries measures. *J Biol Chem.* 274:15797-802.

Faber, G. 1999. *Pharmacology and Therapeutics.* 84:327.

Fisher, L.W., A.M. Heegaard, U. Vetter, W. Vogel, W. Just, J.D. Termine, and M.F. Young. 1991. Human biglycan gene. Putative promoter, intron-exon junctions, and chromosomal localization. *J Biol Chem.* 266:14371-7.

Fox. 2003. *FEBS Lett.* 27:537.

Ganellin, C., and G. Durant. 1981. Burgers Medicinal Chemistry. Wiley. 487-552 pp.

Gardina, P.J., and M.D. Manson. 1996. Attractant signaling by an aspartate chemoreceptor dimer with a single cytoplasmic domain. *Science.* 274:425-6.

Glasel, J.A. and M.P. Deutcher. 1995. Introduction to Biophysical Methods for Protein and Nucleic Acids Research. Academic Press. Chapter 3.

Glaser, R.W. 1993. Antigen-antibody binding and mass transport by convection and diffusion to a surface: a two-dimensional computer model of binding and dissociation kinetics. *Anal Biochem.* 213:152-61.

Godfrey, E.W., and E.M. Shooter. 1986. Nerve growth factor receptors on chick embryo sympathetic ganglion cells: binding characteristics and development. *J Neurosci.* 6:2543-50.

Grimes, M.L., J. Zhou, E.C. Beattie, E.C. Yuen, D.E. Hall, J.S. Valletta, K.S. Topp, J.H. LaVail, N.W. Bunnett, and W.C. Mobley. 1996. Endocytosis of activated TrkA: evidence that nerve growth factor induces formation of signaling endosomes. *J Neurosci.* 16:7950-64.

Hawkins, S., S. Russell, M. Baier, and J. Winter. 1993. *J MOI Biol.* 234:958.

Hefti, F. 1986. Nerve growth factor promotes survival of septal cholinergic neurons after fimbrial transections. *J Neurosci.* 6:2155-62.

Hefti, F., J. Hartikka, and B. Knusel. 1989. Function of neurotrophic factors in the adult and aging brain and their possible use in the treatment of neurodegenerative diseases. *Neurobiol Aging.* 10:515-33.

Heinz, D.W., W.A. Baase, F.W. Dahlquist, and B.W. Matthews. 1993. How amino-acid insertions are allowed in an alpha-helix of T4 lysozyme. *Nature.* 361:561-4.

Hestermann, E.V., J.J. Stegeman, and M.E. Hahn. 2000. Relative contributions of affinity and intrinsic efficacy to aryl hydrocarbon receptor ligand potency. *Toxicol Appl Pharmacol.* 168:160-72.

Holden, P.H., V. Asopa, A.G. Robertson, A.R. Clarke, S. Tyler, G.S. Bennett, S.D. Brain, G.K. Wilcock, S.J. Allen, S.K. Smith, and D. Dawbarn. 1997. Immunoglobulin-like domains define the nerve growth factor binding site of the TrkA receptor. *Nat Biotechnol.* 15:668-72.

Horwell, D.C. 1995. The 'peptoid' approach to the design of non-peptide, small molecule agonists and antagonists of neuropeptides. *Trends Biotechnol.* 13:132-4.

Hosang, M., and E.M. Shooter. 1985. Molecular characteristics of nerve growth factor receptors on PC12 cells. *J Biol Chem.* 260:655-62.

Huber, L.J., and M.V. Chao. 1995. A potential interaction of p75 and trkA NGF receptors revealed by affinity crosslinking and immunoprecipitation. *J Neurosci Res.* 40:557-63.

Ibanez, C.F. 1994. Structure-function relationships in the neurotrophin family. *J Neurobiol.* 25:1349-61.

Ibanez, C.F. 1995. Neurotrophic factors: from structure-function studies to designing effective therapeutics. *Trends Biotechnol.* 13:217-27.

Ibanez, C.F. 1998. Emerging themes in structural biology of neurotrophic factors. *Trends Neurosci.* 21:438-44.

Ibanez, C.F. 2002. Jekyll-Hyde neurotrophins: the story of proNGF. *Trends Neurosci.* 25:284-6.

Ibanez, C.F., T. Ebendal, G. Barbany, J. Murray-Rust, T.L. Blundell, and H. Persson. 1992. Disruption of the low affinity receptor-binding site in NGF allows neuronal survival and differentiation by binding to the trk gene product. *Cell.* 69:329-41.

Ibanez, C.F., T. Ebendal, and H. Persson. 1991. Chimeric molecules with multiple neurotrophic activities reveal structural elements determining the specificities of NGF and BDNF. *Embo J.* 10:2105-10.

Ibanez, C.F., F. Hallbook, T. Ebendal, and H. Persson. 1990. Structure-function studies of nerve growth factor: functional importance of highly conserved amino acid residues. *Embo J.* 9:1477-83.

Ibanez, C.F., L.L. Ilag, J. Murray-Rust, and H. Persson. 1993. An extended surface of binding to Trk tyrosine kinase receptors in NGF and BDNF allows the engineering of a multifunctional pan-neurotrophin. *Embo J.* 12:2281-93.

Ip, N.Y., T.N. Stitt, P. Tapley, R. Klein, D.J. Glass, J. Fandl, L.A. Greene, M. Barbacid, and G.D. Yancopoulos. 1993. Similarities and differences in the way neurotrophins interact with the Trk receptors in neuronal and nonneuronal cells. *Neuron*. 10:137-49.

Jin, L., B.M. Fendly, and J.A. Wells. 1992. High resolution functional analysis of antibody-antigen interactions. *J Mol Biol*. 226:851-65.

Jing, S., P. Tapley, and M. Barbacid. 1992. Nerve growth factor mediates signal transduction through trk homodimer receptors. *Neuron*. 9:1067-79.

Kandel E.R., J.H. Schwartz, T.M. Jessell, 2000, Principles of Neural Science, Fourth Edition, Pub. McGraw-Hill, Chapters 1, 13, 58.

Kaplan, D., and T. Hunter. 1991. *Cell*. 65:895.

Kaplan, D.R., B.L. Hempstead, D. Martin-Zanca, M.V. Chao, and L.F. Parada. 1991a. The trk proto-oncogene product: a signal transducing receptor for nerve growth factor. *Science*. 252:554-8.

Kaplan, D.R., D. Martin-Zanca, and L.F. Parada. 1991b. Tyrosine phosphorylation and tyrosine kinase activity of the trk proto-oncogene product induced by NGF. *Nature*. 350:158-60.

Kaplan, D.R., and F.D. Miller. 2000. Neurotrophin signal transduction in the nervous system. *Curr Opin Neurobiol*. 10:381-91.

Kelley, R.F., and M.P. O'Connell. 1993. Thermodynamic analysis of an antibody functional epitope. *Biochemistry*. 32:6828-35.

Kenakin, T. 1996. *TIPS*. 17:190.

Kenakin, T., and O. Onaran. 2002. The ligand paradox between affinity and efficacy: can you be there and not make a difference? *Trends Pharmacol Sci*. 23:275-80.

Klein, R. 1994. *FASEB J*. 8:738.

Klein, R., D. Conway, L.F. Parada, and M. Barbacid. 1990. The trkB tyrosine protein kinase gene codes for a second neurogenic receptor that lacks the catalytic kinase domain. *Cell*. 61:647-56.

Klein, R., S.Q. Jing, V. Nanduri, E. O'Rourke, and M. Barbacid. 1991. The trk proto-oncogene encodes a receptor for nerve growth factor. *Cell*. 65:189-97.

Klein, R., L.F. Parada, F. Coulier, and M. Barbacid. 1989. trkB, a novel tyrosine protein kinase receptor expressed during mouse neural development. *Embo J*. 8:3701-9.

Klotz, I.M. 1985. Ligand--receptor interactions: facts and fantasies. *Q Rev Biophys*. 18:227-59.

Kobe, B., and J. Deisenhofer. 1994. The leucine-rich repeat: a versatile binding motif. *Trends Biochem Sci*. 19:415-21.

Kojima, S., T. Nakayama, G. Kuwajima, H. Suzuki, and T. Sakata. 1999. TrkB mutant lacking the amino-terminal half of the extracellular portion acts as a functional brain-derived neurotrophic factor receptor. *Biochim Biophys Acta*. 1420:104-10.

Kong, H., J. Boulter, J.L. Weber, C. Lai, and M.V. Chao. 2001. An evolutionarily conserved transmembrane protein that is a novel downstream target of neurotrophin and ephrin receptors. *J Neurosci*. 21:176-85.

Krommer, L. 1987. *Science*. 235:214.

Kullander, K., D. Kaplan, and T. Ebendal. 1997. Two restricted sites on the surface of the nerve growth factor molecule independently determine specific TrkA receptor binding and activation. *J Biol Chem*. 272:9300-7.

Kurucz, I., A. Hilbert, A. Kapus, D. Medgyesi, G. Koncz, G. Sarmay, A. Erdei, and J. Gergely. 2000. Bacterially expressed human Fc gamma RIIb is soluble and functionally active after in vitro refolding. *Immunol Lett.* 75:33-40.

Lai, W.H., and H.J. Guyda. 1984. Characterization and regulation of epidermal growth factor receptors in human placental cell cultures. *J Clin Endocrinol Metab.* 58:344-52.

Laich, A., and R.B. Sim. 2001. Complement C4bC2 complex formation: an investigation by surface plasmon resonance. *Biochim Biophys Acta.* 1544:96-112.

Lamballe, F., P. Tapley, and M. Barbacid. 1993. trkC encodes multiple neurotrophin-3 receptors with distinct biological properties and substrate specificities. *Embo J.* 12:3083-94.

Lamm, O. 1929. *Ark Mat Astron Fys.* 21B:2.

Lauffenburger, D.A., and J.J. Linderman. 1993. Receptors, Models for Binding, Trafficking and Signaling. Oxford University Press. Chapters 1-4 pp.

Layer, P.G., and E.M. Shooter. 1983. Binding and degradation of nerve growth factor by PC12 pheochromocytoma cells. *J Biol Chem.* 258:3012-8.

Lee, K.F., E. Li, L.J. Huber, S.C. Landis, A.H. Sharpe, M.V. Chao, and R. Jaenisch. 1992. Targeted mutation of the gene encoding the low affinity NGF receptor p75 leads to deficits in the peripheral sensory nervous system. *Cell.* 69:737-49.

Limbird, L. 1986. A Short Course on Theory and Methods. Martinus Nijhoff, Boston.

Linderman, J.J., and D.A. Lauffenburger. 1988. Analysis of intracellular receptor/ligand sorting in endosomes. *J Theor Biol.* 132:203-45.

Linstrom-Lang, K., and J. Schellman. 1959. *Enzymes.* 1:443.

Lipshultz, C., Y. Li, and S. Smith-Gill. 2000. *Methods.* 20:310-318.

Luo, J., J. Zhou, W. Zou, and P. Shen. 2001. Antibody-antigen interactions measured by surface plasmon resonance: global fitting of numerical integration algorithms. *J Biochem (Tokyo).* 130:553-9.

Mahadeo, D., L. Kaplan, M.V. Chao, and B.L. Hempstead. 1994. High affinity nerve growth factor binding displays a faster rate of association than p140trk binding. Implications for multi-subunit polypeptide receptors. *J Biol Chem.* 269:6884-91.

Malmquist, M., and R. Karlsson. 1997. *Curr Opin Chem Biol.* 1:378.

Martin-Zanca, D., R. Oskam, G. Mitra, T. Copeland, and M. Barbacid. 1989. Molecular and biochemical characterization of the human trk proto-oncogene. *Mol Cell Biol.* 9:24-33.

McDonald, N.Q., R. Lapatto, J. Murray-Rust, J. Gunning, A. Wlodawer, and T.L. Blundell. 1991. New protein fold revealed by a 2.3-A resolution crystal structure of nerve growth factor. *Nature.* 354:411-4.

McDonnell, J.M. 2001. Surface plasmon resonance: towards an understanding of the mechanisms of biological molecular recognition. *Curr Opin Chem Biol.* 5:572-7.

Meakin, S.O., and E.M. Shooter. 1991. Molecular investigations on the high-affinity nerve growth factor receptor. *Neuron.* 6:153-63.

Meakin, S.O., and E.M. Shooter. 1992. The nerve growth factor family of receptors. *Trends Neurosci.* 15:323-31.

Meakin, S.O., U. Suter, C.C. Drinkwater, A.A. Welcher, and E.M. Shooter. 1992. The rat trk protooncogene product exhibits properties characteristic of the slow nerve growth factor receptor. *Proc Natl Acad Sci U S A.* 89:2374-8.

Middlemas, D.S., R.A. Lindberg, and T. Hunter. 1991. trkB, a neural receptor protein-tyrosine kinase: evidence for a full-length and two truncated receptors. *Mol Cell Biol.* 11:143-53.

Myszka, D.G. 1999. Improving biosensor analysis. *J Mol Recognit.* 12:279-84.

Myszka, D.G., R.W. Sweet, P. Hensley, M. Brigham-Burke, P.D. Kwong, W.A. Hendrickson, R. Wyatt, J. Sodroski, and M.L. Doyle. 2000. Energetics of the HIV gp120-CD4 binding reaction. *Proc Natl Acad Sci U S A.* 97:9026-31.

Neet, K.E., and R.B. Campenot. 2001. Receptor binding, internalization, and retrograde transport of neurotrophic factors. *Cell Mol Life Sci.* 58:1021-35.

Nicholls, A., K.A. Sharp, and B. Honig. 1991. Protein folding and association: insights from the interfacial and thermodynamic properties of hydrocarbons. *Proteins.* 11:281-96.

Niederhauser, O., M. Mangold, R. Schubenel, E.A. Kusznir, D. Schmidt, and C. Hertel. 2000. NGF ligand alters NGF signaling via p75(NTR) and trkA. *J Neurosci Res.* 61:263-72.

Ninkina, N., M. Grashchuck, V.L. Buchman, and A.M. Davies. 1997. TrkB variants with deletions in the leucine-rich motifs of the extracellular domain. *J Biol Chem.* 272:13019-25.

Novotny, J., R.E. Bruccoleri, and F.A. Saul. 1989. On the attribution of binding energy in antigen-antibody complexes McPC 603, D1.3, and HyHEL-5. *Biochemistry.* 28:4735-49.

Oddie, G.W., L.C. Gruen, G.A. Odgers, L.G. King, and A.A. Kortt. 1997. Identification and minimization of nonideal binding effects in BIAcore analysis: ferritin/anti-ferritin Fab' interaction as a model system. *Anal Biochem.* 244:301-11.

Orengo, C.A., A.E. Todd, and J.M. Thornton. 1999. From protein structure to function. *Curr Opin Struct Biol.* 9:374-82.

Panayotatos, N., E. Radziejewska, A. Acheson, R. Somogyi, A. Thadani, W.A. Hendrickson, and N.Q. McDonald. 1995. Localization of functional receptor epitopes on the structure of ciliary neurotrophic factor indicates a conserved, function-related epitope topography among helical cytokines. *J Biol Chem.* 270:14007-14.

Perez, P., P.M. Coll, B.L. Hempstead, D. Martin-Zanca, and M.V. Chao. 1995. NGF binding to the trk tyrosine kinase receptor requires the extracellular immunoglobulin-like domains. *Mol Cell Neurosci.* 6:97-105.

Peters, J.W., M.H. Stowell, and D.C. Rees. 1996. A leucine-rich repeat variant with a novel repetitive protein structural motif. *Nat Struct Biol.* 3:991-4.

Qiao, Z.S., Z.Y. Guo, and Y.M. Feng. 2001. Putative disulfide-forming pathway of porcine insulin precursor during its refolding in vitro. *Biochemistry.* 40:2662-8.

Rabizadeh, S., J. Oh, L.T. Zhong, J. Yang, C.M. Bitler, L.L. Butcher, and D.E. Bredesen. 1993. Induction of apoptosis by the low-affinity NGF receptor. *Science.* 261:345-8.

Radeke, M.J., T.P. Misko, C. Hsu, L.A. Herzenberg, and E.M. Shooter. 1987. Gene transfer and molecular cloning of the rat nerve growth factor receptor. *Nature.* 325:593-7.

Raffioni, S., R.A. Bradshaw, and S.E. Buxser. 1993. The receptors for nerve growth factor and other neurotrophins. *Annu Rev Biochem.* 62:823-50.

Roback, J., H. Palfrey, and B. Wainer. 1992. *Comments Dev Biol.* 1:311-.

Robertson, A.G., M.J. Banfield, S.J. Allen, J.A. Dando, G.G. Mason, S.J. Tyler, G.S. Bennett, S.D. Brain, A.R. Clarke, R.L. Naylor, G.K. Wilcock, R.L. Brady, and D. Dawbarn. 2001. Identification and structure of the nerve growth factor binding site on TrkA. *Biochem Biophys Res Commun.* 282:131-41.

Robinson, R.C., C. Radziejewski, D.I. Stuart, and E.Y. Jones. 1995. Structure of the brain-derived neurotrophic factor/neurotrophin 3 heterodimer. *Biochemistry*. 34:4139-46.

Rodriguez-Tebar, A., and Y.A. Barde. 1988. Binding characteristics of brain-derived neurotrophic factor to its receptors on neurons from the chick embryo. *J Neurosci*. 8:3337-42.

Rodriguez-Tebar, A., G. Dechant, R. Gotz, and Y.A. Barde. 1992. Binding of neurotrophin-3 to its neuronal receptors and interactions with nerve growth factor and brain-derived neurotrophic factor. *Embo J*. 11:917-22.

Ross, A.H., M.C. Daou, C.A. McKinnon, P.J. Condon, M.B. Lachyankar, R.M. Stephens, D.R. Kaplan, and D.E. Wolf. 1996. The neurotrophin receptor, gp75, forms a complex with the receptor tyrosine kinase TrkA. *J Cell Biol*. 132:945-53.

Ross, G.M., I.L. Shamovsky, G. Lawrance, M. Solc, S.M. Dostaler, D.F. Weaver, and R.J. Riopelle. 1998. Reciprocal modulation of TrkA and p75NTR affinity states is mediated by direct receptor interactions. *Eur J Neurosci*. 10:890-8.

Rothberg, J.M., J.R. Jacobs, C.S. Goodman, and S. Artavanis-Tsakonas. 1990. slit: an extracellular protein necessary for development of midline glia and commissural axon pathways contains both EGF and LRR domains. *Genes Dev*. 4:2169-87.

Ruffolo Jr, R., E. Rosing, and J. Waddell. 1979. Receptor interactions of imidazolines. I. Affinity and efficacy for alpha adrenergic receptors in rat aorta. *J Pharmacol Exp Ther*. 209:429-436.

Ruffolo Jr, R., and J. Waddell. 1983. Aromatic and benzylic hydroxyl substitution of imiadzolines and phenylethamines: differences in activity with alpha-1 and alpha-2 receptors. *J Pharmacol Exp Ther*. 224:559-566.

Ryden, M., and C.F. Ibanez. 1997. A second determinant of binding to the p75 neurotrophin receptor revealed by alanine-scanning mutagenesis of a conserved loop in nerve growth factor. *J Biol Chem*. 272:33085-91.

Saragovi, H., and K. Burgess. 1999. *Exp Opin Ther Patents*. 9:737.

Saragovi, H.U., and M.C. Zaccaro. 2002. Small molecule peptidomimetic ligands of neurotrophin receptors, identifying binding sites, activation sites and regulatory sites. *Curr Pharm Des*. 8:2201-16.

Schechter, A.L., and M.A. Bothwell. 1981. Nerve growth factor receptors on PC12 cells: evidence for two receptor classes with differing cytoskeletal association. *Cell*. 24:867-74.

Schneider, R., and M. Schweiger. 1991. The yeast DNA repair proteins RAD1 and RAD7 share similar putative functional domains. *FEBS Lett*. 283:203-6.

Schuck, P. 1997a. Reliable determination of binding affinity and kinetics using surface plasmon resonance biosensors. *Curr Opin Biotechnol*. 8:498-502.

Schuck, P. 1997b. Use of surface plasmon resonance to probe the equilibrium and dynamic aspects of interactions between biological macromolecules. *Annu Rev Biophys Biomol Struct*. 26:541-66.

Schuck, P., and A.P. Minton. 1996. Analysis of mass transport-limited binding kinetics in evanescent wave biosensors. *Anal Biochem*. 240:262-72.

Shamovsky, I.L., G.M. Ross, R.J. Riopelle, and D.F. Weaver. 1999. The interaction of neurotrophins with the p75NTR common neurotrophin receptor: a comprehensive molecular modeling study. *Protein Sci*. 8:2223-33.

Soppet, D., E. Escandon, J. Maragos, D.S. Middlemas, S.W. Reid, J. Blair, L.E. Burton, B.R. Stanton, D.R. Kaplan, T. Hunter, and et al. 1991. The neurotrophic factors brain-derived neurotrophic factor and neurotrophin-3 are ligands for the trkB tyrosine kinase receptor. *Cell.* 65:895-903.

Stevens, R.C. 2000. Design of high-throughput methods of protein production for structural biology. *Structure Fold Des.* 8:R177-85.

Sutter, A., R.J. Riopelle, R.M. Harris-Warrick, and E.M. Shooter. 1979. Nerve growth factor receptors. Characterization of two distinct classes of binding sites on chick embryo sensory ganglia cells. *J Biol Chem.* 254:5972-82.

Tatsuno, I., M. Homma, K. Oosawa, and I. Kawagishi. 1996. Signaling by the Escherichia coli aspartate chemoreceptor Tar with a single cytoplasmic domain per dimer. *Science.* 274:423-5.

Thoenen, H. 1991. The changing scene of neurotrophic factors. *Trends Neurosci.* 14:165-70.

Thoenen, H. 1995. Neurotrophins and neuronal plasticity. *Science.* 270:593-8.

Tsoulfas, P., D. Soppet, E. Escandon, L. Tessarollo, J.L. Mendoza-Ramirez, A. Rosenthal, K. Nikolics, and L.F. Parada. 1993. The rat trkC locus encodes multiple neurogenic receptors that exhibit differential response to neurotrophin-3 in PC12 cells. *Neuron.* 10:975-90.

Ultsch, M.H., C. Wiesmann, L.C. Simmons, J. Henrich, M. Yang, D. Reilly, S.H. Bass, and A.M. de Vos. 1999. Crystal structures of the neurotrophin-binding domain of TrkA, TrkB and TrkC. *J Mol Biol.* 290:149-59.

Urfer, R., P. Tsoulfas, L. O'Connell, J.A. Hongo, W. Zhao, and L.G. Presta. 1998. High resolution mapping of the binding site of TrkA for nerve growth factor and TrkC for neurotrophin-3 on the second immunoglobulin-like domain of the Trk receptors. *J Biol Chem.* 273:5829-40.

Urfer, R., P. Tsoulfas, L. O'Connell, D.L. Shelton, L.F. Parada, and L.G. Presta. 1995. An immunoglobulin-like domain determines the specificity of neurotrophin receptors. *Embo J.* 14:2795-805.

Urfer, R., P. Tsoulfas, D. Soppet, E. Escandon, L.F. Parada, and L.G. Presta. 1994. The binding epitopes of neurotrophin-3 to its receptors trkC and gp75 and the design of a multifunctional human neurotrophin. *Embo J.* 13:5896-909.

Valenzuela, D.M., P.C. Maisonpierre, D.J. Glass, E. Rojas, L. Nunez, Y. Kong, D.R. Gies, T.N. Stitt, N.Y. Ip, and G.D. Yancopoulos. 1993. Alternative forms of rat TrkC with different functional capabilities. *Neuron.* 10:963-74.

Van Regenmortel, M.H. 2001. Analysing structure-function relationships with biosensors. *Cell Mol Life Sci.* 58:794-800.

Watson, F.L., M.A. Porcionatto, A. Bhattacharyya, C.D. Stiles, and R.A. Segal. 1999. TrkA glycosylation regulates receptor localization and activity. *J Neurobiol.* 39:323-36.

Weskamp, G., and L.F. Reichardt. 1991. Evidence that biological activity of NGF is mediated through a novel subclass of high affinity receptors. *Neuron.* 6:649-63.

Wiesmann, C., Y. Muller, and A. de Vos. 2000. Ligand-binding sites in Ig-like domains of receptor tyrosine kinases. *J Mol Med.* 78:247-260.

Wiesmann, C., M.H. Ultsch, S.H. Bass, and A.M. de Vos. 1999. Crystal structure of nerve growth factor in complex with the ligand-binding domain of the TrkA receptor. *Nature*. 401:184-8.

Williams D.A., T.L. Lemke, 2002, Foye's Principles of Medicinal Chemistry, Fifth Edition, Pub. Lippincott Williams & Wilkins, Chapters 1-6.

Williams, L.R., S. Varon, G.M. Peterson, K. Wictorin, W. Fischer, A. Bjorklund, and F.H. Gage. 1986. Continuous infusion of nerve growth factor prevents basal forebrain neuronal death after fimbria fornix transection. *Proc Natl Acad Sci U S A*. 83:9231-5.

Wilson, I., and R. Stanfield. 1993. *Curr Opin Struct Biol*. 3:113.

Windisch, J.M., B. Auer, R. Marksteiner, M.E. Lang, and R. Schneider. 1995b. Specific neurotrophin binding to leucine-rich motif peptides of TrkA and TrkB. *FEBS Lett*. 374:125-9.

Windisch, J.M., R. Marksteiner, M.E. Lang, B. Auer, and R. Schneider. 1995c. Brain-derived neurotrophic factor, neurotrophin-3, and neurotrophin-4 bind to a single leucine-rich motif of TrkB. *Biochemistry*. 34:11256-63.

Windisch, J.M., R. Marksteiner, and R. Schneider. 1995a. Nerve growth factor binding site on TrkA mapped to a single 24-amino acid leucine-rich motif. *J Biol Chem*. 270:28133-8.

Wirtz, P., and B. Steipe. 1999. Intrabody construction and expression III: engineering hyperstable V(H) domains. *Protein Sci*. 8:2245-50.

Wolf, D.E., C.A. McKinnon, M.C. Daou, R.M. Stephens, D.R. Kaplan, and A.H. Ross. 1995. Interaction with TrkA immobilizes gp75 in the high affinity nerve growth factor receptor complex. *J Biol Chem*. 270:2133-8.

Wolf, D.E., C. McKinnon-Thompson, M.C. Daou, R.M. Stephens, D.R. Kaplan, and A.H. Ross. 1998. Mobility of TrkA is regulated by phosphorylation and interactions with the low-affinity NGF receptor. *Biochemistry*. 37:3178-86.

Woo, S.B., and K.E. Neet. 1996. Characterization of histidine residues essential for receptor binding and activity of nerve growth factor. *J Biol Chem*. 271:24433-41.

Woo, S.B., C. Whalen, and K.E. Neet. 1998. Characterization of the recombinant extracellular domain of the neurotrophin receptor TrkA and its interaction with nerve growth factor (NGF). *Protein Sci*. 7:1006-16.

Woodruff, N.R., and K.E. Neet. 1986. Inhibition of beta nerve growth factor binding to PC12 cells by alpha nerve growth factor and gamma nerve growth factor. *Biochemistry*. 25:7967-74.

Woodward, C. 1993. Is the slow exchange core the protein folding core? *Trends Biochem Sci*. 18:359-60.

Woodward, C., I. Simon, and E. Tuchsen. 1982. Hydrogen exchange and the dynamic structure of proteins. *Mol Cell Biochem*. 48:135-60.

Xu. 1997. *Nature*. 385:741.

Yan, H., and M.V. Chao. 1991. Disruption of cysteine-rich repeats of the p75 nerve growth factor receptor leads to loss of ligand binding. *J Biol Chem*. 266:12099-104.

Yano, H., and M.V. Chao. 2000. Neurotrophin receptor structure and interactions. *Pharm Acta Helv*. 74:253-60.

Yennawar, N. 1995. *J Am Chem Soc*. 117:577.

Yuen, E.C., and W.C. Mobley. 1996. Therapeutic potential of neurotrophic factors for neurological disorders. *Ann Neurol*. 40:346-54.

Zaccaro, M.C., L. Ivanisevic, P. Perez, S.O. Meakin, and H.U. Saragovi. 2001. p75 Co-receptors regulate ligand-dependent and ligand-independent Trk receptor activation, in part by altering Trk docking subdomains. *J Biol Chem.* 276:31023-9.

Zavodszky, P., J. Kardos, Svingor, and G.A. Petsko. 1998. Adjustment of conformational flexibility is a key event in the thermal adaptation of proteins. *Proc Natl Acad Sci U S A.* 95:7406-11.

Zeder-Lutz, G., R. Wenger, M.H. Van Regenmortel, and D. Altschuh. 1993. Interaction of cyclosporin A with an Fab fragment or cyclophilin. Affinity measurements and time-dependent changes in binding. *FEBS Lett.* 326:153-7.

Appendix I

Sequences of the Trk Receptors and Neurotrophins

A number of recombinant TrkA, TrkB and TrkC proteins were engineered for expression in bacteria and yeast. Listed below are the amino acid sequences for all mammalian Trk species expressed and for the neurotrophins. All Trk and neurotrophin sequences are from the Swiss Protein Data Bank (SwissProt).

NGF (Murine)

```
        10         20         30         40         50         60
         |          |          |          |          |          |
MSMLFYTLIT AFLIGVQAEP YTDSNVPEGD SVPEAHWTKL QHSLDTALRR ARSAPTAPIA

        70         80         90        100        110        120
         |          |          |          |          |          |
ARVTGQTRNI TVDPRLFKKR RLHSPRVLFS TQPPPTSSDT LDLDFQAHGT IPFNRTHRSK

       130        140        150        160        170        180
         |          |          |          |          |          |
RSSTHPVFHM GEFSVCDSVS VWVGDKTTAT DIKGKEVTVL AEVNINNSVF RQYFFETKCR

       190        200        210        220        230        240
         |          |          |          |          |          |
ASNPVESGCR GIDSKHWNSY CTTTHTFVKA LTTDEKQAAW RFIRIDTACV CVLSRKATRR
```

BDNF

```
        10         20         30         40         50         60
         |          |          |          |          |          |
MTILFLTMVI SYFGCMKAAP MKEANIRGQG GLAYPGVRTH GTLESVNGPK AGSRGLTSLA

        70         80         90        100        110        120
         |          |          |          |          |          |
DTFEHVIEEL LDEDQKVRPN EENNKDADLY TSRVMLSSQV PLEPPLLFLL EEYKNYLDAA

       130        140        150        160        170        180
         |          |          |          |          |          |
NMSMRVRRHS DPARRGELSV CDSISEWVTA ADKKTAVDMS GGTVTVLEKV PVSKGQLKQY

       190        200        210        220        230        240
         |          |          |          |          |          |
FYETKCNPMG YTKEGCRGID KRHWNSQCRT TQSYVRALTM DSKKRIGWRF IRIDTSCVCT
```

```
    247
     |
LTIKRGR
```

NT-3

```
         10          20          30          40          50          60
          |           |           |           |           |           |
MSILFYVIFL AYLRGIQGNN MDQRSLPEDS LNSLIIKLIQ ADILKNKLSK QMVDVKENYQ

         70          80          90         100         110         120
          |           |           |           |           |           |
STLPKAEAPR EPERGGPAKS AFQPVIAMDT ELLRQQRRYN SPRVLLSDST PLEPPPLYLM

        130         140         150         160         170         180
          |           |           |           |           |           |
EDYVGSPVVA NRTSRRKRYA EHKSHRGEYS VCDSESLWVT DKSSAIDIRG HQVTVLGEIK

        190         200         210         220         230         240
          |           |           |           |           |           |
TGNSPVKQYF YETRCKEARP VKNGCRGIDD KHWNSQCKTS QTYVRALTSE NNKLVGWRWI

        250     257
          |       |
RIDTSCVCAL SRKIGRT
```

TrkA (Rattus norvegicus)

```
          10          20          30          40          50          60
           |           |           |           |           |           |
MLRGQRHGQL GWHRPAAGLG GLVTSLMLAC ACAASCRETC CPVGPSGLRC TRAGTLNTLR

          70          80          90         100         110         120
           |           |           |           |           |           |
GLRGAGNLTE LYVENQRDLQ RLEFEDLQGL GELRSLTIVK SGLRFVAPDA FHFTPRLSHL

         130         140         150         160         170         180
           |           |           |           |           |           |
NLSSNALESL SWKTVQGLSL QDLTLSGNPL HCSCALLWLQ RWEQEDLCGV YTQKLQGSGS

         190         200         210         220         230         240
           |           |           |           |           |           |
GDQFLPLGHN NSCGVPSVKI QMPNDSVEVG DDVFLQCQVE GQALQQADWI LTELEGTATM

         250         260         270         280         290         300
           |           |           |           |           |           |
KKSGDLPSLG LTLVNVTSDL NKKNVTCWAE NDVGRAEVSV QVSVSFPASV HLGKAVEQHH

         310         320         330         340         350         360
           |           |           |           |           |           |
WCIPFSVDGQ PAPSLRWFFN GSVLNETSFI FTQFLESALT NETMRHGCLR LNQPTHVNNG

         370         380         390         400         410         420
           |           |           |           |           |           |
```

```
NYTLLAANPY GQAAASIMAA FMDNPFEFNP EDPIPVSFSP VDTNSTSRDP VEKKDETPFG

        430         440         450         460         470         480
         |           |           |           |           |           |
VSVAVGLAVS AALFLSALLL VLNKCGQRSK FGINRPAVLA PEDGLAMSLH FMTLGGSSLS

        490         500         510         520         530         540
         |           |           |           |           |           |
PTEGKGSGLQ GHIMENPQYF SDTCVHHIKR QDIILKWELG EGAFGKVFLA ECYNLLNDQD

        550         560         570         580         590         600
         |           |           |           |           |           |
KMLVAVKALK ETSENARQDF HREAELLTML QHQHIVRFFG VCTEGGPLLM VFEYMRHGDL

        610         620         630         640         650         660
         |           |           |           |           |           |
NRFLRSHGPD AKLLAGGEDV APGPLGLGQL LAVASQVAAG MVYLASLHFV HRDLATRNCL

        670         680         690         700         710         720
         |           |           |           |           |           |
VGQGLVVKIG DFGMSRDIYS TDYYRVGGRT MLPIRWMPPE SILYRKFSTE SDVWSFGVVL

        730         740         750         760         770         780
         |           |           |           |           |           |
WEIFTYGKQP WYQLSNTEAI ECITQGRELE RPRACPPDVY AIMRGCWQRE PQQRLSMKDV

        790       799
         |         |
HARLQALAQA PPSYLDVLG
```

TrkA (Human)

```
         10          20          30          40          50          60
          |           |           |           |           |           |
MLRGGRRGQL GWHSWAAGPG SLLAWLILAS AGAAPCPDAC CPHGSSGLRC TRDGALDSLH

         70          80          90         100         110         120
          |           |           |           |           |           |
HLPGAENLTE LYIENQQHLQ HLELRDLRGL GELRNLTIVK SGLRFVAPDA FHFTPRLSRL

        130         140         150         160         170         180
          |           |           |           |           |           |
NLSFNALESL SWKTVQGLSL QELVLSGNPL HCSCALRWLQ RWEEEGLGGV PEQKLQCHGQ

        190         200         210         220         230         240
          |           |           |           |           |           |
GPLAHMPNAS CGVPTLKVQV PNASVDVGDD VLLRCQVEGR GLEQAGWILT ELEQSATVMK

        250         260         270         280         290         300
          |           |           |           |           |           |
SGGLPSLGLT LANVTSDLNR KNLTCWAEND VGRAEVSVQV NVSFPASVQL HTAVEMHHWC

        310         320         330         340         350         360
          |           |           |           |           |           |
IPFSVDGQPA PSLRWLFNGS VLNETSFIFT EFLEPAANET VRHGCLRLNQ PTHVNNGNYT
```

```
       370         380         390         400         410         420
        |           |           |           |           |           |
LLAANPFGQA SASIMAAFMD NPFEFNPEDP IPVSFSPVDT NSTSGDPVEK KDETPFGVSV

       430         440         450         460         470         480
        |           |           |           |           |           |
AVGLAVFACL FLSTLLLVLN KCGRRNKFGI NRPAVLAPED GLAMSLHFMT LGGSSLSPTE


       490         500         510         520         530         540
        |           |           |           |           |           |
GKGSGLQGHI IENPQYFSDA CVHHIKRRDI VLKWELGEGA FGKVFLAECH NLLPEQDKML

       550         560         570         580         590         600
        |           |           |           |           |           |
VAVKALKEAS ESARQDFQRE AELLTMLQHQ HIVRFFGVCT EGRPLLMVFE YMRHGDLNRF

       610         620         630         640         650         660
        |           |           |           |           |           |
LRSHGPDAKL LAGGEDVAPG PLGLGQLLAV ASQVAAGMVY LAGLHFVHRD LATRNCLVGQ

       670         680         690         700         710         720
        |           |           |           |           |           |
GLVVKIGDFG MSRDIYSTDY YRVGGRTMLP IRWMPPESIL YRKFTTESDV WSFGVVLWEI

       730         740         750         760         770         780
        |           |           |           |           |           |
FTYGKQPWYQ LSNTEAIDCI TQGRELERPR ACPPEVYAIM RGCWQREPQQ RHSIKDVHAR

       790    796
        |      |
LQALAQAPPV YLDVLG
```

TrkB (Rattus norvegicus)

```
         10          20          30          40          50          60
          |           |           |           |           |           |
MSPWPRWHGP AMARLWGLCL LVLGFWRASL ACPMSCKCST TRIWCTEPSP GIVAFPRLEP

         70          80          90         100         110         120
          |           |           |           |           |           |
NSIDPENITE ILIANQKRLE IINEDDVEAY VGLKNLTIVD SGLKFVAYKA FLKNGNLRHI

        130         140         150         160         170         180
          |           |           |           |           |           |
NFTRNKLTSL SRRHFRHLDL SDLILTGNPF TCSCDIMWLK TLQETKSSPD TQDLYCLNES

        190         200         210         220         230         240
          |           |           |           |           |           |
SKNTPLANLQ IPNCGLPSAR LAAPNLTVEE GKSVTISCSV GGDPLPTLYW DVGNLVSKHM

        250         260         270         280         290         300
          |           |           |           |           |           |
NETSHTQGSL RITNISSDDS GKQISCVAEN LVGEDQDSVN LTVHFAPTIT FLESPTSDHH
```

```
       310         320         330         340         350         360
        |           |           |           |           |           |
WCIPFTVRGN PKPALQWFYN GAILNESKYI CTKIHVTNHT EYHGCLQLDN PTHMNNGDYT

       370         380         390         400         410         420
        |           |           |           |           |           |
LMAKNEYGKD ERQISAHFMG RPGVDYETNP NYPEVLYEDW TTPTDIGDTT NKSNEIPSTD

       430         440         450         460         470         480
        |           |           |           |           |           |
VADQTNREHL SVYAVVVIAS VVGFCLLVML LLLKLARHSK FGMKGPASVI SNDDDSASPL


       490         500         510         520         530         540
        |           |           |           |           |           |
HHISNGSNTP SSSEGGPDAV IIGMTKIPVI ENPQYFGITN SQLKPDTFVQ HIKRHNIVLK

       550         560         570         580         590         600
        |           |           |           |           |           |
RELGEGAFGK VFLAECYNLC PEQDKILVAV KTLKDASDNA RKDFHREAEL LTNLQHEHIV

       610         620         630         640         650         660
        |           |           |           |           |           |
KFYGVCVEGD PLIMVFEYMK HGDLNKFLRA HGPDAVLMAE GNPPTELTQS QMLHIAQQIA

       670         680         690         700         710         720
        |           |           |           |           |           |
AGMVYLASQH FVHRDLATRN CLVGENLLVK IGDFGMSRDV YSTDYYRVGG HTMLPIRWMP

       730         740         750         760         770         780
        |           |           |           |           |           |
PESIMYRKFT TESDVWSLGV VLWEIFTYGK QPWYQLSNNE VIECITQGRV LQRPRTCPQE

       790         800         810         820
        |           |           |           |
VYELMLGCWQ REPHTRKNIK NIHTLLQNLA KASPVYLDIL G
```

TrkB (Mouse)

```
        10          20          30          40          50          60
         |           |           |           |           |           |
MSPWLKWHGP AMARLWGLCL LVLGFWRASL ACPTSCKCSS ARIWCTEPSP GIVAFPRLEP

        70          80          90         100         110         120
         |           |           |           |           |           |
NSVDPENITE ILIANQKRLE IINEDDVEAY VGLRNLTIVD SGLKFVAYKA FLKNSNLRHI

       130         140         150         160         170         180
         |           |           |           |           |           |
NFTRNKLTSL SRRHFRHLDL SDLILTGNPF TCSCDIMWLK TLQETKSSPD TQDLYCLNES

       190         200         210         220         230         240
         |           |           |           |           |           |
SKNMPLANLQ IPNCGLPSAR LAAPNLTVEE GKSVTLSCSV GGDPLPTLYW DVGNLVSKHM
```

```
       250         260         270         280         290         300
        |           |           |           |           |           |
NETSHTQGSL RITNISSDDS GKQISCVAEN LVGEDQDSVN LTVHFAPTIT FLESPTSDHH

       310         320         330         340         350         360
        |           |           |           |           |           |
WCIPFTVRGN PKPALQWFYN GAILNESKYI CTKIHVTNHT EYHGCLQLDN PTHMNNGDYT

       370         380         390         400         410         420
        |           |           |           |           |           |
LMAKNEYGKD ERQISAHFMG RPGVDYETNP NYPEVLYEDW TTPTDIGDTT NKSNEIPSTD

       430         440         450         460         470         480
        |           |           |           |           |           |
VADQSNREHL SVYAVVVIAS VVGFCLLVML LLLKLARHSK FGMKGPASVI SNDDDSASPL

490         500         510         520         530         540
|           |           |           |           |           |
HHISNGSNTP SSSEGGPDAV IIGMTKIPVI ENPQYFGITN SQLKPDTFVQ HIKRHNIVLK

550         560         570         580         590         600
|           |           |           |           |           |
RELGEGAFGK VFLAECYNLC PEQDKILVAV KTLKDASDNA RKDFHREAEL LTNLQHEHIV

610         620         630         640         650         660
|           |           |           |           |           |
KFYGVCVEGD PLIMVFEYMK HGDLNKFLRA HGPDAVLMAE GNPPTELTQS QMLHIAQQIA

670         680         690         700         710         720
|           |           |           |           |           |
AGMVYLASQH FVHRDLATRN CLVGENLLVK IGDFGMSRDV YSTDYYRVGG HTMLPIRWMP

730         740         750         760         770         780
|           |           |           |           |           |
PESIMYRKFT TESDVWSLGV VLWEIFTYGK QPWYQLSNNE VIECITQGRV LQRPRTCPQE

790         800         810         820
|           |           |           |
VYELMLGCWQ REPHTRKNIK SIHTLLQNLA KASPVYLDIL G
```

TrkB (Human)

```
         10          20          30          40          50          60
          |           |           |           |           |           |
MSSWIRWHGP AMARLWGFCW LVVGFWRAAF ACPTSCKCSA SRIWCSDPSP GIVAFPRLEP

         70          80          90         100         110         120
          |           |           |           |           |           |
NSVDPENITE IFIANQKRLE IINEDDVEAY VGLRNLTIVD SGLKFVAHKA FLKNSNLQHI

       130         140         150         160         170         180
        |           |           |           |           |           |
NFTRNKLTSL SRKHFRHLDL SELILVGNPF TCSCDIMWIK TLQEAKSSPD TQDLYCLNES

       190         200         210         220         230         240
        |           |           |           |           |           |
```

```
SKNIPLANLQ IPNCGLPSAN LAAPNLTVEE GKSITLSCSV AGDPVPNMYW DVGNLVSKHM

       250        260        270        280        290        300
        |          |          |          |          |          |
NETSHTQGSL RITNISSDDS GKQISCVAEN LVGEDQDSVN LTVHFAPTIT FLESPTSDHH

       310        320        330        340        350        360
        |          |          |          |          |          |
WCIPFTVKGN PKPALQWFYN GAILNESKYI CTKIHVTNHT EYHGCLQLDN PTHMNNGDYT

       370        380        390        400        410        420
        |          |          |          |          |          |
LIAKNEYGKD EKQISAHFMG WPGIDDGANP NYPDVIYEDY GTAANDIGDT TNRSNEIPST

       430        440        450        460        470        480
        |          |          |          |          |          |
DVTDKTGREH LSVYAVVVIA SVVGFCLLVM LFLLKLARHS KFGMKGPASV ISNDDDSASP
       490        500        510        520        530        540
        |          |          |          |          |          |
LHHISNGSNT PSSSEGGPDA VIIGMTKIPV IENPQYFGIT NSQLKPDTFV QHIKRHNIVL

       550        560        570        580        590        600
        |          |          |          |          |          |
KRELGEGAFG KVFLAECYNL CPEQDKILVA VKTLKDASDN ARKDFHREAE LLTNLQHEHI

       610        620        630        640        650        660
        |          |          |          |          |          |
VKFYGVCVEG DPLIMVFEYM KHGDLNKFLR AHGPDAVLMA EGNPPTELTQ SQMLHIAQQI

       670        680        690        700        710        720
        |          |          |          |          |          |
AAGMVYLASQ HFVHRDLATR NCLVGENLLV KIGDFGMSRD VYSTDYYRVG GHTMLPIRWM

       730        740        750        760        770        780
PPESIMYRKF TTESDVWSLG VVLWEIFTYG KQPWYQLSNN EVIECITQGR VLQRPRTCPQ

       790        800        810        820
        |          |          |          |
EVYELMLGCW QREPHMRKNI KGIHTLLQNL AKASPVYLDI LG
```

TrkC (Rattus norvegicus)

```
         10         20         30         40         50         60
          |          |          |          |          |          |
MDVSLCPAKC SFWRIFLLGS VWLDYVGSVL ACPANCVCSK TEINCRRPDD GNLFPLLEGQ

         70         80         90        100        110        120
          |          |          |          |          |          |
DSGNSNGNAS INITDISRNI TSIHIENWRG LHTLNAVDME LYTGLQKLTI KNSGLRNIQP

        130        140        150        160        170        180
          |          |          |          |          |          |
RAFAKNPHLR YINLSSNRLT TLSWQLFQTL SLRELRLEQN FFNCSCDIRW MQLWQEQGEA
```

```
       190         200         210         220         230         240
        |           |           |           |           |           |
RLDSQSLYCI SADGSQLPLF RMNISQCDLP EISVSHVNLT VREGDNAVIT CNGSGSPLPD

       250         260         270         280         290         300
        |           |           |           |           |           |
VDWIVTGLQS INTHQTNLNW TNVHAINLTL VNVTSEDNGF TLTCIAENVV GMSNASVALT

       310         320         330         340         350         360
        |           |           |           |           |           |
VYYPPRVVSL VEPEVRLEHC IEFVVRGNPT PTLHWLYNGQ PLRESKIIHM DYYQEGEVSE

       370         380         390         400         410         420
        |           |           |           |           |           |
GCLLFNKPTH YNNGNYTLIA KNALGTANQT INGHFLKEPF PESTDFFDFE SDASPTPPIT

       430         440         450         460         470         480
        |           |           |           |           |           |
VTHKPEEDTF GVSIAVGLAA FACVLLVVLF IMINKYGRRS KFGMKGPVAV ISGEEDSASP
       490         500         510         520         530         540
        |           |           |           |           |           |
LHHINHGITT PSSLDAGPDT VVIGMTRIPV IENPQYFRQG HNCHKPDTYV QHIKRRDIVL

       550         560         570         580         590         600
        |           |           |           |           |           |
KRELGEGAFG KVFLAECYNL SPTKDKMLVA VKALKDPTLA ARKDFQREAE LLTNLQHEHI

       610         620         630         640         650         660
        |           |           |           |           |           |
VKFYGVCGDG DPLIMVFEYM KHGDLNKFLR AHGPDAMILV DGQPRQAKGE LGLSQMLHIA

       670         680         690         700         710         720
        |           |           |           |           |           |
SQIASGMVYL ASQHFVHRDL ATRNCLVGAN LLVKIGDFGM SRDVYSTDYY REGPYQKGPF

       730         740         750         760         770         780
        |           |           |           |           |           |
SVSWQQQRLA ASAASTLFNP SGNDFCIWCE VGGHTMLPIR WMPPESIMYR KFTTESDVWS

       790         800         810         820         830         840
        |           |           |           |           |           |
FGVILWEIFT YGKQPWFQLS NTEVIECITQ GRVLERPRVC PKEVYDVMLG CWQREPQQRL


       850         860
        |           |
NIKEIYKILH ALGKATPIYL DILG
```

TrkC (Human)

```
        10          20          30          40          50          60
         |           |           |           |           |           |
MDVSLCPAKC SFWRIFLLGS VWLDYVGSVL ACPANCVCSK TEINCRRPDD GNLFPLLEGQ
```

```
        70         80         90        100        110        120
         |          |          |          |          |          |
DSGNSNGNAN INITDISRNI TSIHIENWRS LHTLNAVDME LYTGLQKLTI KNSGLRSIQP

       130        140        150        160        170        180
         |          |          |          |          |          |
RAFAKNPHLR YINLSSNRLT TLSWQLFQTL SLRELQLEQN FFNCSCDIRW MQLWQEQGEA

       190        200        210        220        230        240
         |          |          |          |          |          |
KLNSQNLYCI NADGSQLPLF RMNISQCDLP EISVSHVNLT VREGDNAVIT CNGSGSPLPD

       250        260        270        280        290        300
         |          |          |          |          |          |
VDWIVTGLQS INTHQTNLNW TNVHAINLTL VNVTSEDNGF TLTCIAENVV GMSNASVALT

       310        320        330        340        350        360
         |          |          |          |          |          |
VYYPPRVVSL EEPELRLEHC IEFVVRGNPP PTLHWLHNGQ PLRESKIIHV EYYQEGEISE


       370        380        390        400        410        420
         |          |          |          |          |          |
GCLLFNKPTH YNNGNYTLIA KNPLGTANQT INGHFLKEPF PESTDNFILF DEVSPTPPIT

       430        440        450        460        470        480
         |          |          |          |          |          |
VTHKPEEDTF GVSIAVGLAA FACVLLVVLF VMINKYGRRS KFGMKGPVAV ISGEEDSASP

       490        500        510        520        530        540
         |          |          |          |          |          |
LHHINHGITT PSSLDAGPDT VVIGMTRIPV IENPQYFRQG HNCHKPDTYV QHIKRRDIVL

       550        560        570        580        590        600
         |          |          |          |          |          |
KRELGEGAFG KVFLAECYNL SPTKDKMLVA VKALKDPTLA ARKDFQREAE LLTNLQHEHI

       610        620        630        640        650        660
         |          |          |          |          |          |
VKFYGVCGDG DPLIMVFEYM KHGDLNKFLR AHGPDAMILV DGQPRQAKGE LGLSQMLHIA

       670        680        690        700        710        720
         |          |          |          |          |          |
SQIASGMVYL ASQHFVHRDL ATRNCLVGAN LLVKIGDFGM SRDVYSTDYY RLFNPSGNDF

       730        740        750        760        770        780
         |          |          |          |          |          |
CIWCEVGGHT MLPIRWMPPE SIMYRKFTTE SDVWSFGVIL WEIFTYGKQP WFQLSNTEVI


       790        800        810        820        830        839
         |          |          |          |          |          |
ECITQGRVLE RPRVCPKEVY DVMLGCWQRE PQQRLNIKEI YKILHALGKA TPIYLDILG
```

Appendix II

Based upon predicted average hydrophobicity and secondary structure, neurotrophin primary structure is divided into distinct regions I through VII. These regions are illustrated below, based upon the primary structure of rat NGF (Ibanez et al. 1991). Regions VI and VII are the N and C terminal regions respectively of the neurotrophins.

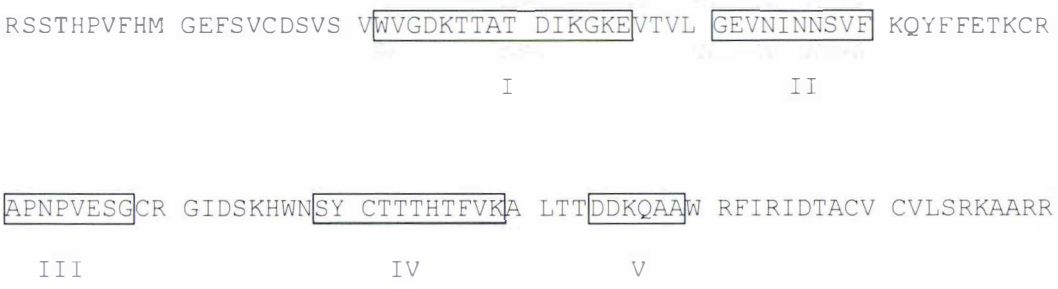

Appendix III

Molecular Weights of MBP-fusion Proteins

The molecular weight of MBP is ~ 42700 Daltons

TrkA	MW Daltons
LRR2	45410
LRR	51019
C1LRR12	53253
LRR23C2	53437
C1LRR	60781
LRRC2	57341
Ig1+Ig2	67028
C2Ig1+Ig2	84484
ED	85086

TrkB	MW Daltons
C1LRR	61521
LRRC2	57025
C1LRRC2	62545
Ig1+Ig2	68883
ED	87336

TrkC	MW Daltons
ED	87370

Appendix IV

Charged Residues on the surfaces of Neurotrophins

NGF, BDNF and NT-3, produced with Grasp software (Nichols et al. 1991), show considerable differences in charge distribution on the surfaces of the proteins. From an NMR[1] study of the two peptides, the TrkA peptide is all random coil, while the TrkB peptide has significant α-helical secondary structure. It is possible that the dissimilar kinetics displayed by the two peptides, arises from the difference in charge distribution on the surfaces of the neurotrophins, as well as the solution structure of the peptides.

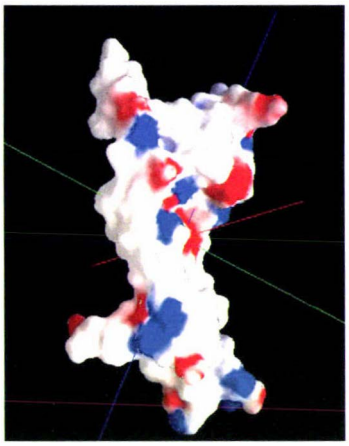

Figure 1A Charge distribution on the surface of NGF.

Above is shown the Grasp determined charge distribution on the surface of an NGF monomer, determined from the homodimer structure of NGF, (McDonald et al. 1991). Positive charges are depicted in blue, while negative charges are shown in red. In order to make a direct comparison of the charge distributions on the surfaces of all three neurotrophins, the charge distribution was plotted with a color range of -5 for negative charge to +5 for the positive charge. Each neurotrophin is displayed with the N-terminus oriented to the lower left and the dimer interface to the right.

[1] Spectra collected by Vladimir Basus , Department of Pharmaceutical Chemistry, UCSF.

Table 1A Charged Residues on the Surface of NGF.

Positively Charged	Negatively Charged
25 Lys	11 Glu
32 Lys	16 Asp
34 Lys	24 Asp
50 Arg	30 Asp
57 Lys	35 Glu
59 Arg	41 Glu
69 Arg	55 Glu
74 Lys	65 Glu
88 Lys	72 Asp
95 Lys	72 Asp
100 Arg	84 His
114 Arg	93 Asp
115 Lys	94 Glu
	105 Asp

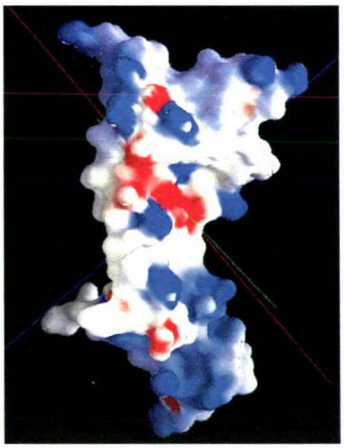

Figure 2A Charge distribution on the surface of BDNF monomer; modeled from an BDNF/NT-3 heterodimer structure (Robinson et al. 1995).

Table 2A Charged Residues on the Surface of BDNF.

Positively Charged		Negatively Charged	
25	Lys	14	Asp
26	Lys	24	Asp
41	Lys	30	Asp
46	Lys	40	Glu
50	Lys	55	Glu
57	Lys	66	Glu
65	Lys	106	Asp
69	Arg		
73	Lys		
74	Arg		
75	His		
81	Arg		
88	Arg		
95	Lys		
96	Lys		
97	Arg		
101	Arg		
104	Arg		
112	Thr		
116	Lys		

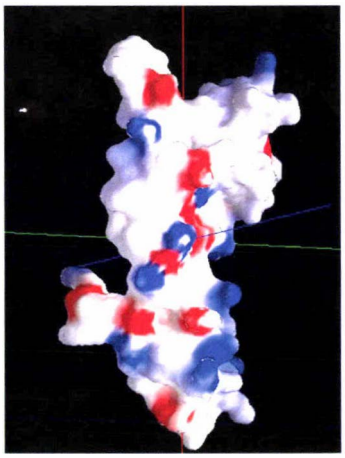

Figure 3A Charge distribution on the surface of NT-3 modeled from the homodimer structure of NT-3 (Butte et al. 1997).

Table 3A Charged Residues on the Surface of NT-3.

Positively Charged		Negatively Charged	
24	Lys	10	Glu
31	Arg	14	Glu
49	Lys	15	Asp
56	Arg	17	Glu
58	Lys	23	Asp
61	Lys	29	Asp
64	Lys	54	Glu
68	Arg	59	Glu
80	Lys	72	Asp
87	Arg	92	Glu
95	Lys	105	Asp
100	Arg		
103	Arg		
114	Arg		